

Analysis of activating Fc gamma receptors and IgG subclasses in the mouse model of cytomegalovirus infection

Inaugural-Dissertation

zur Erlangung des Doktorgrades
der Mathematisch-Naturwissenschaftlichen Fakultät
der Heinrich-Heine-Universität Düsseldorf

vorgelegt von

Katrin Ehrhardt
aus Celle

Düsseldorf, November 2016

aus dem Institut für Virologie
der Heinrich-Heine-Universität Düsseldorf

Gedruckt mit der Genehmigung der
Mathematisch-Naturwissenschaftlichen Fakultät der
Heinrich-Heine-Universität Düsseldorf

Referent: Prof. Dr. Hartmut Hengel, Insitut für Virologie

Korreferent: Prof. Dr. Johannes Hegemann, Insitut für Funktionelle Genomforschung
der Mikroorganismen

Tag der mündlichen Prüfung: 25.01.2017

TABLE OF CONTENT

TABLE OF CONTENT	4
LIST OF FIGURES AND TABLES	8
ABBREVIATIONS	11
SUMMARY	13
ZUSAMMENFASSUNG	14
1. INTRODUCTION	16
1.1. Antibodies	16
1.1.1. Antibody as part of the adaptive immune system	16
1.1.2. Antibody structure and classes	17
1.1.3. IgG and IgG subclasses	19
1.1.4. The immune response: induction of antibodies	19
1.1.5. IgG mediated effector functions	21
1.1.6. Antibody therapies: antibody engineering and clinical use	24
1.2. Mouse Fc receptors	24
1.2.1. Fc receptors (FcRs)	24
1.2.2. Fc binding proteins expressed by pathogens	25
1.2.3. Mouse FcγRs	26
1.2.4. FcγR effector mechanisms	32
1.2.5. Importance of FcγRs in the control of viral infections	36
1.3. Cytomegalovirus	36
1.3.1. Burden of Cytomegalovirus infection	36
1.3.2. Transmission and epidemiology of HCMV	37
1.3.3. Herpesviruses	37
1.3.4. Cytomegalovirus structure, replication cycle, and immune response	38
1.4. Therapy of CMV disease	42
1.4.1. Antiviral drugs	42
1.4.2. Vaccination	43
1.4.3. Passive immunization: prevention and treatment of CMV infection with adoptively transferred antibodies	43
1.5. Objectives of the thesis	46
2. RESULTS	48
2.1. Impact of FcγRs in the primary phase of MCMV infection <i>in vivo</i> : studies in FcγR deficient mouse strains	48
2.1.1. Activating FcγRs contribute to viral control in primary MCMV infection <i>in vivo</i>	48
2.1.2. Absence of a single activating FcγRs is compensated by remaining FcγRs in primary MCMV infection	51
2.1.3. FcγR deficient mice possess elevated total and MCMV specific serum IgG titers	53
2.1.4. Characterization of the immune cell population in the SG of MCMV infected FcRγ-KO vs. FcRγ-HET mice	55
2.2. <i>In vitro</i> FcγR activation assay is a unique tool to quantify FcγR activation by immune complexes	58
2.2.1. Responsiveness of the FcγR-ζ reporter cells to immune complexes	61
2.3. Generation of a recombinant MCMV expressing an ectopic antigen	62
2.3.1. Choice and description of the ectopic model antigen	62
2.4. Generation and characterization of mAbs possessing identical variable regions but different IgG subclasses	67

2.4.1. Comparison of the mouse IgG subclasses	67
2.4.2. Characterization of the parental mAb used for grafting of the variable domain: OKT8 mouse anti-human CD8 IgG2a κ	72
2.4.3. Generation of an expression vector containing the IgG2c constant region	72
2.4.4. <i>In silico</i> predication of N- and O-glycosylation sites in the OKT8 Fv	72
2.4.5. Expression of recombinant OKT8 mAbs in a transduced murine myeloma cell	73
2.4.6. Absence of immune complex resembling IgG aggregates in the purified recombinant OKT8 mAb preparations	74
2.5. IgG subclass dependent Fc binding to Fc γ Rs	80
2.6. P3X-derived recombinant OKT8 mAbs reveal a selective IgG subclass dependent Fc γ R activation pattern <i>in vitro</i>	81
2.7. Influence of the cellular source of recombinant mAb for their Fc γ R activation capabilities	83
2.8. Influence of MCMV infection on IgG subclass dependent Fc γ R activation pattern <i>in vitro</i>	91
2.8.1. CMV encodes viral Fc γ Rs	91
2.8.2. The IgG subclass hierarchy for the Fc γ Rs activation is unchanged on MCMV infected cells vs. non-infected cells	92
2.8.3. Magnitude of Fc γ R activation on MCMV infected cells in comparison to non-infected cells	92
2.9. <i>In vitro</i> Fc γ R activation capacities are equal for BALB/c and C57BL/6 derived Fc γ RIII	96
2.9.1. Comparison of the extracellular domains of the Fc γ Rs derived from C57BL/6 and BALB/c mice	96
2.9.2. IgG subclass dependent Fc binding of BW:Fc γ RIII- ζ BALB/c vs. C57BL/6	97
2.9.3. IgG subclass dependent <i>in vitro</i> Fc γ R activation of BW:Fc γ RIII- ζ BALB/c vs. C57BL/6	98
3. DISCUSSION	101
3.1. Impact of Fc γ Rs for the immune control of MCMV <i>in vivo</i>	101
3.1.1. Activating Fc γ Rs contribute to the control of primary MCMV infection in the SG	101
3.1.2. Redundant function of Fc γ Rs	102
3.1.3. Role of antiviral antibody response in primary MCMV infection, recurrent infection, and latency	103
3.1.4. Immune cell populations possibly exerting Fc γ R dependent control of MCMV in the SG	104
3.2. Optimization of IgG based therapies: IgG subclass dependent activation of Fc γ Rs	105
3.2.1. Unique Fc γ R activation pattern of each IgG subclass	105
3.2.2. IgG subclass dependant Fc γ R activation <i>in vivo</i>	106
3.2.3. IgG2c substitutes genetically for IgG2a in certain mouse strains but is functionally different	107
3.2.4. Fc γ R polymorphisms and their relevance for the affinity to IgG	108
3.2.5. The IgG subclass dependent capability to trigger distinct Fc γ Rs is modified by the Fc glycan composition	109
3.2.6. MCMV mediated alteration of the IgG subclasses dependent Fc γ R activation	110
3.3. Perspective	111
3.3.1. Predictive value of the <i>in vitro</i> Fc γ R activation assay	111
3.3.2. The past and the future of an IgG based therapy against HCMV	111
4. Experimental procedures	113
4.1. Molecular biological methods with nucleic acids	113
4.1.1. Molecular cloning	113
4.1.2. Concentration of nucleic acids	113
4.1.3. RNA isolation and DNA digestion	113
4.1.4. Methods based on the polymerase chain reaction (PCR)	114
4.1.5. Generation of DNA fragments with restriction endonucleases	117
4.1.6. Agarose gel electrophoresis	118
4.1.7. Purification of DNA fragments	118
4.1.8. Dephosphorylating of linearized plasmids	118
4.1.9. Ligation of DNA fragments	118
4.1.10. TOPO-TA-Cloning	119
4.1.11. Transformation of <i>E.coli</i>	119

4.1.12. Isolation of DNA from bacteria	120
4.1.13. Determination of the orientation of an insert in a plasmid	120
4.1.14. Sequencing	120
4.1.15. Generation of recombinant MCMV by BACmid mutagenesis	121
4.1.16. Cryopreservation of bacteria	122
4.1.17. Southern Blot	122
4.2. Protein biochemical methods	123
4.2.1. Determining Protein Concentrations	123
4.2.2. Lysates for SDS PAGE and Western Blot	124
4.2.3. SDS PAGE – Separation of proteins by molecular weight	124
4.2.4. Protein staining with colloidal Coomassie	125
4.2.5. Western Blot - Detection of specific proteins	125
4.2.6. Native PAGE - Detection of native proteins and complex	126
4.2.7. Antibody purification	126
4.2.8. Immunoprecipitation of protein complexes	128
4.3. Cytological methods	129
4.3.1. Cultivation of eukaryotic cells	129
4.3.2. Cryopreservation of eukaryotic cells	129
4.3.3. Preparation of primary Mouse Embryonal Fibroblasts (MEF)	130
4.3.4. Transient transfection of eukaryotic cells	130
4.3.5. Generation of stable cell lines	130
4.4. Virological methods	132
4.4.1. Infection of cells with MCMV	132
4.4.2. <i>In vitro</i> Amplification of MCMV and Purification of a virus stock	132
4.4.3. Quantification of MCMV virus titer	133
4.4.4. <i>In vitro</i> growth kinetics of recombinant MCMV viruses	134
4.4.5. Antibody neutralization test (plaque reduction test)	134
4.5. Immunological methods	135
4.5.1. Enzyme-linked immunosorbent assay (ELISA)	135
4.5.2. <i>In vitro</i> FcγR activation assay and IL-2 sandwich ELISA	136
4.5.3. Flow Cytometry	136
4.6. <i>In vivo</i> experiments in the mouse model	138
4.6.1. Genotyping of mice strains	138
4.6.2. Intraperitoneal injection of mice	139
4.6.3. Blood collection and serum preparation	139
4.6.4. Harvest of mouse organs	139
4.7. Miscellanea	140
4.7.1. Generation and characterization of BW:FcγR-ζ reporter cell lines	140
4.7.2. Generation and characterization of a recombinant MCMV hCD8 mutant	141
4.7.3. Generation of hCD8 expressing cell lines	145
4.7.4. Generation and characterization of mAbs possessing identical variable regions but different IgG subclasses	146
4.7.5. <i>In vitro</i> FcγR activation assay on influenza infected target cells	154
5. Material	156
5.1. Devices	156
5.2. Consumables	157
5.3. Cell culture media and supplements	158
5.4. Chemicals and Biochemicals	159
5.5. Buffers and Solutions	159
5.6. Antibodies	162
5.7. Kits	164
5.8. Enzymes	164
5.9. Primer	165

5.10. Plasmids and BACmids	166
5.11. Viruses	167
5.12. Bacteria	167
5.13. Cells	167
5.14. Mouse strains	168
5.15. Software	168
6. SUPPLEMENT	170
6.1. Characterisation of the immune cell populations in the SG	170
6.2. Structure of the human CD8 $\alpha\alpha$ homodimer	170
6.3. Polymorphisms of mouse IgG subclasses	170
6.4. Characterization of the parental mAb used for grafting of the variable domains: OKT8 mouse-anti-human CD8 IgG2 $\alpha\kappa$	172
6.4.1. Secretion of mAb by the OKT8 hybridoma	172
6.4.2. Antigen binding specificity of OKT8	173
6.5. Reproducibility of the <i>in vitro</i> Fc γ R activation assay	174
6.5.1. Cultivation duration of BW:Fc γ R– ζ reporter cells	174
6.5.2. Batch of produced mAbs	175
6.6. Hierarchy of Fc γ R activation by distinct subclasses is independent of the duration of infection	177
6.7. Differential <i>in vitro</i> Fc γ R activation by mAbs targeting the ectodomain of M2 of Influenza A viruses	178
6.8. Overview of generated plasmid, BACmids, and cell lines	181
6.8.1. Generated plasmids and BACmids	181
6.8.1. Generated cell lines	182
REFERENCE LIST	183
ACKNOWLEDGEMENTS	199
CURRICULUM VITAE	200

LIST OF FIGURES AND TABLES

- FIGURE 1.1. Simplified representation of the five antibody classes.
- FIGURE 1.2. The structure of IgG molecules.
- FIGURE 1.3. Overview of IgG mediated antiviral effector mechanisms.
- FIGURE 1.4. FcγR – IgG interaction.
- FIGURE 1.5. Fc glycoforms.
- FIGURE 1.6. Effector functions of FcγRs.
- FIGURE 1.7. Cytomegalovirus structure, virion, and infected cells.
-
- FIGURE 2.1. Fcγ deficient mice display a viral load in the SG whereas FcγRIV is dispensable for control of primary MCMV infection.
- FIGURE 2.2. Fcγ deficient mice display a higher viral load and delayed clearance in the SG in primary MCMV infection.
- FIGURE 2.3. Fcγ deficient mice display a higher viral load and delayed clearance in the SG in primary MCMV infection.
- FIGURE 2.4. FcγRIII is dispensable for the control of primary MCMV infection.
- FIGURE 2.5. FcγRI is dispensable for the control of primary MCMV infection.
- FIGURE 2.6. Fcγ deficient mice display a higher IgG, MCMV specific IgG, and MCMV neutralizing antibody serum titers in primary MCMV infection.
- FIGURE 2.7. Fcγ deficient mice display a higher viral load and delayed clearance in the SG in primary MCMV infection.
- FIGURE 2.8. Characterization of the immune cell population in the SG in MCMV infected Fcγ-KO vs. Fcγ-HET mice.
- FIGURE 2.9. Characterization of the immune cell population in the SG in MCMV infected Fcγ-KO vs. Fcγ-HET mice.
- FIGURE 2.10. Construction of FcγR-ζ chimeras and the principle of the FcγR-ζ activation assay.
- FIGURE 2.11. Selective and antibody concentration dependent BW:FcγR-ζ activation by opsonized target cells.
- FIGURE 2.12. The *in vitro* replication kinetics of MCMV hCD8 and MCMV hCD4 are comparable to the control MCMV Δm157 Luc on fibroblasts.
- FIGURE 2.13. Surface expression of the ectopic antigens hCD8 and hCD4 and the viral glycoprotein gB on infected fibroblasts.
- FIGURE 2.14. Anti-hCD8 mAbs fail to neutralize MCMV hCD8 virions *in vitro*.
- FIGURE 2.15. *In vivo* replication kinetics of MCMV hCD8 in comparison to MCMV Δm157 Luc in immune compromised RAG1 x Fcγ-KO mice.
- FIGURE 2.16. Differences in the amino acid sequence between the mouse IgG subclasses.
- FIGURE 2.17. Phylogenetic tree.
- FIGURE 2.18. Amino acid polymorphism within in the hinge and C_H2 domain of the IgG subclasses.
- FIGURE 2.19. Anticipated FcγR binding sites.
- FIGURE 2.20. Multiple amino acid sequence alignment of the different IgG2c heavy chain sequences.
- FIGURE 2.21. The OKT8 hybridoma cell line produces IgG aggregates.
- FIGURE 2.22. IgG aggregates activate the BW:FcγR-ζ cells in the absence of antigen.
- FIGURE 2.23. Absence of IgG aggregates in purified recombinant OKT8 mAbs.
- FIGURE 2.24. Detection of IgG aggregates and monomers by analytical Size Exclusion Chromatography.

- FIGURE 2.25. Antibodies from different sources exhibit dissimilar mobility in native PAGE.
- FIGURE 2.26. IgG subclass dependent Fc binding to BW:FcγR-ζ reporter cells.
- FIGURE 2.27. Recombinant OKT8 subclass switch mAbs (P3X) reveal a selective IgG subclass dependent FcγR activation pattern *in vitro*.
- FIGURE 2.28. BW:FcγRIII-ζ can also be strongly triggered by weak activating IgG subclasses applying increased IgG concentrations.
- FIGURE 2.29. Influence of the mAb source and MCMV infection for selective IgG subclass dependent FcγRI activation pattern *in vitro*.
- FIGURE 2.30. Influence of the mAb source and MCMV infection for selective IgG subclass dependent FcγRIII activation pattern *in vitro*.
- FIGURE 2.31. Influence of the mAb source and MCMV infection for selective IgG subclass dependent FcγRIV activation pattern *in vitro*.
- FIGURE 2.32. Influence of the mAb source and MCMV infection for selective IgG subclass dependent FcγRII activation pattern *in vitro*.
- FIGURE 2.33. Overview of the IgG subclass dependent activation of the distinct BW:FcγR-ζ reporter cells.
- FIGURE 2.34. Fc binding by viral FcγRs of MCMV hCD8 infected fibroblasts.
- FIGURE 2.35. hCD8 surface expression in hCD8 transduced fibroblasts is altered dependent on the duration of MCMV infection.
- FIGURE 2.36.A Influence of MCMV and MCMV Δm138 infection for selective IgG subclass dependent BW:FcγR-ζ activation pattern *in vitro*.
- FIGURE 2.36.B Influence of MCMV and MCMV Δm138 infection for selective IgG subclass dependent BW:FcγR-ζ activation pattern *in vitro*.
- FIGURE 2.37. Extracellular domain of FcγRIII.
- FIGURE 2.38. BW:FcγRIII-ζ with the extracellular domain of C57BL/6 or BALB/c bind different IgG subclasses similarly.
- FIGURE 2.39. Comparison of the *in vitro* activation of FcγRIII composed of the extracellular domain from BALB/c or C57BL/6 by recombinant OKT8 mAbs.
-
- FIGURE 4.1. Scheme of 5'RACE.
- FIGURE 4.2. Generation of recombinant CMV virus particles by BACmid mutagenesis via site-specific recombination (FRT/FLP).
- FIGURE 4.3. Transduced BW: FcγR-ζ demonstrate high levels of surface expression of the chimeric receptors and binding of mouse IgG.
- FIGURE 4.4. Scheme of the insert, which was integrated into the MCMV BACmid C3X Δm157-FRT.
- FIGURE 4.5. Restriction endonuclease digest and Southern Blot confirm the predicated DNA band pattern of the generated BACmids for MCMV hCD8 and MCMV hCD4.
- FIGURE 4.6. Verification of hCD8 surface expression of hCD8 transduced cell lines.
- FIGURE 4.7. IgG structure and strategy for exchange of the constant regions of the heavy chain (C_H1-C_H3) and light chain (C_L).
- FIGURE 4.8. Identified sequences for OKT8 V_H and V_L by 5'RACE.
- FIGURE 4.9. Expression and secretion of recombinant OKT8 mAbs produced in stably transfected HEK293T cells.
- FIGURE 4.10. The recombinant OKT8 mAbs produced in stably transfected HEK293T and CHO cells bind to their antigen.
- FIGURE 4.11. The recombinant OKT8 mAbs produced in transduced P3X cells bind to their antigen.

FIGURE 4.12.	Purification of the recombinant OKT8 mAbs by Protein G affinity chromatography.
FIGURE S1.	Flow cytometry gating strategies to characterize the immune cell population in the SG in MCMV infected FcRγ-KO vs. FcRγ-HET mice.
FIGURE S2.	Schematic representation of the structure of the human CD8αα homodimer.
FIGURE S3.	Amino acid polymorphism within IgG subclasses.
FIGURE S4.	Secretion of OKT8 mAbs into the cell culture supernatant.
FIGURE S5.	OKT8-APC binds to human but not to mouse T cells.
FIGURE S6.	The OKT8 mAb binds to human but not to mouse T cells.
FIGURE S7.	Influence of time of MCMV infection for selective IgG subclass dependent FcγRII activation pattern <i>in vitro</i> .
FIGURE S8.	Reproductively of the <i>in vitro</i> FcγRIII activation assay.
FIGURE S9.	Hierarchy of distinct FcγR activation by individual IgG subclasses is independent on the IgG batch.
FIGURE S10.	<i>In vitro</i> FcγR activation by polyclonal immune serum and anti-M2 mAbs.
TABLE 1.1.	Mouse FcRs.
TABLE 1.2.	Mouse FcγRs.
TABLE 2.1.	Sequence identity of the domains of the different IgG subclasses.
TABLE 2.2.	Comparison of the amino acid sequence of the FcγR extracellular domain from C57BL and BALB/c mouse strains.
TABLE 4.1.	Standard PCR Program.
TABLE 4.2.	Standard PCR conditions.
TABLE 4.3.	cDNA synthesis reaction mix.
TABLE 4.4.	Touch down PCR program for a high fidelity polymerase.
TABLE 4.5.	Reaction mixture for analytical and preparative digestion with restriction endonucleases.
TABLE 4.6.	IgG2c HC sequences in different databases.
TABLE S1.	<i>In vitro</i> FcγR activation by polyclonal immune serum and anti-M2 mAbs - statistical analysis.

ABBREVIATIONS

ADCC	antibody-dependent cell cytotoxicity	Log	logarithm
aka	also known as	Luc	Luciferase gene
APC	allophycocyanin	mAb	monoclonal antibody
APC	professional antigen-presenting cell	MCMV	mouse cytomegalovirus
BCR	B cell receptor	MCS	multiple cloning site
CD	cluster of differentiation	MEF	mouse embryonic fibroblast
cDNA	complementary DNA	MHC	major histocompatibility complex
CH	constant domain of the antibody HC	MIEP	major immediate early promoter
CL	constant domain of the antibody LC	mRNA	messenger RNA
CMV	cytomegalovirus	MW	molecular weight
Ctrl	control	MWCO	molecular weight cut off
D	delta, deletion mutant	neg	negative
DC	dendritic cell, pDC: plasmacytoid, cDC: conventional	NK	natural killer cell
DL	detection limit	Nr.	number
dCTP	deoxycytidine triphosphate	ns	not significant
DMEM	Dulbecco's Modified Eagle medium	OD	optical density
DNA	deoxyribonucleic acid	OKT8	clone of mouse anti human CD8 IgG2aK
dNTP	deoxynucleotide triphosphate	ORF	open reading frame
dpi	days post infection	ORI	origin of replication
E.coli	Escherichia coli	PAA	polyacrylamide
ELISA	enzyme-linked immunosorbent assay	PAGE	polyacrylamide gel electrophoresis
Fab	Fragment antigen binding	PBMCs	peripheral blood mononuclear cells
Fc	Fragment crystallisable	PBS	phosphate buffered saline
FcεR1γ	gamma chain	PCR	polymerase chain reaction
FcγR	Fc gamma receptor	PE	phycoerythrin
FcR	Fc Receptor	PGS	Protein G Sepharose
FcRγ	see FcεR1g	pH	potentia hydrogenii (lat.)
FcRn	Fc receptor neonatal	PNGase F	Peptide-N-Glycosidase F
FCS	Fetal Calf Serum	POD	peroxidase (horseradish peroxidase)
FITC	fluorescein isothiocyanate	pos	positive
FITC	Fluorescein isothiocyanate	RAG	recombination-activating gene
gB	HCMV/MCMV glycoprotein B	RNA	ribonucleic acid
GFP	green fluorescent protein	RPMI	Roswell Park Memorial Institute (medium)
HC	heavy chain of an antibody	RSV	respiratory syncytial virus
hCD8	human CD8	RT	room temperature
HCMV	human cytomegalovirus	RT	room temperature
HET	heterozygous	SD	standard deviation
HHV	human herpesvirus	SDS	sodium dodecyl sulphate
hi	high	SEC	size exclusion chromatography
HIV	human immunodeficiency virus	SEM	standard error of the mean
hpi	hours post infection	SG	salivary glands
HSV	herpes simplex virus	TCR	T cell receptor
i.p.	intraperitoneal	TEMED	Tetramethylethylenediamine
IFN-γ	interferon gamma	TGF-β	transforming growth factor beta
Ig domain	immunoglobulin domain	TH	CD4 helper T cell
IgA /D /E /M	immunoglobulin A/D/E/M	TM	melting temperature
IgG	immunoglobulin G	TNF	tumor necrosis factor
IL	interleukin	UV	Ultraviolet light
int	intermediate	v/v	volume/volume
IP	immunoprecipitation	VH	variable domain of the antibody HC
IRES	internal ribosome entry site	VL	variable domain of the antibody LC
ITAM / ITIM	immunoreceptor tyrosine-based activation/ inhibitory motif	VSB	virus standard buffer
IVIG	intravenous immunoglobulin	VSV	Vesicular stomatitis virus
KO	knockout	VZV	varicella zoster virus
LC	light chain of an antibody	w/v	weight/volume
		wpi	weeks post infection
		wt	wild type

UNITS

°C	Celsius degrees
μ (μl, μg, μM)	micro (-litre, -gram, -molar)
μCi	microcurie
A	Ampere
d	day(s)
g	gram
h	hour(s)
kb	kilobase
kDa	kilodalton
l	litre
M	molarity
m (ml, mg, mM)	mili (-litre, -gram, -molar)
min	minute
MOI	multiplicity of infection (PFU/cell)
ng	nanogram
nm	nanometer
PFU	plaque forming unit
RLU	relative light units
rpm	rounds per minute
s	second
V	Volt
w	weeks

AMINO ACIDS

A	Ala	Alanine
C	Cys	Cysteine
D	Asp	Aspartic Acid
E	Glu	Glutamic Acid
F	Phe	Phenylalanine
G	Gly	Glycine
H	His	Histidine
I	Ile	Isoleucine
K	Lys	Lysine
L	Leu	Leucine
M	Met	Methionine
N	Asn	Asparagine
P	Pro	Proline
Q	Gln	Glutamine
R	Arg	Arginine
S	Ser	Serine
T	Thr	Threonine
V	Val	Valine
W	Trp	Tryptophan
Y	Tyr	Tyrosine

SUMMARY

Herpesviral infections are lifelong persistent with phases of latency and recurrence. Human cytomegalovirus (HCMV) causes morbidity and mortality in immuno-compromised patients and after congenital transmission. In the latter situation, no approved therapeutic options exist. The administration of intravenous IgG (IVIG) containing CMV specific antibodies showed varying results. However, the IVIG preparations and their mode of action are not well characterized. Besides neutralization, IgGs exert diverse effector functions by the activation of Fc gamma receptor (FcγRs) via their constant Fc part. Recent studies demonstrated the crucial impact of FcγRs for the antiviral immune response against virus infections including HIV and influenza. To define the role of FcγRs and IgG subclasses in CMV infection and to provide proof of concept, the mouse model of CMV (MCMV) was utilized. In mice, five IgG subclasses, three activating FcγRs, and one inhibitory FcγR exist. Mice deficient in the expression of all activating FcγRs (FcRγ-KO) displayed a higher and prolonged MCMV replication in the salivary glands (SG), an organ important for horizontal transmission of the virus. Furthermore, FcRγ-KO mice displayed reduced numbers of NK cells (14 dpi) and macrophage (28 dpi) in the SG during MCMV infection. This result suggests the involvement of FcγRs in the phase of primary MCMV infection. Mice lacking one of the activating FcγRs controlled the virus comparable to control mice suggesting redundant roles for the activating FcγRs. To dissect further the relative importance of FcγRs in MCMV infection, future investigation of FcγR double deficient mice and / or a recurrent infection model is required. In addition, the optimization of therapeutic IgG was systematically approached focusing on FcγR dependent effector functions of non-neutralizing IgG antibodies. To this end, a set of recombinant subclasses switched IgGs and a recombinant MCMV efficiently expressing the ectopic cognate antigen (human CD8) were constructed. A reporter cell based assay was established to analyse and compare FcγR activation capabilities of mouse IgG *in vitro*. The predictive value of this *in vitro* FcγR activation assay was demonstrated when analysing influenza A virus (IVA) non-neutralizing IgG monoclonal antibodies specific for the M2e antigen. Their FcγR-mediated protection against lethal IAV disease *in vivo* correlated very well with the reporter cell data (cooperation with X. Saelens, Ghent). The *in vitro* FcγR activation capabilities of the IgG subclass switch variants were assessed using hCD8 expressing target cells revealing a unique IgG subclass dependent activation pattern for each of the FcγRs. IgG2a was the most potent subclass clearly differing from IgG2c which had been suggested to be broadly similar to IgG2a. IgG2c was surprisingly weak in FcγRIII activation, while only slightly less potent or comparable in activating the other FcγRs. Because most laboratory mouse strains only possess IgG2a or IgG2c, this finding is of general interest when evaluating FcγR dependent IgG effector functions in different transgenic mouse models. Next, the IgG switch variants were produced in different cell lines (mouse myeloma P3X63Ag8.653, human HEK293T, hamster CHO) associated with a differential composition of their Fc glycan at position Asn297. The pattern of FcγR activation by the distinct subclasses changed modestly for HEK293T but drastically for CHO compared to the myeloma derived recombinant antibodies. Some subclasses, e.g. IgG1, were more affected than others, e.g. IgG2a. Therefore, the subclass and Fc glycan composition affect the FcγR activation capabilities of IgG antibodies. When comparing hCD8 transduced with MCMV infected cells, the IgG subclass hierarchy for the activation of respective FcγRs was not altered but the overall magnitude of activation was greatly diminished. This inhibition is likely caused by MCMV-encoded FcγRs like m138, which antagonize host FcγRs. In the next step, the relative protective effect of the IgG switch variants and their glycan make-up will be assessed during MCMV hCD8 infection of mice.

ZUSAMMENFASSUNG

Herpesvirale Infektionen persistieren lebenslang mit Phasen der Latenz und Reaktivierung. Das humane Cytomegalovirus (HCMV) verursacht Morbidität und Mortalität in immunkompromittierten Patienten und nach Übertragung im Mutterleib. Für die letztere Situation existiert bisher keine zuverlässige Therapie. Die Wirksamkeit von intravenösem IgG (IVIg), welches CMV spezifische Antikörper enthalten, wird kontrovers berichtet. Jedoch sind die IVIg Präparate und deren Wirkungsweise nur wenig charakterisiert. Neben der Neutralisation vermitteln IgG Antikörper diverse Effektorfunktionen über die Aktivierung von Fc gamma Rezeptoren (FcγRs) mittels ihres konstanten Fc Teils. Aktuelle Studien demonstrieren die entscheidende Bedeutung der FcγRs für die antivirale Immunantwort gegen Virusinfektionen wie HIV und Influenza. Um die Rolle der FcγRs und der IgG Subklassen in der CMV Infektion zu definieren und um den grundsätzlichen Nachweis ihrer Wirksamkeit zu erbringen, wurde das CMV-Mausmodell (MCMV) verwendet. Mäuse besitzen fünf IgG Subklasse, drei aktivierende FcγRs und einen inhibierenden FcγR. Die fehlende Expression aller aktivierenden FcγRs führt bei Mäusen (FcγR-KO) zu einer höheren und verlängerten MCMV Replikation in der Speicheldrüse, einem Organ, das für die horizontale Ausbreitung des Virus wichtig ist. Des Weiteren zeigten diese Mäuse eine reduzierte Anzahl an NK Zellen und Makrophagen 14 bzw. 28 Tage nach Infektion in der Speicheldrüse. Diese Ergebnisse unterstützen die Hypothese einer Beteiligung der FcγRs bei der primären MCMV Infektion. Mäuse, denen ein aktivierender FcγR fehlt, kontrollieren das Virus vergleichbar wie Kontrollmäuse, was eine redundante Rolle für die aktivierenden FcγRs impliziert. Um die relative Bedeutung der FcγR in der MCMV Infektion weiter auf zu auflösen, sollten zukünftig zweifach FcγR defiziente Mäuse und / oder ein Modell der reaktivierten MCMV Infektion untersucht werden. Anschließend wurde ein systematischer Forschungsansatz zur Optimierung therapeutischer IgG mit dem Fokus auf FcγR abhängige Effektorfunktionen von nicht neutralisierenden IgG Antikörpern verfolgt. Zu diesem Zweck wurde ein Set von rekombinanten IgGs mit ausgetauschten Subklassen und ein rekombinantes MCMV Virus, das das ektopische Antigen (humanes CD8) effizient exprimiert, konstruiert. Des Weiteren wurde ein auf Reporterzellen basierender *in vitro* Test etabliert, mit dem die FcγR-Aktivierungsfähigkeiten von murinen Antikörperproben analysiert und verglichen werden können. Zuerst wurde der Vorhersagewert des *in vitro* FcγR Aktivierungstest mit nicht neutralisierenden monoklonalen Antikörpern, die spezifisch für das M2e Antigen von Influenza A Virus sind, demonstriert. Deren FcγR vermittelte Schutzwirkung gegen die letale IAV Erkrankung *in vivo* korrelierte sehr gut mit den Reporterzellen generierten Daten (Kooperation mit X. Saelens, Ghent). Die Bestimmung der FcγR Aktivierungsfähigkeiten des IgG Subklassensets auf hCD8 exprimierenden Zielzellen ergab ein einzigartiges IgG Subklassen abhängiges Aktivierungsmuster für jeden FcγR. IgG2a war die potenteste Subklasse und unterschied sich somit eindeutig von IgG2c, was die allgemeine Annahme, dass IgG2c sehr ähnlich zu IgG2a sei, widerlegt. IgG2c was erstaunlich schwach in der Aktivierung von FcγRIII, aber nur leicht schwächer oder vergleichbar in der Aktivierung der anderen FcγRs. Da die meisten Inzuchtstämme entweder über IgG2a oder IgG2c verfügen, sind die o.g. Ergebnisse von großer Bedeutung für die Beurteilung von FcγR abhängigen IgG Effektorfunktionen in verschiedenen transgenen Mausmodellen. Als nächstes wurden die IgG Subklassen in verschiedenen Zelllinien produziert (murines Myelom P3X63Ag8.653, humane HEK293T, vom Hamster stammende CHO) welches in einer unterschiedlichen Zusammensetzung des Fc Teil assoziierten Glykans an Position Asn297 resultiert. Die FcγR-Aktivierungsmuster bestimmter Subklassen haben sich moderat für die aus HEK293T Zellen und stark für die aus CHO Zellen stammenden rekombinanten Antikörper im

Vergleich zu den aus dem Myelom stammenden Antikörpern verändert. Einige Subklassen, z.B. IgG1, waren dabei stärker betroffen als andere, z.B. IgG2a. Folglich bestimmt sowohl die Subklasse als auch die Zusammensetzung des Fc-Glykans die FcγR Aktivierungseigenschaften von IgG Antikörpern. Die Hierarchie der IgG Subklassen für die FcγR Aktivierung ändert sich nicht auf MCMV infizierte Zielzellen im Vergleich zu hCD8 transduzierten Zellen, aber die Stärke der Aktivierung wird stark reduziert. Diese Inhibition der zellulären FcγRs wird wahrscheinlich von MCMV-kodierten FcγR, wie m138, verursacht. Im nächsten Schritt soll die relative Schutzwirkung der IgG Subklassen und deren Glykanzusammensetzung in der MCMV hCD8 Infektion *in vivo* untersucht werden.

1. INTRODUCTION

1.1. Antibodies

1.1.1. Antibody as part of the adaptive immune system

The recognition of foreign structures, e.g. pathogens or toxins, is the basis of the immune response. The innate immune response is rapidly available. It recognizes certain foreign structures of pathogens that have passed the physical protective barriers based on conserved biochemical structures (e.g. LPS as a component of the bacterial cell membrane or dsRNA of viruses), so-called pattern associated molecular patterns (PAMPs). PAMPs activate pattern recognition receptors (PRR), e.g. toll like receptors (TLR), which are expressed on the cell surface or intracellularly. In contrast, the adaptive immune system is able to mount responses targeting a specific foreign structure and to establish a long lasting memory. It needs more time to develop, because it adapts precisely to the specific foreign structure. Furthermore, the adaptive immune response consists of a humoral and cellular branch. Antibodies, also named immunoglobulins, are a part of the humoral response whereby these soluble large “Y”-shaped complexes (1.1.2.) are secreted by B cells. Each antibody binds to a specific target, the antigen. Antibodies are able to trigger multiple effector functions (1.1.5.), which mediate the neutralization or destruction and elimination of the foreign structure. Antibodies are a part of the adaptive immune response but activate effector functions exerted by innate and adaptive components of the immune system. The generation of antibodies is an essential component of immune responses and antibody deficiencies lead frequently to severe and possibly persistent infections. On the other hand, antibodies can cause autoimmune diseases if recognizing self-antigens thereby destructing cells or tissue.

Due to their extremely high antigen specificity, antibodies are unrivalled as diagnostic markers, as tools for diagnostic and research methods, and they are a platform for engineering highly effective therapeutic reagents (1.1.6.). Furthermore, the protection by most vaccines relies on the induction of pathogen-specific antibodies. Vaccination / immunization was even applied before the discovery of antibodies. The first immunization based on the inoculation of smallpox virus containing material (also named variolation) was reported at the end of the 16th century. The hazardous methods of variolation were refined by E. Jenner by the usage of cowpox virus from human lesions, which leads to mild disease but nevertheless protected against smallpox virus disease and resulted in the development of the first vaccine in the late 18th century (Riedel et al., 2005).

The earliest reference to antibody came from E. von Behring, S. Kitasato, and E. Wernicke one century later. Serum from immunized animals was able to protect animals from diphtheria. This discovery resulted in a passive serum therapy for humans. Around 1900, P. Ehrlich proposed the “side-chain theory” (side chain = receptor) about the origin, function, and structure of the antibodies. His theory included the fact, that antibodies first serve as receptors on certain cells and after binding to their antigen, the specific antibody is synthesized and released into the blood. 60 years later, the antibody structure and amino acid sequence was resolved by G. Edelman and R. Porter independently (Elgert, 1998). In the middle of the 20th century, the cell type producing antibodies, namely plasma cells (matured B cells), was described by A. Fagraeus. Furthermore, D. Talmage and F. Burnet proposed the clonal selection theory stating that naïve B cells generate antibodies with a single specificity, which

first served as surface receptor and antigen binding leads to the clonal expansion of the counter-specific B cells and their maturation into plasma cells secreting the soluble form of the antibody (Burnet, 1980). In the 1970ies, the genetic mechanism for the generation of antibodies (1.1.4.2.), which is responsible for the enormous antibody diversity, was discovered by S. Tonegawa (reviewed in Tonegawa, 1983). At the same time, the invention of the hybridoma technology by G. Köhler and C. Milstein enabled the production monoclonal antibodies (Köhler et al., 1975) representing the beginning of the modern era of (antibody) research.

1.1.2. Antibody structure and classes

Antibodies serve two purposes: (1) They are expressed as a membrane bound form on the surface of B cells to sense their specific antigen (B cell receptor, BCR) which leads to cell activation (together with further costimulatory signals, e.g. CD4 T cell help). (2) The secreted soluble form, the antibody, exerts its antigen specific effector functions at a distance from the producing B cell. The expression of the soluble form is accomplished by a shortened C-terminus produced by alternative splicing of the mRNA.

Immunoglobulins are heterotetrameric proteins composed of two identical heavy and two identical light chains connected by intramolecular disulphide bonds and further non-covalent interaction giving rise to the classical “Y”-shape (Figure 1.1). Their structure can be functionally divided: on the one hand, the two identical variable domains bind to the specific antigen (Fab: antigen binding fragment) and on the other hand, the constant domain (Fc: crystallisable fragment) specifies localization and effector functions of the soluble antibody. The antibody chains are composed of repeated anti-parallel β -sheets, called Ig domain. The light chains possess two and the heavy chains four to five Ig domains, whereby the N-terminal domain has a variable sequence. The pairing of the variable domain of the light (VL) and the heavy (VH) chain creates the antigen-binding site (paratope). Each variable domain contains three hypervariable loops (CDR: complementary-determining region) in-between the beta-sheet frame work, which determine the antigen specificity. The variable domains (V_H and V_L) and the first constant Ig domains (C_{H1} and C_L) form the Fab fragment, which is separated by an unstructured and therefore flexible sequence, the hinge region, from the constant part (C_{H2} - C_{H3} or C_{H2} - C_{H4}).

Mammals possess five antibody classes, which are assigned according to their heavy chain: IgA, IgD, IgE, IgG, and IgM (Figure 1.1.). The heavy chain is named after the corresponding Greek letters: α , δ , ϵ , γ , and μ . The term “isotype” specifies the heavy chain and is therefore a synonym for Ig class or IgG subclass. Even though the classes exhibit a similar structure, the protein sequences are relatively dissimilar resulting in different numbers of Ig like domains, numbers and positions of intra- / intermolecular disulphide bonds, N- and O-glycosylation sites, and the length of the hinge. IgM and IgE do not contain a hinge region but an additional C_H domain. IgM and IgA form oligomers induced by a tailpiece, an 18 amino acids cysteine rich sequence at their C-terminus. An associated peptide, the J-chain, facilitates oligomerization and secretion. A membrane-bound form exists for all classes. Furthermore, two variants of light chains exist, kappa and lambda, but the kappa light chain is much more frequent in mice (~95%).

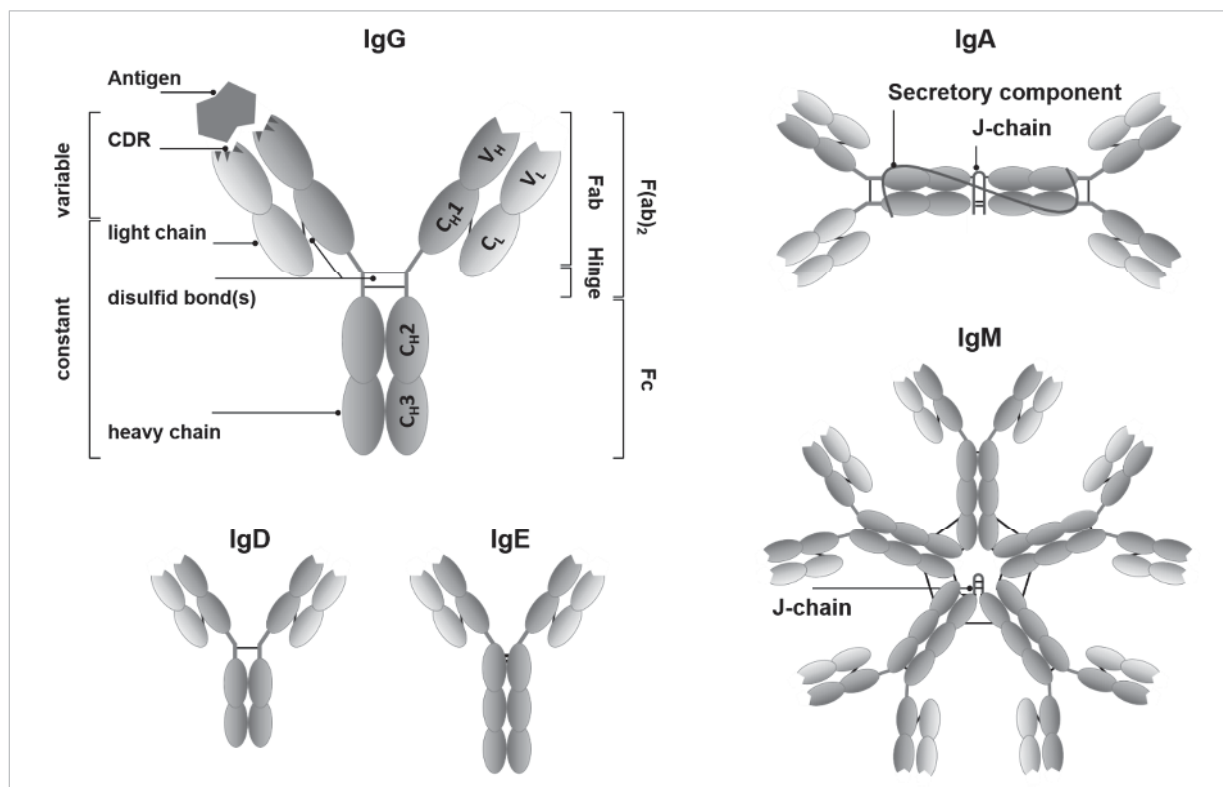


FIGURE 1.1. Simplified representation of the five antibody classes, which differ in the number of Ig domains and the oligomer formation. In the mouse, the IgG class can be divided into 5 subclasses. The J-chain facilitates oligomerization and secretion. IgA exists as monomer and on mucosal surfaces / secretes as dimer associated with the secretory component which is the cleaved extracellular domain of the polymeric immunoglobulin receptor (pIgR). The pIgR mediates the secretion of IgA and IgM. IgM forms pentamers and rarely hexamers without J-chain. N- and O-Glycosylation sites are not shown and differ between classes. Also the amount and position of disulfide bonds (black lines) differ between classes and IgG subclasses especially in the hinge region, which is lacking in IgM and IgE. HC: heavy chain, LC light chain. Sizes are not to scale. Figure adapted from Kenneth, 2012 and Kindt et al., 2006.

The serum abundance of the different antibody classes depends on age and typically is: IgG >>> IgA > IgM > IgD > IgE.

- IgM is the first Ig class produced in the primary immune response. IgM does not undergo affinity maturation (1.1.4.1.; 1.1.4.2.) resulting in a lower antigen affinity as other Ig classes. This is overcome by the formation of pentamers, which increases the avidity of the molecule due to the higher number of antigen binding sites. IgM is found mainly in the blood stream leading and a potent activator of the complement system. It is a diagnostic marker for the acute exposure to a pathogen or immunogen. Furthermore, low titers of polyreactive IgM ("natural" antibodies) exists even in naïve individuals as a first line of defence.
- IgD serves as well as BCR and is mostly co-expressed with IgM on the surface of B cells. Soluble IgD has very low serum concentrations and a short half-life. Its function is unknown.
- IgA is present as monomer in the blood and as dimer on mucosal surfaces / secretes (tears, breast milk, sweat, intestine, etc.) where it is mediating local immunity.
- IgE has a short half-life and very low serum concentration. It is rather bound to FcεRI, which is expressed by certain immune cells (mast cells and basophils). Their activation is attributed with allergic reactions (type I immediate hypersensitivity) and parasitic worm infections.
- IgG is the most abundant class present in the serum. It is important in preventing reinfection by bacteria and viruses and it represents the predominant class induced in a secondary immune response. It accounts for 15% of all serum proteins and represents 75% of all Ig classes. In addition, IgG is present in the extracellular fluid. The high abundance is also a consequence of its

long half-life, which is regulated by the neonatal Fc gamma receptor (FcRn, 1.2.1.). Additionally, the FcRn transports IgGs across the placenta into the fetal blood stream. The effector functions (1.1.5.) are neutralization, complement fixation, and FcγR activation whereby the latter two are influenced by the IgG subclass.

1.1.3. IgG and IgG subclasses

This study focuses on IgG mediated effector functions. An IgG molecule has a molecular weight of approximately 150 kD composed of the two heavy chains with 50 kD and the two light chains with 25 kD each. The IgG structure is shown in Figure 1.1. and 1.2. In mice, five IgG subclasses exist: IgG1, IgG2a, IgG2b, IgG2c, and IgG3. Laboratory mouse strains typically possess either IgG2a or IgG2c (3.2.3). The IgG subclasses differ mostly in the flexible hinge region. A detail comparison is presented in 2.4.1. Furthermore, IgGs possess a conserved N-glycosylation site at Asparagine 297 in the C_H2 domain of the Fc part. The glycan consists of a biantennary core heptasaccharide with variable additions of fucose, galactose, and / or sialic acid leading to a high heterogeneity of the glycan composition of IgG molecules. The conformation of the Fc part is horseshoe like due to non-covalent interaction of the C_H3 domains of both heavy chains and the opening between the C_H2 domains. The Fc glycan modulates the conformation of the Fc part and differences in the glycan composition influence the effector function triggered by the IgG molecule (1.2.3.5.). Therefore, the effector function of the IgG subclasses are determined by the amino acid sequence of the Fc part and the composition of the Fc associated glycan (Bournazos et al., 2015).

Besides the structural differences, the IgG subclasses are differentially induced. Dependent on the pathogen, CD4 T cell differentiation is driven towards T helper cell type 1 or 2 (T_H1 or T_H2). Intracellular pathogens including viruses generally induce a T_H1 response resulting in interferon gamma (IFN-γ) as predominant cytokine and efficient class switching to IgG2a (Coutelier et al., 1988). In contrast, T_H2 cells secrete IL-4 and IL-5 and leading to a high level of IgG1 (and IgE) and TGF-β inducing IgG2b (and IgA) (Mosmann et al, 1989). IgG1 represents the predominant subclass elicited by protein immunogens (Coutelier et al., 1987). Furthermore, mouse IgG3 is the only T cell-independent IgG (1.1.4.1.). It is directed primarily against carbohydrates and antigen containing repeating epitopes.

1.1.4. The immune response: induction of antibodies

1.1.4.1. B cell activation

Naïve B cells express a membrane bound antibody molecule (IgM, IgD) together with two signalling modules (Igα and Igβ) on their surface forming the so-called B cell receptor (BCR). Binding of an antigen to the BCR leads to the internalization, processing, and presentation of peptides derived from the antigen by MHC II molecules on the cell surface. For the full activation of the B cell, the presented peptide has to be recognized by a CD4 T cell. This CD4 T cell had to be activated beforehand by a professional antigen-presenting cell (APC), which had encountered the antigen as well. The CD4 T and B cell recognize the same antigen (also whole virus or bacteria) but generally different epitopes of the antigen. The activated B cells expand clonally. Some differentiate to IgM-secreting plasma cells while others undergo further maturation. Multiple rounds of expansion, somatic hypermutation of the variable regions, and subsequent selection of B cells with increased affinity to their antigen lead to the affinity maturation of the antibody. Additionally, Ig class switch is induced resulting in the association

of the variable regions with the constant region of another Ig (sub)class. These B cells terminally differentiate in to Ig secreting plasma cells or memory B cells. The processes described are regulated by follicular helper T cells, follicular DCs, and the cytokine milieu. (Kenneth, 2012)

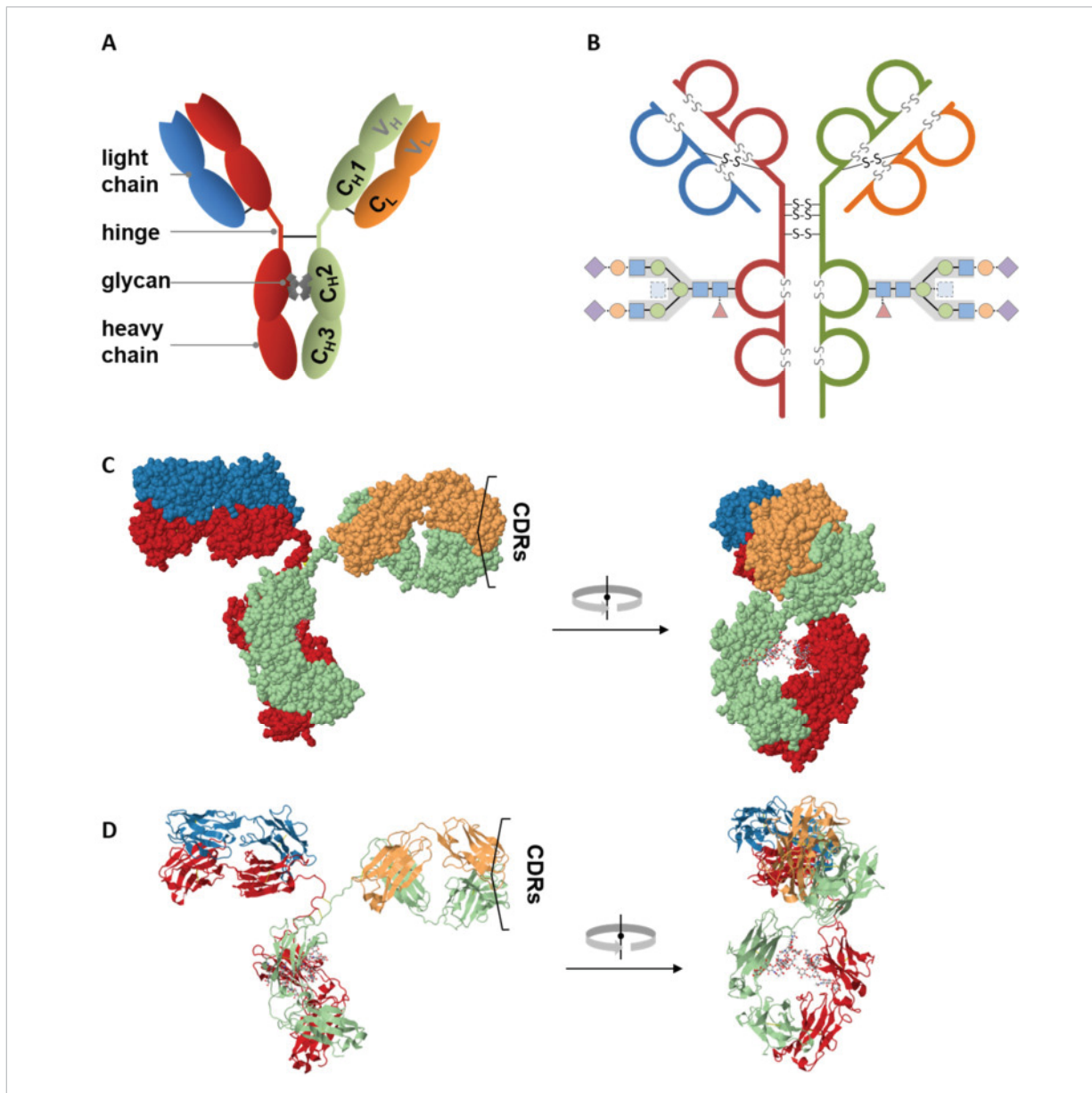


FIGURE 1.2. The structure of IgG molecules. A. Scheme with annotations (C: constant region, V: variable region, H: heavy chain, L: light chain) B. Scheme of the polypeptide chains with intra- and intermolecular disulfide bonds (grey and black, respectively) and of the glycan composition at Asn297 (grey: invariable backbone, red: fucose, blue: GlcNAc, green: mannose, orange: galactose, purple: sialic acid, light blue: bisecting GlcNAc present mainly in human). C, D. X-ray based structure model of a mouse IgG2a (RCSB PDB: 1IGT, JSmol viewer, Harries et al, 1997). Figures were generated with the JSmol viewer of RCSB Protein Database. C. Space fill model D. ribbon model visualizing the secondary structure consisting of beta-sheets representing Ig domains, disulfide bonds are in yellow.

In addition, an alternative pathway to activate B cells can be triggered by certain microbial antigens, for example bacterial DNA or polysaccharides. Thereby, the activation signal is provided by the antigen itself instead of the CD4 T cell. The signal provided by the antigen can be the engagement of pattern recognition receptors (PRR) or the extensive crosslinking of the BCR by repeating epitopes. This pathway is called thymus-independent (TI) in contrast to the B cell activation with CD4 T cell help, which is thymus-dependent (TD). TI antigens lead to short lived plasma cells with limited class switch.

In contrast, TD antigens induce affinity maturation, class switch, and differentiation into long-lived memory cell or plasma cells. TD antigens are proteins or polysaccharide coupled to proteins. (Kenneth, 2012)

1.1.4.2. Genetic level

The diversity of the variable region is created by the combination of a limited number of inherited genes and is further altered in the activated B cell by somatic hypermutation. Each B cell expresses one specific antibody / BCR, which is generated by an irreversible rearrangement of genomic DNA segments (somatic recombination).

First, the variable region of the heavy chains is formed and paired with a germline encoded light chain surrogate. If the pre-BCR is successfully formed, the B cell expands and the variable region of the light chain is rearranged. The mature B cells possess BCRs of the type IgM and IgD.

In more detail, the exon for the variable region of the heavy chain is generated by the combination of three segments (V variable, D diverse, J joining) and exon of the light chain consists of two segments (V, D), whereby the V/D/J segments are randomly chosen from the respective gene segment cluster. These recombination processes is called V(D)J recombination. It also causes nucleotide deletions or insertions at the joints resulting in further diversification. After antigen encountering and activation of the B cells, point mutations are introduced into the variable regions (somatic hypermutation) facilitating the affinity maturation.

Antibody class switch enables the coupling of one antigen specificity with a specific Fc part resulting in distinct effector functions. Therefore, daughter cells of the same B cell can form an antibody with the same antigen specificity but with different antibody (sub)classes. Class switch is mainly regulated by follicular CD4 T cells and the type of cytokine which they secrete. The connection of the exon for variable domain with the exons for a certain heavy chain is realized by irreversible DNA recombination (non-homologous end joining). The order of the heavy chain exons in the mouse *Igh* locus is: C μ (IgM; *Igh-6*) / C δ (IgD; *Igh-5*) – C γ 3 (IgG3; *Igh-8*) – C γ 1 (IgG1; *Igh-4*) – C γ 2b (IgG2b; *Igh-3*) – C γ 2a/c (IgG2a/c; *Igh-1aa/ab*) – C ϵ (IgE; *Igh-7*) – C α (IgA; *Igh-2*). Alternative splicing permits co-production of IgM and IgD. (Kenneth, 2012; Schroeder et al., 2010)

1.1.5. IgG mediated effector functions

As soluble extracellular molecules, antibodies participate in the defence against extracellular and intracellular pathogens like bacteria, viruses (including virus infected cells), and soluble antigens e.g. toxins. Due to the bifunctional nature of antibodies, the effector functions can be separated into Fab and Fc dependent functions. The Fab binds to its specific antigen with high affinity whereas the Fc part determines the antibody class specific effector functions. This and the following section focus on the IgG mediated effector functions to enveloped viruses (Figure 1.3; Forthal, 2014).

1.1.5.1. Fab dependent effector functions

The variable domain of the Fab mediates the binding to the antigen. If the binding of the antibody to a pathogen prevents the infection of a target cell *in vitro*, it is classified as neutralizing. Interference can

occur at different stages of virion (virus particle) entry or egress (Reading et al., 2007). Typically, the attachment or the entry of the virion into the target cell can be blocked sterically by the antibodies or by the prevention of conformational changes, which are necessary to induce the fusion of the virus envelope with the plasma membrane. It might also take place in endosomes, allowing the endocytosis of the virus but not its escape into the cytoplasm e.g. by uncoating. For viruses, which bud from the plasma membrane, repression of virion assembly and release might occur (Klasse et al., 2002; de Parseval et al., 1997). Moreover, cell-to-cell spread of viruses can be inhibited (Burioni et al. 1994; Pantaleo et al. 1995; Mannini-Palenzona et al., 1998). Taken together, the capacity to neutralize is a function of the epitope and it is dependent on the affinity and concentration of the antibody. A high concentration of antibodies is required. The neutralization capacity of an antibody is determined *in vitro* and might differ dependent on the target cell. One theory argues that the epitope itself is irrelevant and neutralization relies solely on the epitope density and occupancy with antibodies (Parren et al., 2001). Neutralization is important for the defence of extracellular pathogens like viruses and is mediated mainly by the IgG antibodies (Dimmock et al., 1993; Burton et al., 2001).

Moreover, cross-linking of pathogens or soluble antigens is trapping them in aggregates. The process is called agglutination and the aggregate are named immune complex. Their size is dependent on the ratio of antigens and antibodies and neutralizing as well as non-neutralizing antibodies contribute. The formation of immune complexes is Fab dependent but their elimination is generally mediated by Fc dependent mechanisms. To note, cluster of antibodies bound to the surface of pathogens or infected cells are termed immune complex.

1.1.5.2. Fc dependent effector functions

While neutralization is effective against extracellular pathogens or toxins, recruitment of effector molecules or /and cells to the Fc part triggers an immune reaction against intracellular pathogens like viruses and tumor cells. While the Fab dependent neutralization of virions can prevent the infection of cells, Fc mediated effector functions mostly act at later steps of the viral replication cycle aiming at the elimination of already infected cells. Neutralizing and non-neutralizing antibodies can initiate Fc dependent responses. Two effector systems can be distinguished: (1) the complement system and (2) Fc gamma receptors (FcγRs). Fundamental is the low affinity of the effector molecules to monomeric antibodies to prevent initiation of the effector mechanism in absence of antigen. In immune complexes, the number of binding sides for the effector molecules is increased leading to a sufficient avidity. Binding of the antibody to the antigen might also induce subtly conformation changes in the antibody Fc domain increasing its affinity to effector molecules (Janda et al., 2016). Nevertheless, monomeric antibodies are bound to FcγR on the surface of immune cells ("cytophilic IgG"), but they don't lead to their activation in the absence of the antigen (Lanier et al., 1983).

a) Complement system

Focusing on the FcγRs in this study, the complement system is only described briefly. The complement system consists of small inactive proteins participating in a cascade of subsequent proteolytic activation and furthermore receptors for complement compounds on distinct cell types. The outcomes include the induction of an inflammatory response, attraction of phagocytes by chemotaxis, opsonization (facilitated phagocytosis), immune complex formation and removal, and the lysis of pathogens or infected cells (CDC: complement dependent cytotoxicity). The lysis is accomplished by the

formation of transmembrane channels called membrane attack complex (MAC). The complement system can be activated by three different converging pathways. Antibodies initiate mainly the classical pathway, whereby the first compound (C1q) binds to IgM or IgG containing immune complexes starting the cascade. Due to its oligomeric nature, IgM is the most potent Ig class for complement activation. It was shown that complement cascade is activated by all IgG subclasses whereby IgG2c was not tested. Dependent on the experimental system, the efficacy of a single subclass to fix complement appears to be different (Neuberger et al., 1981; Hirayama et al., 1982; Ey et al., 1979, Maeda et al., 1986; Michaelsen et al., 2004; Uchida et al., 2004). Even within the same subclass, mAbs react differently (Seino et al., 1993; Stewart et al., 1988). In line with these observations, Garred et al. (1989) reported that the IgG subclass pattern of complement activation depends on the epitope density and the concentration of antibody and complement.

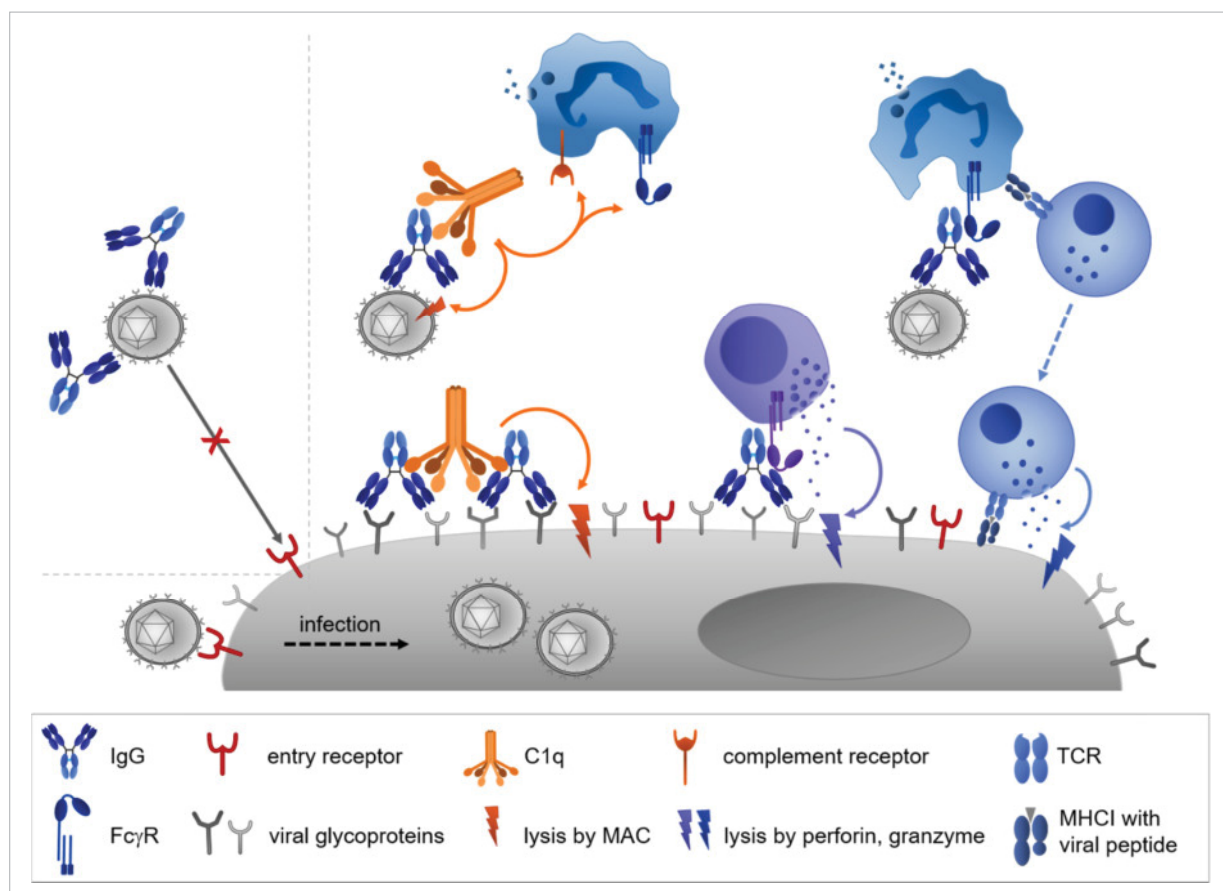


FIGURE 1.3. Overview of IgG mediated antiviral effector mechanisms. Neutralizing antibodies prevent the infection of the target cell by interfering with attachment, entry, or egress (not shown) of the virus. This function is independent of the IgG subclass in contrast to Fc mediated effector functions, which are complement or FcγR mediated. The complement system consists of numerous humoral factors which are activated in a cascade and receptors expressed by mainly immune cells. It induces agglutination, opsonization, chemotaxis, and lysis of cells or enveloped viruses by the membrane attack complex (MAC). Furthermore, various effector functions are exerted by immune cells after engagement of FcγRs like phagocytosis, cytotoxicity (ADCC, antibody dependent cellular cytotoxicity), secretion of proinflammatory substances, facilitation of T cell priming, etc. Immune complex associated with complement factors can be removed by binding to complement receptors or FcγR. To note. immune complexes are represented by only one or two IgG molecules in this figure.

b) Cellular mediated effector functions via Fc receptors and Fc gamma receptors (FcRs, FcγRs)

Via Fc receptors, antibodies connect the humoral with the cellular response. Since they are expressed on immune cell subsets of the innate and adaptive immunity, both branches of the immune system are impacted by the activation of FcRs. Notably, the specificity of the adaptive immune response is linked to the potent effector mechanisms of the innate immune cells. Most FcRs are involved in the

elimination of pathogens. Another class, which is mainly present on epithelial and / or endothelial cells, delivers distinct antibody classes by transcellular transport (transcytosis) to their site of action. FcRs and their effector functions are described in detail in the next chapter (1.2.).

1.1.6. Antibody therapies: antibody engineering and clinical use

IgG antibodies exhibit a remarkable therapeutic potential due to their high specificity and long serum half-life. Monoclonal antibodies are the fastest growing group of pharmaceutical molecules. In the late 1980s, the first mAb, OKT3, was licensed and in 2014 nearly 50 antibodies have been approved in the US or Europe for the treatment of cancer, autoimmune diseases, infections, and as prevention of organ transplant rejection (Ecker et al., 2015; Irani et al., 2015). The most common effector functions for therapeutic antibodies are the block or activation of a signalling cascade by binding the receptor or ligand, the recruitment of immune system inducing clearance / killing of the target (by FcγR and / or complement engagement), or a combination of mechanisms. Antibody therapeutics are often combined with conventional therapies like chemotherapy for cancer. For example, Rituximab, an anti-CD20 mAbs, induces deletion of B cells by the induction of apoptosis in addition to complement and FcγRs induced cytotoxicity (Maloney et al., 2002). Furthermore, therapeutic mAbs can have a vaccinal effect inducing long-term cellular immune responses due to FcγR engagement on APCs (DiLillo et al., 2015).

Furthermore, multiple IgG functions can be modified:

- (1) In- or decrease of Fc effector functions (FcγR, complement, and FcRn engagement) are realized by deletion of the Fc region, insertion of point mutations in the constant domains, or by altering the Fc glycan composition. In addition, bispecific mAbs, which recognize separate antigens with each Fab, are able to recruit and physically link immune cells to the desired target cell.
- (2) Pharmacokinetics and biodistribution can be altered using a variety of antibody formats including small molecules like F(ab)₂, scFv (V_L and V_H connected with a linker peptide), and Fc-fusion proteins.
- (3) Drugs can be targeted via antibody drug conjugates.

Only one humanized mAb against viral infection is approved so far (RSV-specific Synagis®) although the majority of vaccine relies mainly on the protection by antibodies. Further mAbs against viruses are currently developed (listed in Irani et al., 2015 and Marasco et al., 2007). Therefore, it is important to understand further the exact IgG effector function and immune evasive mechanisms of the pathogen to improve the clinical use of antibodies against viral diseases.

1.2. Mouse Fc receptors

1.2.1. Fc receptors (FcRs)

FcRs trigger potent and manifold effector function by linking the humoral with the cellular and the high specificity of the adaptive with the powerful effector functions of the innate immune response (1.1.5.2.). Several specific receptors for the Fc portion of different antibody classes are known. Generally, these are cell surface receptors specific for the Fc portion of one or two distinct Ig classes (Table 1.1). In contrast, TRIM21 is the only intracellular FcR known. In addition, C-type lectin receptors

like FcεRII (CD23) and SIGNR1 (CD209b; human: DC-SIGN) bind to the glycan of the IgE or IgG Fc part, respectively, with a preference for certain glycan compositions.

Fc Receptor	Ligand	Full or alternative name	Expression profile	Main Function
FcμR	IgM		B cells	IgM homeostasis; regulation of humoral immune responses
Fcα/μR	IgM, IgA		B cells, macrophages, non-hematopoietic cells in secondary lymphoid organs	pathogen elimination
plgR	IgM, dimeric IgA	polymeric Immuno-globulin receptor	mucosal epithelium	transcellular transport of polymeric Ig
FcγRI FcγRIIB FcγRIII FcγRIV	IgG (IgE**)	CD64 CD32 CD16 -	immune cell subsets dependent on distinct FcγR (1.2.2.2.)	FcγRI/III/IV: Activation; FcγRIIB: Inhibition; pathogen elimination, immune modulation (1.2.4.)
FcRn	IgG	neonatal Fc receptor, Brambell receptor	Endothelium (also placenta), epithelium subset, immune cell subsets e.g. DCs, monocytes / macrophages	Transcytosis (also of maternal IgG to fetus), prolongation of half-life
FcεRI	IgE		mast cells, basophiles, DCs*, neutrophils*	allergic reaction, immune response to parasites
TRIM21	IgM, IgA, IgG	tripartite motif-containing protein 21	Immune cells, endothelium subset; intracellular receptor	Direction of cytosolic pathogens to proteasomal degradation

TABLE 1.1. Mouse FcRs and their ligands, expression profile, and function. * in infection; **binding of IgE with a very low affinity, except FcγRI; (Bruhns et al., 2015; Sakamoto et al., 2001; Honjo et al., 2012)

Functionally, FcRs can be divided in signalling or transporting receptors. To the latter category belong plgR and FcRn. PlgR transports IgA and IgM unidirectional across the epithelial cells into the intestinal lumen. The FcRn binds IgG in a pH dependent manner in the intestinal lumen or endosomes and mediates intracellular sorting. Thereby, it enables IgG homeostasis (recycling, prolongation of IgG half-life) and bi-directional transcytosis, which also includes the transport of maternal IgG to the bloodstream of the fetus. The FcRn is also expressed in immune cells like phagocytes and APCs. In concert with FcγRs, the FcRn is involved in the phagocytosis of immune complexes and IgG opsonized pathogens and enhancement of antigen (cross-)presentation on MHC I and MHC II (Vidarsson et al., 2006; Baker et al., 2011 and 2014). All other FcR belong to the first category and their main functions are listed in Table 1.1. The only intracellular FcR is TRIM21, which is expressed in almost all cell types and highly in immune cells. It binds to IgM, IgA, or IgG bound to non-enveloped viruses present in the cytosol and directs them to proteasomal degradation (Foss et al, 2015). The mechanism was termed antibody-dependent intracellular neutralization (ADIN; Foss et al, 2015). It also activates intracellular signalling (e.g. via NF-κB) to combat infection.

1.2.2. Fc binding proteins expressed by pathogens

Besides host expressed FcR, certain pathogens express Fc binding proteins to evade the host's immune response. A wide range of bacteria exhibit Fc binding proteins on their surface and in soluble form (Becker et al., 2014). They bind to the Fc part of antibodies of various mammalian species with different affinities dependent on species, Ig class, and subclass. By binding the Fc portion, the antibody effector mechanisms are diminished either by competing with cellular FcγRs and C1q for the binding site on the IgG molecule (Sidorin et al, 2011; Léonetti et al., 1999) or by prevention of crosslinking and therefore signalling of host FcγRs and BCRs (Fabiana et al., 2013; Becker et al., 2014). Many Fc binding

proteins interact with further compounds of blood in addition to IgG. Protein A and Protein G from *Staphylococcus aureus* and *Streptococcus* respectively are well studied and commonly used for antibody purification. In addition, an FcR is present on the protozoa *Schistosoma* (Loukas et al., 2001) and viruses were reported to exhibit Fc binding proteins like mouse hepatitis virus and hepatitis C virus (Oleszak et al., 1990; Maillard et al., 2004). Herpesviruses like HSV and CMV express so called viral FcγRs (vFcγR) on their virions and on the infected host cells interfering with the activation of the host FcγRs by antibody bipolar bridging (3.2.6.).

1.2.3. Mouse FcγRs

Fc gamma receptors specific for IgG (FcγRs) are expressed on most immune cells except for T cells and differ in their cellular expression pattern and affinity to IgG and IgG subclasses (Table 1.2). The triggered effector functions are dependent on the immune cell type, the FcγR expression profile, the IgG molecule (subclass, glycosylation), and involvement of other signalling molecules. Effector functions include direct mechanisms for pathogen clearance and immunomodulatory functions (1.2.4.). By immunomodulation of innate immune cells, FcγRs are involved in regulating the adaptive immune response like priming of T cells. Furthermore, inhibitory FcγRIIB on DCs and B cells control the production and specificity of their ligands (IgGs).

Two classes of FcγRs can be separated: activating and inhibitory. Cellular coexpression of the two classes determines the threshold for cell activation. In mice, three activating (FcγRI / CD64, FcγRIII / CD16, FcγRIV) and one inhibitory FcγR (FcγRIIB / CD32) exists (Table 1.2.).

1.2.3.1. Structure of FcγRs

All FcγRs consist of an alpha chain, a type I transmembrane protein composed of two or three Ig like domains. Thus, they belong to the immunoglobulin gene superfamily. This alpha chain mediates binding of IgG or particularly IgG containing immune complexes. Intracellular signalling is initiated by immunoreceptor tyrosine-based motifs for activation or inhibition (ITAMs or ITIMs). In the inhibitory FcγRIIB, the ITIM is located in the cytosolic domain. Activating FcγRs (FcγRI/III/IV) are complexed with an accessory signalling module, the gamma chain (alternative names FcεR1γ or FcRγ). The gamma chain contains the ITAM and forms dimers. Furthermore, the accessory signalling module is essential for efficient surface expression. As exception, the (human) FcγRIII can be associated with the homodimers of the gamma chain (with preference), CD3 zeta chain, or heterodimers in human NK cells (Lanier et al, 1989; Letourneur et al., 1991). In fact, in HCMV seropositive individuals a unique NK cell subset possessing FcγRIII associated with the CD3 zeta was identified (Lee et al., 2015; Zhang et al., 2013). Based on the structural requirement for the interaction, the association of mouse FcγRIII with the CD3 zeta chain is predicted to be absent (Kurosaki et al., 1991).

1.2.3.2. Expression levels of FcγRs

FcγRs are expressed on most immune cells and commonly activating and inhibiting FcγR are co-expressed on the same cell with the exception of NK / NKT cells, which only express the activating FcγRIII, and B cells, which only possess the inhibitory FcγRIIB (Table 1.2.). The low affine FcγRIII and FcγRIIB have the broadest expression profile and are present on the majority of myeloid cells and granulocytes. The inhibitory FcγRIIB is highly expressed on B cells, monocytes / macrophages, DCs, and

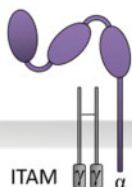



Structure					
Name		FcγRI	FcγRIV	FcγRIII	FcγRII
		CD64	-	CD16	CD32
Nr. of amino acids		404	240	267	329
Function		activation			inhibition
Affinity to IgG		high	medium	low	
Binding of IgG subclasses**				IgG1	IgG1
		IgG2a	IgG2a	IgG2a	IgG2a
			IgG2b	IgG2b	IgG2b
Expression	Lymphoid			NK, NKT	B cell
	Myeloid	Mono/Macro*, DC*	Mono/Macro*, DC?	Mono/Macro, DC	Mono/Macro, DC
	Granulocyte		Neutro	Neutro, Baso, Eosino, Mast	Neutro, Baso, Eosino, Mast

TABLE 1.2. Mouse FcγRs. Structure, functional outcome, number of amino acids, affinity and specificity for IgG subclasses, and cellular expression profiles are shown. FcγRs are type I glycoproteins with two or three Ig like domains in their ligand binding alpha chain. Activating FcγRs are associated with an accessory signaling molecule, the gamma chain, which obtains an intracellular ITAM (immunoreceptor tyrosine-based activation motif). The inhibitory FcγRIIB signals through an ITIM (immunoreceptor tyrosine-based inhibition motif) in the cytoplasmic domain of the alpha chain. Mono: monocytes. Macro: macrophages, DC: dendritic cells; Neutro: neutrophils, Baso: basophils, Eosino: eosinophils, Mast: mast cells; * expression on subsets, ** IgG2c subclass not tested, ? under debate (adapted from Bruhn et al., 2015; Guillems et al., 2014; Kim et al., 2006)

granulocytes with the exception that the expression level on neutrophils is low. FcγRIII is highly expressed on monocytes / macrophages, DCs, granulocytes, and low amount are present on NK cells (Biburger et al., 2011; Guillems et al., 2014). In contrast, the high affine FcγRI and medium affine FcγRIV have a narrower expression profile. FcγRI is restricted to tissue-resident macrophages and monocyte derived DCs (Mancardi et al., 2013). Negligible to no expression of FcγRI was observed on circulating immune cells (Bruhns et al., 2015). FcγRIV is highly expressed by patrolling monocytes (Ly6C^{low} subset) and to lower amount on tissue-resident macrophages and neutrophils while the expression on DCs is controversial (Biburger et al., 2011; Guillems et al., 2014; Nimmerjahn et al., 2005; Kitamura et al., 2007). Relative expression levels of activating and inhibitory FcγR vary between cell types and set the threshold for cell activation. FcγR expression levels are not static and influenced by inflammation. In general inflammatory cytokines / mediators (e.g. T_H1 cytokines like IFN-γ, complement compound C5a, bacterial LPS) tend to upregulate activating receptors and downregulate the inhibitory receptor and vice versa T_H2 cytokines (e.g. IL-4). Nevertheless, the effect can also be cell type specific. The regulation of FcγRs expression is coupled with the regulation of the IgG subclass switch and exerted by the same cytokines: IFN-γ induces IgG2a (T_H1), TNF-β IgG2b, and IL-4 IgG1 (T_H2) (Coffman et al., 1989; Finkelman et al., 1990; 1.1.3.). Furthermore, the maturation state of the immune cells can affect FcγRs expression level. For example, DC downregulate FcγR expression after

antigen encounter as well as B cells when maturing into plasma cells. The particular Fc γ R expression profiles of DC subsets and their role for T cell activation is discussed by Guillems et al., 2014.

The IgG subclasses possess different affinities for the distinct Fc γ Rs. Their potential to activate effector functions is dictated by the relative affinity of IgGs for activating vs. inhibitory Fc γ Rs, which is also termed activation-to-inhibition (A/I) ratio. The A/I ratio of IgG2a is the highest whereas IgG1 possess a small value of the tested subclasses. This suggests that IgG2a mediated effector functions are less influenced by the inhibitory Fc γ RIIB than IgG1 (Nimmerjahn et al., 2005)

To mention, also Fc γ R expression of non-hematopoietic cells has been detected but the functions are still unclear (reviewed in Anderson et al., 2015). Furthermore, Fc γ RIII expression was detected on $\gamma\delta$ -T cells (Couzi et al., 2012).

1.2.3.3. Signalling of Fc γ Rs

Fc γ R signalling is initiated by their crosslinking via immune complexes. This is a common mode of activation of receptors, which signal through accessory modules e.g. T and B cell receptor. Clustering of Fc γ Rs by immune complexes triggers their relocation to lipid rafts, which are membrane subdomains enriched in signalling molecules. Engagement of activating Fc γ Rs leads to the phosphorylation of the ITAM in the accessory gamma chain by SCR protein kinases followed by the recruitment of SYK protein kinases. The downstream signalling consists of a cascade of kinases mediated phosphorylation reactions. This leads to the activation of transcription factors and consequently gene expression, which determine the cellular responses (Getahun et al., 2015). Co-engagement of the inhibitory Fc γ Rs leads to phosphorylation of the ITIM motive and the recruitment and activation of SHIP kinase, which interferes with the ITAM induced signalling cascade and formation of the immune synapse. Furthermore, the activated SHIP inhibits cell proliferation. Crosslinking of the inhibitory Fc γ RIIB on B cells with or without the BCR balances B cell activation or induces apoptosis, respectively. The induction of apoptosis is independent of the ITIM (1.2.4.4.). The detailed intracellular signalling cascades are not the scope of this work and therefore not described in further details (reviewed by Getahun et al., 2015).

1.2.3.4. Recognition of IgG

Commonly, high and low affine receptors are discriminated. The affinity for monomeric antibodies varies by 2 - 3 logs between the Fc γ Rs (Fc γ RI-IV). Fc γ RI is a high affine receptor which binds monomeric IgG with similar affinity as immune complexes whereas Fc γ RII and Fc γ RIII are low affine receptors. The definition of Fc γ RIV as high or medium affine receptor is still under debate (Bruhns et al., 2015; Guillems et al., 2011; Nimmerjahn et al., 2005 and 2006). Fc γ RIV is herein assigned as medium affine. The high and medium affine Fc γ RI and Fc γ RIV have the narrowest expression profile and specificity for IgG subclasses binding IgG2a and IgG2a / IgG2b respectively. The low affine receptors bind all IgG subclasses except IgG3. The affinity of the IgG2c subclass was not determined yet.

As reminder, Fc γ Rs are only activated by immune complexes and not by monomeric IgG although monomeric IgG does bind to Fc γ Rs (1.1.5.2). Studying the activation of Fc γ Rs, using immune complexes is fundamental. To note, the association constant (K_A), which quantifies the affinity of two interaction partners, is commonly measured by surface plasmon resonance with immobilization of either the Fc γ R or IgG while the other component is applied in solution (e.g. Nimmerjahn et al., 2006). Therefore, the affinity measurements of the Fc γ R-IgG interaction in the absence of the antigen might not reflect the potency of single IgG subclasses for their Fc γ R activation. Nevertheless, the affinity of FcRs to

monomeric antibodies is discussed in the context of IgG subclass dependent FcγR activation capacities (3.2.1.).

FcγRs display a conserved structure and IgG binding mode. The Ig like domains are termed D1 - D3, with D1 at the N terminus. FcγRI is the only receptor with three Ig like domains whereby D1 and D2 are homologue to the domains of the other FcγRs. Mutational analyses and crystal structures for mostly human FcγRs and IgG mapped the binding sites. The D2 domain and the joining loop of the D1 and D2 domains of the FcγRs and the lower hinge region and the upper C_H2 domain of the IgG have been identified as interaction sites, whereby binding orders the lower hinge conformation (Figure 1.4; Sondermann et al., 2000). Therefore, substitution of certain amino acids in the upper C_H2 domain of the human IgG1 leads to enhanced or diminished FcγRs binding (Lund et al., 1992; Shields et al., 2001; Irani et al., 2015). The FcγR D2 domain intercalates into the groove formed by the two heavy chains of the Fc fragment (Figure 1.4). Binding involves non-covalent interaction via salt bridges, hydrogen, and hydrophobic bonds. The high affinity binding of the (human) FcγRI is mediated by additional interactions of the D2 domain with the lower hinge. In this context, the presence of a unique interaction of the FcγRI-D2 domain with the Fc glycan is debated (Lu et al., 2015; Kiyoshi et al., 2015). The additional D3 domain does not interact directly with the IgG molecule but it is important for maintaining the receptor conformation similarly to the D1 region, which also interacts with the D2 domain non-covalently (Gavin et al., 1998). Most of the IgG Fc residues of the contact region are conserved allowing a common mode for the IgG recognition. In addition, individual Fc-FcγRs interactions mediate IgG subclass specificity. A less conserved loop in the D2 domain of the FcγRs contacts different residues in the Fc inducing slightly altered conformations of the lower hinge in the complex with the individual FcγRs (Shields et al., 2001; Lu et al., 2015). Consequently, the length of the hinge and the Fc glycan composition influence the affinity due to conformational restrains (1.2.3.5.). Although the FcγR binds to both heavy chains, the interaction is asymmetric. It induces a small conformational change in the C_H2 domain and breaks the twofold symmetry of the unbound IgG. Therefore, the stoichiometry of FcγR binding to IgG is 1:1. Furthermore, binding induces no significant conformational changes on the FcγR indicating that clustering instead of conformation changes is the primary mode of activation for FcγRs.

Considering other IgG binding proteins, the binding side for the complement factor C1q partially overlaps with the FcγRs binding site, whereas FcRn, TRIM21, and Protein A / G bind at the interface of the C_H2 - C_H3 domain in a 2:1 stoichiometry (Figure 1.4.). Herpesvirus encoded vFcγRs (1.3.4.5.b) bind to regions distinct from the host FcγRs and C1q binding sides. For HSV-1gE/gI and HCMV gp68 the C_H3 - C_H2 interdomain junction has been identified (Sprague et al., 2008) and HCMV gp95 binds to the lower hinge in addition (Mercé Maldonado, 2011). The binding site for MCMV m138 is unknown, but does not overlap with the host FcγRs (Bigl, 2010). Despite similar binding regions, vFcγRs show particular variations in their IgG-binding modes. In contrast to host FcγRs, vFcγR bind also monomeric IgG with high affinity. HCMV gp68 and gp34 bind all human IgG subclasses (Atalay et al., 2002), HSV-1 gE/gI all expect IgG3 (Armour et al., 2002), and HCMV gp95 and RL13 prefer IgG1 and IgG2 (Mercé Maldonado, 2011; Cortese et al., 2012). MCMV m138 binds only mouse IgG2a and IgG2b (IgG2c was not tested; Budt, unpublished data).

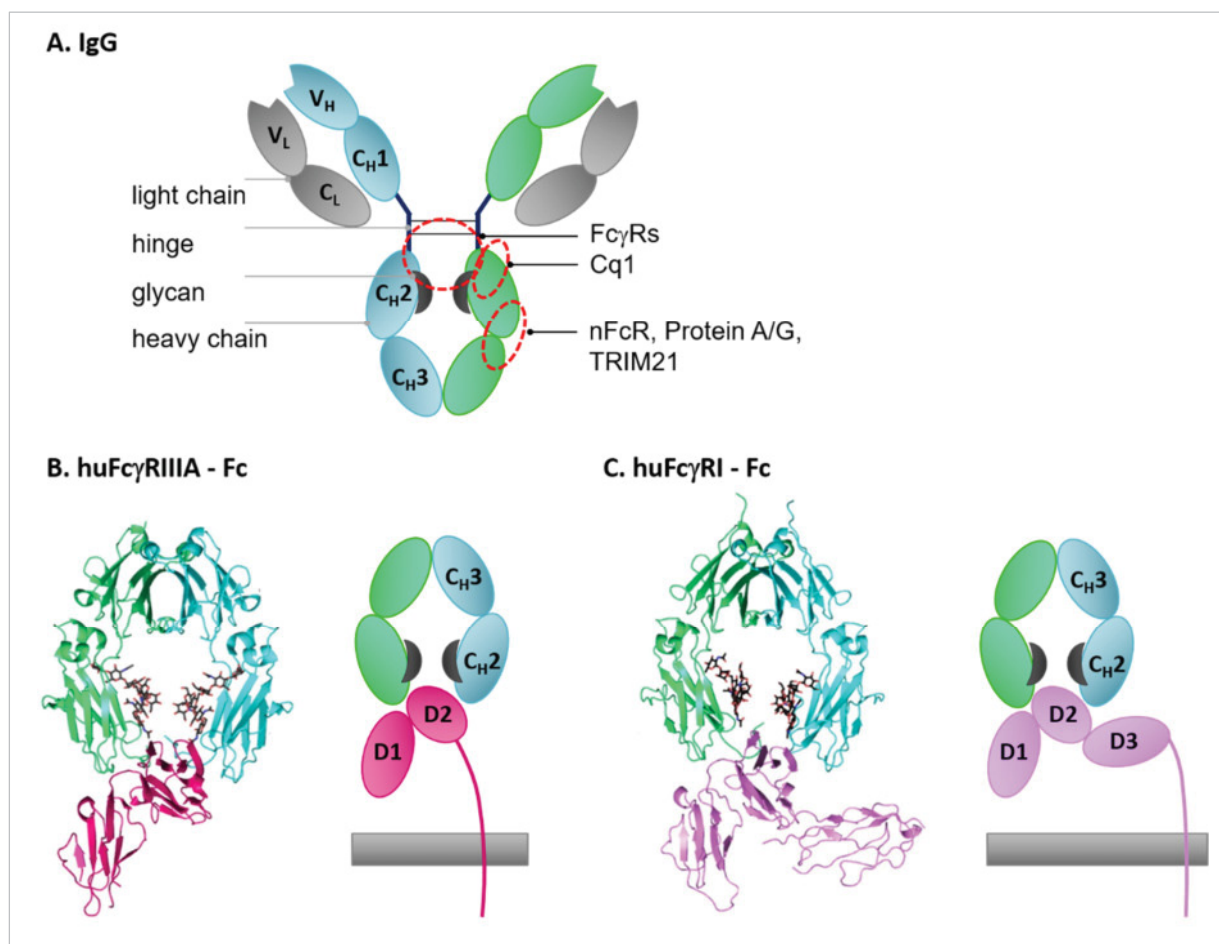


FIGURE 1.4. FcγR – IgG interaction. A. Bindings sites within the IgG molecule for effector proteins. B/C. Ribbon and schematic representations of the extracellular domains of huFcγRIIIA (PDB 3AY4) and huFcγRI (PDB 4X4M) in complex with IgG Fc. The two IgG heavy chains are shown in turquoise and green, the light chains in grey, and the glycan associated with Asn-297 in dark grey. Glycosylation of the FcγRs is not displayed. Modified from Hanson et al., 2015 and Irani et al., 2015.

1.2.3.5. Influence of the Fc glycosylation for the recognition of IgG by FcγRs

IgGs contain only one highly conserved N glycosylation site at Asparagine 297, which is located at the upper C_{H2} and beneath the hinge region. The C_{H2} and C_{H3} form a horseshoe structure with the glycan in the middle thus contributing to the conformation of the Fc domain. The glycan is added posttranslational in the endoplasmic reticulum and it is modified in the Golgi. In general, glycans are located at exposed position on the protein surface. In contrast, the Fc glycan is hidden between the C_{H2} domains resulting a limited access and incomplete modification by the Golgi resident glycosyltransferases (Raymond et al., 2012). Consequently, IgGs commonly possess different glycans at both heavy chains of one molecule and thus Fc glycans are very heterogeneous. Uniquely, the Fc glycan interacts non-covalently with certain amino acids of the C_{H2} domain leading to a partially restricted flexibility of the glycan (Raymond et al., 2012). Thus, the amino acid sequence of the hinge and C_{H2} domain aka the IgG subclass can influence the glycan composition (Jassal et al., 2000; Baudino et al., 2008; Wuhler et al., 2007; Keusch et al., 1996). Moreover, the Fc glycans maintain the quaternary structure and the thermodynamic stability of the Fc domain (Arnold et al., 2007; Huang et al., 2015).

The glycan consists of a conserved core of a bi-antennary heptasaccharide ($GlcNAc_2Man_3GlcNAc_2$; Man = Mannose; GlcNAc = N-Acetylglucosamine) and the heterogeneity arises by variable addition of core fucose, galactose, and terminal sialic acid (Figure 1.2.). In humans, a bisecting GlcNAc can be present. Furthermore, the terminal sialic acid can be linked at two different positions at the galactose. Over 30

different glycan forms have been identified in human sera (Arnold et al., 2007; Wormald et al., 1997). Differences in glycan composition affect the affinity for FcγRs (see below). Its influence on the local C_H2 domain conformation, on the overall C_H2 orientation, and on the motion due to the glycan flexibility are discussed as cause (Subedi et al., 2015; Dalziel et al., 2014.). Whereby restricted glycan flexibility and motion of the C_H2 domain correlates with increasing affinity (Subedi et al., 2014; Huang et al., 2015). IgG deglycosylation reduced drastically or even abolished the binding to FcγRs (Lux et al., 2013).

The human antibody glycan profile and its consequences for antibody effector functions was analysed in a number of studies (reviewed in Böhm et al., 2014). In healthy humans, most IgGs obtain a core fucose, half one terminal galactose (G1) and about one quarter none (G0) or two (G2) terminal galactose whereby ratios of G0 and G2 vary. Bisecting GlcNAc is present in less than one fifth and terminal sialic acid in more than one fifth of molecules (Pucić et al., 2011; Raju et al., 2000).

The glycan composition is also species and cell-specific because the expression of glycosyltransferases varies (Raju et al., 2000). The bisecting GlcNAc is absent in mouse and CHO derived mAbs (Raju et al., 2000; Arnold et al., 2007). Core fucose is common (> 90%) in contrast to sialylation for natural antibodies and recombinant mAbs produced in CHO, HEK293T or murine myeloma cell lines (Raju et al., 2000 and 2012; Mimura et al., 2016). The level of terminal galactosylation is also different dependent on the species or cell line. The predominant form of mouse IgG is G0 and G1, of human IgG it is G1, and for CHO cell derived mAbs G0 (Ye et al., 2009; Nallet et al., 2012, van Berkel et al., 2009, Raju et al., 2000; Pucic et al., 2011; Raju et al., 2012). In addition, the type of saccharide attached can differ between species. The type of sialic acids in human and CHO is NANA (N-acetylneuraminic acid) and in mice it is NGNA (N-glycolylneuraminic acid) (Raju et al., 2000). Despite the related type of saccharide, also the attachment can be dissimilar. Sialic acid can be linked either with α2,3 or α2,6 linkage to the terminal galactose (Raymond et al., 2012) and it differs which branch preferentially carries the terminal galactose in monogalactosylated IgGs (G1) (Raju et al., 2000).

The absence of the core fucose strongly increased the affinity of human IgG to FcγRIIIA and consequently the magnitude of ADCC independent of the IgG subclass and FcγRIIIA polymorphism (Thomann et al., 2016; Shinkawa et al., 2003; Niva et al., 2005; Veomett et al., 2014). Unique glycan-glycan interactions of the IgG and the human FcγRIIIA mediate the high affinity binding in the absence of the core fucose. But only human FcγRIIIA and its mouse orthologue FcγRV but no other FcγRs possess this glycan (Ferrara et al., 2011). The affinity of IgG to the other FcγRs was affected less by the lacking fucose (Shields et al., 2002; Chung et al., 2012; Veomett et al., 2014). In contrast to human IgG subclasses, fucose has a divergent influence on the affinity of the mouse IgG subclasses to mouse FcγRs (Nimmerjahn et al., 2005). Terminal sialic acids exerted anti-inflammatory activities in most studies. A reduced affinity for the classical FcγRs and increased binding to the anti-inflammatory C-type lectin receptor SIGNR1 (human homologue: DC-SIGN) was proposed as mechanism, which has been recently challenged. For example, sialylation was associated with decreased affinity for human FcγRIIIA and consequently reduced ADCC (Scallon et al., 2006) but also no altered or even slightly improved FcγR affinity was found (Thomann et al., 2015). Similarly, data for the effect of terminal galactose are non-conclusive so far (Shinkawa et al., 2003; Thomann et al., 2016; Nimmerjahn et al., 2007).

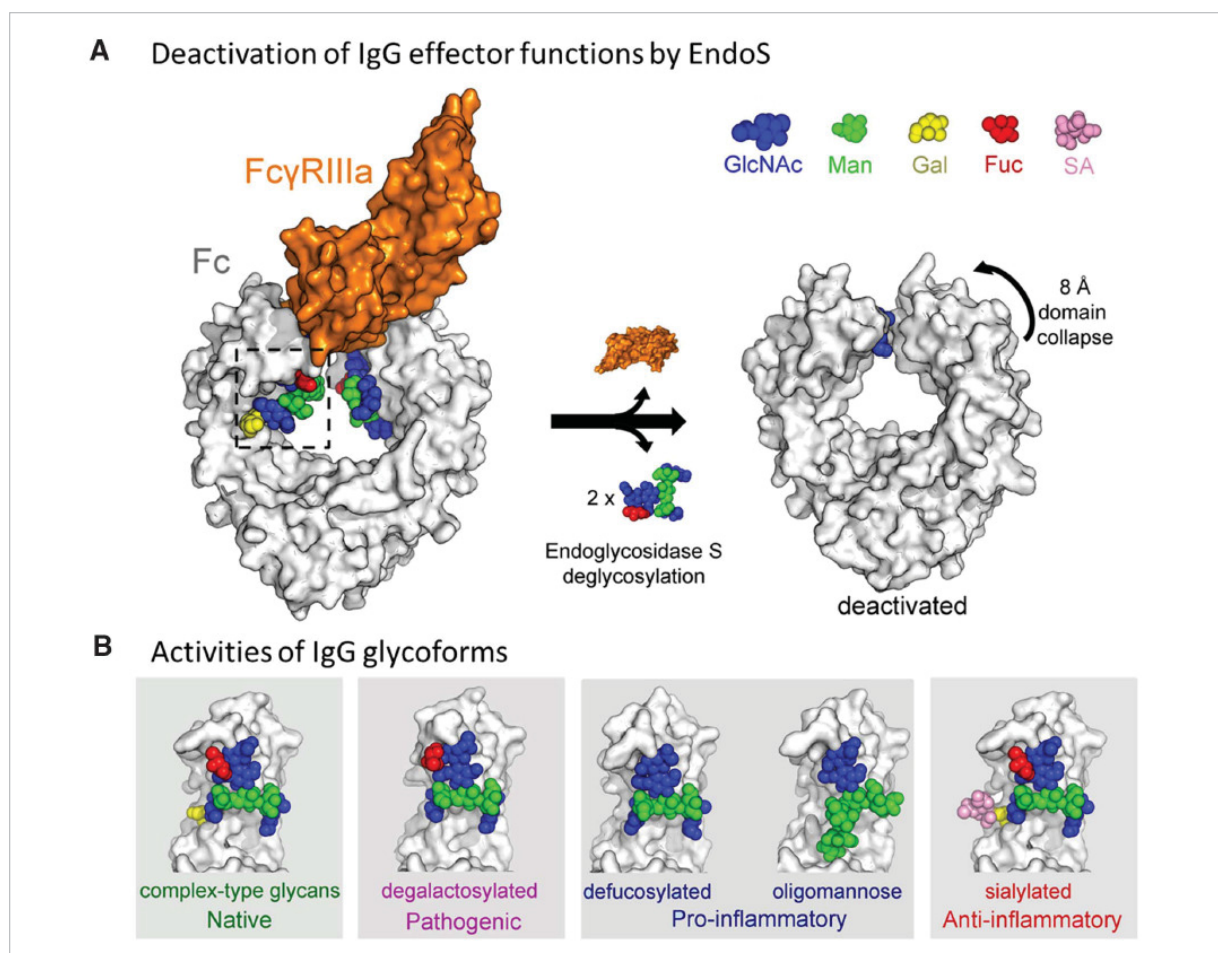


FIGURE 1.5. Fc glycoforms. A. Structure of the Fc - human FcγRIIIA complex and that of the deglycosylated Fc after cleavage by EndoS. B. Crystal structures of different glycoforms associated with various immune responses. Oligomannose-type glycans are generated in the ER and commonly further processed to the complex glycan forms in the Golgi. Only a very small to neglectable proportion of IgGs possess oligomannose-type glycans. From Dalziel et al., 2014.

Moreover, alterations of the glycosylation profile have been found with age, pregnancy, and several inflammatory diseases (Nimmerjahn et al., 2011). For example, a higher percentage of non-galactosylated IgGs (G0) is present in rheumatic arthritis and it is correlating with disease activity (Axford, 1999). The modification of the glycan can turn an antibody in the pro- or anti-inflammatory direction and represents a switch, which is fine-tuned by the immune system whereby deregulation can be associated with disease (Collin et al., 2013; Oefner et al., 2012; Ackerman et al., 2013). In addition, the Fc glycan affects the binding affinity of the complement compound C1q by but not the FcRn-dependent half-life of an IgG molecule. In addition, some C-type lectin receptors (e.g. Dectin-1, SIGNR1 / DC-SIGN, MR, MBL) bind preferentially to certain Fc glycan forms and might act in concert with FcγRs and complement (Collin et al., 2013).

In summary, the affinity of an IgG to FcγRs is determined by its subclass, i.e. amino acid sequence, and it is modified by the N-glycan composition located in the C_H2 domain. Therefore, the choice of the expression system is crucial for the production of recombinant IgGs for therapy (3.2.5.).

1.2.4. FcγR effector mechanisms

FcγR engagement regulates the activation of diverse immune cells and mediates important effector functions against intracellular pathogens like viruses, especially during reinfection. They are

dependent on the type of the effector cell, their FcγR expression profile, and nature of the immune complex concerning IgG subclasses, glycosylation, and size. Effector functions can be direct e.g. pathogen killing or indirect by modulating the immune response, e.g. T cell priming. Typical effector functions are listed below and are summarized in Figure 1.6.

- degranulation and cytotoxicity (ADCC: antibody dependent cytotoxicity)
- secretion of cytokines, proinflammatory mediators, and reactive oxygen species (ROS)
- antigen internalization by receptor mediated endocytosis or phagocytosis (ADCP: antibody dependent phagocytosis)
 - enhance killing of intracellular pathogen and oxidative burst
 - antigen processing, (cross-)presentation, cell maturation of APCs lead to rapid and effective T cell activation
- regulation of B cell activation, antibody production, and plasma cell survival

1.2.4.1. Antibody dependent cytotoxicity (ADCC)

ADCC defines the granule dependent pathogen killing or cytolysis upon IgG-mediated activation of FcγR bearing effector cells. Effector cells are NK cells, monocytes / macrophages, and granulocytes (neutrophils, basophils, eosinophils). FcγR engagement leads to the polarization of the cell mediating extensive cell-to-cell contact between effector and target and the release of the preformed granules containing cytolytic substances in the direction of the target cell. Pores are formed in the target cell membrane by perforin and apoptosis is induced by proteolytic enzymes called granzymes (Kenneth, 2012). Reactive oxygen species and intermediates (ROS / ROI) might be also released. The magnitude of ADCC (potency of killing) is dependent on the type of effector cell, number and type of FcγRs cross-linked, and the target cell type.

1.2.4.2. Antibody dependent phagocytosis

Phagocytic cells are monocytes, macrophages, DCs, and granulocytes. Phagocytosis is the active uptake and endocytosis of particles larger than 0,5 μm into a cell (Aderem et al., 1999). The magnitude of FcγR engagement by opsonizing IgG determines signalling and if the threshold for phagocytosis is reached. In addition to the particle uptake, oxidative burst occurs in contrast to complement mediated phagocytosis (Caron et al., 1998). The phagosome matures into phagolysosome by recruitment and fusion with lysosomes in which the engulfed particle is enzymatically degraded. Functional consequences of the antibody dependent phagocytosis are governed by the cell type: macrophages are specialized in immune complex degradation whereas DC do not perform oxidative burst but are specialized in antigen presentation (1.2.4.3).

1.2.4.3. Modulation of the T cell response

Antigen uptake by FcγR mediated endocytosis or phagocytosis by DCs lead to a stronger adaptive immune response. Antigens are processed rapidly and (cross-)presented on MHC I and MHC II (Regnault et al., 1999). DC maturation induces expression of costimulatory signals resulting in efficient priming of CD4 and CD8 T cells. Furthermore, the memory T cell response is enhanced. Co-stimulatory signals are cell surface receptors and cytokines. FcγRs engagement induced cytokine secretion by other innate immune cells shape the adaptive response as well. In contrast, antigen uptake via pinocytosis or non-receptor mediated endocytosis leads to a slow and low T cell response. Importantly, by regulation of DC activity, FcγRs control if an immunogenic or tolerogenic T cell response is initiated. Thereby, FcγR mediated modulation of antigen uptake, processing, and

presentation by DC, antibodies have a key role in regulation (e.g. polarization) of T cell responses against intracellular pathogens (Regnault et al., 1999; Igiertseme et al., 2004). Even by passively administered mAbs in a tumor therapy model, induction of a long-term T cell response by the engagement of FcγRs on APCs besides direct tumor cell killing by ADCC was evident (DiLillo et al., 2015). Furthermore, it was suggested, that FcγR mediated uptake also changes the presented peptide repertoire (Amigorena et al, 1998).

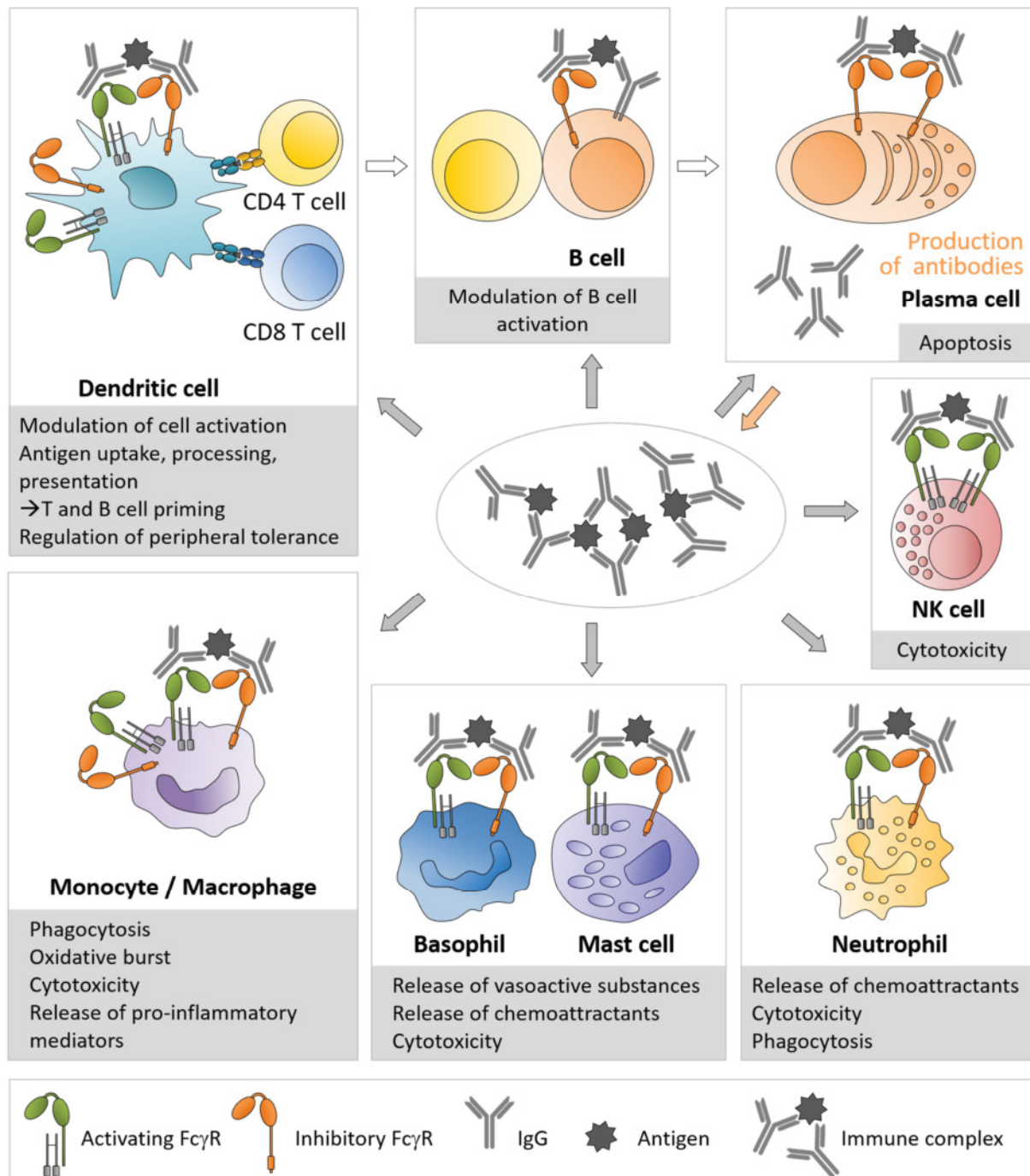


FIGURE 1.6. Effector functions of FcγRs. Immune complexes bind to activating and inhibitory FcγRs expressed on diverse immune cells. Triggered effector functions are indicated in the grey boxes. Immune complexes with a soluble antigen are shown as simplification, but some effector function require effector-target cell (opsonized infected cell or pathogen) contact e.g. cytotoxicity (ADCC). Adapted from Nimmerjahn et al., 2008.

1.2.4.4. Modulation of the immune response by the inhibitory FcγRIIB

FcγRIIB is the only inhibitory FcγR and has a broad expression profile and IgG subclass specificity. Co-engagement with activating FcγRs and other receptors like PRR (e.g. TLR4) modulate the activation threshold of the immune cells. Thereby, FcγRIIB has important roles in balancing the immune response to maintain tolerance and prevent immunopathology. In this line, FcγRIIB deficient mice show elevated immune complex mediated inflammation, phagocytosis, and clearance of pathogens (Nimmerjahn et al., 2006; Takai, 2002). Uncontrolled B cell activation leads to low affinity polyreactive and consequently autoreactive antibodies. As a result, certain mouse strains develop lupus like autoimmune diseases and glomerulonephritis (Tiller et al., 2010).

B cells only express the inhibitory FcγRIIB, which regulates activating signals transduced by the BCR if crosslinked by immune complexes. In particular, B cells express exclusively the FcγRIIB-1 form, a splice variant, which exhibits a modified intracellular domain resulting in a low capacity for endocytosis in contrast to the FcγRIIB-2 form expressed by the other cell types. Besides the ITIM dependent interference with activating signalling cascades, BCR clustering is prevented by an ITIM independent mechanism (Liu et al., 2010). Thereby antibody production and B cell proliferation are inhibited. By FcγRIIB crosslinking without BCR engagement, apoptosis is induced via an ITIM independent pathway. Thereby B cells that lost their antigen specificity due to somatic hypermutation are eliminated. Similarly, the elimination of long-lived plasma cells, which are different from B memory cells and express low to no level of BCR and high level of FcγRIIB, can be achieved. Therefore, FcγRIIB has a central role in regulating antibody responses (after class switch to IgG): it facilitates the production of high affinity IgG antibodies and it maintains peripheral tolerance (Xiang et al., 2007; Ono et al., 1997). Lack of FcγRIIB on DCs enhances antigen specific T cell responses but it also promotes unspecific cell activation by immune complexes normally present in the serum. Since DCs also inactivate autoreactive T cells, FcγRIIB is an important regulator of DC activation and involved in maintaining peripheral T cell tolerance (Nimmerjahn et al., 2006 and 2008).

1.2.4.5. FcγR-deficient mice reveal importance of FcγRs for protection against infection, in inflammation, and in autoimmunity

Several FcγR-deficient mouse strains exist including single gene knockout strains lacking one particular FcγR due to the deletion of the FcγR alpha chain (FcγRI-KO, FcγRIIB-KO, FcγRIII-KO, FcγRIV-KO), mice lacking the expression of all activating FcγRs due to the deletion of the FcRγ chain (FcεR1γ-KO / FcRγ-KO), and combination of these.

The FcRγ-KO mouse is a common model to study the role of activating FcγRs in inflammation / autoimmune diseases, infections, and antibody based therapies because the deletion of the gamma chain abolishes their surface expression; e.g. influenza (Lee et al., 2014; El Bakkouri et al., 2011; Huber et al., 2001), LCMV (Straub et al., 2013), *Brugia malayi* (Gray et al., 2002), *Plasmodium berghei* (Yoneto et al., 2001), anti-CD20 antibody therapy (Hamaguchi et al., 2006), and type II/III hypersensitivity responses (Ji et al., 2002; Wipke et al. 2004; Sylvestre et al., 1994; Clynes et al., 1995). It was demonstrated that these mice have significant defects in antibody mediated effector cell responses like phagocytosis, ADCC, antigen presentation by DCs, and inflammatory responses (Takai et al., 1994 and 1996; Regnault et al., 1999). To note, Barnes et al, 2002 reported that FcRγ-KO mice exhibit a residual FcγRI expression on macrophages with impaired function due to the lack of the FcRγ.

Interpreting the result in the FcγR-KO model, it has to be taken in account that also other receptors rely on the gamma chain as signalling adaptor and are absent in these mice like the high affinity receptor FcεRI for IgE (Takai et al., 2005), the activating NK cell receptor NKp46 (Moretta et al., 2001), and Mincle (macrophage inducible Ca²⁺-dependent C-type lectin; Yamasaki et al., 2008). To dissect the impact of the individual FcγR, the single KO mice are utilized: FcγRIV-KO mice (Nimmerjahn et al., 2005), FcγRIIB (Takai et al., 1996), FcγRIII-KO (Hazenbos et al., 1996), and FcγRI-KO (Barnes et al., 2002; Ioan-Facsinay et al., 2002). Deletion of the only inhibitory FcγRIIB, allows to study its role in the modulation of immune responses (1.2.4.4.).

1.2.5. Importance of FcγRs in the control of viral infections

The role for IgG in the protection from infectious diseases is demonstrated by the increased susceptibility of patients with deficiencies in the antibody response. In addition, FcγR polymorphisms lead to higher susceptibility or more severe courses for certain viral (e.g. influenza, SARS, EBV, HIV) and bacterial infections (Li et al., 2014; Nimmerjahn et al., 2008).

For influenza and HIV / SIV, several studies emphasize the role of FcγRs for their protection or reduced viral load. Mice deficient in the gamma chain and therefore lacking all activating FcγRs are more susceptible to influenza infection (Huber et al., 2001). Furthermore, non-neutralizing antibodies directed against M2 contribute to virus control in wild type but not FcγR deficient mice (Lee et al., 2014). It was suggested that anti-influenza virus antibodies are dependent on FcγRs for their protective effect *in vivo* as demonstrated for broadly neutralizing and non-neutralizing mAb against HA (hemagglutinin) and NA (neuraminidase) (DiLillo et al., 2014 and 2016). Also for HIV / SIV evidences from natural infection, vaccination, and passive antibody transfer experiments with recombinant mAb variants indicate a critical role for FcγRs and non-neutralizing antibodies (Hessell et al., 2007; Boesch et al., 2013; Forthal et al., 2013; Nimmerjahn et al., 2015; Bournazos et al., 2014 and 2015). In addition, mice are protected by transfer of poorly neutralizing antibodies against West Nile virus in a FcγR dependent manner (Vogt et al., 2011).

Of note, FcγR are not only involved in the protection from disease but can promote susceptibility. Antibodies can mediate enhanced virus uptake by FcγRs bearing cells like macrophages in the presence of non-neutralizing or suboptimal concentrations of neutralizing antibodies. This has been reported for some pathogens e.g. dengue virus, HIV, RSV, and *Leishmania major* (Nimmerjahn et al., 2011).

1.3. Cytomegalovirus

1.3.1. Burden of Cytomegalovirus infection

Cytomegalovirus (CMV) infection persists lifelong with alternating phases of latency and reactivation. During reactivation lytic virus replication leads to the production of infectious virus particles. While infection or reactivation in immunocompetent individuals is mostly asymptomatic, it leads to high morbidity and mortality in immunodeficient persons (organ transplant recipients, AIDS patients). CMV represents one of the most important pathogens in organ transplantation. The most frequent symptoms are retinitis, interstitial pneumonia, colitis, hepatitis, and encephalitis (Mocarski et al., 2013). Furthermore, congenital transmission during pregnancy is the second most common cause for

disabilities like hearing loss, mental retardation, and movement impairments (Schleiss, 2013). Therefore, development of a vaccine against congenital CMV infection is a major public health priority.

1.3.2. Transmission and epidemiology of HCMV

HCMV is broadly distributed with a seroprevalence ranging from 50 - 60% in North America and Europe to over 90% in developing countries. CMV infects ductal epithelial cells in secretory organs, which lead to its spread by body fluids and initial infection of mucosal surfaces. Horizontal transmission is mediated by the contact of urine and saliva from young children and occurs also sexually among adults. Primary infection is mostly asymptomatic. Young children shed virus over a long period despite being healthy and thus infection during early childhood is common (Adler, 1991). Another rare mode of infection is the receipt of blood cells or organs from seropositive donors. CMV is classified as opportunistic infection because reactivation is facilitated in immunocompromised individuals.

Vertical transmissions from mother to child can occur intrauterine (congenital), during childbirth or by breast-feeding (perinatal). Primary infection of women during pregnancy leads in 30 – 45% of cases to transmission and reactivation or reinfection with another strains to approx. 1 - 5% (Kenneson et al., 2007). Reinfections result in three quarters of congenital infections in the USA (Wang et al., 2011; Yamamoto et al., 2010). Furthermore, transmission rate and effects on the fetus are dependent on the gestation age. Intrauterine transmission results in infection of 0,2 - 5% of all newborns (Kenneson et al., 2007; Manicklal et al., 2013). About one tenth of these are symptomatic at birth. CMV infection may cause severe long-term sequelae, including progressive sensorineural hearing loss and developmental delay in 40-50% and in 7-15% of symptomatic and initially asymptomatic infected newborns respectively (Naing et al., 2016).

Reactivation during lactation (>95%) and transmission (40%) is frequent but perinatal transmission is not associated with morbidity (Hamprecht et al., 1998) except for premature born infants with underweight (Kurath et al., 2010). Breast-feeding has a major influence on the epidemiology (Boppana et al., 2007) and seroprevalence of HCMV in the population.

1.3.3. Herpesviruses

Herpesviruses are highly prevalent. Their name is derived from the Greek word for creeping and refers to the latent and recurring infections, which are typical for the persisting herpes viruses. They share following characteristics:

1. The common structure is composed of a large, linear dsDNA genome (124–295 kb) within an icosahedral capsid, which is surrounded, by the so-called tegument and a membrane (envelope). The tegument contains viral proteins and miRNAs which function immediately after entry of the virus (pre-immediate early). The virions are about 120-260 nm in size.
2. Virus gene transcription, synthesis of viral DNA, and capsid assembly occurs in the nucleus.
3. Large array of enzymes involved in DNA replication and protein processing
4. They establish life-long persistent infections with phases of latency (non-productive infection) and reactivation (productive infection)
5. Lytic replication

The herpesviruses encompasses three families (Pellett et al., 2013): Herpesviridae (mammals, birds, reptiles), Alloherpesviridae (fish, amphibians), and Malacoherpesviridae (bivalves). The Herpesviridae is further subdivided into the alpha-, beta-, and gammaherpesvirus subfamilies based on genetic and biological properties. For example, alphaherpesviruses display a relatively short reproductive cycle and establish latent infections primarily in sensory ganglia. Betaherpesviruses, of which CMV is a member, have a restricted host range, a long reproduction cycle, and infect a broad range of cells e.g. differentiated hematopoietic, epithelial, and endothelial cells. Gammaherpesviruses are characterized by a narrow host range and establish latency in B or T cells. For human nine herpesviruses have been identified so far (Alphaherpesviruses: herpes simplex virus 1 (HSV-1), herpes simplex virus 2 (HSV-2), varicella zoster virus (VZV); Betaherpesviruses: human cytomegalovirus (HCMV), Human herpesviruses 6A/6B (HHV-6A, HHV-6B), Human herpesviruses 7 (HHV-7); Gammaherpesviruses: Epstein-Barr virus (EBV), Kaposi's sarcoma-associated herpesvirus (HHV-8))

1.3.4. Cytomegalovirus structure, replication cycle, and immune response

1.3.4.1. CMV structure and replication cycle

The genome of HCMV (HHV-5) contains about 235 kb and about 750 translational products have been identified (Stern-Ginossar et al., 2012). The virus replication is strictly regulated with phases of immediately early (IE), early (E), and late (L) gene expression. Furthermore, the virus encodes numerous immune evasion mechanisms facilitating the escape from immune responses and the establishment of latency. Immune evasive strategies are for example modulation of peptide presentation to minimize T cell responses, inhibiting of NK cell activation, and the interference with the IgG effector functions by expressing viral FcγRs (see 1.4.3.4.c).

CMV infects the cell by different mechanisms involving receptor mediated endocytosis or fusion of the viral envelope with the plasma membrane of the host cell. Several viral proteins are involved for virus entry but the required components are dependent on the cell type. The viral genome is present as episome in the nucleus and is replicated by the rolling cycle mechanism. The capsid is assembled at the nuclear membrane and first buds into the perinuclear space (first envelopment). Then the capsid is released into the cytoplasm where it associates with the viral tegument and buds a second time within a special compartment composed of endoplasmic reticulum, Golgi and organelle membranes (viral assembly compartment, secondary envelopment) (Mocarski et al., 2013). The virions are secreted from the cell by exocytosis (Mettenleiter, 2002). Viral glycoproteins are present on the surface of the infected cells. Infected cells frequently become enlarged (cytomegalia, see Figure 1.7.).

1.3.4.2. Mouse Model of CMV: MCMV

CMV is absolutely species specific and the pathogenesis can only be studied in the natural host. The mouse CMV (MCMV) is a common model for the CMV pathogenesis of the mouse (*mus musculus*). Most MCMV structural proteins are homologs to HCMV (Rawlinson et al., 1996; Hudson, 1979). MCMV modulates the host immunity and inflammation similarly as HCMV but different viral genes might be employed. Furthermore, the MCMV model reproduces with reasonable accuracy the antiviral immune response observed in humans to HCMV infection. An advantage of the mouse model is the presence of various transgenic mouse strains allowing to investigate the impact of different immune components (e.g. receptors, cytokines) or cell types for the control of the virus, e.g. FcγR deficient mouse strains.

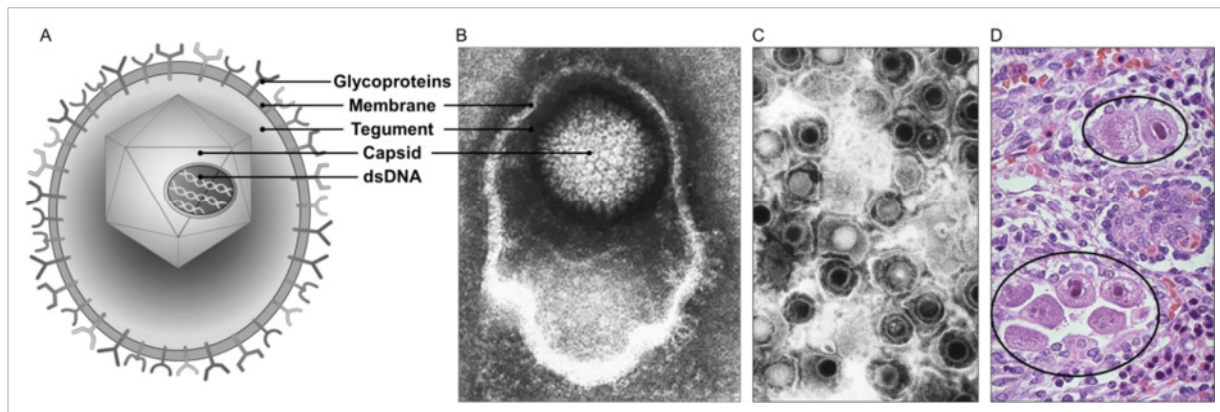


FIGURE 1.7. Cytomegalovirus structure, virion, and infected cells. A. Schematic representation of a CMV virion. B/C. Electron microscopy pictures of herpesvirus virion(s). D. CMV infected cells (circles) in the renal tubular epithelium after congenital infection display a typical enlargement of nucleus and consequently the whole cell (cytomegalia). Sources: B. Linda Stannard, of the Department of Medical Microbiology, University of Cape Town. C. Centers for Disease Control and Prevention, part of the United States Department of Health and Human Services. D. The Internet Pathology Laboratory for Medical Education / The University of Utah Eccles Health Sciences Library.

1.3.4.3. Cell tropism of CMV

Cell and consequently tissue tropism for CMV is broad despite its specific species tropism (Hsu et al., 2009). Target cells for infection are various epithelial cell types (e.g. hepatocytes), endothelial cells, fibroblast, smooth muscle cells, astrocytes, neurons, and myeloid cells (e.g. monocytes / macrophages, dendritic cells, neutrophils) (Grundy et al., 1998). Lymphocytes are not infected. Hepatocytes and vascular endothelial cells are the primary and productive targets (Sacher et al., 2008). Although the myeloid lineage is a common target for infection, certain subtypes are not permissive e.g. cDCs and patrolling (“non-classical”) monocytes / macrophages are MCMV permissive in contrast to pDCs and inflammatory (“classical”) monocytes / macrophages (Alexandre et al., 2014). The predominant target cells types and their contribution to productive infection might also be dependent on the specific tissue. For example, hepatocytes are primary targets but MCMV progeny was only disseminated to liver endothelial cells but not distant organs (Sacher et al., 2008 and 2012). CMV engages myeloid cells for its dissemination in the host during acute infection (Daley-Bauer et al., 2014). Infection of ductal epithelial cells in secretory glands (e.g. salivary gland acinar cells, kidney tubular epithelial cells) leads to transmission via body fluids. Latent CMV genomes have been found in tissue and bone marrow resident myeloid (progenitor) cells. But there, latency might be transient and endothelial cells are proposed as site for long-lasting latency as it was shown for liver and spleen endothelial sinusoidal cell in the MCMV model (Seckert et al., 2013; Koffron et al., 1998). For HCMV, marrow-derived myeloid lineage progenitor cells are the reservoir for latency (Hahn et al., 1998). Due to the tropism of HCMV to certain cell of the central nerve system, encephalitis and progressive hearing loss or retinitis is common after congenital transmission and in AIDS patients, respectively (Cheeran et al., 2009; Maschke et al., 2002).

1.3.4.4 Replication of MCMV *in vivo*

Spread of systemic MCMV infection is proposed to occur in two phases: primary and secondary viremia. First, replication takes place in parenchymal (e.g. hepatocytes) and vascular endothelial cells at primary infection sites (Hsu et al., 2009; Sacher et al., 2008 and 2012). Second, the amplified virus is disseminated (5 - 6 dpi) via the blood stream to distal organs (Daley-Bauer et al., 2014; Collins et al., 1994). Therefore, patrolling macrophages are recruited to the initial sites and hijacked (Sacher et al., 2008; Daley-Bauer et al., 2014; Stoddart et al., 1994). In addition, infected endothelial cells, which

detach and circulate in the blood stream, contribute to systemic MCMV spread (Sacher et al., 2008; Gerna et al., 2004). The relative contribution of endothelial cells to productive infection and total virus load depends on the organ (Sacher et al., 2008). The bulk of progeny in lungs is derived from endothelial cells during the first three days, a lower amount in spleen and kidney and the lowest in liver, where the bulk progeny is produced by hepatocytes (Sacher et al., 2008 and 2012). Furthermore, progeny virus from liver does not contribute significantly to systemic spread (Sacher et al., 2008). Thus, virus productivity and dissemination from an organ is not necessarily related (Sacher et al., 2008).

Administration of MCMV via the intraperitoneal route leads to the infection of mediastinal lymph nodes (macrophages subset), spleen (reticular fibroblasts), and liver (hepatocytes) by cell free virus within the first hours (Hsu et al., 2009). In spleen and liver, viral loads peak at three dpi before immune control limits further replication (Sacher et al., 2008). In other organs like kidneys, lung, heart, or intestines (Hsu et al., 2009), no virus replication was detectable up to 2 dpi and virus loads were reported to reach maximum at 5 – 7 dpi (Collins 1994, Hsu et al., 2009, Stoddart et al., 1994). The salivary glands (SG) are also infected during secondary viremia. The first and productively infected cell type is the acinar glandular epithelial cell (AGECs). Only a low number of acinar epithelial cells are responsible for the virus load in the SG (Jonic et al., 1989). Viral titers increased drastically from 7 to 14 dpi (Daley-Bauer et al., 2014) and peak between 14 and 21 dpi (Stoddart et al., 1996; Manning et al., 1992; Saederup et al., 1999; Henson et al., 1972). The salivary gland is a privileged site for MCMV immune control allowing persistence due to its less stringent immune surveillance (1.3.4.5.). Thus, CMV established a prolonged replication and shedding in this organ for several weeks (Manning et al., 1992) allowing transmission of the virus.

1.3.4.5. Immune response and evasion

a) Immune response to MCMV

CMV is equipped with various immune evasive strategies. Nevertheless, the immune response is crucial for the termination of the productive infection and the maintenance of the virus in a latent state. In case of insufficient immune control, the virus can reactivate and leads to massive replication, which can be eventually lethal. Due to the long coevolution of virus and host, numerous defence and immune evasive strategies developed on both sides and multiple and partially redundant immune effector functions of the innate and adaptive immune system participate in the immune control of CMV. NK cells and interferons exert the immediate control. Infected myeloid cells are responsible for the dissemination of MCMV. Additionally, NK and myeloid cells modulate the antiviral T cell response. T cells are responsible to terminate the productive infection. Virus specific antibodies reduce the viral load and limit reactivation (Klenovsek et al., 2007; Polić et al., 1998; Jonjić et al., 1994).

In detail: MCMV is first sensed by DCs and macrophages resulting in the secretion of chemokines and cytokines including IFN type I. NK cells secrete diverse cytokines (e.g. IFN- γ , TNF- α) and lyse infected cells. Myeloid cells are recruited to the site of infection by CMV encoded cytokines (e.g. MCK2) and are exploited for virus dissemination. In contrast to patrolling monocytes, inflammatory monocytes are not permissive for infection and thus dispensable for dissemination. Nevertheless, they cooperate in shaping the immune response. DCs and NK cells play a role in induction and regulation of subsequent adaptive immune responses (Robbins et al., 2007; Mitrović et al., 2012). Furthermore, $\gamma\delta$ T

cells contribute in the early phase of MCMV immune control and protect immunocompromised mice from lethal MCMV infection comparable to $\alpha\beta$ T cells (CD8 and CD4 T cells) (Khairallah et al, 2015; Sell et al., 2015).

T cells are required for the resolution of the productive infection. CD8 T cell lyse infected cells and produce IFN- γ . CD4 T cells exert multiple effector functions. They are of T_H1 phenotype (Walton et al., 2008), produce cytokines e.g. IFN- γ (Arens et al., 2008), and are essential for the antibody response (Jonjić et al., 1989). Also cytotoxic activity has been noticed (Verma et al., 2015). In the SG, CD4 T cells are crucial for the resolution MCMV infection via IFN- γ (Lucin et al., 1992) and TNF- α (Pavic et al., 1993) which initiated antiviral signalling in non-hematopoietic cells like AGECS (Lucin et al., 1992, Walton et al., 2011). Local APC are deficient in cross presentation and infiltration of cDCs is rare consequently hampering the CD8 T cell response (Walton et al., 2011; Jonjić et al., 1990; Pavić et al., 1993; Thom et al., 2014). In addition, infected AGECS are hidden from CD8 T cells by remarkably efficient downregulation of MHC I by the virus (Lu et al., 2006). Salivary gland resident NK cells seem to be phenotypically distinct (Tessmer et al., 2011; Cortez et al., 2014) and were reported to contribute to MCMV immune control in the SG (Polić et al, 1998). Another unique characteristic of CMV is the expansion of a specific population of memory CD8 T cells (memory inflation) specific for a small variety of viral epitopes (Karrer et al., 2003).

The MCMV specific antibody response begins with the production of IgM followed by class switch to IgG (Lawson et al., 1988). Predominant subclasses are IgG2a in BALB/c and IgG2b/IgG2c in C57BL/6 mice. Virus specific IgGs inflate during persistent infection without altering antibody avidity (Welten et al., 2016; Androsiac, 2012). Neutralizing antibodies are detected late in rather low concentration (Hangartner et al., 2006; Manischewitz et al., 1979). In addition, a hyperimmunoglobulinemia, elevated antigen unspecific IgG antibodies, (Androsiac, 2012) and consequently autoantibodies are induced (Bartholomaeus et al., 1988). Concerning the antigen specificity of the IgG response elicited by CMV, mostly neutralizing antibodies were investigated. Boosting with UV inactivated virus after MCMV infection, over the half of IgG antibodies were directed against gB and less than the half of these gB-specific antibodies were neutralizing (Karbach, 2012). HCMV envelope glycoproteins (gB, gH-gL-gO complex, gM-gN complex) induce neutralizing antibodies, which might recognize strain-specific epitopes e.g. for gN (Pati et al., 2012). The composition of the HCMV envelope glycoproteins determines the cell tropism (fibroblasts or epithelial/endothelial cells) and consequently, the neutralizing capacity of an antibody might be dependent on the cell line tested.

In summary, the immunologic control of MCMV is redundant and relies on multiple cell types and immune effector functions (Polić et al., 1998). E.g. CD8 T cells are sufficient to control MCMV infection (Jonjić et al., 1989; Reddehase et al., 1987), but mice lacking CD8 T cells eliminated infectious virus with clearance kinetics similar to that of normal mice (Jonjić et al., 1990; Jeitziner et al., 2013).

Reactivation can be non-symptomatic despite virus is shed. In the immunocompromised situation, recurrent disease occurs with a different spread and engagement of immune control than in primary infection (Polić et al., 1998). Antibodies, T cells, NK cells and IFN- γ contribute to the maintenance of latency. Recurrent disease is established if multiple components of the immune response are absent indicating also functional redundancy of control mechanism for the maintenance of latency (Polić et al., 1998). The SG were reported as the site of most rapid virus shedding (Polić et al., 1998).

b) Immune evasion

CMVs have co-evolved with their hosts and encode numerous immune evasion mechanisms to disseminate efficiently and establish latency. All levels of host defence are counteracted, but it has to be distinguished the manipulation of directly infected cells (cis) and non-permissive cells (trans). For example is MHC I downregulated in infected cells leading to reduced antigen presentation (cis) and consequently diminished activation of CD8 T cells (trans). In general, mechanisms are: evasion from PRR, inhibition of IFN signalling and IFN induction, diminishing of T cell responses by downregulation of MHC I and MHC II, inhibition of NK cell activation, interference with immune cell cross talk / immune cell homing (e.g. cytokines / chemokines), block of apoptosis, inhibition of antibody effector functions (Hengel et al., 1998; Brinkmann et al., 2015; Corrales-Aguilar et al., 2014; Benedict et al., 2006; Jackson et al., 2011; Nomura et al., 2002). The antibody response is circumvented by three different means: (1) expression of viral FcγR(s), which antagonize the host FcγRs (2) circumvention of complement mediated virolysis and cytolysis by incorporation host complement regulatory proteins into the virion and upregulation on infected cells (Spiller et al., 1996) and (3) induction of a large quantity of non-specific antibodies (hyperimmunoglobulinemia) and non-neutralizing anti-viral antibodies (Pötsch et al., 2011; Welten et al., 2016; Hutt-Fletcher et al., 1983).

The vFcγR are present on the surface of the infected cell and they are incorporated into the virion as well. The HSV-1 encoded vFcγR gE/gI was the first vFcγR characterised. It inhibits neutralization, complement mediated virolysis and cytolysis, and host FcγR activation including ADCC (Dubin et al., 1991, Frank et al., 1989, Corrales-Aguilar et al., 2014). The other alpha herpesviruses like HSV-2 and VZV encode homologs (Budt et al., 2004). Four vFcγR have been identified for HCMV: glycoprotein (gp)34, gp68, gp95 (alternative name RL12), and RL13, which rapidly mutates by propagating the virus *in vitro* (Atalay et al., 2002; Cortese et al., 2012; Mercé Maldonado, 2011). For MCMV, only one vFcγR, m138, was recognised so far (Thäle et al., 1994). In contrast to HSV-1, HCMV vFcγRs do not interfere with neutralization and complement mediated virolysis (Reinhard, 2009; Mercé Maldonado, 2011). For the described vFcγRs, a mechanism of antibody bipolar bridging is evident whereby the antibody binds the antigen with its Fab and simultaneously the Fc part is bound by the vFcγR present on the same cells (Sprague et al., 2006; Corrales-Aguilar et al., 2014). A further function of most vFcγR is their internalization. The exact relevance and intracellular fate of the IgG have not been extensively evaluated and might be different for distinct vFcγRs (Ndjamien et al., 2014 and 2016; Mercé Maldonado, 2011).

1.4. Therapy of CMV disease

1.4.1. Antiviral drugs

Antiviral drugs inhibiting specific stages of the virus replication cycle were developed by targeting viral proteins. For HCMV four nucleoside analogues are currently licensed (Ganciclovir, Valganciclovir, Foscarnet, Cidofovir). However, antiviral drugs have severe side effects due to their toxicity and teratogenicity. Treatment during pregnancy is not suitable for most drugs. Furthermore, these antiviral drugs lead to drug resistant virus mutants.

1.4.2. Vaccination

Vaccination is the most effective mean to prevent infection. There are several promising approaches for a HCMV vaccine in different phases of clinical trials (Plotkin, 2015; Bernstein, 2011; Sung et al., 2010). In the past, some degree of protection was already achieved in different settings. The major drawbacks were the induction of a too low, too short lasting, and too narrow immune responses. Growing knowledge about distinct viral proteins, their immunogenicity, or their participation in different cell tropisms / entry pathways of CMV advanced the vaccination strategy. Therefore, the aim is to trigger humoral and cellular immune responses using antigens, which are protective against a broad range of strains. Vaccination approaches in the MCMV model are not reviewed here. But it has to be mentioned that superinfection is hardly possible with the homologues MCMV strain in contrast to heterologous viruses, indicating that protective immune responses are inducible (Wirtz et al., 2008; Gorman et al., 2006).

1.4.3. Passive immunization: prevention and treatment of CMV infection with adoptively transferred antibodies

Another approach for prevention or treatment of infection is the “passive immunization” with polyclonal or monoclonal antibodies. Polyclonal blood-derived antibody products have been developed for a variety of infectious disease (e.g. anthrax, cytomegalovirus, tetanus toxin, Hepatitis A virus, Hepatitis B virus, respiratory syncytial virus (RSV), VZV, rabies virus, measles, and CMV). IgG is also applied to treat immunodeficiency and antibody mediated autoimmune disorders (Sawyer, 2000; Barahona Afonso et al., 2016). In contrast to the defence of pathogens, immunomodulatory i.e. anti-inflammatory effector functions of the administered high doses of these polyclonal antibody preparations are considered to be responsible for the therapeutic successes in autoimmune diseases (reviewed in Lux et al., 2010; Böhm et al., 2014).

It is a point of matter whether passive immunization with antibody is suitable for prevention / treatment of herpesviruses and CMV infection. The following passage gives an overview about their protective capacities in recurrence / reinfection and passive immunization for HCMV and the MCMV model with regard to immunocompetent and compromised hosts. Vaccination strategies (for HCMV) are already described briefly above (1.4.2.) and therefore not included in the following paragraphs.

1.4.3.1. Prevention and treatment of HCMV infection

Against CMV, hyperimmunoglobulin preparations from a large number of healthy donors with high CMV specific IgG antibody titers (e.g. CytoGam®, Cytotect®) or IVIG preparations (intravenous immunoglobulin G) from donors with unknown CMV serostatus are used. In transplant recipient, antibodies are co-administrated with antiviral drugs, mostly Ganciclovir. Despite wide-ranging usage as prophylactically and / or therapeutically treatment in transplant recipients and intrauterine infection, benefits for the prevention of CMV infection and disease are uncertain (reviewed in Schleiss, 2013; Sawyer, 2000). However, IgG preparations, administration protocols, and parameters to evaluate the efficiency are not standardized and complicate the interpretation and comparison of the different clinical studies.

Administration of CMV-hyperimmunoglobulin was associated with a significantly lower risk of congenital CMV infection in a nonrandomized study (Nigro et al., 2005). The same group reported that many symptoms of congenital CMV infection were caused by placental dysfunction, which was reduced in hyperimmunoglobulin treated women (Maidji et al., 2010; Adler et al., 2009). In their further studies, in utero resolution of the signs of fetal disease and reduction of the severity of disabilities by hyperimmunoglobulin therapy of already primary infected mothers were observed (Nigro et al., 2008 and 2012). Unfortunately, the prevention of congenital infection was not confirmed in a controlled study (Revello et al., 2014). Two randomized phase III studies for the prevention of congenital infection are currently performed (Biotest in Europe, Eunice Kennedy Shriver National Institute of Child Health and Human Development in USA). In addition, approaches with mAbs are under investigation (reviewed in Ohlin et al., 2015).

Despite unclear results for hyperimmunoglobulin application, hints for the beneficial effect of anti-HCMV specific antibodies are evident. Preexisting immunity reduces the intrauterine HCMV transmission from one third who acquiring primary infection during pregnancy to about 1% in reinfection or recurrence of seropositive persons. Moreover, it is associated with less severe sequelae of congenital CMV infection than in primary infection (Fowler et al., 1992 and 2003) and protection against transfusion-associated CMV infection in the immediate postnatal period (Syndman et al., 1995). Furthermore, the quality of antibodies seems to be crucial since transmission during primary infection was associated with lower neutralizing antibody titers and lower avidity despite higher HCMV specific antibody titers (Boppana et al., 1995). Also higher titers of neutralizing antibodies were associated with absence of virus in plasma and protection from HCMV-disease in bone marrow transplant recipients (Schoppel et al., 1998).

In solid organ transplant recipients, studies indicated that immunoglobulins do not reduce CMV disease but reduced the risk of death from CMV disease (Hodson et al., 2007). The benefit for allogeneic stem cell transplant patients is also unclear (Raanani et al., 2009; Boeckh et al., 2001). Because Ganciclovir alone is more effective than immunoglobulins (Sawyer, 2000), the recommendations disfavor the combined therapy except for high risk patients (Avery, 1999) or for treatment of pneumonia in bone marrow and stem cell transplant recipients (Nichols et al., 2000).

1.4.3.2. Prevention and treatment of MCMV infection

The role of antiviral antibodies in MCMV infection was not investigated in such detail as the cellular immune response. Nevertheless, studies in immunocompetent or immunodeficient mice were performed, which evaluate the role of B cells, memory B cells, polyclonal antiviral IgGs, and antiviral mAbs administered either prior or post infection for MCMV replication and the maintenance of latency.

Early studies indicated a prevention of (detectable) MCMV replication by passive immunization with immune serum prior to subcutaneous infection. Nevertheless, development of latency was not altered (Shanley et al., 1981). Administration of immune serum post infection did not limit dissemination of virus in immunocompetent nor immunosuppressed mice (Shanley et al., 1981). Similarly, an even earlier study failed to detect protection from lethal course of infection by administration of immune serum post infection (Starr et al., 1977) probably due to a too low titer of virus specific antibodies in the serum. However, passive immunization prior to lethal MCMV infection permitted survival of mice

(Araullo-Cruz et al., 1978). The efficacy of passive immunization in terms of survival was dependent on the virus dose and CMV specific antibody titers of the immune serum (Araullo-Cruz et al., 1978).

Reduction of the viral load by passive immunization prior or post virus challenge of immunodeficient mice was shown multiple times using MCMV immune sera (Reddehase et al, 1994; Jonjić et al, 1994; Klenovsek et al., 2007; Wirtz et al., 2008) or to a lesser extent by mAbs (Karbach, 2012). Correspondingly, Klenovsek et al. verified that also the transfer of memory B cells in RAG1-KO mice conferred long-term protection from the lethal course of the infection due to antibody production of the (re)activated memory B cells.

In contrast to humans, CMV is not transmitted intrauterinly in the mouse. In the model of MCMV-infected newborn mice treated with immune serum, the titer of infectious virus in the brains was reduced below detection limit and significantly less CNS inflammation was observed in contrast to the untreated control group. Furthermore, a monoclonal antibody (mAb97.3, anti-gB IgG2c) also resulted in the reduction of virus titer in the brain but not as strong as polyclonal immune serum (Cekinović et al, 2008). In addition, maternal infection or vaccination with an attenuated MCMV protected neonatal mice from MCMV disease via placental transfer of antiviral antibodies (Slavuljica et al., 2010).

The exact antibody effector mechanisms mediating protecting in MCMV infection are not known. Complement seems to be dispensable because no difference was seen in mice lacking complement and control mice in passive immunization experiments (Farrell et al., 1991; Bootz, 2014). The role of neutralization is a matter of discussion. CMV specific antibodies inhibit long-distance primary dissemination from the site of entry to target tissues, but also protect from the focal cell-to-cell spread of virus after tissue infection was established in immunocompromised mice (Wirtz et al., 2008). In this study, higher virus neutralizing activity corresponded to a higher antiviral activity and due to γ irradiation (resulting in the elimination of immune cells), Fc γ R mediated effector mechanisms are unlikely and the neutralization of virions might be the most plausible mechanism in this scenario. As described above high titers of neutralizing antibodies seem to counteract HCMV more efficiently (1.4.3.1.). Nevertheless, it has to be noted that MCMV neutralizing antibodies appear late and in low titers post infection (Klenovsek et al., 2007; Araullo-Cruz et al. 1978; Welten et al., 2016). The study of Farrell et al., 1991 compared the protection from lethal MCMV challenge by mAbs with different neutralization capacities. However, these mAbs required complement for *in vitro* neutralization implicating that their neutralizing capacity is not strictly Fab mediated (1.1.5.1.). Nevertheless, no correlation of virus specific ELISA titers with neutralization capacity *in vitro* and no correlation of neutralization capacity *in vitro* with protection *in vivo* were observable indicating that protection *in vivo* might involve other effector mechanisms. The contribution of Fc γ R and therefore cellular mediated effector functions were not yet investigated in primary MCMV infection.

The passive or active immunization experiments did not accomplish sterilizing immunity but the challenge infection typically involved a high and non-physiological dose of virus and a non-natural infection route.

In summary, preventive passive immunization reduced virus load in immunocompetent and immunodeficient mice. However, B cell deficient mice clear primary MCMV infection and establish viral latency with the same kinetics as normal mice indicating a dispensable role in primary infection (Jonjić et al., 1994). These studies are of two different types: gain or loss of function. On the one hand, the presence of antiviral antibodies prior infection (or even post infection in more severely

immunocompromised) provides additional control of virus replication in comparison with the non-treated group. On the other hand, if an antibody response cannot be mounted during the immune response in primary infection, this absence of antibodies might be compensated by other components of the immune system, e.g. T cells. A redundancy and compensatory effect of control mechanisms for CMV is known (1.3.4.5.a). Furthermore, the studies in B cell deficient mice revealed that antibodies limit virus replication and dissemination after recurrence in the immunosuppressed host (Jonjić et al., 1994; Reddehase et al., 1994; Polić et al., 1998, Mutnal et al., 2012). Seropositivity prevents reactivation in mice after γ -irradiation or T-cell depletion but depletion of T and NK cells in B-cell-deficient mice resulted in 100% recurrent infection (Polić et al., 1998; Reddehase et al., 1994).

In conclusion, there is evidence that CMV specific antibodies play a role in controlling CMV infection especially if other components of the immune system are compromised. Their mechanism of action is unclear which hamper the improvement of the clinical application of CMV specific antibodies. In addition, the role of antiviral IgG in primary and secondary infection seems to differ, but the reason behind this is observation is unclear. It could be due to differences in IgG function (e.g. IgG affinity maturation), IgG effector mechanisms (e.g. memory NK cells), or modes of MCMV transmission.

1.4.3.1. Perspectives

Vaccination is not available and sterilizing immunity might not be achievable by passive immunization. The reduction of the viral load and severity of disease is nevertheless highly desirable for immunocompromised patients, transplant recipients, and after congenital infection. Since polyclonal immunoglobulin preparations are not highly standardized and using a single mAb has restricted efficiency, a combination of highly efficient mAbs might be suitable. One step towards an optimization of an IgG based therapy of CMV is the evaluation of the role of Fc γ Rs in the control of MCMV replication and the dependency of the Fc γ R activation on the IgG subclass.

1.5. Objectives of the thesis

The relevant antibody mediated effector functions in CMV infection or of therapeutically administrated IgGs are unclear. The impact of neutralizing antibodies in the immune control of CMV is still under debate whereas complement dependent IgG effector functions seem to be relatively little effective (1.4.3.2.). Growing evidence indicates that Fc γ R mediated cellular responses contribute essentially to the protection from virus infection including influenza and HIV (1.2.5.). Consequently, we hypothesized that Fc γ R contribute to the immune control of CMV. For proof of concept, the mouse model of CMV, MCMV, was chosen because the impact of activating Fc γ Rs can be evaluated *in vivo* by taking advantage of different Fc γ R deficient mouse strains (Fc γ 1-KO, Fc γ 2-KO, Fc γ 3-KO, Fc γ 4-KO mice).

Furthermore, the long-term objective is the assessment and optimal design of IgG based therapy against CMV disease. In a first step, we focus on the evaluations of the role of the IgG subclass and the producing cell line of recombinant mAbs (which influences the Fc glycan composition) for optimal Fc γ R activation. A recently developed Fc γ R activation assay allows to quantify the activation of a distinct Fc γ R by immune complexes *in vitro*, which reflects the natural situation most likely better than affinity measurements of the interaction of monomeric IgG with Fc γ Rs. This assay was established for the mouse Fc γ Rs in this study. We hypothesized that the Fc γ R activation capability of an IgG depends on

the IgG subclass and the producing cell line by editing Fc glycosylation pattern; consequently, systematic optimization of IgGs should be able to improve the antibody-mediated therapeutic effect *in vivo*. To be able to relate the *in vitro* FcγR activation with protective capabilities *in vivo*, non-neutralizing antibodies had to be utilized. No suitable non-neutralizing mAbs specific for a viral protein also expressed on the surface of infected cells were available at the beginning of this study. To this end, an ectopic surface antigen expressed by either a cell line or a recombinant MCMV and a set of recombinant monoclonal antibodies possessing the same variable regions but different IgG subclasses were generated. This system allowed the systematic comparison of the capability of the distinct IgG subclasses to activate the individual FcγRs without and within the context of MCMV infection. The advantage is that this set of recombinant IgG antibodies recognizes the same epitope so that FcγR activation capabilities are solely dependent on the Fc part and not influenced by varying affinities or accessibility of epitopes. Moreover, the direct comparison of the IgG2a subclass expressed by BALB/c related mouse strains with the neglected IgG2c subclass of C57BL/6 related mouse strains was of interest. Although these subclasses are discussed to be allelic variants of one gene, we hypothesised that they are functionally distinct. A previous study comparing the antibody response in infected BALB/c and C57BL/6 mice (Androsiac, 2012) revealed that IgG2a and IgG2c are induced to a different degree in primary MCMV infection. Additionally, MCMV immune sera from these two mouse strains showed a remarkable different capability to activate FcγRIII suggesting that this difference is caused by the distinct IgG subclasses.

2. RESULTS

2.1. Impact of FcγRs in the primary phase of MCMV infection *in vivo*: studies in FcγR deficient mouse strains

IgGs exert diverse effector functions by activation of Fc gamma receptor (FcγRs). The crucial impact of FcγRs for the antiviral immune response against virus infections like HIV and influenza was demonstrated in recent studies (see 1.2.5.). In this work, the role of FcγRs in primary phase of MCMV infection was defined *in vivo* taking advantage of the FcεR1γ-KO mouse (here referred to as FcRγ-KO), which lacks the surface expression of all activating FcγR due to the deletion of the accessory gamma chain (Figure 1.2; Takai et al., 1994). Next, single FcγR deficient mice lacking one of the activating receptors due to a deletion of the FcγR alpha chain (FcγRI-KO, FcγRIII-KO, and FcγRIV-KO) were examined. All mouse strains were on the C57BL/6 background possessing the activating Ly49H receptor on NK cells, which recognize the MCMV encoded MHC I homologue m157 expressed on infected cells. The Ly45H - m157 interaction leads to a strong NK cell response rapidly eliminating MCMV infected cells (Arase et al., 2002). However, the *m157* gene is highly sequence variable in wild mice derived MCMV isolates interacting predominantly with inhibitory Ly49 receptors (Voigt et al., 2003; Corbett et al., 2011). To avoid this unusual NK cell activation elicited by the MCMV virus lab strains (Smith, C3X) in C57BL/6 mice, the MCMV Δm157 deletion mutant is commonly used (Bubić et al., 2004). Here, the MCMV Δm157 Luc mutant (Ohmer et al., 2016) was chosen because it encodes the Firefly luciferase reporter gene allowing determining the viral organ load by luciferase activity (bioluminescence). On one hand, the luciferase activity can be quantified in the homogenized organ itself, which reflects virus gene expression in cells. On the other hand, the amount of the produced virus progeny (i.e. the viral load) in the organ can be determined by infecting target cells with the organ homogenate *in vitro* followed by the quantification of the luciferase activity in the target cells one day post infection (4.4.3.2.). Virions themselves are not detected because luciferase itself is not packaged into the virions.

2.1.1. Activating FcγRs contribute to viral control in primary MCMV infection *in vivo*

First, the contribution of all activating FcγRs for the virus control in primary MCMV infection was evaluated. FcRγ-KO mice and C57BL/6 wild type mice were infected with MCMV Δm157 Luc for 3, 7, 14, 21, and 28 dpi. A one to two log-steps elevated viral load was detectable in the salivary glands (SG) of FcRγ-KO compared to C57BL/6 wild type mice at 14 to 28 dpi (Figure 2.1. A - C). The viral load in the spleen and lungs seemed to be elevated as well but the differences did not reach statistical significance for most tested time points with the given number of mice per group (Figure 2.1.F). The viral load in the liver varied strongly between single mice within the same group whereby no virus was detectable at each time point for some animals in this experiment. No difference in the viral load in the liver was detectable between the mouse strains. Nevertheless, this finding supports the hypothesis that activating FcγRs contribute to the viral control in MCMV infection thus indicating an involvement of non-neutralizing antiviral IgG antibodies.

To dissect the impact of individual FcγRs further, primary MCMV infection was analysed in FcγRIV-KO mice (Nimmerjahn et al., 2005) in comparison to FcγRIV heterozygotes (FcγRIV-HET) and C57BL/6 wild

type mice (Figure 2.1.). Detecting no difference in the viral load of the tested organs implies that the FcγRIV is dispensable for the control of primary MCMV infection.

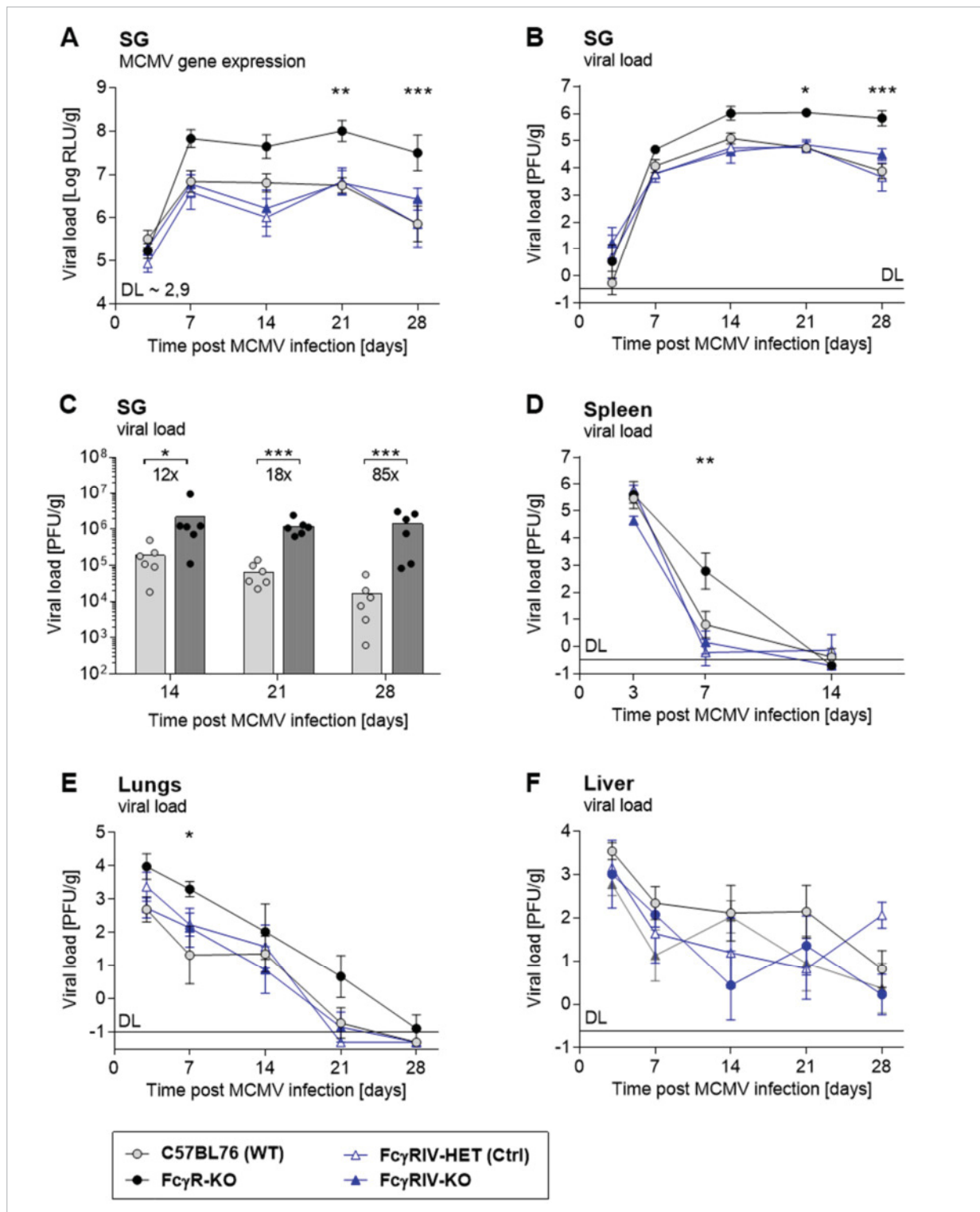


FIGURE 2.1. Fcγ deficient mice display a higher viral load in the SG whereas FcγRIV is dispensable for control of primary MCMV infection. 9 - 14 weeks old FcγR-KO, FcγRIV-KO, FcγRIV-HET, and C57BL/6 wild type mice were infected i.p. with 2×10^5 PFU MCMV Δm157 Luc for 3 to 28 days (5 - 7 mice/group). The viral load in the indicated organs was determined via the luciferase reporter gene activity in the organ homogenate directly (A) or after infection of BIM fibroblasts with the organ homogenate (B-F); DL: detection limit. Triplicate values were determined and means with the standard error of the mean (SEM) or single mice are shown. Two-way ANOVA: * $p < 0,05$; ** $p < 0,01$; *** $p < 0,001$; FcγR-KO vs. C57BL/6 is shown and FcγRIV-KO vs. FcγRIV-HET was not significant (Figure A, B, D, E, F); Students t-test for Figure C; (GraphPad Prism 6). One of two experiments with FcγRIV-KO mice is shown; further experiments with FcγR-KO mice are depicted in additional figures and described in the text.

Detecting an elevated viral load in the SG of MCMV infected FcR γ -KO mice led to the question, how long MCMV persists in this organ in the absence of activating Fc γ Rs. Therefore, the viral load was determined until 84 dpi (Figure 2.2.). A delayed clearance in the SG was reproduced in FcR γ -KO mice in comparison to C57BL/6 wild type mice. Virus gene expression in the SG of FcR γ -KO mice was detectable until 56 dpi and infectious virions up to 84 dpi (in one animal) in contrast to the control group in which MCMV gene expression or infectious virus progeny was only measurable until 28 and 56 dpi respectively. Furthermore, a higher virus gene expression was detectable in the lungs at 28 dpi in FcR γ -KO mice.

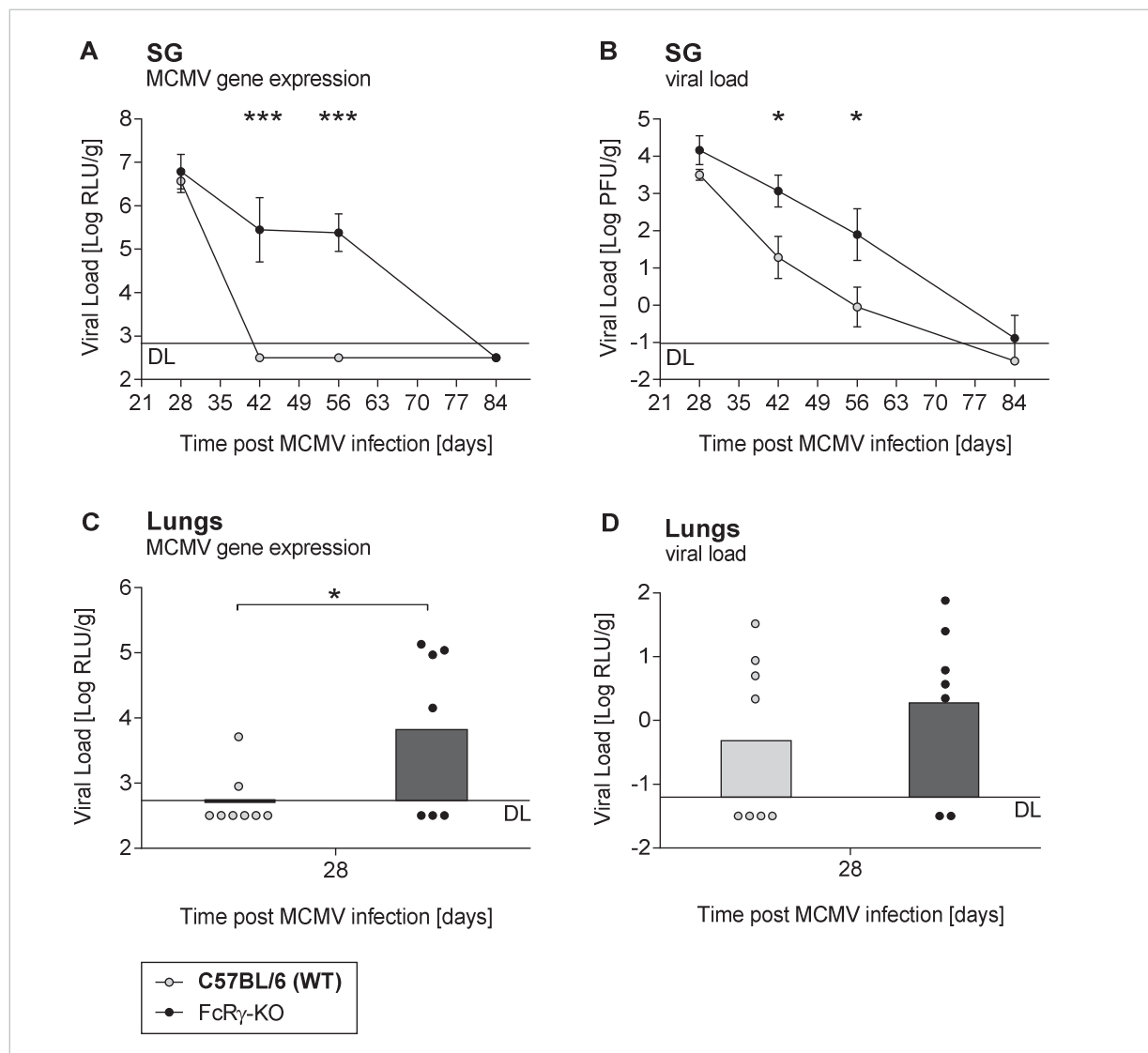


FIGURE 2.2. FcR γ deficient mice display a higher viral load and delayed clearance in the SG in primary MCMV infection. 8 - 14 weeks old FcR γ -KO and C57BL/6 wild type mice were infected i.p with 2×10^5 PFU MCMV Δ m157 Luc for 28 to 84 days (5 - 8 mice/group). The viral load in the SG and lungs was determined via the luciferase reporter gene activity in the organ homogenate directly (A, C) and after infection of BIM fibroblasts with the organ homogenate (B, D); For the lungs only 28 dpi was analysed. DL: detection limit. Triplicates were determined and means with SEM or single mice are shown. Two-way ANOVA (A,B) or student's t-test (C,D): * $p < 0,05$; ** $p < 0,01$; *** $p < 0,001$; (GraphPad Prism 6).

Further validating this phenotype, MCMV infection of FcR γ -KO mice were compared to heterozygous control mice (FcR γ -HET) at selected time points post infection. In general, heterozygous mice are superior controls in comparison to wild type mice. Variations in the genetic background and variations eventually resulting from different housing (e.g. microbial commensals), which may arise using wild type controls that were bred separately from the transgenic mice, are excluded.

An increase in the viral load in the SG was consistently reproduced for 14, 21, 28, 42, and 56 dpi mostly reaching statistical significance in various experiments. Moreover, a tendency of a higher viral load in the lungs and liver was observable in most experiments reaching significance in some cases. Exemplarily, the viral loads in the SG and liver at 28 and 42 dpi is shown in Figure 2.3. The lungs were not titrated in this case because MCMV replication is usually abrogated in this organ late in infection in contrast to liver (Figure 2.1. and 2.2.). In addition, the viral load in the SG, liver, and lungs at 14 and 28 dpi are presented in Figure 2.7.

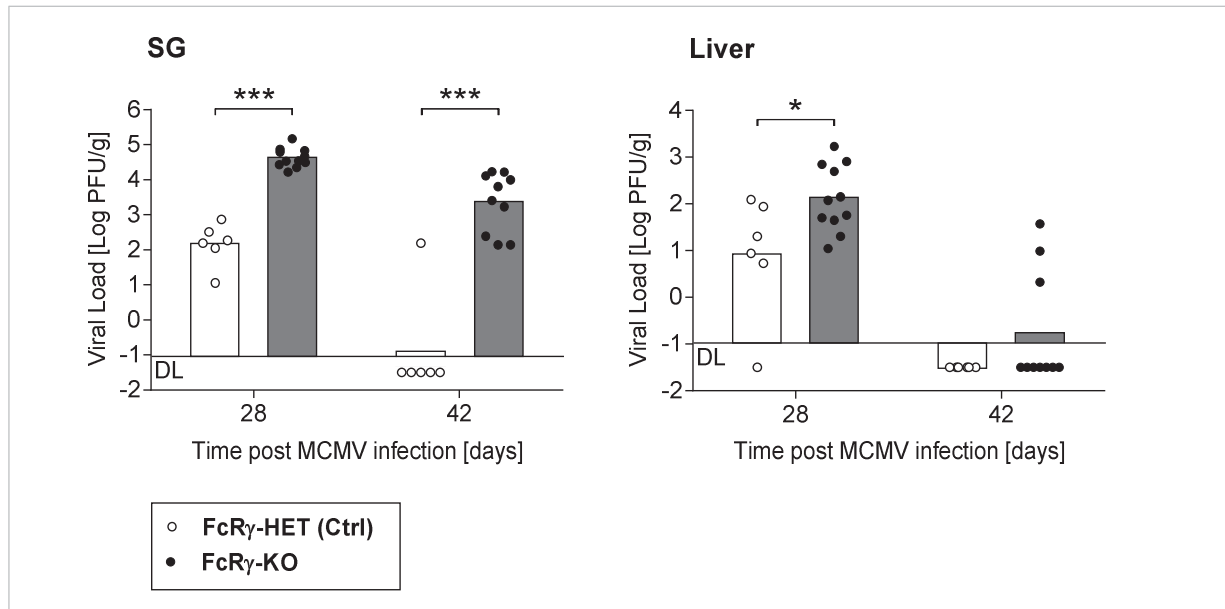


FIGURE 2.3. FcγR deficient mice display a higher viral load and delayed clearance in the SG in primary MCMV infection. 8 - 11 weeks old FcγR-KO and FcγR-HET control mice were infected i.p. with 2×10^5 PFU MCMV $\Delta m157$ Luc for 28 or 42 days (6 - 11 mice/group). The viral load in the SG and liver was determined via the luciferase reporter gene activity after infection of BIM fibroblasts with the organ homogenate; DL: detection limit. Triplicates were determined. Bars represent the mean and dots single mice. Two-way ANOVA: * $p < 0,5$; ** $p < 0,05$; *** $p < 0,01$; (GraphPad Prism 6).

SUMMARY

- *FcγR-KO mice, which lack the expression of all activating FcγRs, displayed elevated and prolonged viral loads especially in the SG demonstrating a contribution of the activating FcγRs in the immune control of the MCMV infection.*
- *The contribution of FcγRs indicates an involvement of non-neutralizing antiviral IgG antibodies for the control of MCMV infection.*
- *FcγRIV is dispensable for the control of primary MCMV infection.*

2.1.2. Absence of a single activating FcγRs is compensated by remaining FcγRs in primary MCMV infection

Since an elevated and prolonged MCMV replication in the SG of FcγR-KO mice but not in mice selectively lacking FcγRIV was observed, FcγRIII-KO (Hazenbos et al., 1996; Figure 2.4) and FcγRI-KO (Barnes et al., 2002; Ioan-Facsinay et al., 2002; Figure 2.5) mice were tested next. FcγRIII is of special interest because it is the only FcγR expressed on NK cells in the mouse. However, no difference in the viral load was observed in the SG 4 to 56 dpi comparing FcγRIII-KO to C57BL/6 wildtype mice. Unexpectedly, the viral load was even reduced in the spleen in the FcγRIII-KO mice at 4 dpi. As further control, FcγRIII-KO mice were compared to FcγRIII heterozygous mice (FcγRIII-HET) at an early (4 dpi)

and a late (28 dpi) time point post infection (Figure 2.4C). No difference was detected in the spleen, lung, liver, and SG. Thus, the differences in the viral load in the spleen of FcγRIII-KO mice in comparison to wild type control mice was not reproduced with heterozygous control mice. The unchanged control of the MCMV infection in FcγRIII-KO mice suggests that FcγRIII and therefore NK cell mediated ADCC is dispensable for the control of primary MCMV infection in this setting.

Similar to the FcγRIV-KO and FcγRIII-KO mice, no difference in the viral load was measurable in the spleen and SG of FcγRI-KO mice in comparison to heterozygous control mice (FcγRI-HET) 3 to 42 dpi. Additionally, the detection of virus by the luciferase activity was compared with plaque formation resulting in the same results (Figure 2.5.B vs. 2.5.C).

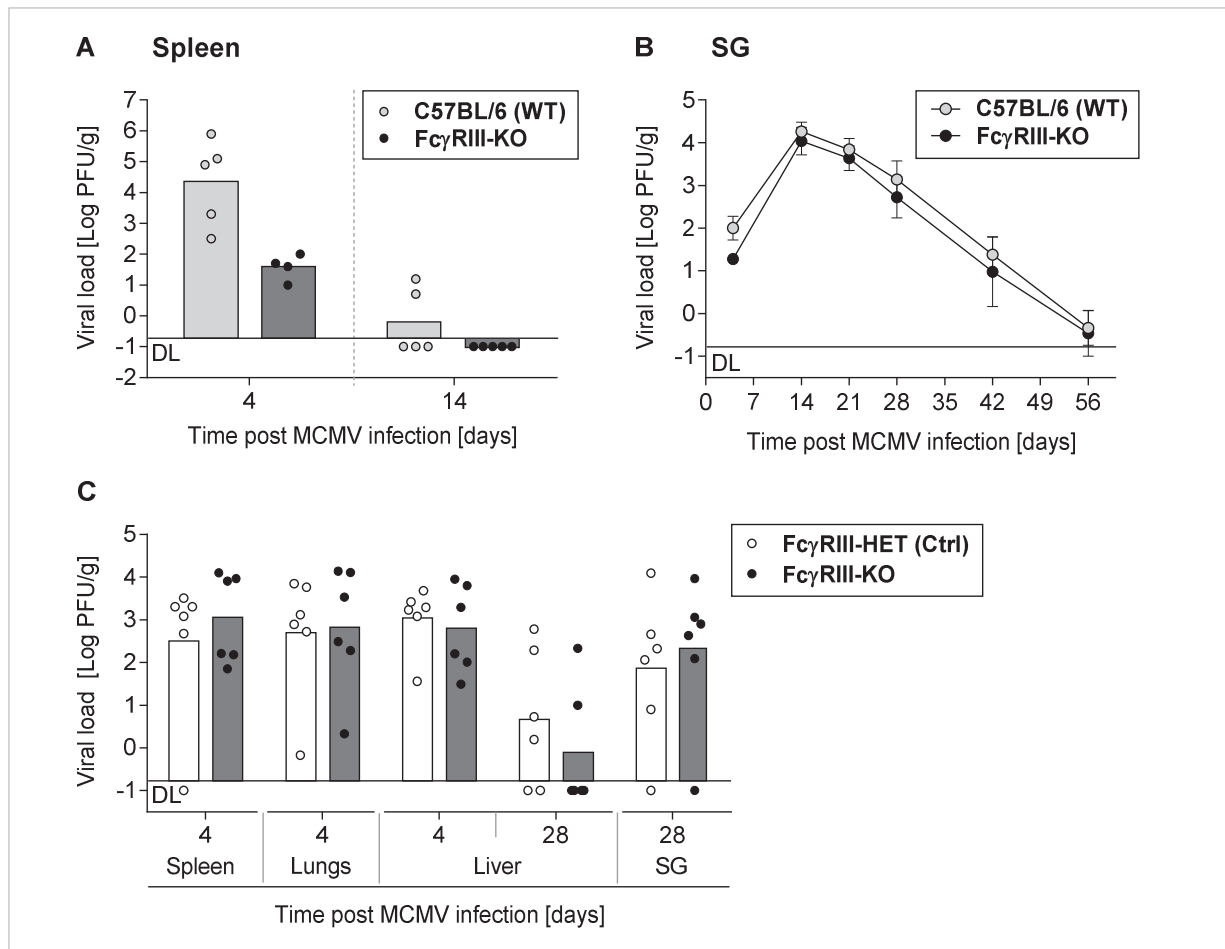


FIGURE 2.4. FcγRIII is dispensable for the control of primary MCMV infection. A+B: 8 - 10 weeks old FcγRIII-KO or C57BL/6 wildtype mice were infected i.p. with 2×10^5 PFU MCMV $\Delta m157$ Luc for 4 to 56 days (4 - 5 mice/group). C: FcγRIII-KO or FcγRIII-HET control mice were infected for 4 or 28 days (6 mice/group). The viral load in the indicated organs was determined via the luciferase reporter gene activity after infection of BIM fibroblasts with the organ homogenate; DL: detection limit. Means with SEM are shown. Two-way ANOVA: spleen 4 dpi $p = 0,001$, other n.s. (GraphPad Prism 6); both with FcγRIII-KO mice performed experiments are shown.

SUMMARY

- Similar to FcγRIV, FcγRI and FcγRIII are dispensable for the control of primary MCMV infection if only one activating FcγR is absent.
- In contrast to the absence of all FcγRs, the absence of a single activating FcγRs might be compensated by the other two remaining FcγRs in primary MCMV infection indicating functional redundancy of the individual (activating) FcγRs.

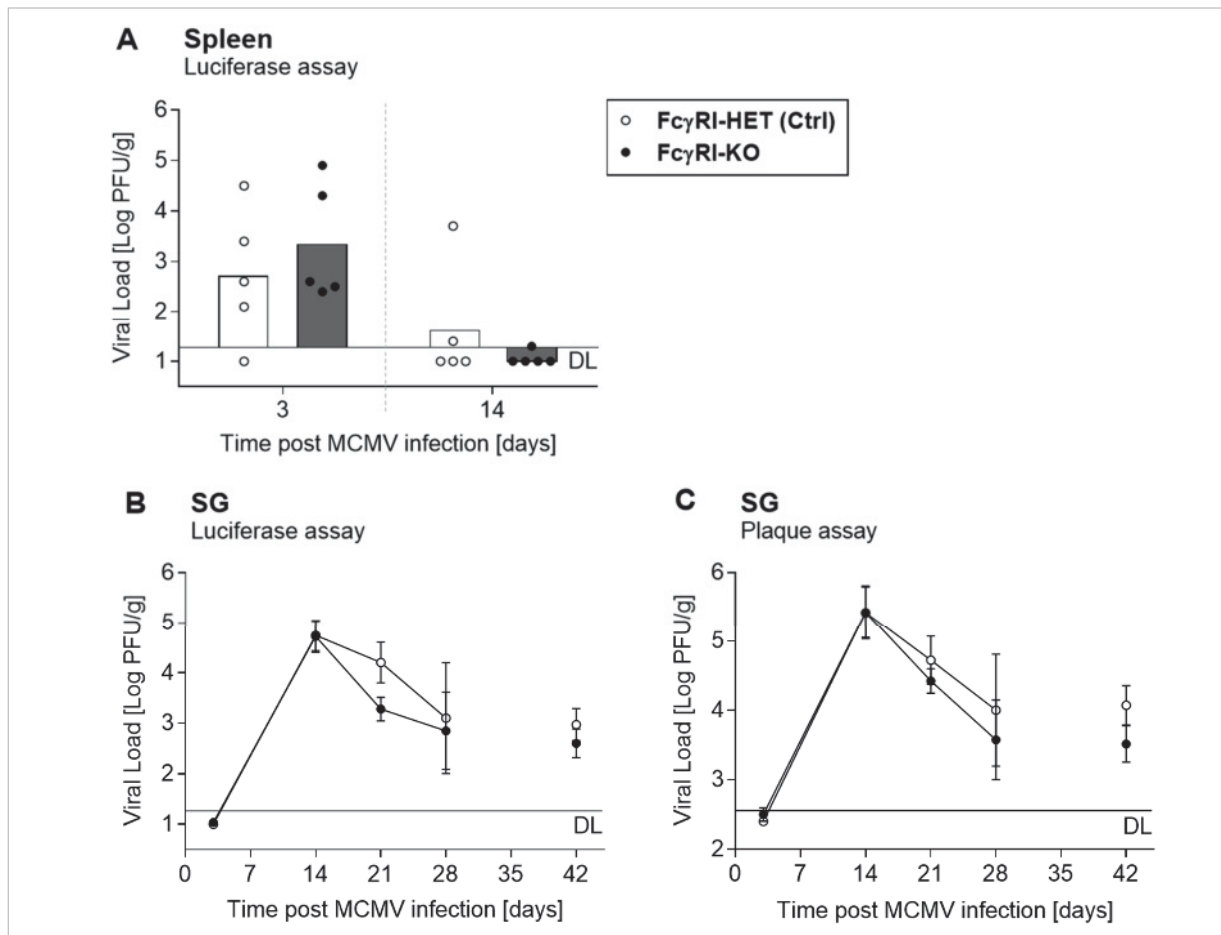
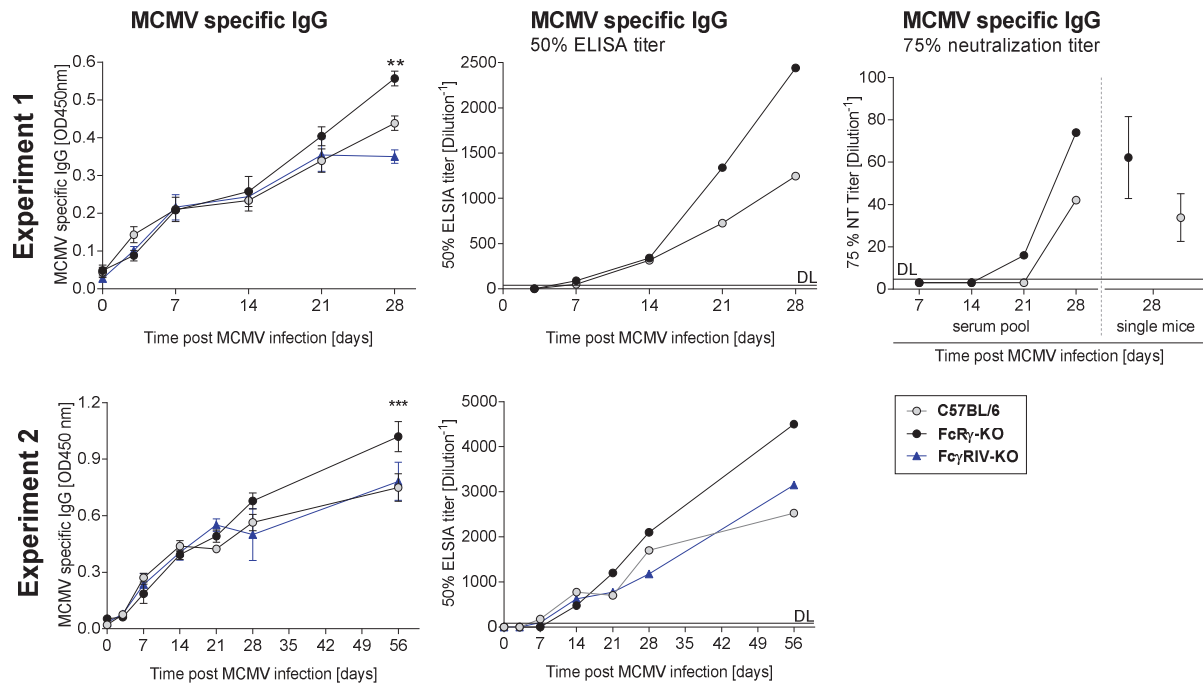


FIGURE 2.5. FcγRI is dispensable for the control of primary MCMV infection. 8 -12 weeks old FcγRI-KO or FcγRI-HET mice were infected i.p. with 2×10^5 PFU MCMV Δm157 Luc for 3 to 28 (4 - 5 mice/group). In addition, 6 - 7 mice/group were infected for 42 days. The viral loads in spleen and SG were determined via the luciferase reporter gene activity after infection of CIM fibroblasts with the organ homogenate (A, B) and by plaque assay on MEF (C); DL: detection limit. Means with SEM or single mice are shown; Two-way ANOVA: n.s. (GraphPad Prism 6); one of two experiments with FcγRI-KO mice is shown.

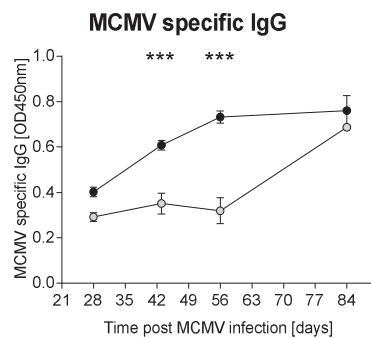
2.1.3. FcγR deficient mice possess elevated total and MCMV specific serum IgG titers

FcγR deficient mice displayed an increased and prolonged viral load in the SG as well as by trend elevated viral loads in other organs. To verify that these effects are caused by the lack of the expression of the activating FcγRs and not due to a diminished IgG response to MCMV, the MCMV specific IgG level in the serum was quantified by ELISA (Figure 2.6). FcγR-KO mice revealed a higher IgG titer in comparison to C57BL/6 wild type mice upon 21 to 28 dpi. The 50% ELISA titer was calculated using serial dilutions of serum pools from the individual mice for each time point detecting increased MCMV specific serum IgG levels upon 21 dpi. The MCMV specific IgG serum titer of infected wildtype mice seemed to reach the level of the FcγR-KO mice at the latest analysed time point (84 dpi). Increased IgG titers were not reported for FcγR-KO mice. FcγRIV-KO mice exhibited comparable MCMV specific IgG serum titers to C57BL/6 wild type mice. In addition, the overall IgG serum titer was quantified revealing a strongly elevated IgG level in FcγR-KO mice even at early time points post infection. The remarkably high amount of total IgG (hypergammaglobulinemia) was already observed before in MCMV infected wild type mice (Androsiac, 2012, Price et al., 1993; Karupiah et al., 1998).

A. Acute and persistent infection



B. Late persistent infection



C. Acute and persistent infection

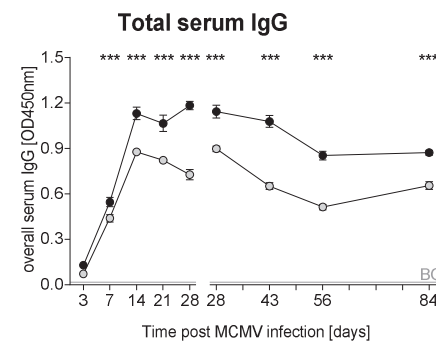


FIGURE 2.6. FcRγ deficient mice display a higher IgG, MCMV specific IgG, and MCMV neutralizing antibody serum titers in primary MCMV infection. 8 - 14 weeks old FcRγ-KO, FcγRIV-KO, and C57BL/6 wildtype mice were infected i.p. with 2×10^5 PFU MCMV Δm157 Luc and blood was obtained from the heart under thoracotomy (A. Experiment 1: see Figure 2.1; B: see Figure 2.2, A. Experiment 2: 3 mice/ group). MCMV specific IgG serum titer was quantified by ELISA using coated lysate of MCMV infected MEF incubated with 1/200 serum dilutions. For quantification of the total serum IgG, a 10^{-4} dilution of serum pools was coated. The 50% ELISA Titer was determined by graded dilutions of serum pools. For the determination of the 75% neutralization titer, 10^3 PFU of MCMV Δm157 Luc were first incubated with graded dilutions of complement inactivated serum pools at 37°C for 90 min. The virus-serum mix was added to BIM fibroblasts and one dpi the virus titer was measured by luciferase reporter gene activity. DL: detection limit. Triplicates were determined and means with SEM and SD for the total serum IgG are shown. Two-way ANOVA: * $p < 0,5$; ** $p < 0,05$; *** $p < 0,01$; (GraphPad Prism 6). ELISAs determining MCMV specific and total IgG titers were performed at least twice; 50% ELISA titers were determined once and 75% neutralization titers were determined twice for 28 dpi and once for all other time points (due to limited serum amounts).

Additionally, the 75% neutralization titer was determined illustrating that the FcRγ-KO also possess a higher amount of MCMV neutralizing serum antibodies (IgG and IgM) in accordance with the elevated MCMV specific IgG serum levels. As reported (Manischewitz et al., 1979; Hangartner et al., 2006), the first neutralizing antibodies were detected late, 21 to 28 dpi, in contrast to all MCMV specific IgGs antibodies. Elevated levels of MCMV neutralizing IgGs might reduce the viral load, which on the other hand is increased due to the lack of the activating FcγRs. Thus, the magnitude of virus control by FcγR might be partially masked by the increased level of neutralizing IgG leading to underestimation of the contribution of the FcγRs in this experimental setting at least at later time points of infection.

SUMMARY

- *FcR γ -KO mice possess higher total, MCMV specific, and MCMV neutralizing IgG serum level in comparison to control mice*

2.1.4. Characterization of the immune cell population in the SG of MCMV infected FcR γ -KO vs. FcR γ -HET mice

The SG become MCMV-infected during the second viremia (1.3.4.4.). FcR γ -KO mice showed elevated and prolonged viral load in this organ after primary MCMV infection. FcR γ s are expressed on a variety of immune cells, but their activation also influences non-FcR γ bearing immune cells e.g. via soluble mediators. To define the role of the activating FcR γ s, the immune cell populations in the SG were characterized in FcR γ -KO and FcR γ -HET mice. Two time points post infection were analysed. In addition, the viral load was determined. As seen before, the viral load was only modestly increased at 14 dpi, whereas an increase of two log steps was detectable at 28 dpi in FcR γ -KO mice (Figure 2.7).

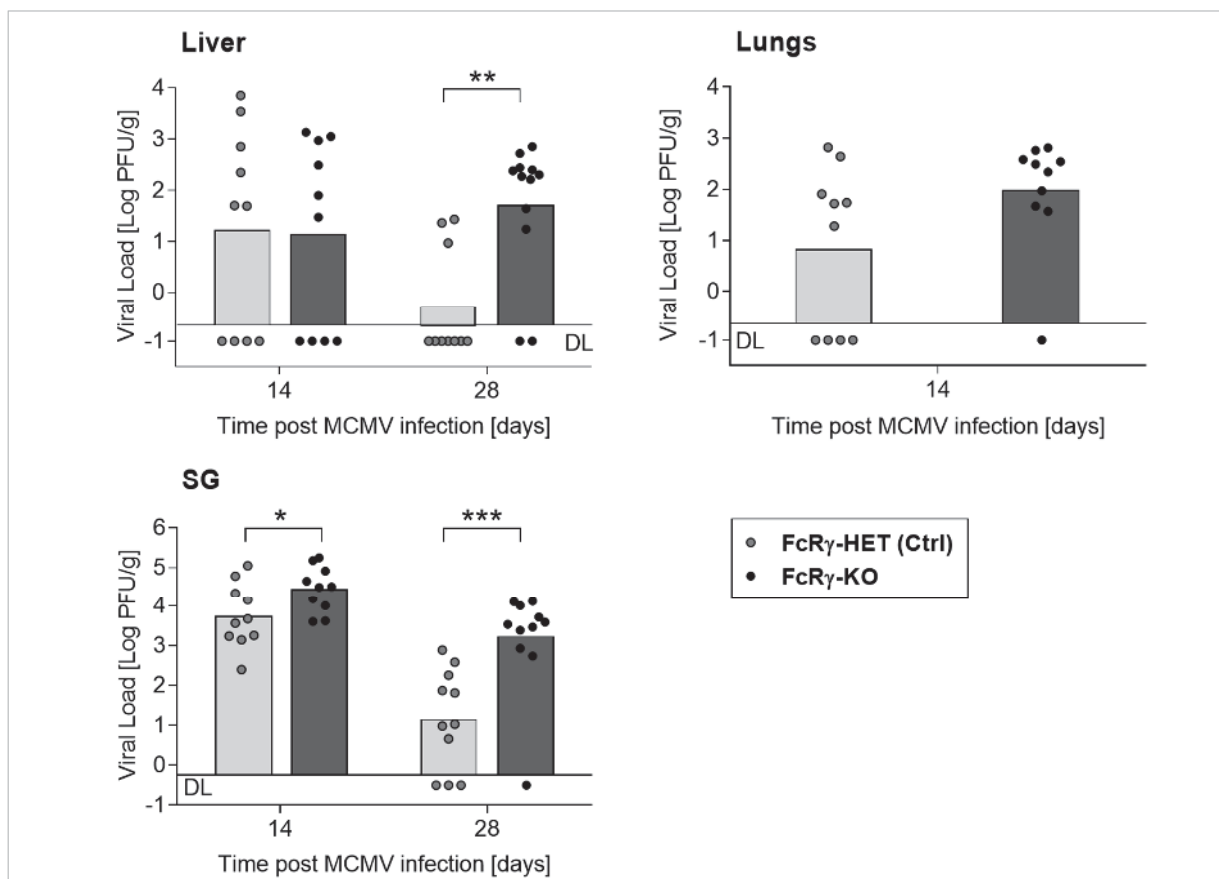


FIGURE 2.7. FcR γ deficient mice display a higher viral load and delayed clearance in the SG in primary MCMV infection. 8 - 12 wks old FcR γ -KO and FcR γ -HET control mice were infected with 2×10^5 PFU MCMV Δ m157 Luc i.p. for 14 or 28 (10 - 12 mice/group). The viral loads in the SG, liver, and lungs were determined via the luciferase reporter gene activity of organ homogenate incubate BIM fibroblasts; DL: detection limit. Triplicates were determined. Bars indicate the mean and dots single mice. For lungs, only the earlier time point was analysed. Student's t-test if no data points < DL, otherwise Man-Whitney: * $p < 0,5$; ** $p < 0,05$; *** $p < 0,01$; (GraphPad Prism 6).

The SG were harvested, the tissue was mechanically and enzymatically dissolved, and the immune cells were separated by density gradient centrifugation (4.5.3.1.). Finally, the immune cell populations were characterized by cell surface markers via flow cytometry. Living (DAPI negative) and single cells (FSC (A) vs. FSC (H)) were gated. Two different staining approaches addressing distinct cell populations were pursued. The gating strategies are shown in Figure S1. To analyse T cells, CD8 or CD4 positive

cells were gated in the CD3 positive population. B cells were identified by gating on CD19 positive cells in the CD3 negative population. The B and T cell activation marker CD86 was analysed in the CD4 T cells ($CD3^{pos}CD4^{pos}$), CD8 T cell ($CD3^{pos}CD8^{pos}$), and B cell ($CD3^{neg}CD19^{pos}$) populations as well. To characterize NK and myeloid cells, B and T cells were excluded by selecting CD3 negative and CD19 negative cells. Subsequently, the majority of NK cells was recognized by their DX5 expression. Moreover, F4/80 identified macrophages in the DX5 negative population. To classify DCs and monocytes, the cell surface markers CD11c and CD11b were used (hi: high; int: intermediate; low: low expression level). The $CD11c^{hi}CD11b^{int}$ population contains DCs, the $CD11c^{low}CD11b^{int/hi}$ population monocytes, and the $CD11c^{int}CD11b^{neg}$ population plasmacytoid DCs (pDCs). Concerning monocytes and macrophages, the degree of expression of distinct surface markers is also dependent on the (resident) tissue. To note, the absolute cell numbers were not determined and the flow cytometry analysis of different time points post infection was performed in separated experiments.

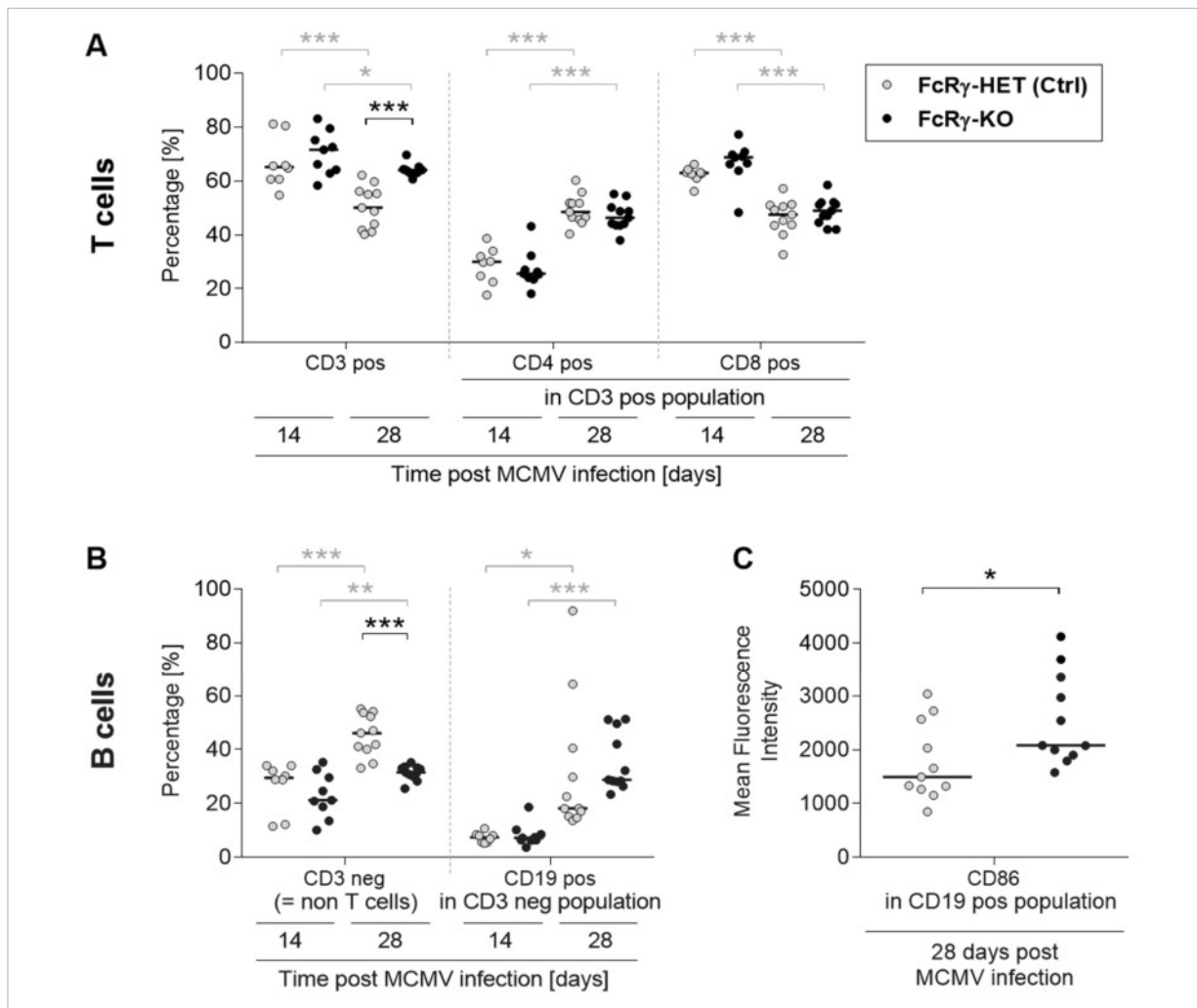


FIGURE 2.8. Characterization of the immune cell population in the SG in MCMV infected FcR γ -KO vs. FcR γ -HET mice. 8 - 12 wks old FcR γ -KO and FcR γ -HET control mice were infected i.p. with 2×10^5 PFU MCMV $\Delta m157$ Luc for 14 or 28 (10 - 12 mice/group). Surface staining was performed with CD3-PE, CD19-APC, CD8-FITC, CD4-PerCP-Cy5.5, and CD86-PE-Cy7. Dead cells were excluded by DAPI staining. Cells were measured by flow cytometry (BD FACS Canto II, FACS Diva software) and analysed with FlowJo (Tree Star Inc). Horizontal lines represent the median; Student's t-test: * $p < 0,5$; ** $p < 0,05$; *** $p < 0,01$; black: comparison between mouse strains, grey: comparison between time points; (GraphPad Prism 6). MFI: mean fluorescence intensity.

FcR γ -KO mice had an elevated percentage of CD3 positive cells (Figure 2.8.A). This population contains mainly T cells (>90%) because NKT are absent in the SG in naïve and MCMV infected mice (Tessmer et

al., 2011). This tendency reached statistical significance in one of two experiments performed. Furthermore, the CD3 positive cell population is decreasing during infection (Figure 2.8.B). Ratios of CD4 and CD8 T cells were comparable between KO and HET-mice and are consistent with previous findings (Campbell et al., 2008; Cavanaugh et al., 2003), but it changes during the course of infection. The percentage of CD4 T cells, which are the main effector cell type exerting antiviral functions, increased during infection leading to equal amounts of both T cell subsets at 28 dpi when viral load was dropping in heterozygous mice (Figure 2.8.A). The percentage of CD19 positive B cells increased also during the course of infection (Figure 2.8.B). By trend, FcγR-KO exhibited a higher percentage of B cells at 28 dpi. The activation status was characterized by CD86, which seems to be elevated on B cells from FcγR-KO mice 28 dpi (Figure 2.8.C) but CD86 expression was not altered on CD4 or CD8 T cells comparing both mouse strains (data not shown).

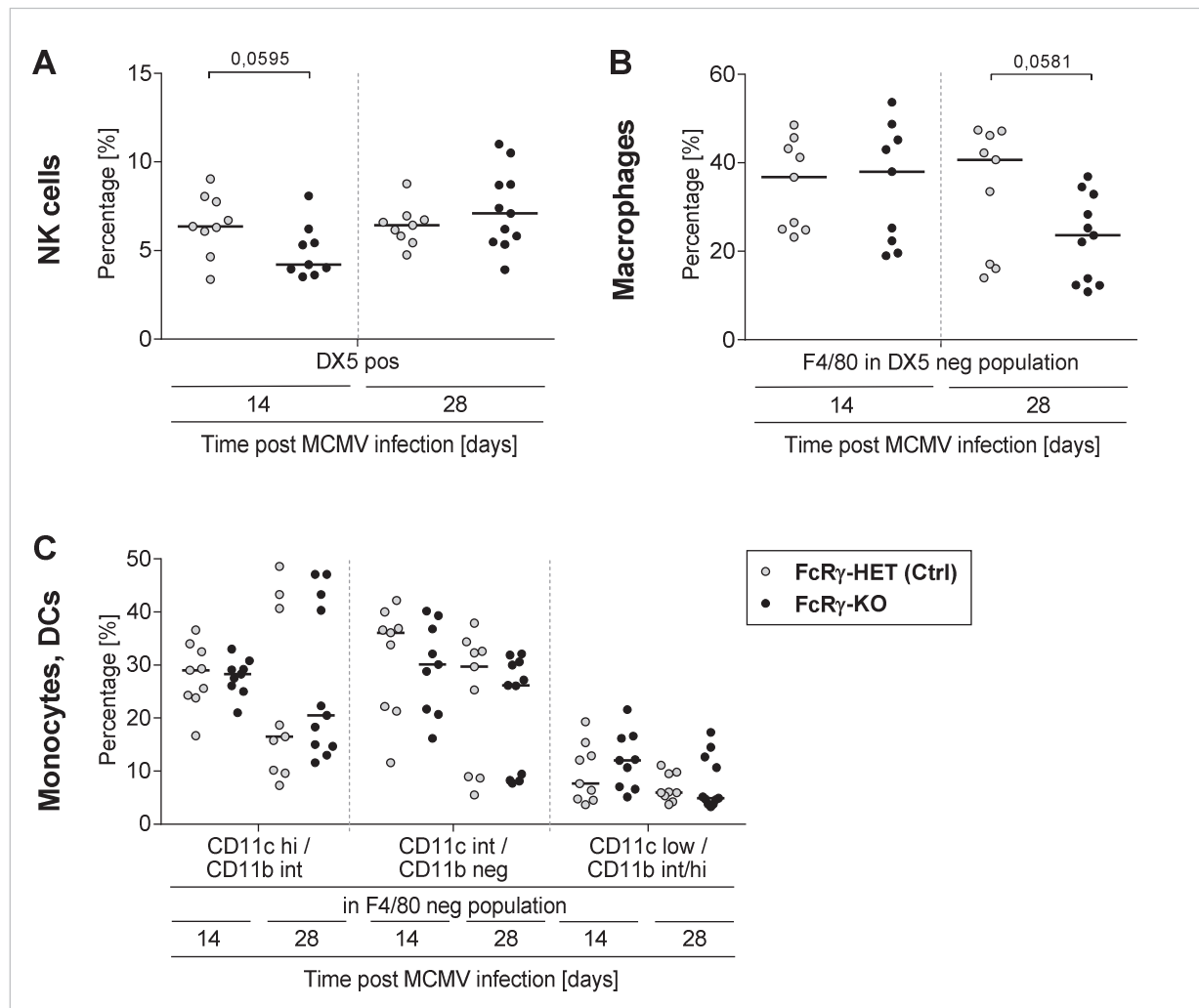


FIGURE 2.9. Characterization of the immune cell population in the SG in MCMV infected FcRγ-KO vs. FcRγ-HET mice. 8 -12 wks old FcRγ-KO and FcRγ-HET control mice were infected i.p. with 2×10^5 PFU MCMV Δ m157 Luc for 14 or 28 (10 - 12 mice/group). Surface staining was performed with CD3-PerCP, CD19-PerCP, DX5-PE-Cy7, F4/80-PE, CD11c-APC, CD11b, and APC-Cy7. Dead cells were excluded by DAPI staining. Cells were measured by flow cytometry (BD FACS Canto II, FACS Diva software) and analysed with FlowJo (Tree Star Inc). Horizontal lines represent the median. Student's t-test was performed to compare KO and HET mice within the same day: * $p < 0.05$; ** $p < 0.01$; *** $p < 0.001$; (GraphPad Prism 6).

The percentage of NK cells ($CD3^{\text{neg}}CD19^{\text{neg}}DX5^{\text{pos}}$) was slightly reduced in FcRγ-KO mice at 14 dpi but not anymore at 28 dpi (Figure 2.9.A). Similar amounts of NK cells were found in FcRγ-HET mice at 14 and 28 dpi consistent with findings from Cavanaugh et al., 2003. No difference in the CD11c or CD11b

expression on the NK cells was detectable in-between the mouse strains, but the CD11c expression was decreased at 28 dpi in comparison to 14 dpi (data not shown). The percentage of macrophages (CD3^{neg}CD19^{neg} F4/80^{pos}) was slightly decreased in the FcγR-KO mice at 28 dpi (Figure 2.9.B). Using CD11c and CD11b expression levels, the populations containing monocytes (CD11c^{low}CD11^{int/hi}) and DCs (cDCs in CD11c^{hi}CD11b^{int}, pDCs in CD11c^{int} CD11b^{neg}) were defined (Figure 2.8.C). No obvious differences in these subset were detectable in-between the mouse strains. The next step would be the characterization of the FcγR expression of the SG resident cell populations in the control mice. Additionally to the determination of the percentage of certain immune cell population, the absolute numbers would give further information as well. An additional late time point could clarify if the loss of macrophages is transient or lasting. Furthermore, functional assays determining the amount of virus specific CD4 T cells and their capacity to secrete cytokines would reveal if the loss of FcγR affect CD4 T cell priming by APCs or if the loss of virus control is a direct effect of the functional impairment of innate immune cells.

SUMMARY

- *Immune cell populations at 14 and 28 days post MCMV infection in the SG:*
 - *The percentage of T cells (CD3 positive cells) decreased during the time course of infection.*
 - *The percentage of CD4 T cells increased during the time course of infection.*
 - *The percentage of B cells increased during the time course of infection.*
- *Comparison of immune cell populations (14 and 28 dpi) in the SG of MCMV infected FcγR deficient mice (FcγR-KO) versus control mice (FcγR-HET):*
 - *The percentage of T cells (CD3 positive cells) was slightly elevated in FcγR-KO mice.*
 - *The activation status of B cells was slightly elevated in FcγR-KO mice.*
 - *The percentage of NK cells was slightly reduced at 14 dpi in FcγR-KO mice.*
 - *The percentage of macrophages was slightly reduced at 28 dpi in FcγR-KO mice.*

2.2. In vitro FcγR activation assay is a unique tool to quantify FcγR activation by immune complexes

Assessing the activation capabilities of distinct antibodies for the individual FcγRs is of essential importance for the development of therapeutic IgGs or for the improvement of vaccinations. Our group developed a new method to quantify IgG mediating FcγR activation *in vitro*, which allows measuring the activation of any human FcγR by defined immune complexes (Corrales-Aguilar et al., 2013). This new method is essential because no reliable methodology was existing to measure FcγR activation capabilities of IgG *in vitro*. Although several *ex vivo* ADCC assay have been developed, these assays share the disadvantage to rely on primary FcγRIII positive NK (isolated or in PBMCs). In addition, the expression of further FcγRs (CD32A/B) by human NK cells is discussed (Morel et al., 1999). Primary NK cells lead to highly variable results due to the heterogeneity of the cell population and between donors. Furthermore, the availability of these effector cells is limited because they cannot be maintained in cell culture. Except for NK cells, more than one activating FcγR can be co-expressed on primary immune cells, which hinders the analysis of a defined FcγR. The classical ADCC assay relies on the lysis of radioactively labelled and opsonized target cells by primary NK cells and the released ⁵¹Cr is quantified as measure for FcγRIII activation / ADCC. In most refined ADCC assays, the radioactivity was substituted by e.g. fluorescent dyes (Kantakamalakul et al., 2006; Lichtenfels et al., 1994; Gómez-Román et al., 2006). To achieve reliability, it is crucial to improve the effector cells, e.g. using a

homogenous effector cell population expressing only one defined FcγR. In first attempts, a T cell line was transduced with human FcγRIII, FcRγ, and a luciferase reporter gene controlled by the IL-2 promoter or αβ T cells were transduced with a fusion protein thereof (Parekh et al., 2012; Clémenceau et al., 2006).

As surrogate marker, numerous studies evaluated the binding affinity of monomeric IgG to distinct FcγR (by surface plasmon resonance). However, this does not represent the natural situation for FcγR activation by immune complexes *in vivo*. First, evidence exists that the binding to the antigen can induce conformational changes of the Fc domain, which might consequently influencing Fc effector functions (Kota et al., 1991; Janda et al., 2010, 2012, and 2016; Eryilmaz et al., 2013; Tian et al., 2015). Second, the affinity of binding to FcγRs does not necessarily predict the magnitude of the FcγR activation. Increased binding affinity of antibodies (by amino acid mutation in the Fc part and defucosylation) did not translate into enhanced ADCC beyond a certain threshold (Masuda et al., 2007). Third, the valence of immune complexes can enhance their binding capabilities (avidity) to cellular expressed FcγRs in contrast to monomeric IgGs. Likewise, the size of the immune complex can further enhance avidity (Lux et al., 2013). This argues against a possible predication of FcγR activation by a certain IgG *in vivo* based on *in vitro* protein-protein interaction affinity data and emphasises the importance of an *in vitro* FcγR activation assay.

The *in vitro* FcγR activation assay, which was developed in our group, combines a clonal effector cell line expressing a distinct FcγR and an easy quantifiable readout (Corrales-Aguilar et al., 2013). The principle of the assay is the activation of a signalling cascade by FcγR cross-linking which leads to a quantitative and easy measurable readout. To this end, the extracellular domain of the FcγR, which binds to the Fc part of IgGs, was fused to the signal transduction unit of the TCR, which is the transmembrane and cytoplasmic domain of the CD3-zeta chain (Figure 2.10.A). Expression and cross-linking of this FcγR-ζ chimera expressed by the TCR negative BW5147 T cell hybridoma allows the activation of the natural TCR signalling cascade resulting in quantitative secretion of IL-2 (Figure 2.10.B). The mouse BW5147 (ATCC TIB-47™) thymoma cells lack functional expression of TCR α, β, γ and ζ chains (Bonifacino et al., 1988; Letourneur et al, 1989; Wegener et al., 1992) and endogenous Fc receptor expression (Daëron et al., 1985). IL-2 secretion can be restored by transfection of CD3-ζ or chimaeras with CD3-ζ by utilizing the intracellular TCR signal transduction machinery (Wegener et al., 1992). The IL-2 amount is quantified by a sandwich ELISA and it serves as a surrogate marker for the magnitude of the FcγR activation. FcγR cross-linking and activation is achieved by exposure of the reporter cells to immune complexes. Different immune complexes are suitable: IgG coated surfaces, soluble complexes of aggregated or agglutinated IgGs, opsonized virions, and opsonized (infected) cells. As expected, monomeric IgG, virions, or cells alone as well as bound F(ab)₂ fragments are not able to activate the BW:FcγR-ζ reporter cells (Corrales-Aguilar et al., 2013).

The generation of the BW:FcγR-ζ reporter cell lines for the murine FcγRI, FcγRII, FcγRIII, and FcγRIV is described in 4.7.1. The parental BW5147 cell line was transduced with lentiviral particles to achieve stable expression of the chimeric FcγR-ζ chimaeras. The FcγR-ζ surface expression and Fc binding capabilities of the BW:FcγR-ζ reporter cell lines were verified by flow cytometry (4.7.1.).

2.2.1. Responsiveness of the FcγR-ζ reporter cells to immune complexes

To confirm the selective activation of the BW:FcγR-ζ cells by immune complexes, the reporter cell lines were co-cultivated with MCMV or mock infected MEF cells that were preincubated (i.e. opsonized) with MCMV immune serum (28 dpi, BALB/c) or naïve serum (BALB/c). As expected, only infected cells opsonized with immune serum were able to trigger IL-2 secretion of the reporter cells (Figure 2.11). To show that the amount of secreted IL-2 correlated with the magnitude of activation, i.e. amount of immune complexes, the reporter cells were co-cultivated with MCMV infected MEF opsonized with graded concentrations of the immune serum. As anticipated, the amount of secreted IL-2 decreases with higher serum dilution. Furthermore, no IL-2 secretion was detectable for parental BW5147.

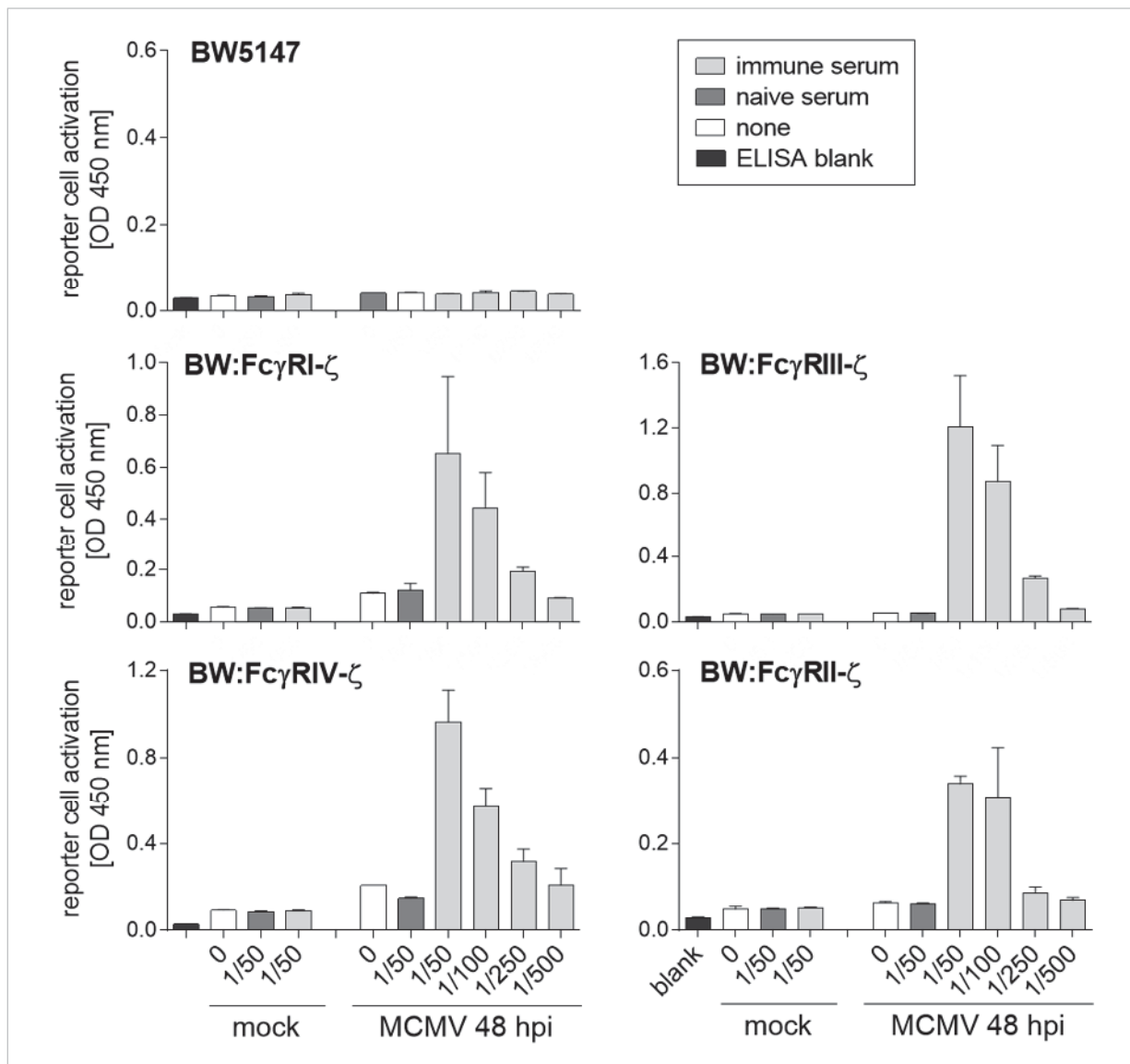


FIGURE 2.11. Selective and antibody concentration dependent BW:FcγR-ζ activation by opsonized target cells. MEF were infected with MOI 0,5 for 48 h with MCMV C3X_{MCK2}- and co-cultivated with 2×10^5 BW5147 or BW:FcγR-ζ cells overnight in the presence of the indicated dilutions of MCMV immune (MCMV C3X_{MCK2}-, 28 dpi, BALB/c) or naïve (BALB/c) serum. Each serum dilution was determined in duplicates. IL-2 secretion, the surrogate marker for the reporter cell activation, was quantified by IL-2 sandwich ELISA. Data were analysed with Prism 6 (GraphPad Software) and means with SD are shown.

SUMMARY

- The generated reporter cells (BW:FcγRI-ζ, BW:FcγRII-ζ, BW:FcγRIII-ζ, and BW:FcγRIV-ζ) were functional as demonstrated by their high FcγR-ζ surface expression, Fc binding capabilities, and their selective and concentration dependent activation by immune complexes.

2.3. Generation of a recombinant MCMV expressing an ectopic antigen

2.3.1. Choice and description of the ectopic model antigen

The long-term goal is the evaluation of anti-viral IgG for its protective potential and by this means improving the anti-CMV IgG based immunotherapy (1.5.). This study focuses in particular on the role of the FcγR activation capabilities of IgG. For this reason, an experimental approach had to be developed that avoids any confounding neutralization capacity of the MCMV-specific IgG. Since no non-neutralizing mAbs specific for a viral protein, which is expressed on the surface MCMV infected cells, were available, a system of an ectopic neoantigen antigen and recombinant neoantigen-specific IgG antibodies was generated. This ectopic antigen had to fulfil certain conditions to be suitable. First, it had to be a cell surface protein, which is easily expressed and not involved in protein complexes. Furthermore, it should be functionally inert and not leading to the neutralization of virus particles if incorporated into the membrane of the virion. To be able to generate recombinant IgG switch variants of a mAb recognizing the neoantigen, the last requirement was the availability of a hybridoma cell line to generate cDNAs of the IgG heavy and light chains. Cloning of the sequences for the variable regions from the heavy and the light chain from the hybridoma cell line allows the generation of recombinant mAbs possessing the same variable regions, but exchanged IgG subclasses.

Another advantage of an ectopic neoantigen expressed by the MCMV genome is that its expression (time point and amount) can be controlled by the choice of the promoter. Using the HCMV MIEP, an early and strong expression (4.7.2.1.; 2.3.2.2.) allows optimal conditions for the proof of concept. This proof might be difficult to achieve when focusing on only one natural viral antigen because most envelope proteins are rather expressed late during the replication cycle and the plasma membrane density is low since MCMV virions bud from intracellular compartments (1.3.4.1.; Jean Beltran et al., 2014).

For the reasons listed above, the human CD8 gene and the OKT8 hybridoma cell line (ATCC Number: CRL-8014; Reinherz et al., 1980), which produces a mouse anti human CD8 alpha IgG2a kappa, was chosen. The OKT8 antibody binds to the extracellular domain of the CD8 alpha molecule, but the precise binding site is not known.

There are two isoforms of the CD8 protein, alpha and beta, each encoded by different genes. Both are type-1 transmembrane protein with four domains: an N-terminal Ig like domain, a membrane proximal stalk, a transmembrane, and short cytosolic domain (Figure S2). The Ig like domain is N- and the stalk is O-glycosylated. The protein has a molecular weight of 32-34 kDa, thus it is rather small. CD8 forms disulphide-linked dimers, CD8αβ and the less common CD8αα. The CD8 dimer binds very weakly to invariant α3 domains of MHC I. The TCR - MHC I interaction is needed to form a stable TCR-MHC I - CD8 complex between the CD8 T cells and the antigen-presenting cells or target cells.

The mouse and the human CD8α molecules have approximately a sequence identity of 49% and the hCD8 is able to bind the mouse LCK (Höllander et al 1992). Human and mouse CD8αα have a common binding mode to peptide loaded MHC I, but species-specific characteristics exist (Gao et al., 2000).

Nevertheless, for the purposes to use the hCD8 as an ectopic antigen in the context of MCMV, it is an adequate candidate, because MCMV does not infect lymphocytes. Therefore, no interference of the human CD8 molecule is expected in the mouse system when expressed on the surface of infected cells.

SUMMARY

- The human CD8 molecule was chosen as model antigen because it fulfils following requirements:
 - cell surface expression
 - no complex posttranscriptional modifications
 - no complex formation with other proteins
 - availability of a hybridoma cell line, which produces a mAb specific for the antigen.

2.3.2. Characterization of the newly generated MCMV hCD8 and MCMV hCD4 virus mutants

The generation of a recombinant MCMV expressing the hCD8 antigen is described in 4.7.2. In addition, a corresponding virus mutant expressing another neoantigen, the human CD4, was also generated serving as control in *in vitro* assays and *in vivo* experiments.

2.3.2.1. *In vitro* replication kinetics

The size and nature of an inserted gene can lead to a growth deficiency of a recombinant virus. Therefore, the *in vitro* replication kinetics was analysed. Two growth curves comprising the time points 1 - 7 dpi were performed per virus mutant, namely MCMV hCD8, MCMV hCD4, and the control MCMV Δ m157 Luc (Figure 2.12). Infecting with a low MOI of 0,01, the virus titer in the supernatant increased linearly until it reached the maximum at 5 - 6 dpi. As expected, starting with a tenfold higher MOI (MOI = 0,1) resulted in a more rapid production of the maximum viral titer at 5 dpi. A decrease was observed at 7 dpi most likely caused by degradation of the shed virus due to suboptimal conditions e.g. lack of uninfected target cells and suboptimal composition of the supernatant after the prolonged cultivating period. Importantly, no differences were detectable between the different virus mutants and the control.

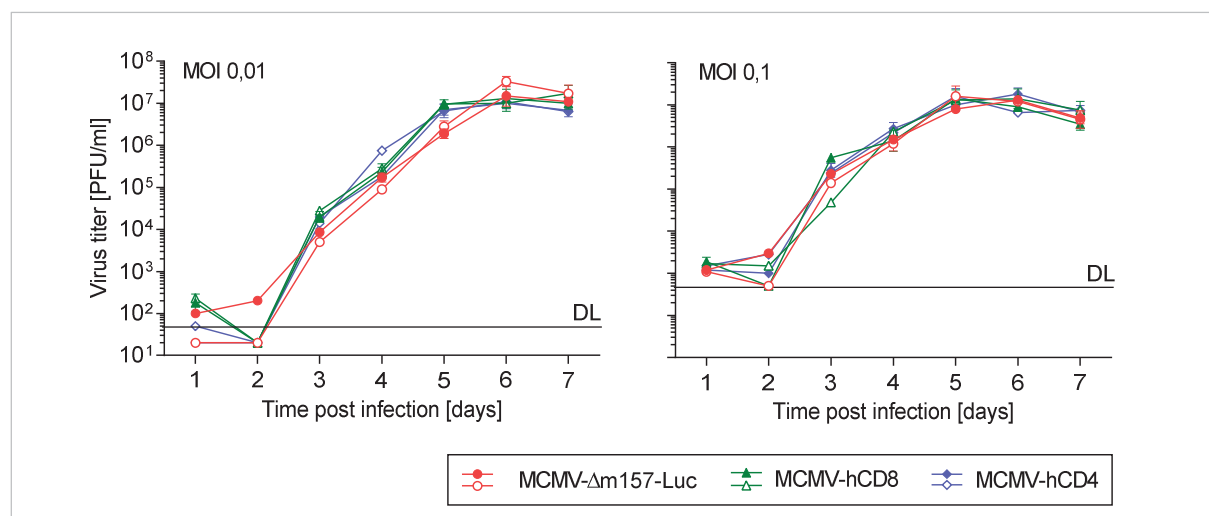


FIGURE 2.12. The *in vitro* replication kinetics of MCMV hCD8 and MCMV hCD4 are comparable to the control MCMV Δ m157 Luc on fibroblasts. MEF were infected with the MOI of 0,1 and 0,01 in a 24 well plate format. The supernatant was collected at the indicated time points and stored at -80°C. Per virus and time point two wells were infected. Each well was plaque titrated in duplicates. DL: detection limit.

2.3.2.2. Surface expression of the ectopic antigen hCD8 / hCD4 and the viral gB on infected cells

After the verification of the intact viral replication *in vitro*, the expression of the ectopic antigen was analysed and compared to the gB surface expression on infected cells at different time points post infection by flow cytometry (Figure 2.13, 4.5.3.). At all tested time points, a robust gB expression was detectable for the newly generated virus strains, MCMV hCD8 and MCMV hCD4, and it was comparable to the control MCMV Δ m157 Luc. The hCD8 expression on MCMV hCD8 infected cells was mostly independent of the analysed time points post infection, whereas the hCD4 expression of MCMV hCD4 infected cells was lower at 1 dpi, but increased at later time points. A double staining of hCD8 / hCD4 and gB (Figure 2.13.B) proved that all infected cells express the ectopic antigen. The OKT4-FITC antibody led to lower fluorescence signals than the APC labelled equivalent, which is the cause for the difference in the CD4 signal magnitudes in the histogram compared to the dot blots. Taken together, the newly generated recombinant MCMV hCD8 and MCMV hCD4 viruses showed consistent surface expression of their ectopic antigen.

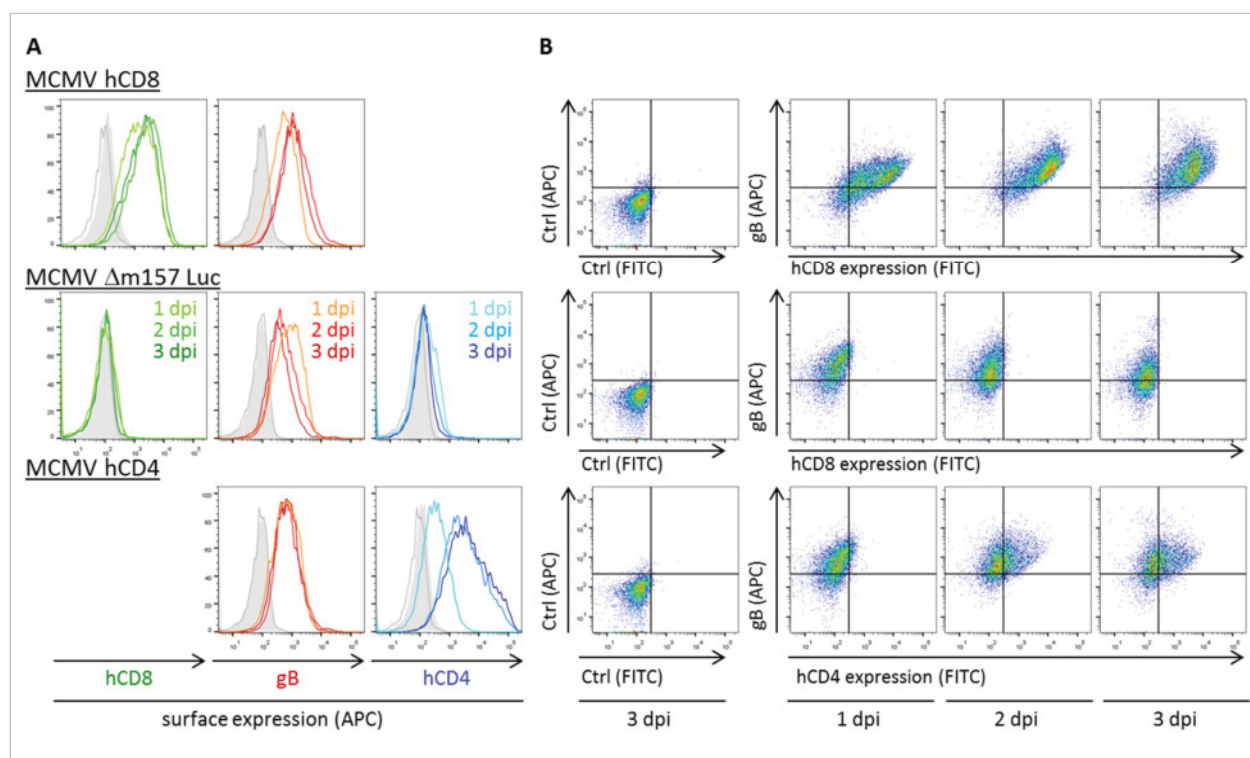


FIGURE 2.13. Surface expression of the ectopic antigens hCD8 and hCD4 and the viral glycoprotein gB on infected fibroblasts . BIM cells were infected with MOI 2 of MCMV hCD8, MCMV hCD4, and MCMV Δ m157 Luc at 3, 2, and 1 day prior the analysis. The ectopic antigens were stained with anti-hCD8 (OKT8-FITC/APC) or anti-hCD4 (OKT4-FITC/APC) respectively. gB was stained with MCMV1.01 which was detected with an goat anti mouse IgG-Cy5 (Ctrl APC). As controls APC or FITC labelled mAbs or the 2nd antibody were used. At least 3×10^4 cells were measured by flow cytometry (BD FACS Canto II, FACS Diva software) and analysed with FlowJo (Tree Star Inc.). Living cells (DAPI negative) in the FSC(A) / SSC(A) gate are displayed. A. Histograms, grey solid: control stained cells 3 dpi, grey line: unstained cell 3 dpi, green line: anti-hCD8, red line: anti-gB, blue line: anti-hCD8. B. Dot plots demonstrating gB vs. hCD8 / hCD4 expression of different time points post infection.

2.3.2.3. MCMV hCD8 virions are not neutralized by anti-hCD8 antibodies

As mentioned, the goal of this work is the evaluation of antiviral effector mechanism of non-neutralizing antibodies in dependency of the IgG subclass. To this end, the ectopic neo-antigen hCD8 was chosen, which was expressed by the MCMV genome. It is very unlikely that hCD8 molecules are incorporated into the virions. Nevertheless, with regard to *in vivo* experiments, a neutralizing effect of the utilized anti-hCD8 antibodies had to be formally excluded. A classical neutralization test was

performed, which bases on the pre-incubation of the virions with antibodies prior to the addition of the virus-antibody-mixture to target cells. The MCMV hCD8 mutant was incubated with two concentrations of the anti-hCD8 mAbs recognizing the same epitope but possessing different IgG subclasses. The mAbs are based on the OKT8 hybridoma derived mouse anti-human CD8 antibody and therefore they are referred to as recombinant OKT8 mAbs. Their generation and characterization is described in detail in 4.7.4. As negative controls, no and a mAb against an irrelevant antigen (OKT4: mouse anti-hCD4, IgG2b) were chosen. The anti-MCMV gB mAb 97.3 (IgG2c, Cekinović et al., 2008) is neutralizing and served as positive control. It reduced the viral load in the higher concentration of 4 μ g by 99% and in the lower concentration of 1 μ g by 78% (Figure 2.14). The neutralization capacity of an antibody is the function of its variable domains and theoretically independent of the subclass. Nevertheless, the whole IgG subclass panel (IgG1, IgG2a, IgG2b, IgG2c, and IgG3) of the recombinant anti-hCD8 OKT8 mAbs was tested. As expected, the virus titers in these samples were comparable to the negative control for both tested mAb concentrations. Therefore, the recombinant OKT8 mAbs were not able to neutralize the MCMV hCD8 virions.

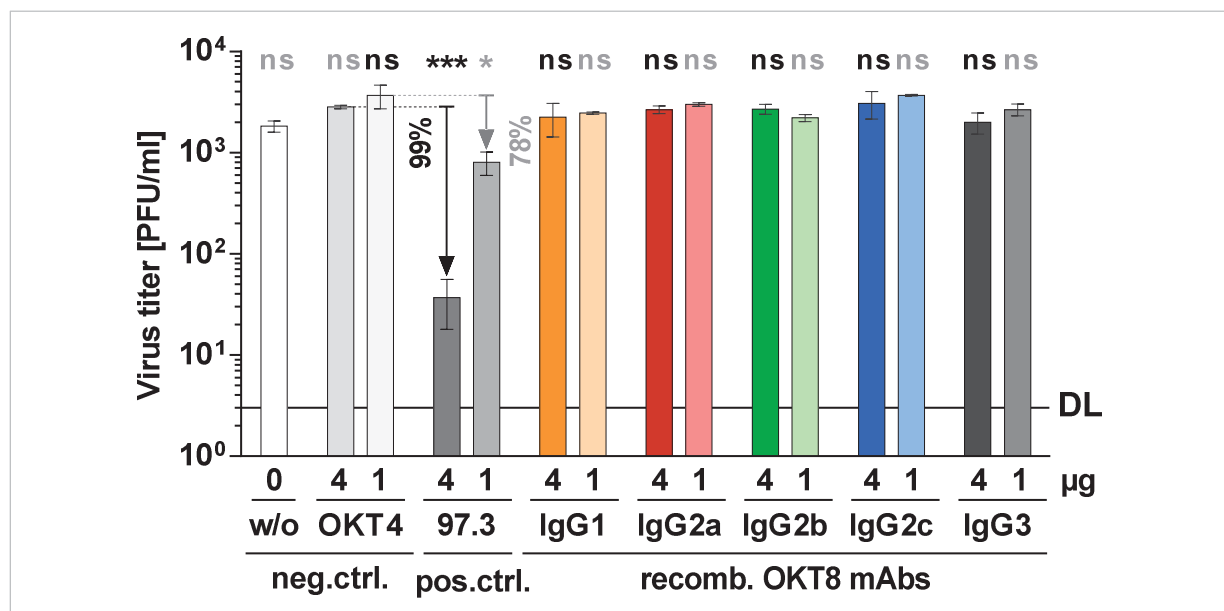


FIGURE 2.14. Anti-hCD8 mAbs fail to neutralize MCMV hCD8 virions *in vitro*. 670 PFU of MCMV hCD8 were incubated with 1 or 4 μ g of a distinct mAb for 70 min at 37°C and titrated in a 1/5 dilution series in triplicated on MEF. The mAbs OKT4 and 97.3 were purified from hybridoma supernatant and the recombinant OKT8 mAbs were purified from HEK293T supernatant. The detection limit (DL) is 3 PFU/ml. Means with standard deviation are shown. Samples with 1 or 4 μ g mAb were compared to their corresponding OKT4 negative control (1 μ g: grey or 4 μ g: black) with the t-test: * $p < 0,05$; ** $p < 0,01$; *** $p < 0,001$ (GraphPad Prism 6).

2.3.2.4. *In vivo* replication kinetics of MCMV hCD8

Last, the *in vivo* replication kinetics of MCMV hCD8 were determined in immunocompromised mice lacking adaptive immunity (T and B cells) and the expression of activating Fc γ Rs (RAG1 x Fc γ -KO). In order to evaluate the antiviral capacities of mAbs in passive immunization experiments, it is beneficial to use mice which don't mount their own antibody response against the virus, e.g. RAG1-KO mice. Furthermore, the RAG1 x Fc γ -KO mice are a suitable loss of function control for passive immunization experiments due to the additional lack of the Fc γ Rs (Bootz, 2014). Therefore, the MCMV hCD8 replication was analysed in these double knockout mice (Figure 2.15.). They were infected with 1×10^5 PFU of MCMV hCD8 or MCMV Δ m157 Luc. The body weight was comparable for mice infected with either virus until 9 dpi. At later time points, mice infected with MCMV hCD8 lost weight less rapidly

suggesting a lower viral load. The viral load was determined at 5, 14, and 19 dpi revealing no differences in the spleen and liver. In contrast, a lower viral load was observable in the SG for MCMV hCD8 leading to a statistically significant difference at 19 dpi. Mice losing more than 20% of their initial body weight were euthanized. For this reason, it was not possible to analyse later time points post infection. Taken together, the MCMV hCD8 replication seemed to be slightly reduced *in vivo* in comparison to MCMV Δ m157 Luc. Nevertheless, the MCMV hCD8 virus is suitable to analyse the protective capabilities of anti-hCD8 antibodies *in vivo*.

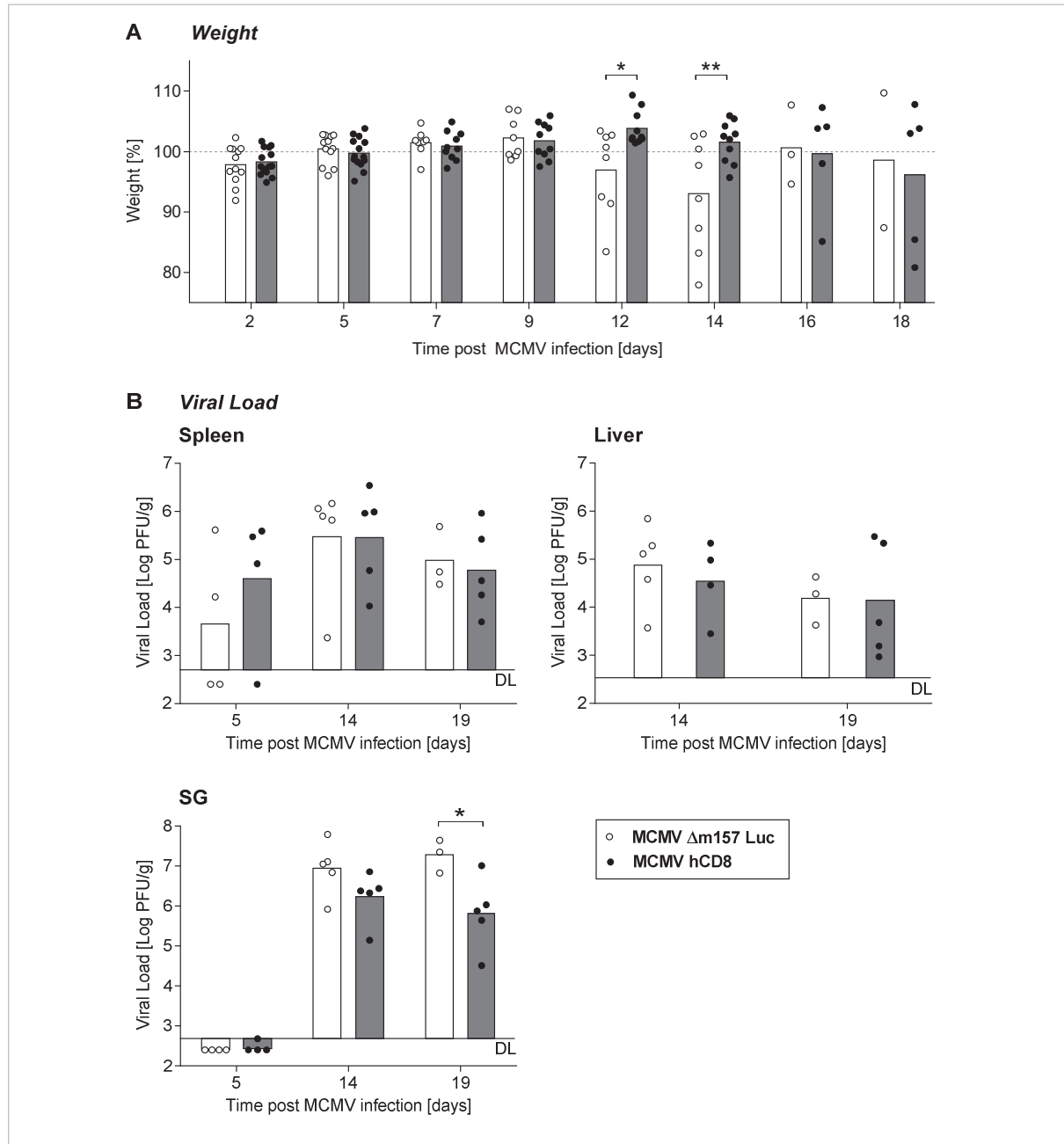


FIGURE 2.15. *In vivo* replication kinetics of MCMV hCD8 in comparison to MCMV Δ m157 Luc in immune compromised RAG1 x FcR γ -KO mice. 8 - 9 weeks old RAG1 x FcR γ -KO mice were infected i.p. with 1×10^5 PFU MCMV Δ m157 Luc or MCMV hCD8 for 5 to 19 days (3 - 5 mice/group). A. The body weight was monitored and is expressed as percentage in relation to the weight one day prior infection (100%). B. The viral load in the indicated organs were quantified by plaque assay; the viral load in the liver was too low at 5 dpi for a valid evaluation due to the toxicity of the liver homogenates for the target cells. DL: detection limit. Triplicates were determined and means are shown. Two-way ANOVA: * $p < 0,05$; ** $p < 0,01$; *** $p < 0,001$; (GraphPad Prism 6).

SUMMARY

- *In vitro* replication kinetics of the MCMV hCD8 and MCMV hCD4 viruses were comparable to the control virus.
- The MCMV hCD8 and MCMV hCD4 viruses showed consistent expression of their ectopic antigen on the surface of infected fibroblasts.
- MCMV hCD8 virions are not neutralized by anti-hCD8 antibodies.
- The MCMV hCD8 replication in immunocompromised mice seemed slightly reduced in the SG in comparison to the control virus leading to less weight loss.
- The MCMV hCD8 virus is suitable to test the protective capabilities of anti-hCD8 antibodies *in vivo*.

2.4. Generation and characterization of mAbs possessing identical variable regions but different IgG subclasses

Recombinant monoclonal antibodies possessing the same variable region but different IgG constant regions, i.e. the different IgG subclasses, were generated. In other words, monoclonal antibodies with the same affinity for the antigen but different effector functions were created to allow the direct correlation of the effector functions, e.g. FcγR activation, with the IgG subclass. Structural features of the different IgG subclasses are described in 2.4.1.

To this end, the variable regions were cloned into expression vectors containing the constant region of the different heavy chains (IgG subclasses) or the light chain (4.7.4., Figure 4.7.). These IgG subclass switched recombinant mAbs were produced by co-transfection or co-transduction of an expression vector for the HC and LC into mammalian cells and purified by Protein G chromatography (4.7.4.).

To facilitate the characterization of the recombinant OKT8 mAbs in settings with and without MCMV infection *in vitro*, stable hCD8 expressing cell lines were generated by lentiviral transduction (4.3.5.2.) e.g. HeLa hCD8, CIM hCD8, BIM hCD8, and NIH hCD8 (4.7.3.).

2.4.1. Comparison of the mouse IgG subclasses

This work focuses on the IgG subclass dependent FcγR activation. The FcγR binding sites are located in the hinge and C_H2 domain of the IgG molecule. Therefore, the differences in the amino acid sequence of the IgG subclasses were analysed in detail.

The sequence alignment comparing the constant regions of the heavy chain is shown in Figure 2.16B and a schematic representation focusing on the variations in the hinge region is presented in Figure 2.16A. Furthermore, the sequence of the defined regions is listed in Table 2.1. and a phylogenetic tree is shown in Figure 2.17. Slightly different annotations for the sequence representing the C_H1 - C_H3 domains and the hinge exist (Vidarsson et al, 2014; Lefranc et al., 2005; Wenig et al., 2001; Bloom et al, 1997; Dangl et al., 1988). Here these regions were assigned according to the Ig like domains for IgG2a in the P01864 (UniProt Database). The hinge was defined as sequence between C_H1 and C_H2 with the core hinge including the cysteines for the interchain disulphide binds.

The position of the cysteine residues forming the intrachain disulphide bonds and the N-glycosylation site (Asn297) are highly conserved among all subclasses. IgG2a and IgG2c are the subclasses most similar to each other (85% sequence identity) and share the second highest identity with IgG2b (79%). Among IgG subclasses, the sequence identity ranges from 67 - 85% percent while identity with other Ig classes (IgM, IgA, IgE, IgD, and IgG) is reduced to 22 – 37% (data not shown). In contrast, the human

A

Hinge region: Amount of AA	IgG1	IgG2a	IgG2b	IgG2c	IgG3
Upper	5	8	10	9	10
Core	6	6	10	10	4
(Cysteines)	(3)	(3)	(4)	(3)	(1)
Lower	5	8	8	8	8
Total	16	22	28	27	22

[illegible]

Most variations are found in the hinge region resulting in a different length and number of disulphide bonds (Figure 2.16.). IgG1 possess the shortest hinge region (16 AA). The hinges of IgG2a and IgG3 have an intermediate length (22 AA), whereas IgG2b and IgG2c have long ones (27 and 28 AA respectively). IgG1, IgG2a, and IgG2c exhibit three interchain disulphide bonds in the hinge, while

IgG2b possess four and IgG3 only one. Despite the different length and number of disulphide bonds of the hinge of IgG2a and IgG2c, their amino acid sequence is the most similar among all subclasses. Comparing the Ig domains (C_H1, C_H2, C_H3), the C_H3 domains is the most variable. Of note, the intrachain disulphide bond coupling the IgG1 heavy to the light chains lays within the upper hinge region in contrast to the other IgG subclasses possessing this cysteine in the C_H1 domain.

Sequence identity [%]		> 90%		> 80%		< 40%	
Subclass	Domain	IgG1	IgG2a	IgG2b	Ig2c	IgG3	MW
IgG1	C _H 1		86	83	84	71	81
	Hinge		38	31	25	10	26
	C _H 2		71	70	72	76	72
	C _H 3		65	54	62	65	62
	full		72	67	70	68	69
IgG2a	C _H 1	86		86	95	73	85
	Hinge	38		82	64	56	60
	C _H 2	71		94	95	83	86
	C _H 3	65		59	70	60	64
	full	72		79	85	71	77
IgG2b	C _H 1	83	86		87	73	82
	Hinge	31	82		63	36	53
	C _H 2	70	94		92	83	85
	C _H 3	54	59		62	55	58
	full	67	79		79	68	73
IgG2c	C _H 1	84	95	87		72	85
	Hinge	25	64	63		38	48
	C _H 2	72	95	92		81	85
	C _H 3	62	70	62		58	63
	full	70	85	79		68	76
IgG3	C _H 1	71	73	73	72		72
	Hinge	10	56	36	38		35
	C _H 2	76	83	83	81		81
	C _H 3	65	60	55	58		60
	full	68	71	68	68		69

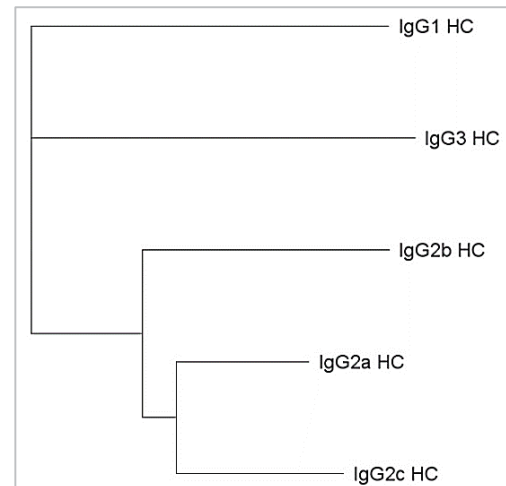


FIGURE 2.17. Phylogenetic tree based on the heavy chain sequences shown in Figure 5.25B. The tree was generated with Geneious 6 (Blosum 62 matrix).

TABLE 2.1. Sequence identity of the domains of the different IgG subclasses based on the heavy chain sequences shown in Figure 5.25B (Clustal Omega). The C_H2 – C_H3 interdomain sequence was not included.

Next, the polymorphism within an IgG subclass was analysed by using the NCBI *Basic Local Alignment Search Tool (protein blast)*. Variations in the amino acid sequence of the hinge and C_H2 region are shown in Figure 2.18. All allelic sequences of a specific subclass were highly similar exhibiting a sequence identity of 98 - 100%. For IgG2c, the sequence originating from the MAI mouse revealed a sequence identity of 94%. Because of the evolutionary distance, it was not included in the analysis; nevertheless, the sequence is shown in Figure 2.17. Additionally one database entry shared only an identity of 96% in the IgG2b subclass. In summary, no or very rare amino acid changes are found in the hinge and C_H2 region within the same IgG subclass. Therefore, the heavy chain sequences used for the generation of the recombinant mAbs represent the respective subclass present in (laboratory) mice strains allowing drawing general conclusions about the IgG subclass dependent FcγR activation in the mouse model.

As described, the amino acid sequence of IgG2a and IgG2c differs in 15% with most alterations in the hinge and C_H3 regions. It is still debated if IgG2c is an allelic variant of IgG2a or a separated gene and consequently a separate subclass. On the one hand, the high divergence IgG2a versus IgG2c was explained by a possible gene conversion of IgG2a with IgG2b gene (*Igh-3*) in certain mouse strains (Schreier et al., 1981; Ollo et al 1983) implying that IgG2a and IgG2c are allelic variants in majority strains of mice (Zhang et al., 2012; exception MAI strain: g2b - g2c - g2a; Morgado et al., 1989). The other theory suggests that a duplication of the ancestral IgG2a/c locus gave rise to IgG2a and IgG2c as

separated subclasses encoded by tandemly arranged genes. Both subclasses are commonly present in natural population of mice (e.g. certain European, East Asian, Japanese, Chinese, Indian wild mice) while one gene was deleted in most inbred mouse strains (IgG2a [*Igh1a*, *c*, *d*, *e*, or *j*]: BALB/c, C58, 129, DBA/2, RF, AKR, NZB, C3H, PL/J, NMRI; IgG2c [*Igh-1b*]: C57BL/6, C57BL/10, SJ, SM/J, NOD; Morgado et al., 1989 and 1993; Jouvin-Marche et al., 1989; Martin et al., 1997; Dognin et al., 1981). To mention, no mice containing IgG2b-IgG2c were found in the natural population (Jouvin-Marche et al., 1989). For simplification, IgG2a and IgG2c were referred as different subclasses in this work, but the controversial origin of the genes has to be kept in mind.

<p>IgG1 $\Sigma 53$ (99-100%)</p> <p>Hinge</p> <p>PRDCG^{-CG}CKPCICTVPEV</p> <p>C_H2</p> <p>SSVFIFPPKPKDVLITITLPKVTCTVVVDISKDDPEVQFSWFVDDVEVHTAQT^{K(10)}PREEQ^{H(5)}NSTFRSVSELPIMHQDWL^PNGKEFKCRVN SAAFPAPIEKTIS</p>
<p>IgG2a $\Sigma 26$ (98-100%)</p> <p>Hinge</p> <p>PRGPTIKPCPPCKCPAPNLLGG</p> <p>C_H2</p> <p>PSVFIFPPKIKDVLMLISLSP^{M(14)}VTCVVVDVSEDDPDVQISWVFNNEV^{H(12)}TAQTQTHREDYNSTLRVVSALPIQHQDWMMSGKEFKCKV NNK^{D^{A(10)}}LPAPIERTIS</p>
<p>IgG2b $\Sigma 17$ (96, 98-100%)</p> <p>Hinge</p> <p>PSGP^ITSTINPCPPCKECKCPAPNLEGG</p> <p>C_H2</p> <p>PSVFIFPPNIKDVLMISLTPKVTCTVVVDVSEDDPDV^{RQ(14)}ISWVFNNEV^HTAQTQTHREDYNSTIRVVS^{A^{H(1)}T(8)}LPQHQDWMMSGKEFKC KVNNKDLPS^APIERTIS</p>
<p>IgG2c $\Sigma 8$ (98-100%)</p> <p>Hinge</p> <p>PRVPITQNPCPPLKEC^{HQ^{RV}}PPCAAPDLLGG</p> <p>C_H2</p> <p>PSVFIFPPKIKDVLMLISLSPMVTCTVVVDVSEDDPDVQISWVFNNEVHTAQTQTHREDYNSTLRVVSALPIQHQDWMMSGKEFKCKVNNRA LPSPIEKTIS</p>
<p>IgG3 $\Sigma 7$ (99-100%)</p> <p>Hinge</p> <p>PRIPKPSTPPGSSCPPGNILGG</p> <p>C_H2</p> <p>PSVFIFPPKPKDALMISLTPKVTCTVVVDVSEDDPDVHVSFVDNKEVHTAWTQPREAQYNSTFRVVSALPIQHQDWMRGKEFKCKVNNK ALPAPIERTIS</p>

FIGURE 2.18. Amino acid polymorphism within in the hinge and C_H2 domain of the IgG subclasses. A. The sequences were identified by *NCBI protein blast* in database of non-redundant protein sequences for *mus musculus* (taxid 10090). The query sequences were the heavy chain sequences present in the pFUSE vectors of InVivogen and the newly cloned IgG2c heavy chain (4.7.4.1.). Sequences with a cover of $\geq 98\%$ (IgG1 $\geq 99\%$) and a sequence identity of $> 86\%$ were compared. Amino acid substitutions are coloured in green and the superscript specifies the alternative amino acids with the number of affected sequences in brackets. The light green colour indicates that the amino acid substitution was only present in one sequence. Grey color marks one IgG2b HC sequence with a sequence identity of only 96%; – deletion, + insertion, Σ number of compared sequences with the sequence identity comparing the whole sequence in brackets. Missing of one or two AA at the N- and C-terminus was not included. C_H1-C_H3 annotation from P0186/Figure 2.25B, bold N: N-glycosylation side at Asn297. All domains and NCBI sequence identification numbers (gi) are listed in the supplement (6.3.).

The positions of the anticipated Fc γ R binding site on the IgG molecules are displayed in Figure 2.19. The indicated binding sites were predicted by homology modelling to resolved human IgG-Fc γ R interactions and mutagenesis analysis (Hogarth et al., 2012; Arduin et al., 2015; Baudino et al., 2008a,

2008b, and 2008c; Caaveiro et al., 2015). The mutation of aspartic acid in the upper C_H2 domain (D265A) abrogates FcγR binding and *in vivo* activity for IgG1, IgG2a, and IgG2b (Baudino et al., 2008b). The natural three amino acid deletion in the lower hinge of IgG1 is partially responsible for its inability to engage FcγRIV. Replacement of the lower hinge of IgG1 with the sequence of IgG2b partially restored binding to FcγRIV (same affinity as for FcγRIII, but less than wt IgG2b for FcγRIV), increased binding to FcγRIII, but did not alter affinity to FcγRIIB. Deletion of these three amino acids in IgG2b strongly diminishes binding to all FcγRs indicating that IgG1 might have a unique interaction side with FcγRIIB and lacks an integration site for FcγRIV. These changed affinities translated to a moderate increased activity *in vivo* for mutated IgG1 and a reduction of activity of mutated IgG2b to wt IgG1 level (Baudino et al., 2008a). Furthermore, the second leucine in this region is involved in the high affinity binding of IgG2a to FcγRI (Baudino et al., 2008c) and the mutation of both leucines reduced binding to all FcγRs (Arduin et al., 2015). Both leucines are conserved in IgG2c but in no other IgG subclass.

To note, although most differences are located in the upper and core hinge of the IgG subclasses, the FcγR binding sites are located in the lower hinge and C_H2 region (1.2.3.4.; Figure 2.19). Still, the lower hinge is the most diverse in comparison of all binding sites. Surprisingly, binding sites seem to be conserved in the IgG3 subclass although it does not activate FcγRs indicating that not only the amino acid sequence determines binding affinity to FcγRs. To mention, the Fab arm flexibility and spanning distance is dependent on the length of the upper hinge, which ranges from five to 10 amino acids for mouse IgG subclasses. For low epitope density, this might also affect the functionality of the different subclasses.

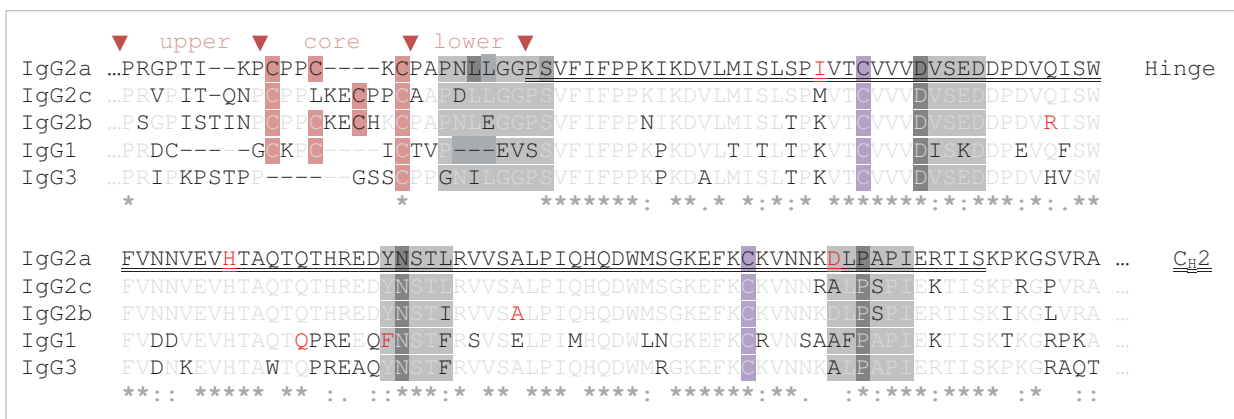


FIGURE 2.19. Anticipated FcγR binding sites on the basis of crystallographic homology modelling to human IgG1 with FcγRII/IIIA and mutagenesis analysis and flanking amino acids are displayed as grey boxes (Hogarth et al., 2012; Arduin et al., 2015; Baudino et al., 2008a, 2008b, and 2008c). Not all amino acids interact with the FcγRs and important amino acids are marked dark grey, e.g. the N-glycosylation site. FcγRs interact with the hinge of both IgG heavy chains, C_H2 located box 1 and 2 on one heavy chain and box 3 on the other chain. Amino acid polymorphisms found in at least two sequences (see A) are highlighted red. Cysteines participating in inter- and intra-chain disulphide bonds of the heavy chains are marked red and purple respectively.

SUMMARY

- The position of the cysteine residues forming the intrachain disulphide bonds and the N-glycosylation site (Asn297) are highly conserved among all subclasses
- The IgG subclasses differ most in the hinge region (amino acid sequence, length, number of disulphide bonds).

- *Only very little polymorphic variations within one subclass exist.*
- *IgG2a and IgG2c are the subclasses most similar to each other and share the second highest sequence identity with IgG2b.*

2.4.2. Characterization of the parental mAb used for grafting of the variable domain: OKT8 mouse anti-human CD8 IgG2a_κ

The human hCD8 was chosen as a model antigen as described in 2.3.1. An available cell line producing a mouse anti-human CD8 mAb was the OKT8 hybridoma (Reinherz, 1980; ATCC Number: CRL-8014). The mAb is an IgG2a with kappa light chain and it binds to the extracellular domain of the CD8 alpha molecule. Before starting with the identification of the variable regions of the OKT8 mAb and grafting them on the different IgG subclasses (4.7.4.), the OKT8 hybridoma derived mAb was tested to fulfil the following requirements (6.4.): (1) secretion of mAb (6.4.1.), (2) binding of the mAb to its antigen (6.4.2.), (3) exclusion of any cross reactivity with mouse CD8 (6.4.2.). The OKT8 hybridoma was considered suitable.

2.4.3. Generation of an expression vector containing the IgG2c constant region

For the constant part of the heavy chain of IgG1, IgG2a, IgG2b, and IgG3 expression vectors were available (pFUSE, InVivogen). Accordingly, an expression vector with the IgG2c heavy chain was generated using cDNA from C57BL/6 splenocytes (4.7.4.1.). The cloned coding sequence was compared to sequences available in databases (Table 4.6.). The multiple alignments of chosen sequences is shown in Figure 2.20 revealing a complete identity to most sequences and only a variation in maximal 6% of the amino acid residues among some of the IgG2c alleles.

2.4.4. *In silico* predication of N- and O-glycosylation sites in the OKT8 Fv

In approximately 20% of IgGs (Jefferis, 2007) the variable domains (Fv) exhibits a potential N-glycosylation site with the consensus motif: NX[S,T], X≠P. Nevertheless, the existence of the consensus motif does not guarantee the usage of this site e.g. because structural properties may influence their accessibility. In contrast to Fc-associated carbohydrate, the function of Fv glycosylation is not well characterized. It can affect stability, half-life, and binding characteristics of Abs and BCRs. The Fv being glycosylated would add another layer of complexity for the mAb production process since it was shown that the origin of the producing cell line influence the glycan structure (1.2.3.5.) and this may alter the antigen binding properties of the mAb. The identified sequences for the OKT8 VH and VL (4.7.4.2.) were analysed with the NetNGlyc1.0 Server and the NetOGlyc4.0 Server (Steentoft et al., 2013) to predict potential N- or O-glycosylation sites respectively. The OKT8 VL contains the motif NQSP (positions 25-28) but this one was predicated to be non-glycosylated due to the 28P. No further N- or O-glycosylation sites were found.

SUMMARY

- *No N- and O-glycosylation sites were predicted in variable regions of the OKT8 mAb.*

However, investigating here the role of the IgG subclasses for FcγR activation in the murine system, the recombinant OKT8 antibodies should be equipped with “murine” glycans. Resembling the natural situation as closely as possible, the recombinant OKT8 mAbs were produced in a murine myeloma cell line (4.7.4.4.), although the glycosylation can change in cancer cells (Hu et al., 2014). In addition, the recombinant OKT8 mAbs were produced in HEK293T and CHO transfectants (4.7.4.3.). A myeloma cell line consists of cancerous plasma cells, which are immortal and do not produce antibodies. Typically, they are used to create hybridoma cells by fusion of the myeloma cells with IgG secreting plasma cells isolated from immunized mice. In addition, they are suspension cells facilitating the production of larger amounts of supernatant. Because transfection of DNA into murine cell lines is ineffective, pseudotyped lentiviral particles were used to transduce the murine myeloma line enabling the stable expression of the recombinant OKT8 mAbs genes due to their integration into the cell genome. Therefore, the OKT8-HC and OKT8-LC genes were inserted into the lentiviral transfer vector puc2CL6IPwo or puc2CL6INwo respectively and the myeloma cell line P3X63Ag8.6533 (ATCC CRL-1580), which is abbreviated here as P3X, was transduced with the generated lentiviral particles (4.3.5.2.).

First, a small volume of IgG containing supernatant was produced and the expression, secretion, and antigen binding of the recombinant OKT8 IgG switch variants produced in the different cell lines were verified (4.7.4.5.). Next, the recombinant OKT8 mAbs were purified and concentrated by Protein G chromatography from a larger volume of supernatant (4.7.4.6.).

2.4.6. Absence of immune complex resembling IgG aggregates in the purified recombinant OKT8 mAb preparations

During cell culture and purification of mAbs, IgG aggregates can be formed e.g. by the interaction of partially unfolded molecules. These aggregates resemble immune complexes. Consequently, they are highly potent in FcγR activation in absence of the antigen. The amount of intracellular IgG aggregation varies between hybridoma cell lines. Furthermore, environmental conditions and the purification process may also cause aggregation e.g. due to suboptimal pH; for instance during the acidic elution from the Protein G affinity chromatography column.

To analyse the purified mAbs, native PAGEs (4.2.6.) and analytical Size Exclusion Chromatography (SEC, 4.2.7.3.) were performed. In a native PAGE, non-reducing and non-denaturation conditions allow the separation of whole protein complexes such as antibodies in a porous gel matrix by applying an electric field. The electrophoretic mobility of a protein complex is dependent on the molecular weight, shape and charge. The proteins were visualized by Coomassie staining (4.2.4.). A more sensitive method is the SEC, whereat the porous column matrix determines the accessibility and therefore the retention of different sized molecules. Here the SEC was performed with a Superdex 200 10/300 GL (GE Healthcare) in an analytical scale.

2.4.6.1. IgG aggregates are present in the OKT8 hybridoma supernatant

The OKT8 hybridoma produces IgG aggregates, which can be observed in the self-made as well as in the commercially available OKT8 mAb preparations (eBioscience) (Figure 2.21 and 2.23). A ladder of bands is visible in the native PAGE consisting of monomers, dimers and higher aggregates, which correspond to the peaks in the SEC elution profile (Figure 2.21). The void volume (V_0) of the column was approx. 9,5 ml. Therefore, all complexes with a molecular weight > 600 kDa are eluted with the V_0 . There is a delay comparing the OD values of the SEC elution profile and the concentrations of the

fractions caused by the distance of the UV flow cell measuring the OD and the fractionation. The Protein G purified OKT8 mAbs from the hybridoma were used in the following analyses as standard to define the size of IgG aggregates.

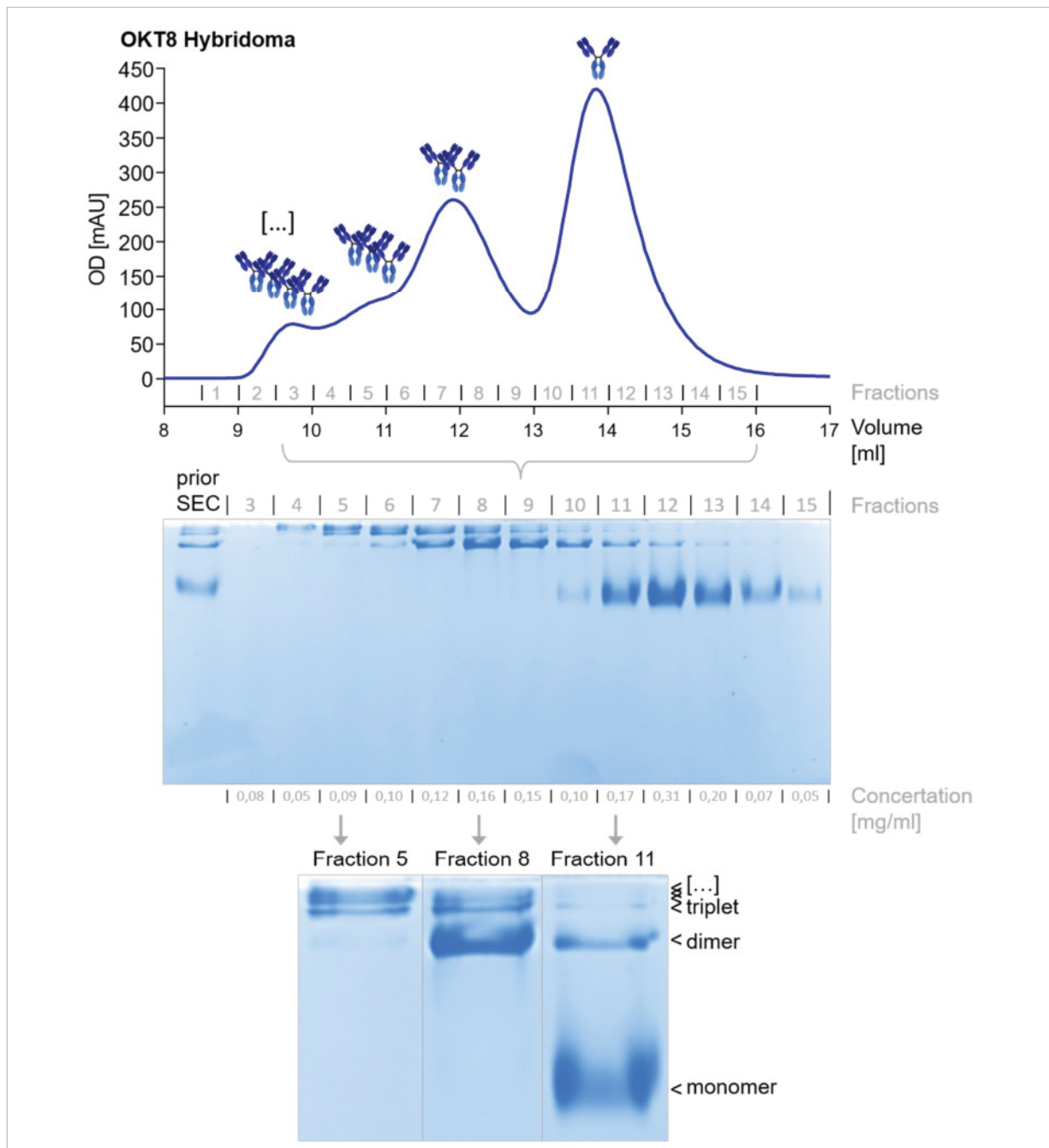


FIGURE 2.21. The OKT8 hybridoma cell line produces IgG aggregates detectable by Size Exclusion Chromatography and native PAGE. 250 µg of the Protein G purified OKT8 mAb preparation was separated by SEC (Superdex 200 10/300 GL, GE Healthcare). 0,5 ml fractions were collected, 40 µl was separated by 10% PAA PAGE for 4 h, and stained with colloidal coomassie (InstantBlue, Expedeon). 8 µg of Protein G purified OKT8 mAb was applied as control (prior SEC). The sizes of the eluted IgG aggregates of the corresponding SEC peaks are indicated by the number of IgG molecule which were estimated on the basis of the native PAGE. The protein concentration was determined based on the absorption at 280 nm.

2.4.6.2. IgG aggregates are capable to activate FcγR in the absence of antigen

IgG aggregates resemble immune complexes and are able to activate FcγRs in the absence of antigen as shown in Figure 2.22. The FcγR reporter cell activation by the Protein G purified OKT8 hybridoma supernatant (Figure 2.21, sample “prior SEC”) was compared on HeLa cells and HeLa cells expressing the hCD8 antigen (HeLa hCD8). This OKT8 mAb preparation was capable of activating the reporter cells

dose-dependently in the absence of hCD8 antigen. However, a higher concentration of the OKT8 mAbs was required in the absence of the antigen to achieve reporter cell activation to comparable level that was obtained in the presence of the antigen. In the presence of the antigen, immune complexes are formed by monomeric IgGs in addition to the already existing IgG aggregates. This leads to a stronger Fc γ R reporter cell activation than in the absence of the antigen. Of course, also the IgG aggregates can bind their antigen resulting in the formation of even larger complexes. However, if the size of the immune complexes also influence the magnitude of Fc γ R activation is not predictable from this experiment. Therefore, the preparation of aggregate free mAbs is crucial to study Fc γ R activation *in vitro* and especially *in vivo*.

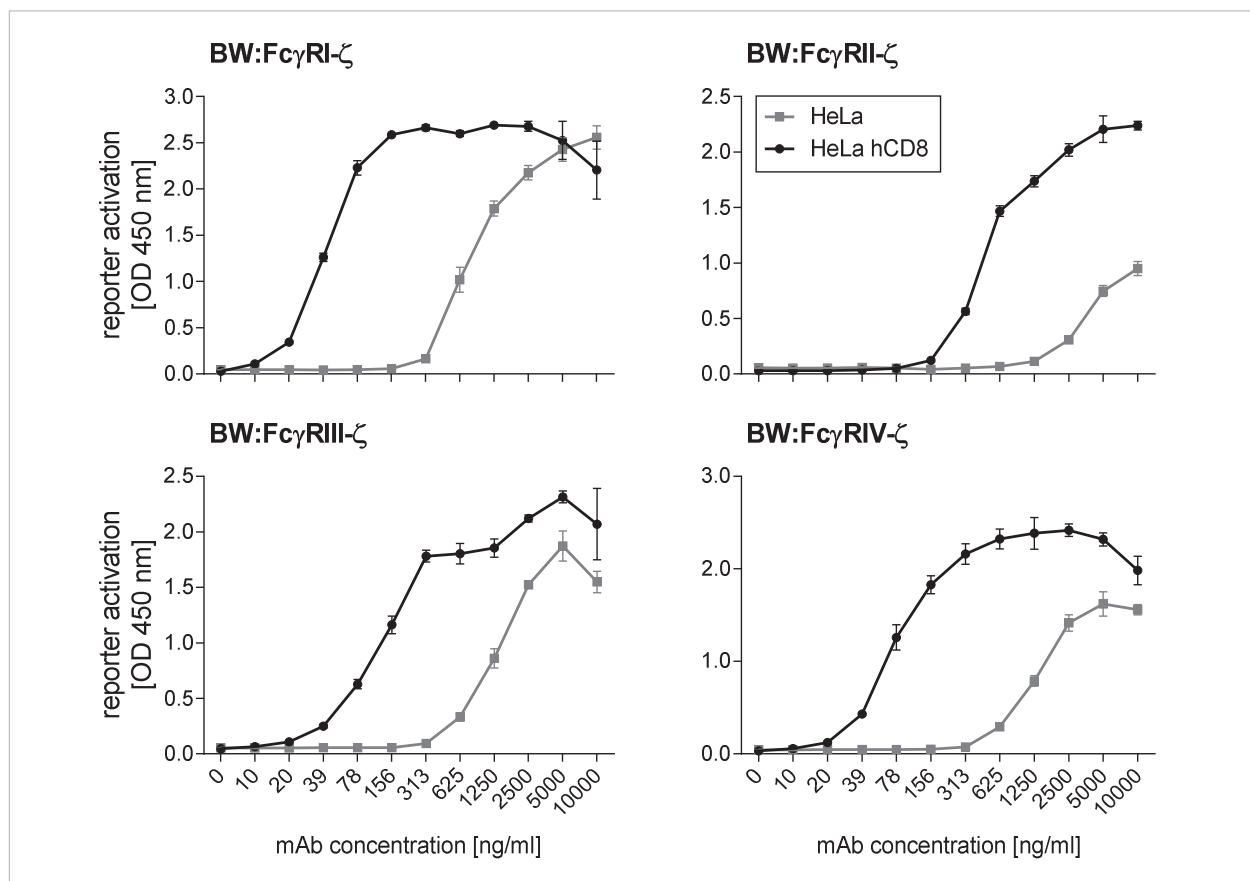


FIGURE 2.22. IgG aggregates activate the BW:Fc γ R- ζ cells in the absence of antigen. HeLa or HeLa hCD8 cells were opsonized with graded dilutions of Protein G purified OKT8 hybridoma supernatant and co-cultivated with and 2×10^5 reporter cells overnight. IL-2 was quantified in a sandwich ELISA. Colorimetric reaction was stopped after 40 s for BW:Fc γ RI- ζ , 130 s for BW:Fc γ RII- ζ , 75 s for BW:Fc γ RIII- ζ , and 50 s for BW:Fc γ RIV- ζ . Triplicates were measured. The data were analysed with GraphPad Prism and means with SD are shown. One out of two experiments is shown.

2.4.6.3. IgG aggregates are absent in the recombinant OKT8 mAb preparations

The next step was to assure the absence of IgG aggregates in the recombinant OKT8 mAb preparations. Analysing the recombinant OKT8 mAbs produced in HEK293T, CHO, and P3X cells by native PAGE, no IgG aggregates were visible in contrast to the OKT8 hybridoma derived preparations (Figure 2.23). Moreover, the band representing monomeric IgG molecules was diffuse in comparison to the OKT8 hybridoma derived mAbs but similar to mouse IgG, which was purified from serum. The absence of aggregates in the recombinant OKT8 mAb preparations was confirmed by SEC (Figure 2.24E- G). The retention volumes (V_R) of the recombinant OKT8 mAbs were comparable to the V_R of IgG from mouse serum and the monomeric fraction of the OKT8 hybridoma derived mAbs. The same amount of mouse serum IgG was analysed multiple times to illustrate the reproducibility of the

method (Figure 2.24A). Furthermore, graded concentrations of OKT8 hybridoma derived mAbs demonstrate the different sized IgG aggregates, i.e. their V_R , and the concentration dependency of the peak height (Figure 2.24B). Moreover, the SEC supports the accuracy of the concentrations of the recombinant OKT8 mAbs, which were determined based on the adsorption at 280 nm (4.2.1.).

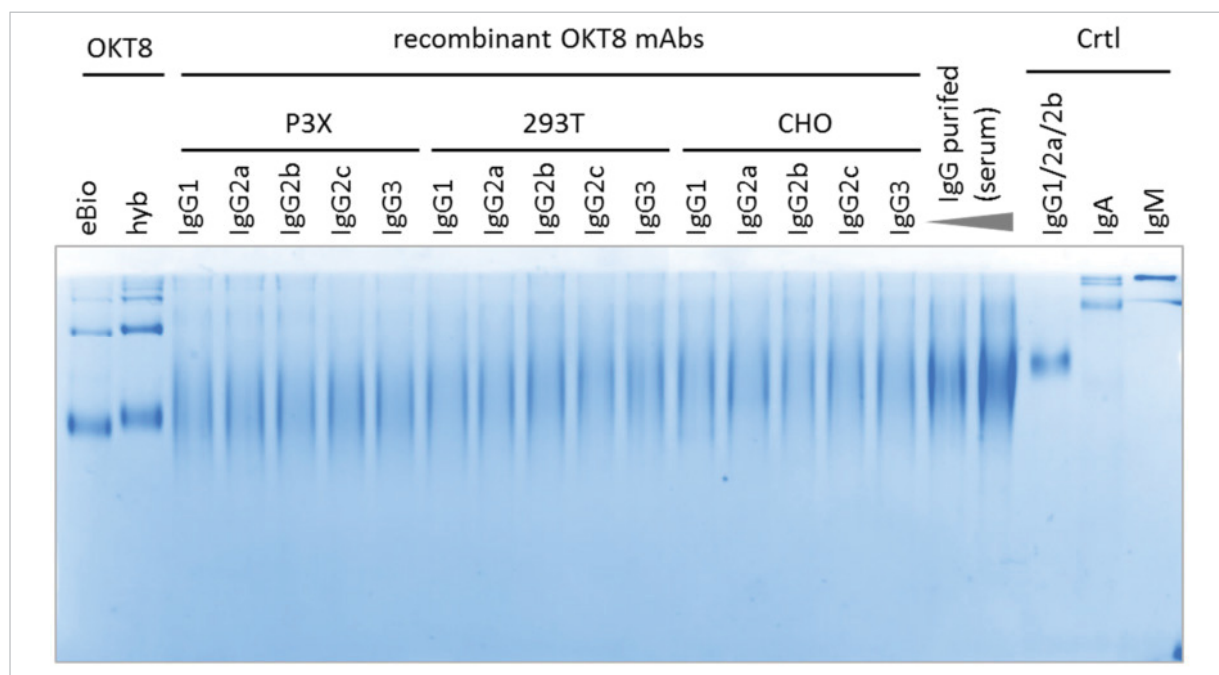


FIGURE 2.23. Absence of IgG aggregates in purified recombinant OKT8 mAbs. 4 μ g of recombinant OKT8 mAbs were separated by 10% native PAGE for 3,5 h and stained with colloidal Coomassie (InstantBlue, Expedeon). As controls, 4 μ g Protein G purified (hyb) or commercially available (eBio) OKT8 mAbs and purified mouse serum IgG (5,7 and 8,6 μ g; ChromePure, Dianova) were applied. The molecular weight is indicated by the Ig class specific controls IgG: ~150 kDa, IgA: ~350 kDa, IgM: ~900 kDa (2 - 2,5 μ g; Southern Biotech).

SUMMARY

- High amounts of IgG aggregates are present in the OKT8 hybridoma supernatant.
- The hybridoma derived OKT8 IgG aggregates are capable to activate all $Fc\gamma R$ s in the absence of their antigen.
- No IgG aggregates were detectable in the recombinant OKT8 mAb preparations (SEC, native PAGE)

2.4.6.4. Antibodies from different sources exhibit dissimilar electrophoretic mobility in native PAGE

Detecting the different migration properties of the IgG bands in the native PAGE for antibodies derived from the OKT8 hybridoma vs. the recombinant and serum purified IgGs (Figure 2.23), a larger spectrum of antibodies from different sources was analysed (Figure 2.25). MABs derived from hybridoma cell lines, which were produced in cell culture or as ascites, exhibit a more condensed band with different electrophoretic mobility. To note, both analysed OKT8 preparations formed aggregates but the electrophoretic mobility seemed to be slightly different. IgGs derived from MCMV infected BALB/c mice showed comparable characteristics as the recombinant OKT8 mAbs and the mouse serum IgG. The dissimilar electrophoretic mobility of IgGs derived from diverse sources suggested that the N-glycan present in the Fc part might differ. An additional glycosylation located in the variable regions (2.4.4.) may also increase the molecular weight of a particular mAb. Nevertheless, the migration properties of the band for the recombinant OKT8 mAbs and the mouse serum derived IgGs might suggest that the glycans of these antibodies are more heterogeneous than of IgGs derived from hybridoma cell lines. A differential glycan composition could be verified as cause for the different

migration properties if the mAbs, after enzymatic deglycosylation, show comparable electrophoretic mobility that represents the molecular weight of their amino acid backbones.

SUMMARY

- Antibodies from different sources exhibited dissimilar bands (broadness, mobility) in native PAGE.
- The recombinant OKT8 mAbs displayed a broad band and mobility comparable to IgG purified from mouse serum in contrast to hybridoma-derived mAbs.

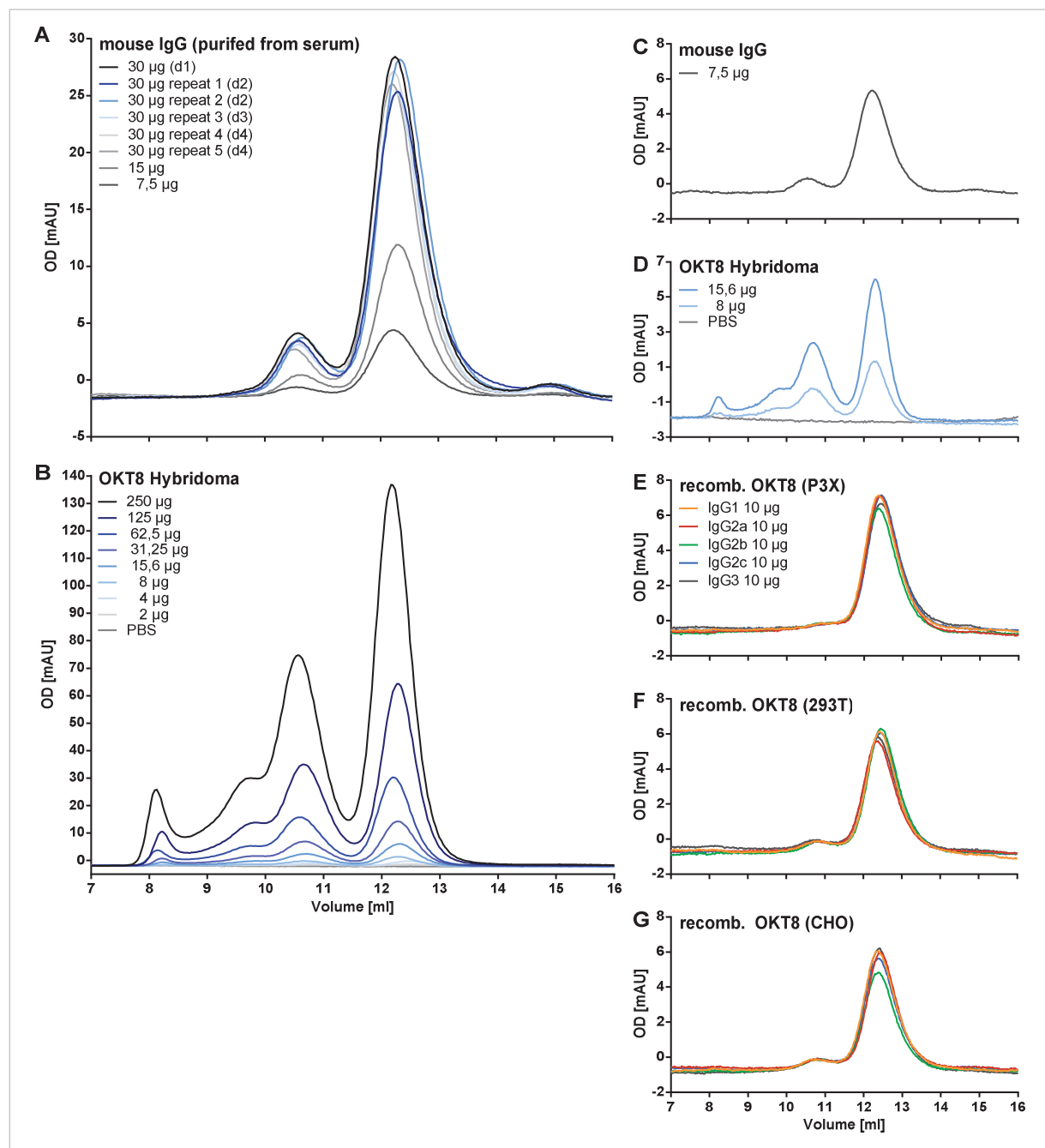


FIGURE 2.24. Detection of IgG aggregates and monomers by analytical Size Exclusion Chromatography. Indicated amounts of IgG were separated by a Superdex 200 10/300 GL column (GE Healthcare) ($V_0 \sim 7.8$ ml). A. Elution profiles of purified IgG from mouse serum (ChromPure, Dianova). Repeated measurements at different days (d) demonstrate the reproducibility. B. Elution profiles of graded amounts of Protein G purified OKT8 mAbs indicate the different sized IgG aggregates and the concentration dependency of the peak height. E-F. Elution profiles of the recombinant OKT8 mAbs produced in P3X, HEK293T, or CHO cells in comparison with similar amounts of purified mouse IgG (C) and purified OKT8 mAbs (D) are shown. OD of the elution profiles were adjusted to OD at 9 ml of purified mouse IgG d1 (A), 7, 5 ml at OKT8 250 µg (B), and at 11 ml of IgG1 P3X (E), HEK293T (F) or CHO (G) respectively for the overlay.

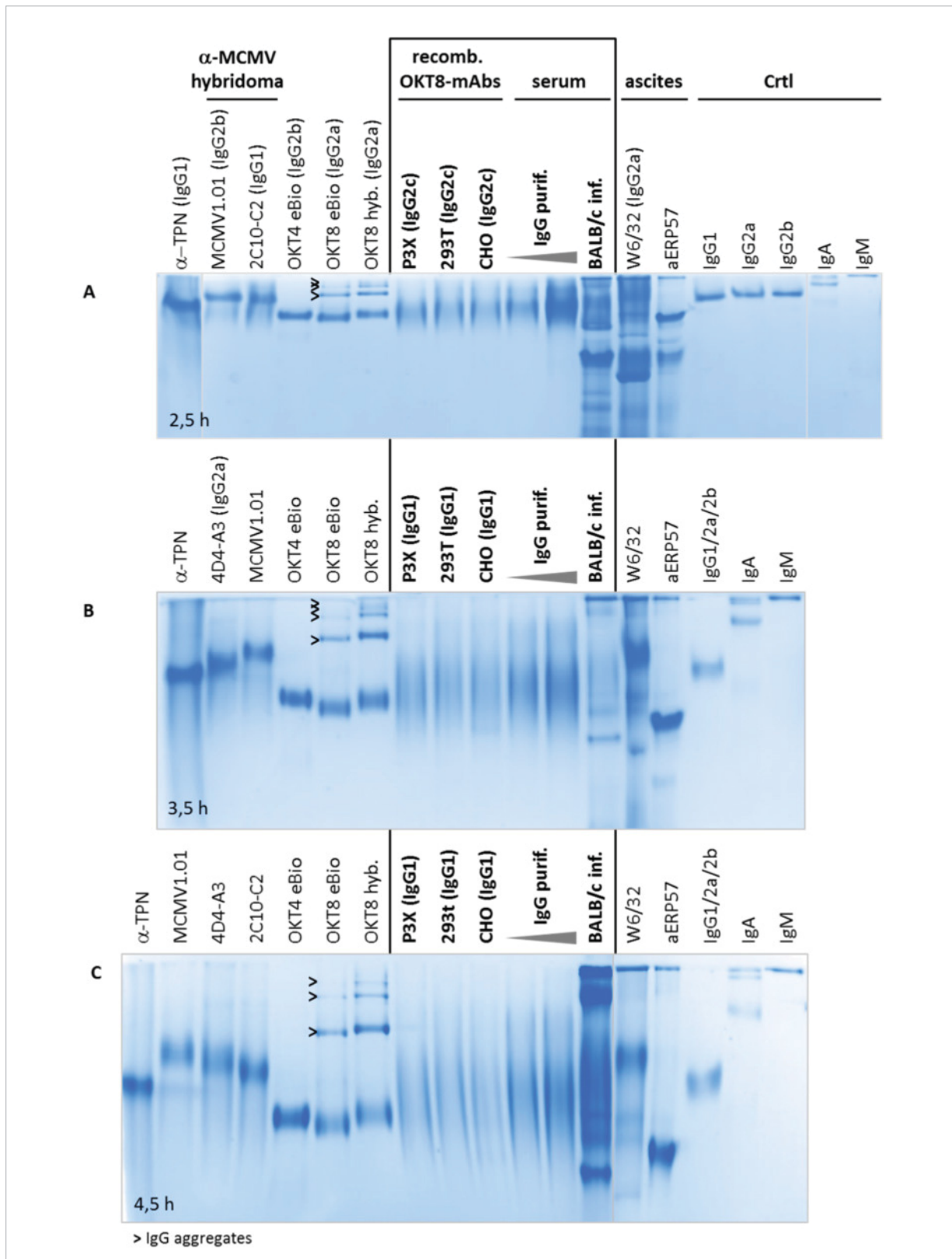


FIGURE 2.25. Antibodies from different sources exhibit dissimilar mobility in native PAGE. Antibodies were separated by 10% native PAGE for 2,5 (A), 3,5 h (B) or 4,5 h (C) and stained with colloidal Coomassie (InstantBlue, Expedeaon). Following amounts were applied: recomb. OKT8 mAbs, OKT8, OKT4 4 µg; anti-MCMV mAbs (MCMV1.01 anti-gB; 4D4-A3 anti-m46; 2C10-C2 anti-pp89) 2 - 4 µg; anti-TPN 4 - 5 µg; BALB/c MCMV immune serum 28 dpi and ascites 0,75 - 1 µl; purified mouse serum IgG 5,7 and 23 µg (A)/8,6 µg(B)/11,4 µg (C) (ChromPure, Dianova). The molecular weight is indicated by the Ig class specific controls IgG: ~150 kDa, IgA: ~350 kDa, IgM: ~ 900 kDa (2 - 2,5 µg; Southern Biotech).

2.5. IgG subclass dependent Fc binding to FcγRs

First, the IgG subclass dependent Fc binding of monomeric IgG to the FcγR-ζ was tested. Unbiased detection of different IgG subclasses is problematic when using secondary antibodies because these reagents recognize the different IgG subclasses with variable efficiency (4.7.4.5.). An anti-light chain antibody was also tested but was not suitable due to its poor performance. Another option is the direct (covalently) fluorophore labelling of the mAbs, but the concentration of the recombinant OKT8 mAbs was not sufficient. Therefore, the biotinylated IgG isotype panel from Genetex was used, which was detected with a fluorophore-coupled streptavidin (Figure 2.26).

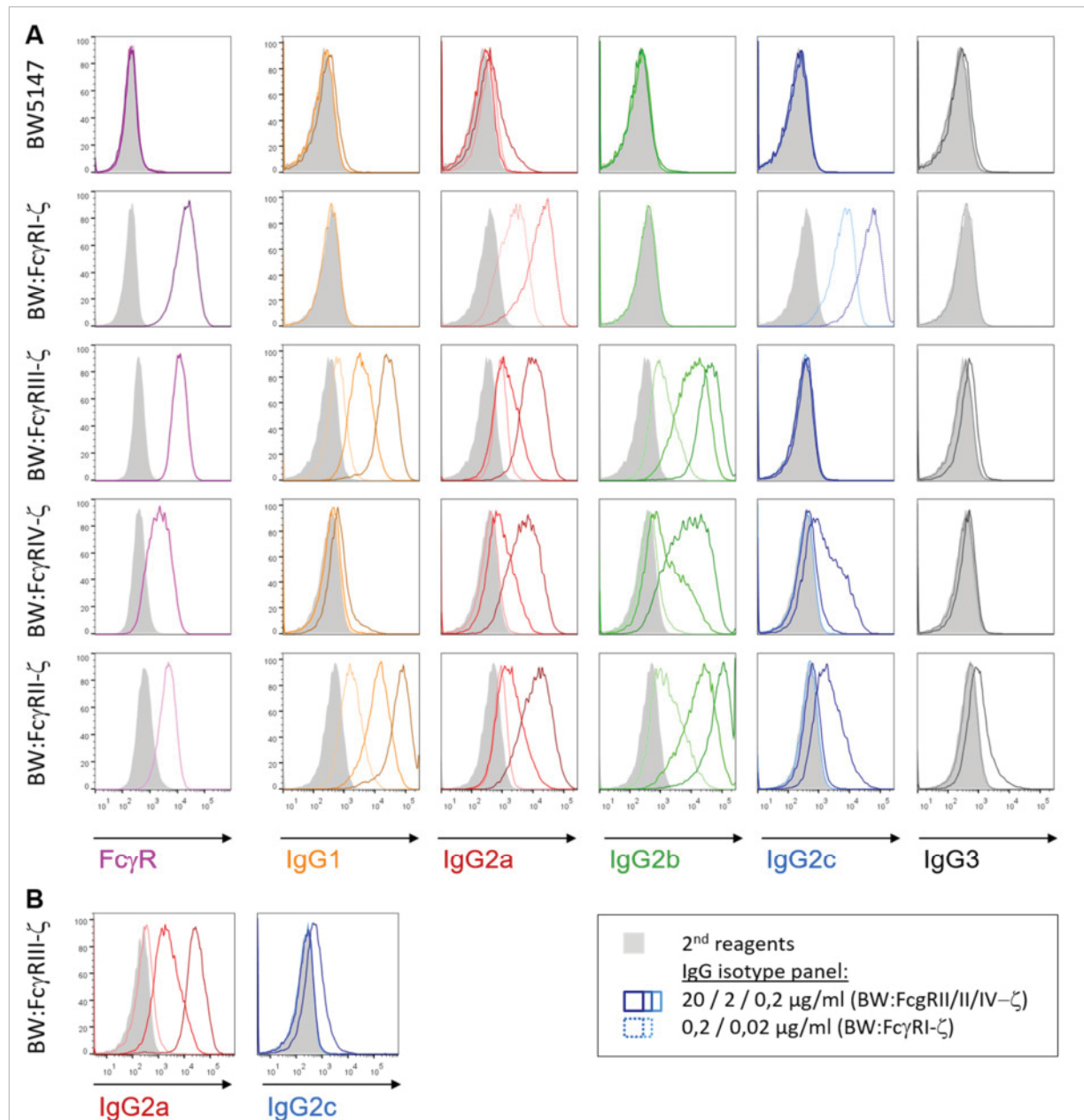


FIGURE 2.26. IgG subclass dependent Fc binding to BW:FcγR-ζ reporter cells. Parental BW5147 or BW:FcγR-ζ cells were stained with the respective anti-FcγR, which was detected with an goat anti rat FITC 2nd antibody, or with graded concentrations of the biotinylated IgG isotype panel from Genetex (20 μg/ml, 2 μg/ml, 0,2 μg/ml; BW:FcγRI-ζ 0,2 μg/ml, 0,02 μg/ml), which were detected with Streptavidin-APC. 3 x 10⁴ cells were measured by flow cytometry (BD FACS Canto II, FACS Diva software) and analysed with FlowJo (Tree Star Inc). Histograms represent living single cells in the FSC/SSC gate for the IgG isotype panel and single cells in the FSC/SSC gate for the FcγR staining. Detection reagent incubated cells are shown in grey / solid.

Parental BW5147 cells served as negative control. The high affinity BW:FcγRI–ζ strongly bound IgG2a and IgG2c and as expected, no binding of the other subclasses was detected. This cell line had to be incubated with reduced concentrations of the IgG isotype panel to remain within the detectable range emphasizing its high affinity IgG binding. BW:FcγRIII–ζ bound IgG1, IgG2a, and IgG2b. Binding of IgG2c was very weak and only occasionally detectable (Figure 2.26B). For BW:FcγRIV–ζ binding of IgG2a, IgG2b, and IgG2c was measurable whereas the BW cells expressing the inhibitor FcγRII as chimaera bound all IgG subclasses and surprisingly also to a small extent IgG3. IgG2c seems to be bind weaker than IgG2a to BW:FcγRIV–ζ and BW:FcγRII–ζ.

SUMMARY

- *Each of the BW:FcγR–ζ cell lines displayed a unique binding pattern of the individual (monomeric) IgG subclasses.*
- *BW:FcγRIII–ζ bound IgG2c surprisingly weak.*
- *BW:FcγRI–ζ bound IgG2a and IgG2c with high affinity.*
- *IgG2a was efficiently bound by all BW:FcγR–ζs, whereas IgG3 was not bound.*

2.6. P3X-derived recombinant OKT8 mAbs reveal a selective IgG subclass dependent FcγR activation pattern *in vitro*

The aim is the evaluation of the IgG subclass dependent activation of the distinct FcγRs (*in vitro*). The affinity of an antibody to its epitope and furthermore the location of an epitope within the antigen might influence the capability of this antibody to activate FcγRs. To be able to compare the IgG subclass dependency of the FcγRs activation independent these effects, recombinant mAbs possessing the same variable region or in other words mAbs recognizing the same epitope but possessing different IgG subclasses were generated (4.7.4.). A comparable systematic approach including both the IgG2a and the IgG2c subclass was not performed before. Furthermore, the fundamental principle is that FcγRs can only be activated in the presence of the antigen or more precisely by immune complexes avoiding unspecific activation by monomeric IgG. So far, most studies rely solely on the binding affinities of FcγRs to monomeric IgG measured by surface plasmon resonance (SPR). Here, the activation of FcγRs by immune complexes was analysed in this study taking advantage of the newly developed *in vitro* FcγR activation assay (2.2.). BW:FcγR–ζ reporter cells were co-cultivated HeLa hCD8 cells opsonized with P3X derived recombinant OKT8 mAbs bound to (Figure 2.27). The reproducibility of the *in vitro* FcγR assay concerning the cultivation duration of the reporter cells, the mAb batch, and different target cells lines was proven as well (6.5.).

The high affinity FcγRI–ζ was only activated by IgG2a and IgG2c whereas IgG2a was superior to IgG2c for lower concentrations. Similarly, FcγRIV–ζ was only strongly triggered by IgG2a and IgG2c whereby IgG2c seems to be slightly less efficient. Additionally FcγRIV–ζ was activated poorly by IgG2b. FcγRIII–ζ and FcγRII–ζ were activated by all IgG subclasses expect for IgG3. FcγRIII–ζ activation showed a clear functional rank (hierarchy) for the IgG subclasses of IgG2a > IgG1 > IgG2b = IgG2c while the inhibitory FcγRII–ζ was triggered comparable by IgG1, IgG2a, and IgG2c and only slightly less by IgG2b. Comparing biological repetitions (not shown), no differences in the activation capability were detected between IgG2b and IgG2c for FcγRIII–ζ and IgG2a and IgG2c for FcγRII–ζ. However, IgG1 was sporadically slightly less potent than IgG2a and IgG2c for FcγRII–ζ activation. For IgG3, no BW:FcγR–ζ activation was detectable for the tested concentrations. In addition, no activation of the reporter cells

was detected without mAbs or antigen (HeLa cells). The magnitude of activation cannot be compared between BW:FcγR-ζ cell lines for a distinct antibody sample because the FcγR-ζ expression cannot be standardized nor used to normalize activation. Nevertheless, it was observable that lower mAb concentrations were sufficient to activate the high affinity BW:FcγRI-ζ cells in contrast to the other reporter cell lines.

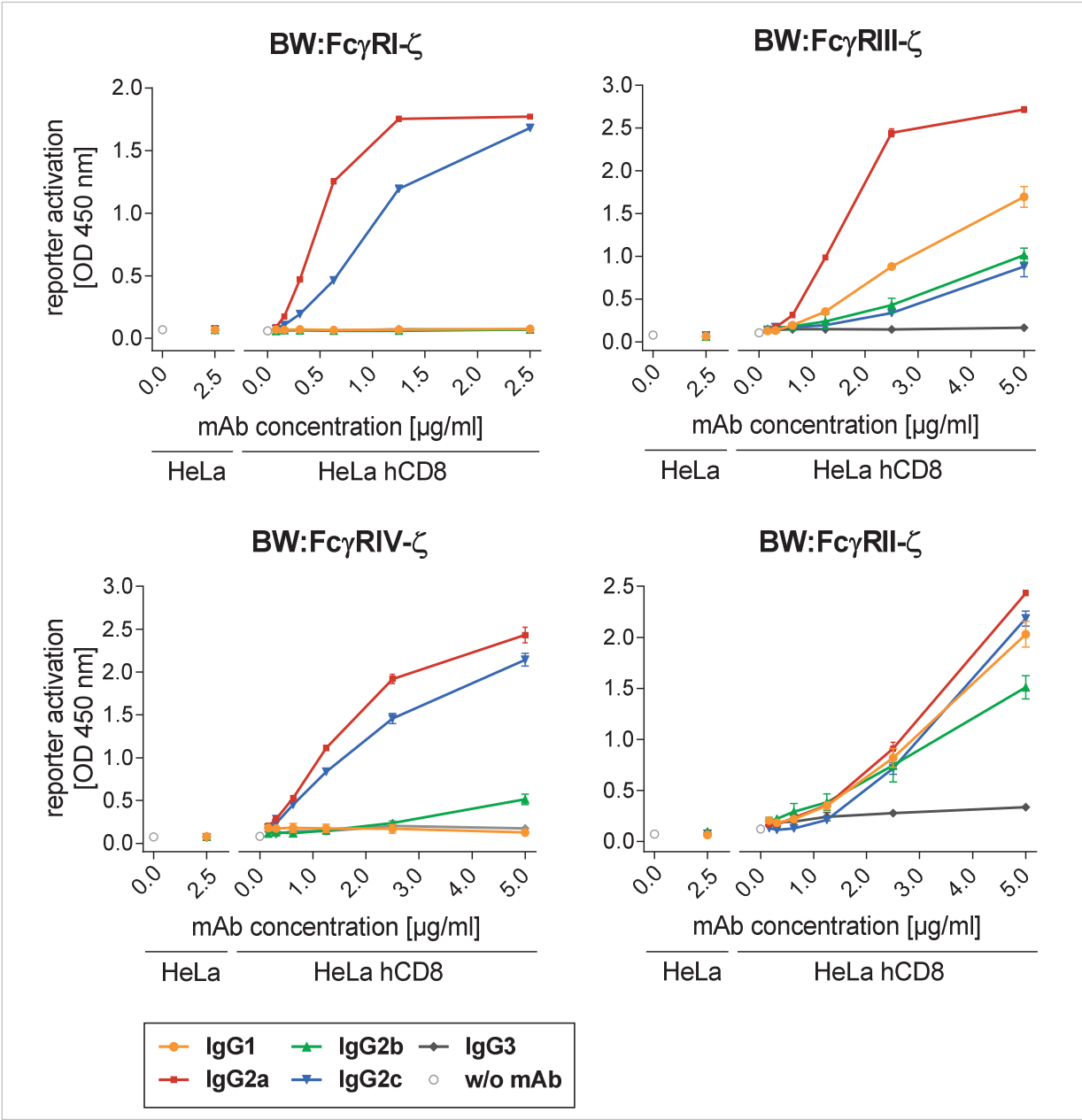


FIGURE 2.27. Recombinant OKT8 subclass switch mAbs (P3X) reveal a selective IgG subclass dependent FcγR activation pattern *in vitro*. HeLa hCD8 or HeLa cells were opsonized with grades concentrations of recombinant P3X derived OKT8 mAbs and co-cultivated with 2×10^5 reporter cells overnight. IL-2, the surrogate marker for FcγR-ζ activation, was quantified by sandwich ELISA. Colorimetric reaction was stopped after 40s for BW:FcγRI-ζ, 90s for BW:FcγRIII-ζ, and 100s for BW:FcγRII-ζ and BW:FcγRIV-ζ. Triplicates were measures. The data were analysed with GraphPad Prism and means with SD are shown. One representative out of minimum three experiments per reporter cell line is shown.

The next question was if weak FcγR activating IgG subclasses become capable to reach maximal FcγR activation like more potent IgG subclasses when their concentration is sufficiently increased. Unfortunately, the concentrations of the recombinant mAbs were limited so that they could not be significantly increased in the FcγR activation assay. Nevertheless, IgG2a reached saturating amounts

for the activation of BW:Fc γ RIII- ζ at the second highest tested concentration and IgG1 might have reached saturating concentration for the highest amount tested (Figure 2.28.). Increasing amounts of IgG2b and IgG2c are linear proportional to the BW:Fc γ RIII- ζ activation suggesting that saturated amounts and maximal activation of BW:Fc γ RIII- ζ are not reached for the tested concentrations of these two subclasses. It was ensured that all measured signals were in the linear range of the colorimetric reaction of the ELISA.

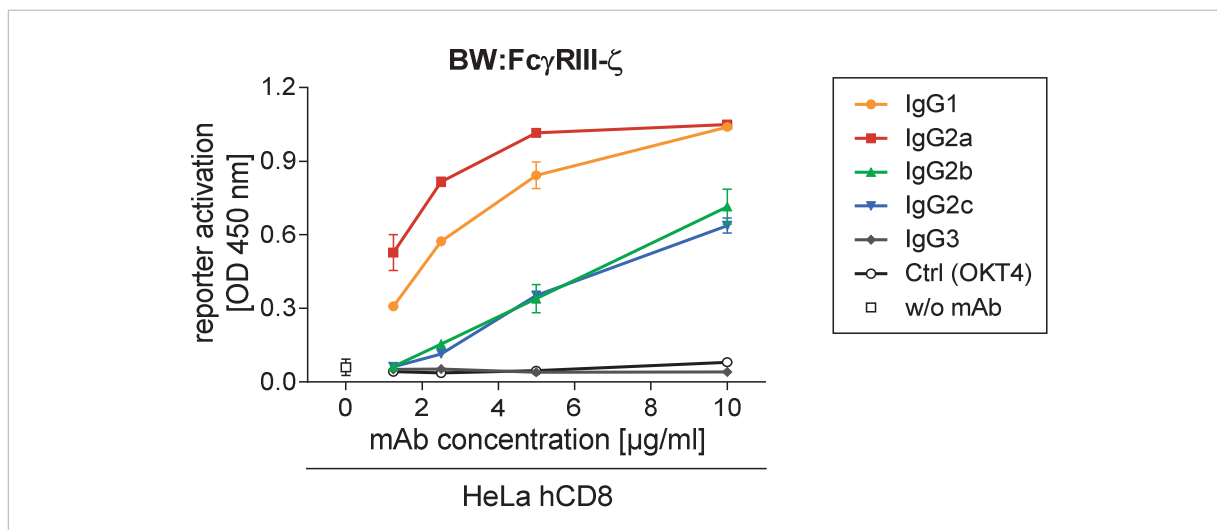


FIGURE 2.28. BW:Fc γ RIII- ζ can also be strongly triggered by weak activating IgG subclasses applying increased IgG concentrations. HeLa hCD8 were co-cultivated with graded concentrations of recombinant P3X derived OKT8 mAbs and 2×10^5 reporter cells overnight. As additional control OKT4, and mouse IgG2b anti-human CD4, was applied. IL-2, the surrogate marker for Fc γ RIII- ζ activation, was quantified by sandwich ELISA. Triplicates were measures. The data were analysed with GraphPad Prism and means with SD are shown.

SUMMARY

- Each BW:Fc γ R- ζ cell line displayed a unique activation pattern dependent on the IgG subclasses.
- BW:Fc γ RII- ζ and BW:Fc γ RIII- ζ were activated by all IgG subclasses except IgG3, whereby BW:Fc γ RI- ζ and BW:Fc γ RIV- ζ displayed a restricted IgG subclass specificity.
- As expected, IgG1 only triggered the activating Fc γ RI in addition to the inhibitory Fc γ RII.
- IgG2a was the most potent IgG subclass in activating all BW:Fc γ R- ζ cell lines.
- IgG2b activated BW:Fc γ RIII- ζ and BW:Fc γ RIV- ζ only weakly.
- IgG2c was only a weak activator for BW:Fc γ RIII- ζ , but it activated the other BW:Fc γ R- ζ s efficiently.
- As expected, no BW:Fc γ R- ζ activation was observed for IgG3.
- BW:Fc γ R- ζ s can be strongly triggered by weak activating IgG subclasses applying increased IgG concentrations as shown exemplary for BW:Fc γ RIII- ζ .

2.7. Influence of the cellular source of recombinant mAb for their Fc γ R activation capabilities

The cell line used for recombinant mAb production influences the Fc glycan composition, which itself may influence the Fc γ R activation due to its location on the C_H2 domain, which his part of the Fc γ R binding site (1.2.3.5.). Therefore, IgG subclass dependent Fc γ R activation was compared for the recombinant OKT8 mAbs produced in a mouse (P3X), human (HEK293T), and hamster (CHO) derived cell lines.

FcγRI

Independent of the cell line in which the mAbs were produced, only IgGs of the subclasses IgG2a and IgG2c were capable to trigger activation of BW:FcγRI–ζ at the tested concentration range (Figure 2.29 left panel). As observed before, P3X derived IgG2a was superior to IgG2c, which was also true for the CHO derived IgGs. The capability of IgG2c was strongly dependent on the producing cell line ranging from weak FcγRI activation if derived from CHO cells, almost as potent as seen for IgG2a derived from P3X, and even slightly more potent than IgG2a if derived from HEK293T cells.

FcγRIII

For BW:FcγRIII–ζ activation, a clear hierarchy of IgG2a > IgG1 > IgG2b = IgG2c was observable for P3X derived IgGs (Figure 2.30 left panel). In comparison, the HEK293T IgG1 had a greatly reduced capability to activate FcγRIII–ζ and HEK293T IgG2c might be marginally better than the corresponding IgG2b. The subclass dependent pattern changed dramatically when these mAbs were produced in CHO cells. Only IgG1 and IgG2a were capable of triggering BW:FcγRIII–ζ and IgG1 gained potential and activated FcγRIII–ζ as strong as IgG2a for the highest tested concentration. There might be minor activation of FcγRIII by CHO derived IgG2c for the highest antibody concentration tested, but this was not robustly reproducible.

FcγRIV

BW:FcγRIV–ζ was triggered by P3X and HEK293T derived IgG2a, IgG2b, and IgG2c (Figure 2.31 left panel). The weakest activation was seen for IgG2b from either P3X or HEK293T. The most potent subclass was IgG2a for P3X derived mAbs but IgG2c for mAbs origination from HEK293T cells. Similar to BW:FcγRI–ζ, CHO derived IgG2a seemed to gain whereas IgG2c lost potential for BW:FcγRIV–ζ activation. CHO derived IgG2b subclass was not capable of triggering FcγRIV–ζ in the tested concentration range.

FcγRII

FcγRII activation differed strongly for the mAbs dependent on the producing cell line. The activation of the inhibitory BW:FcγRII–ζ does not discriminate between the individual P3X derived IgG subclasses as strong as the activating BW:FcγRI–ζs (Figure 2.32 left panel). IgG1, IgG2a, and IgG2c lead to comparable FcγRII–ζ activation whereas IgG2b was a little less potent. All subclasses can still activate FcγRII if produced in HEK293T cell, but with a clear hierarchy of IgG2c > IgG2a > IgG2b > IgG1. The increased capability for HEK293T IgG2c in comparison to the corresponding IgG2a was also seen for the activation of BW:FcγRIII–ζ and BW:FcγRIV–ζ. CHO derived IgG1 and IgG2a were very potent activators of FcγRIIB even at low concentrations, whereby IgG1 was superior to IgG2a for lower concentrations. Moreover, CHO IgG2c was only a weak activator and IgG2b failed to trigger FcγRII–ζ.

To correlate the functional *in vitro* FcγR activation assays with affinity and furthermore the glycan composition, affinity measurements by SPR and glycoforms determination by MS based methods (Stadlmann et al., 2008) were undertaken, but the amounts of the purified mAbs were unfortunately not sufficient for valid results. Other methods like detection of certain glycoforms by lectins in Western Blot or analysing sialylation extent by IEF can be an option for small sample amounts but will give less information than MS.

SUMMARY

- *The Fc γ R activation capacity of a distinct IgG subclass was greatly influenced by the cell line in which the (recombinant) mAb was produced, which is presumably due to a differential glycan composition of the Fc portion.*
- *Some subclasses, like IgG1 and IgG2c, seemed to be more influenced by the cell line in which they were produced in than other subclasses, like IgG2a.*
- *P3X derived recombinant OKT8 mAbs demonstrated the most complex IgG subclass dependent Fc γ R activation pattern.*
- *HEK293T derived IgG1 lost and IgG2c strongly gained activating potential. IgG2c was superior to IgG2a in activating all Fc γ Rs except Fc γ RIII.*
- *CHO derived IgG2b failed to activate any Fc γ R, IgG1 generally gained while IgG2c lost potential in comparison to P3X derived mAbs.*
- *The BW:Fc γ RIII– ζ activation by IgG2c was always weak independent of the producer cell line.*
- *As expected, no BW:Fc γ R– ζ activation was detectable by IgG3 independent of the producer cell line.*
- *All Fc γ Rs were sensitive to changes in the Fc glycoforms and Fc γ RIIB seemed to be the slightly more affected than the other ones.*

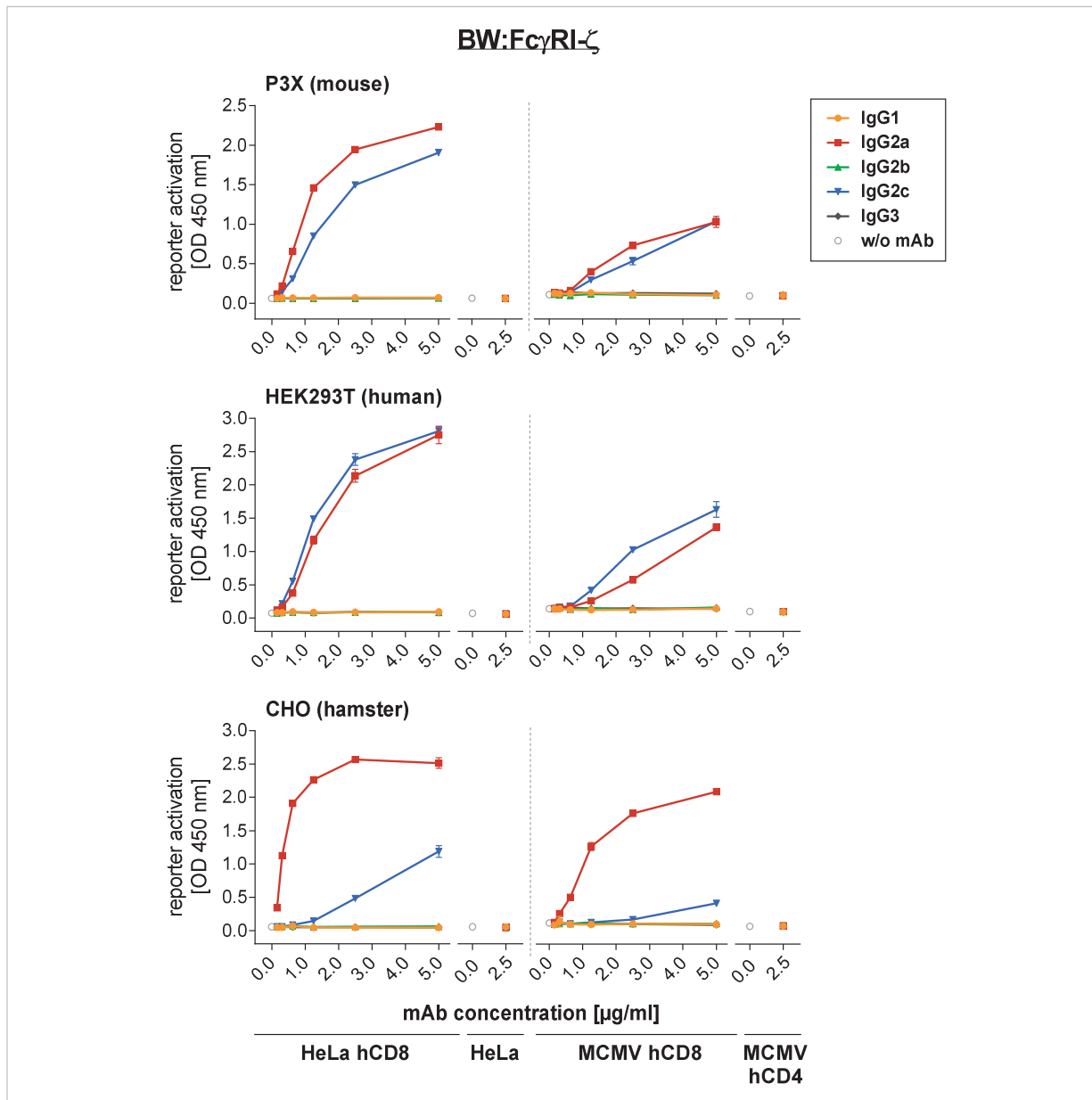


FIGURE 2.29. Influence of the mAb source and MCMV infection for selective IgG subclass dependent FcγRI activation pattern *in vitro*. Target cells were opsonized with grades concentrations of recombinant OKT8 mAbs produced in P3X (mouse), HEK293T (human), or CHO (hamster) cells and co-cultivated with 2×10^5 reporter cells overnight. Target cells were HeLa hCD8 or MCMV hCD8 infected MEF (MOI 1,5; 2 dpi) and HeLa or MCMV hCD4 infected MEF served as controls. IL-2, the surrogate marker for FcγR activation, was quantified by sandwich ELISA. Colorimetric reaction was stopped after 60s for OKT8 (P3X) and OKT8 (CHO), after 70s for OKT8 (HEK293T). Triplicates were measured and duplicates for the highest concentration and controls. The data were analysed with GraphPad Prism and means with SD are shown. One representative out of three experiments is shown.

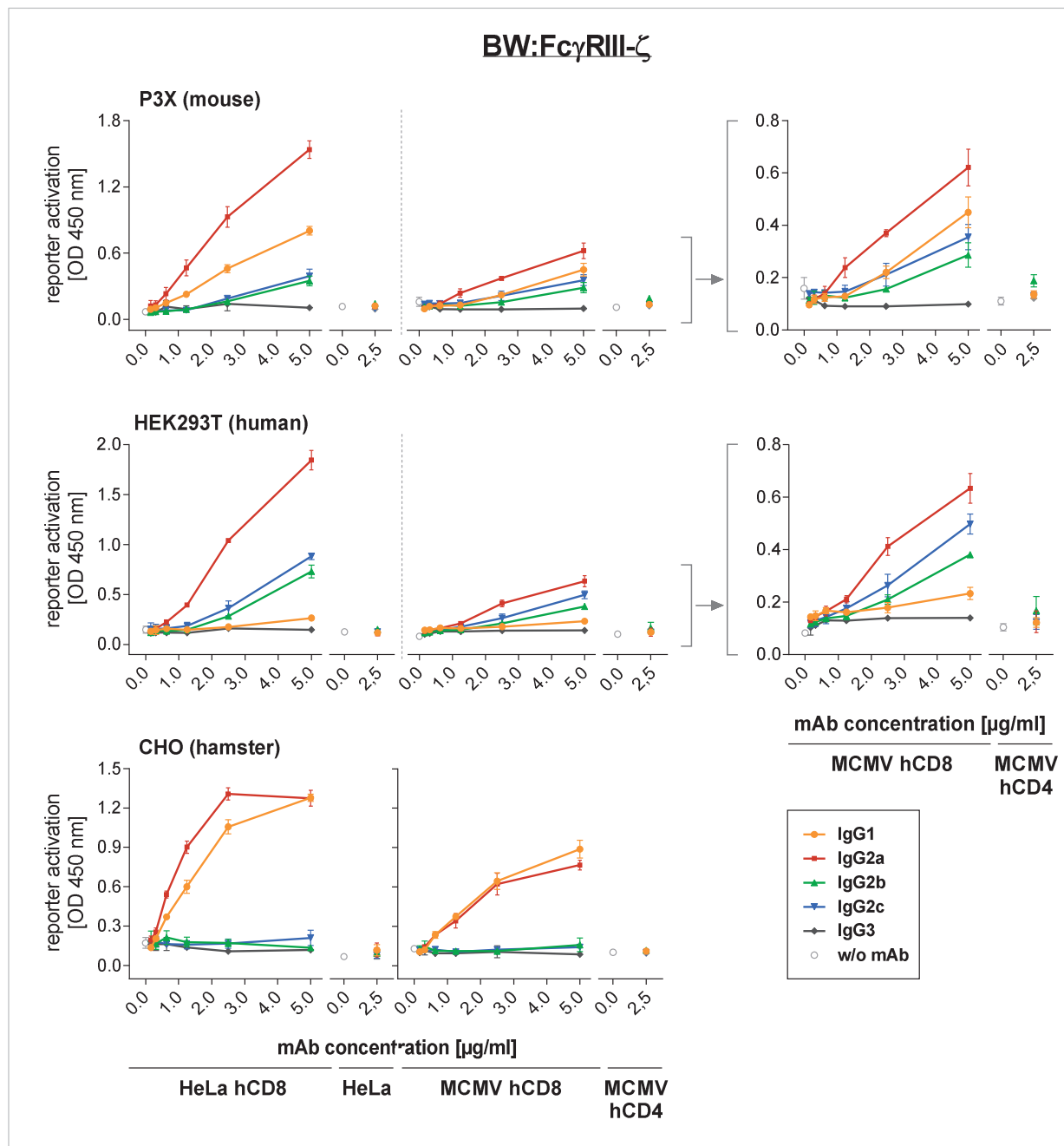


FIGURE 2.30. Influence of the mAb source and MCMV infection for selective IgG subclass dependent FcγRIII activation pattern *in vitro*. Target cells were opsonized with grades concentrations of recombinant OKT8 mAbs produced in P3X (mouse), HEK293T (human), or CHO (hamster) cells and co-cultivated with 2×10^5 reporter cells overnight. Target cells were HeLa hCD8 or MCMV hCD8 infected MEF (MOI 1,5; 2 dpi) and HeLa or MCMV hCD4 infected MEF served as controls. IL-2, the surrogate marker for FcγR activation, was quantified by sandwich ELISA. Colorimetric reaction was stopped after 120s for OKT8 (P3X), 160s for OKT8 (HEK293T), and 50s and 70s for OKT8 (CHO) on HeLa hCD8 and MCMV hCD8 infected MEF respectively. Triplicates were measured and duplicates for the controls. The data were analysed with GraphPad Prism and means with SD are shown. One representative out of four experiments is shown.

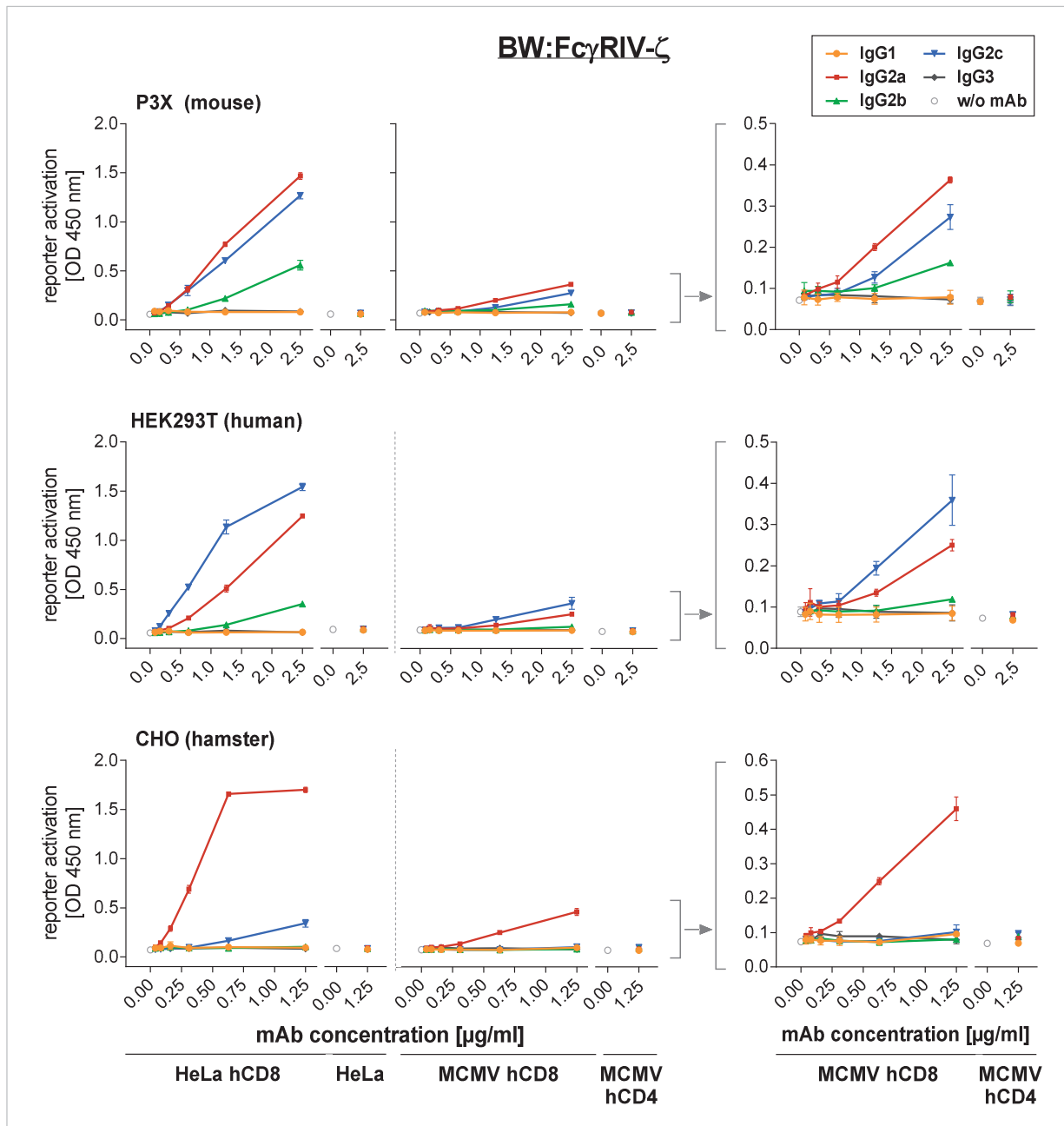


FIGURE 2.31. Influence of the mAb source and MCMV infection for selective IgG subclass dependent Fc γ RIV activation pattern in vitro. Target cells were opsonized with grades concentrations of recombinant OKT8 mAbs produced in P3X (mouse), HEK293T (human), or CHO (hamster) cells and co-cultivated with 2×10^5 reporter cells overnight. Target cells were HeLa hCD8 or MCMV hCD8 infected MEF (MOI 1,5; 2 dpi) and HeLa or MCMV hCD4 infected MEF served as controls. IL-2, the surrogate marker for Fc γ R activation, was quantified by sandwich ELISA. Colorimetric reaction was stopped after 90s except for OKT8 (P3X)/HeLa hCD8 after 60s. Triplicates were measured and duplicates for controls. The data were analysed with GraphPad Prism and means with SD are shown. One representative out of three experiments is shown.

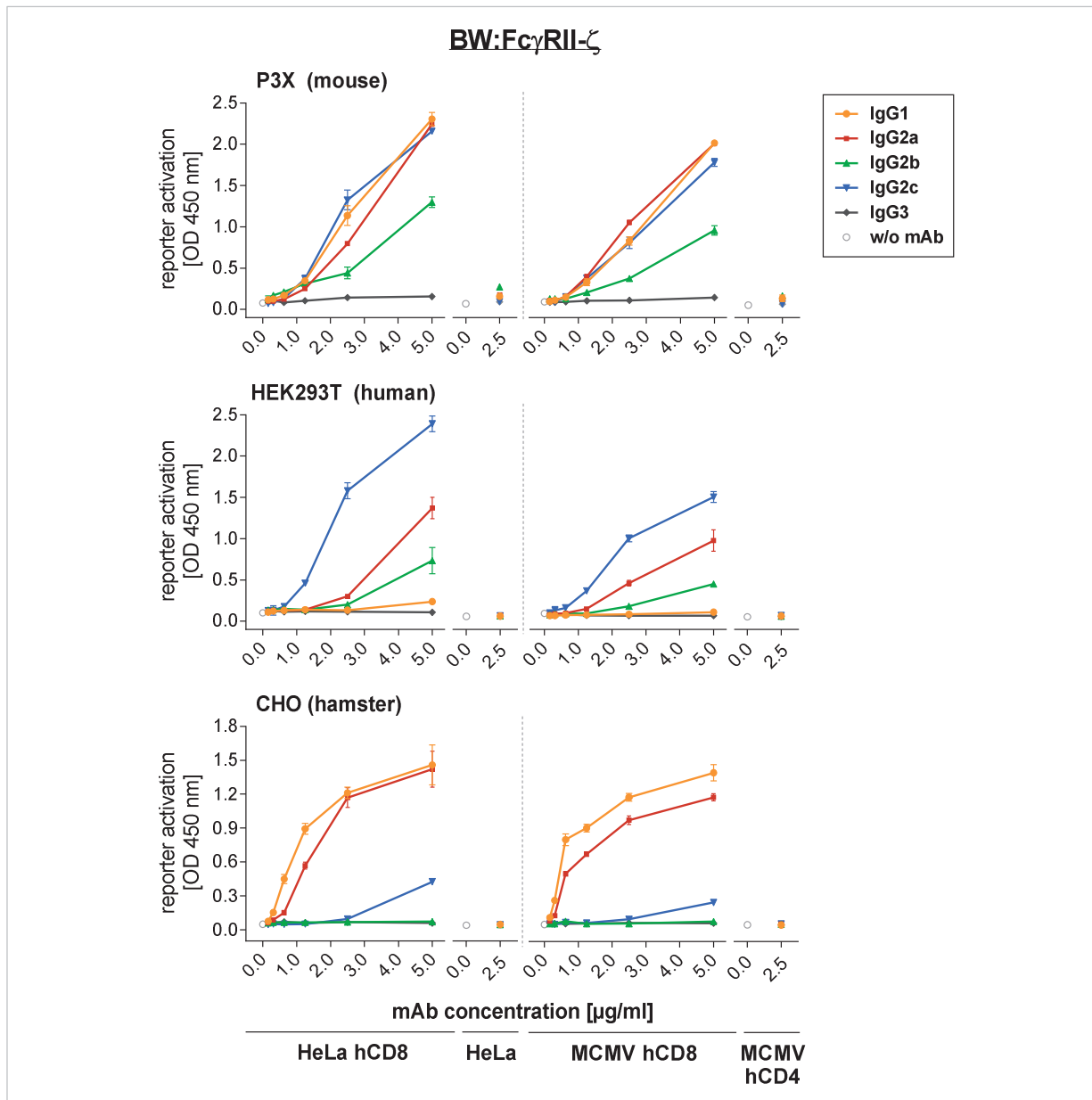


FIGURE 2.32. Influence of the mAb source and MCMV infection for selective IgG subclass dependent FcγRII activation pattern in vitro. Target cells were opsonized with grades concentrations of recombinant OKT8 mAbs produced in P3X (mouse), HEK293T (human), or CHO (hamster) cells and co-cultivated with 2×10^5 reporter cells overnight. Target cells were HeLa hCD8 or MCMV hCD8 infected MEF (MOI 1,5; 2 dpi) and HeLa or MCMV hCD4 infected MEF served as controls. IL-2, the surrogate marker for FcγR activation, was quantified by sandwich ELISA. Colorimetric reaction was stopped after 90s for OKT8 (P3X), 100s for OKT8 (HEK293T), and 60s for OKT8 (CHO). Triplicates were measured and duplicates for the highest concentration and controls. The data were analysed with GraphPad Prism and means with SD are shown. One representative out of three experiments is shown.

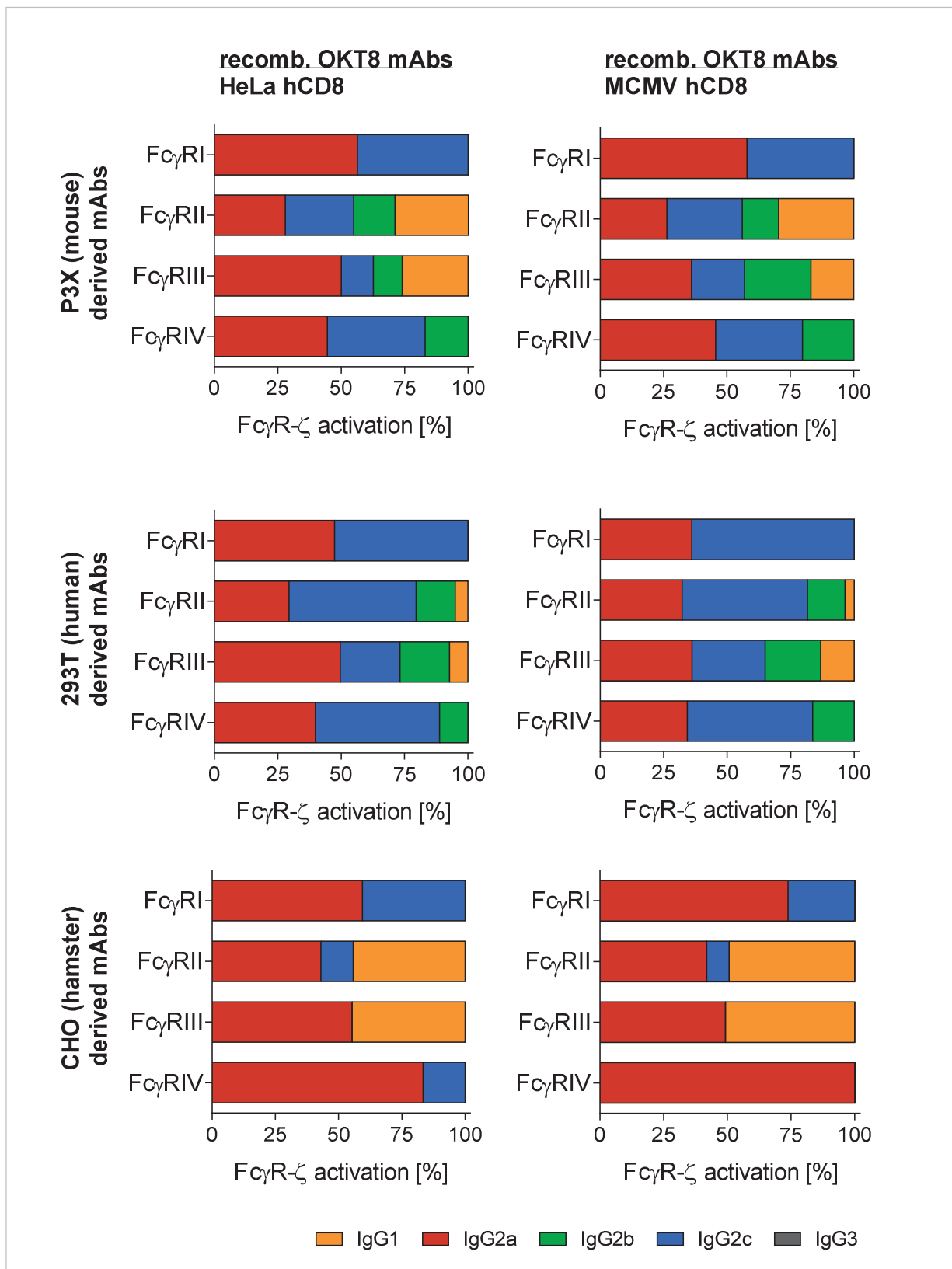


FIGURE 2.33. Overview of the IgG subclass dependent activation of the distinct BW:FcγR-ζ reporter cells. Activation is expressed as percentage on the basis of the data presented in Figure 2.29 – 2.32 for the following data points: FcγRI: second highest concentration (2,5 µg/ml); FcγRII: highest concentration (5 µg/ml); FcγRIII: highest concentration (5 µg/ml), except CHO second highest concentration (2,5 µg/ml); FcγRIV: highest concentration (2,5 µg/ml).

2.8. Influence of MCMV infection on IgG subclass dependent FcγR activation pattern *in vitro*

2.8.1. CMV encodes viral FcγRs

CMV exhibits a broad array of immune evasive function and counteracts host FcγR activation by expressing Fc binding proteins, so called viral FcγRs, on the surface of infected cells. HCMV encodes at least three and for MCMV only one vFcγR, m138, was identified so far (Thäle et al., 1994) (1.3.4.5.b). MCMV infected fibroblast bind Fc as detectable by the extracellular or intracellular staining (Figure 2.34.A). The extracellular staining appears rather weak whereas the intracellular staining reveals a stronger Fc binding. This is a result of the fast internalization and turnover of vFcγRs that has been overserved for HCMV (Master thesis of Anna Reib, 2012).

For MCMV, only one vFcγR, m138, has been identified so far. By immunoprecipitation (IP), at least one further orphan vFcγR is detectable (Figure 2.34B) with a molecular weight of approximately 55 kD. Due to extensive glycosylation, vFcγRs were visible as broad bands in the SDS PAGE. Moreover, deglycosylation sensitive (before glycan progressing in trans-Golgi) and resistant forms (past trans-Golgi) might exist as seen for m138. Using MCMV Δm138 in addition to MCMV hCD8, bands visualising m138 can be clearly identified and distinguished from the orphan FcγR(s). Deglycosylation by PNGase F reveals the size of the protein backbone, which is around 45 kD for the orphan vFcγR.

SUMMARY

- MCMV expresses viral FcγR(s) on the surface of infected cells that bind IgGs.
- At least one further vFcγR with the molecular weight around 55 kDa was detected in addition to m138 in precipitation experiments.

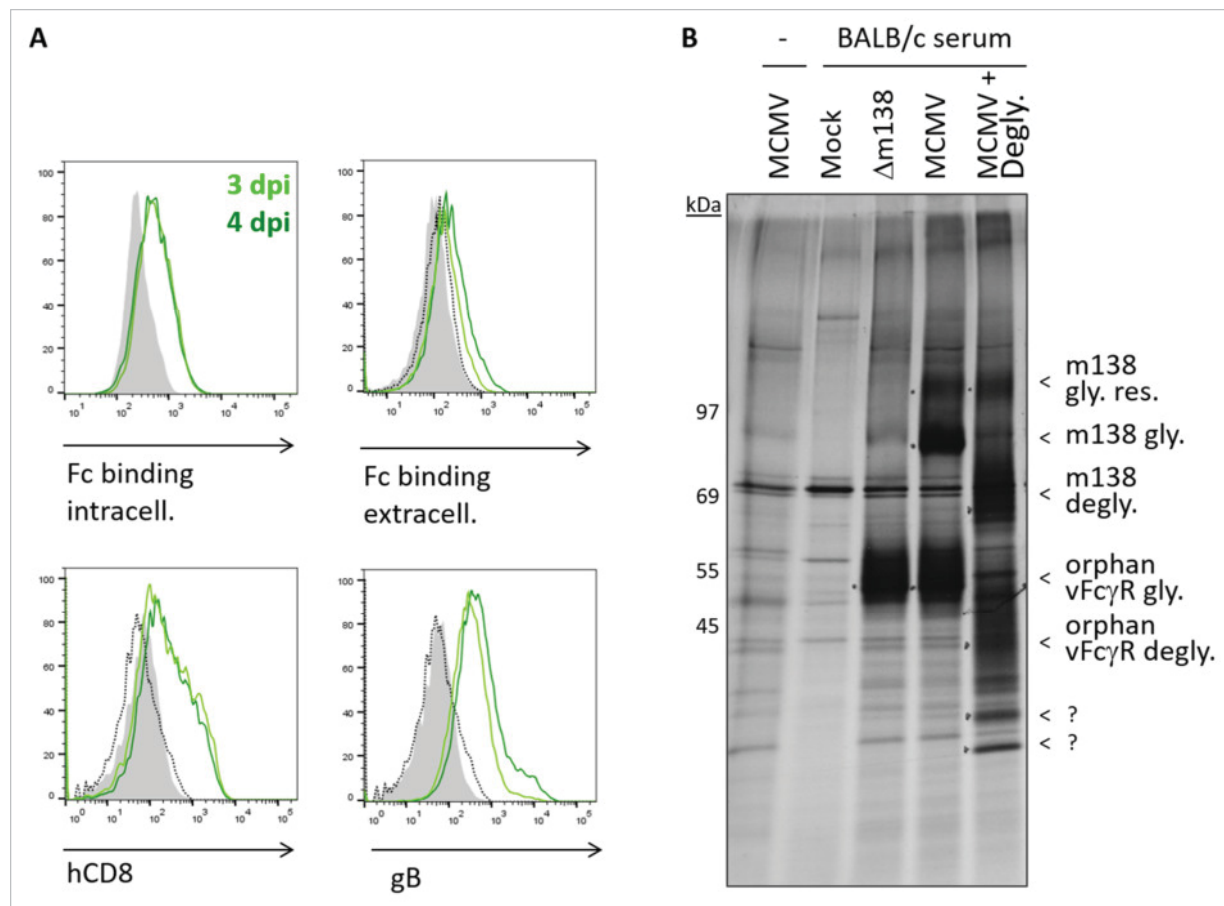


FIGURE 2.34. Fc binding by viral FcγRs of MCMV hCD8 infected fibroblasts. A. BIM fibroblasts were infected with MCMV hCD8 (MOI 3) for 3 and 4 days. Fc binding is shown by extracellular or intracellular staining with Fc-FITC fragment. As controls, the surface expression of hCD8 (OKT8 F(ab)₂) and MCMV gB (MCMV1.01) were detected using goat anti mouse APC. 1,5 - 2,5 x 10⁴ cells were recorded with DB FACS Canto II/FACS Diva and analysed with FlowJo (Tree Star Inc). Living cells (DAPI negative) were gated. Grey solid: mock; black dotted line: 4 dpi unstained; green: 3 dpi; dark green: 4 dpi. B. IP of MCMV encoded vFcγRs. B. MEF were infected for 2 days with MOI 2 of MCMV_{MCK2-Δm138} ("Δm138") or MCMV hCD8 ("MCMV"), metabolically labelled with ³⁵S methionine and cysteine for 2h, and mildly lysed with Digitonin. vFcγRs were precipitated by incubation of the cell lysate with BALB/c naïve serum (10 µl/well) and subsequently precipitated with PGS. Proteins were separated by a discontinuous SDS PAGE (8 - 11,5% PAA). The sample "MCMV + Degly." was treated with PNGase F. gly.: glycosylated; gly.res.: resistant glycosylation; degly.: deglycosylated (by PNGase F); ? unknown. One of three IPs is shown.

2.8.2. The IgG subclass hierarchy for the FcγRs activation is unchanged on MCMV infected cells vs. non-infected cells

To evaluate if the inhibitory effect of the MCMV encoded vFcγRs influences the IgG subclass dependent activation of the FcγR, the *in vitro* FcγR activation capabilities were analysed using infected fibroblasts. MEF were infected with MCMV hCD8 for two to three days to allow sufficient vFcγR expression. As negative control served MCMV hCD4 infected MEF. For a better comparability of the IgG dependency of the activation of the distinct FcγRs (independent on the total signal magnitude), the FcγR activation was expressed as relative activation in Figure 2.33. Remarkably, the IgG subclass hierarchy for the BW:FcγR-ζ activation is comparable between HeLa hCD8 and MCMV hCD8 infected target cells whereas the overall activation seem to be reduced especially for the activating FcγRs (Figure 2.29. - 32., right panel). However, BW:FcγRIII-ζ activation by CHO derived recombinant OKT8 IgG2a was slightly superior to IgG1 on HeLa hCD8 cells but not on MCMV hCD8 infected cells. Similarly, BW:FcγRII-ζ activation by CHO derived recombinant OKT8 IgG2a was slightly weaker than IgG1 on MCMV hCD8 infected cells in contrast to HeLa hCD8 cells, where IgG2a and IgG1 showed comparable activation of FcγRII-ζ for higher concentrations. Thus, CHO derived OKT8 IgG2a might be more affected than the corresponding IgG1 subclass in activating FcγRIII-ζ by the MCMV infection. In addition, the duration of infection (1 – 3 dpi) had no influence on the hierarchy of FcγR activation by the distinct subclasses (6.6.).

SUMMARY

- *The IgG subclass hierarchy of the BW:FcγR-ζs activation was not significantly changed on MCMV hCD8 infected target cells despite the expression of viral FcγR(s).*
- *The magnitude of activation seemed to be diminished especially for the activating FcγRs on MCMV hCD8 infected target cells compared to hCD8 stable expressing cells.*

2.8.3. Magnitude of FcγR activation on MCMV infected cells in comparison to non-infected cells

An overall lower BW:FcγR-ζ activation was observed by MCMV infected target cells in contrast to HeLa hCD8 cells especially with regard to the activating FcγRs. The overall magnitude of the activation could be influenced by the density of antigen and vFcγR on the cell surface of the infected cells. To characterize the magnitude of inhibition by MCMV encoded vFcγRs, the ectopic hCD8 antigen was expressed by a MCMV susceptible cell line, which allows their infection with MCMV and its comparison to mock infected cells. hCD8 expressing mouse fibroblast cell lines were generated by lentiviral transduction (4.7.3.). To exclude an effect of the transduction on the infectivity of the cell lines, MCMV gB surface expression was monitored showing no difference between transduced and

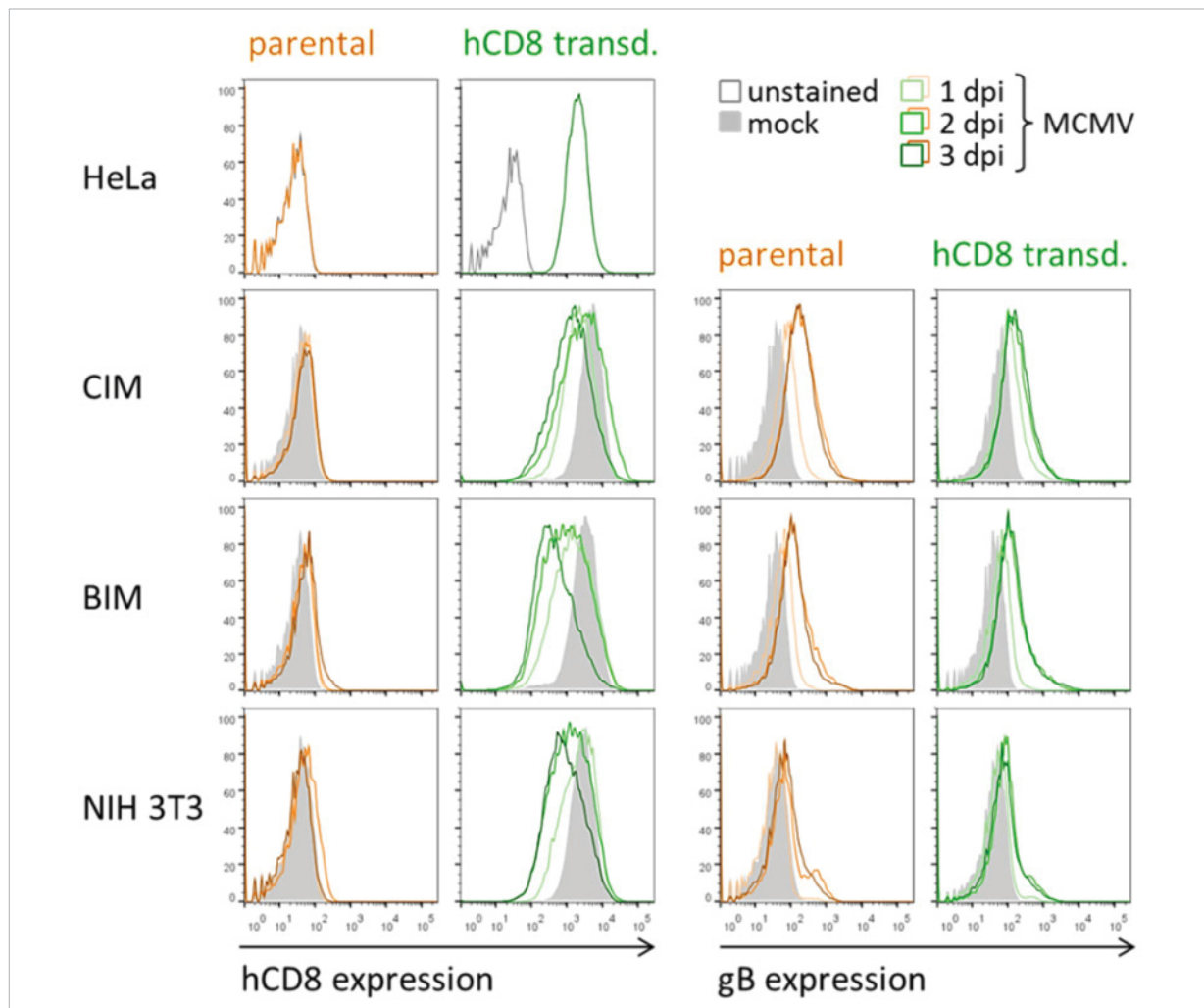


FIGURE 2.35. hCD8 surface expression in hCD8 transduced fibroblasts is altered dependent on the duration of MCMV infection. hCD8 transduced murine fibroblasts cells were infected with MOI 1 of MCMV_{MCK2}- and surface expression of hCD8 (OKT8-APC) and MCMV gB (MCMV1.01 / goat anti mouse APC) were measured by flow cytometry. Mock infected, non-transduced ("parental"), and HeLa hCD8 cells served as control. At minimum 2.5×10^4 cells were measured by flow cytometry (BD FACS Canto II, FACS Diva Software) and analysed with FlowJo (Tree Star Inc). It was gated on living (DAPI negative) and single cells.

non-transduced fibroblast cell lines (Figure 2.35). However, the surface expression of hCD8 was reduced and the reduction was stronger the longer the period of infection lasted. This fact hampers a valid comparison of BW:FcγR-ζ activation by MCMV in comparison to mock infected cells but not a comparison of BW:FcγR-ζ activation on cells infected with comparable well replicating MCMV mutants. Therefore, preliminary experiments evaluating the BW:FcγR-ζ activation with target cells (CIM hCD8) infected with MCMV_{MCK2}- and MCMV_{MCK2}-Δm138, lacking the only identified vFcγR of MCMV, were performed. Mock infected cells served as control. Only very weak (Figure 2.36) to no BW:FcγR-ζ activation was detectable with the infected cells depending on the particular experiment and in contrast to mock cells. In addition, the activation of the inhibitory FcγRII-ζ was highly affected, comparable to the activating FcγRs tested. As expected, the hierarchy of IgG subclass dependency for the activation of the distinct BW:FcγR-ζ was equal for mock infected CIM hCD8 and HeLa hCD8 as seen in the previous experiments expressing the hCD8 antigen by MCMV (MCMV hCD8). Because the reduction of the hCD8 antigen expression on infected cells is rather small (Figure 2.35), these results are compatible with a possible inhibition of the BW:FcγR-ζs by MCMV, e.g. by vFcγR(s). No differences with MCMV wt or MCMV Δm138 infected target cells were obvious for the BW:FcγRII-ζ and FcγRIII-ζ

activation, but possibly a small increase for BW:Fc γ RIV- ζ activation with MCMV Δ m138 infected target cells (which has to be reproduced). These results indicate an inferior impact for m138 as vFc γ R and may suggest a dominant role for the “orphan” vFc γ R(s) (Figure 2.34). Of course, a general disturbance of the reporter cells by the MCMV infected target cell e.g. by cytokines besides the expression vFc γ Rs cannot be excluded. Therefore, the identification of the further MCMV encoded vFc γ R(s) and the analysis of their impact for the host Fc γ R activation using specific MCMV deletion mutations are of high interest.

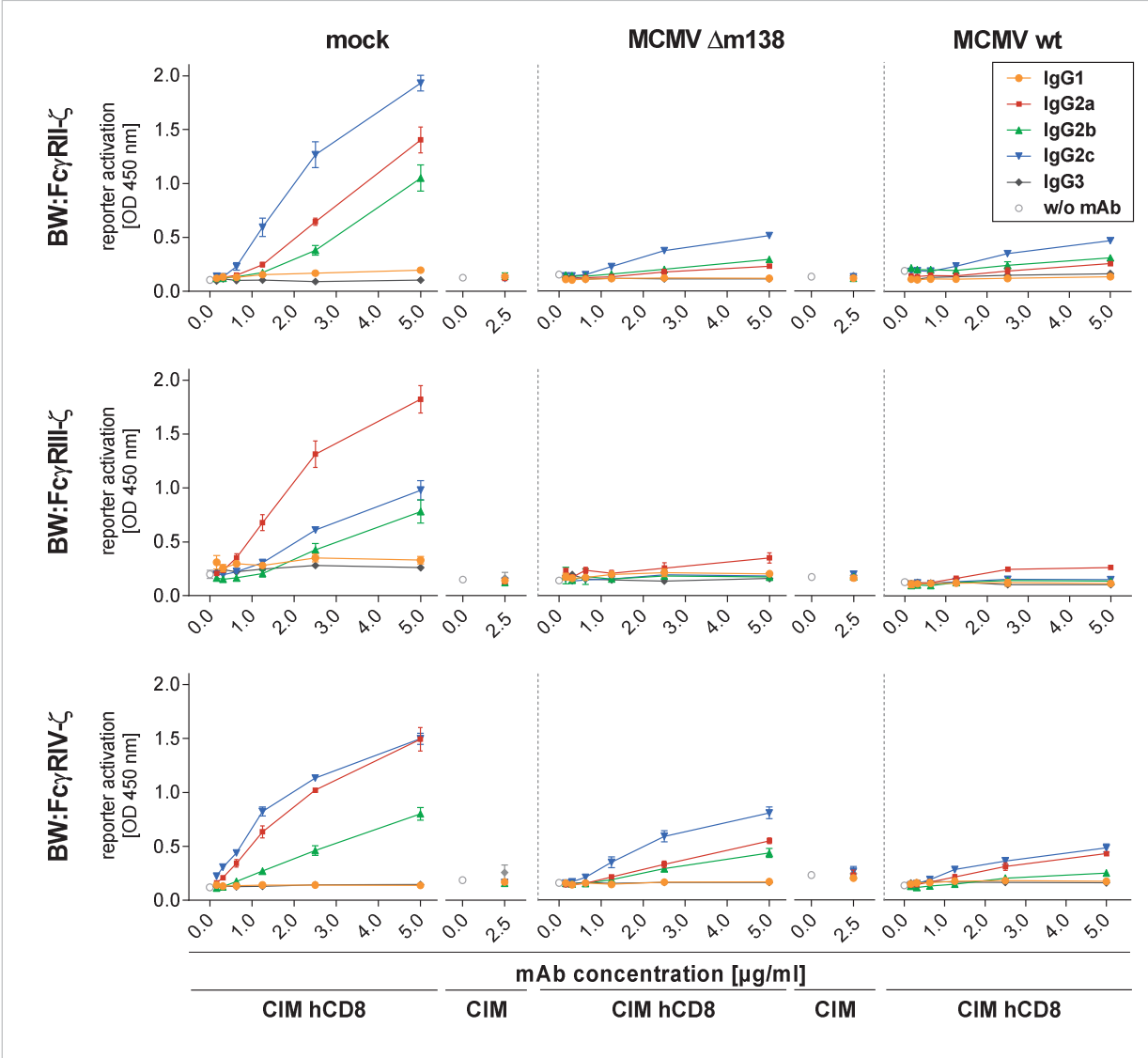


FIGURE 2.36.A Influence of MCMV and MCMV Δ m138 infection for selective IgG subclass dependent BW:Fc γ R- ζ activation pattern *in vitro*. Target cells were opsonized with grades concentrations of recombinant OKT8 mAbs produced in HEK293T cells (human) and co-cultivated with 2×10^5 reporter cells overnight. Target cells were mock, MCMV_{MCK2-}, or MCMV_{MCK2-} Δ m138 infected CIM hCD8 (MOI 1; 2 dpi) whereat CIM served as controls. IL-2, the surrogate marker for Fc γ R activation, was quantified by sandwich ELISA. Colorimetric reaction was stopped after 110 s for BW:Fc γ RII- ζ , 130s for BW:Fc γ RIII- ζ , and 120 s for BW:Fc γ RIV- ζ . Triplicates were measured. The data were analysed with GraphPad Prism and means with SD are shown. One representative out of two experiments is shown.

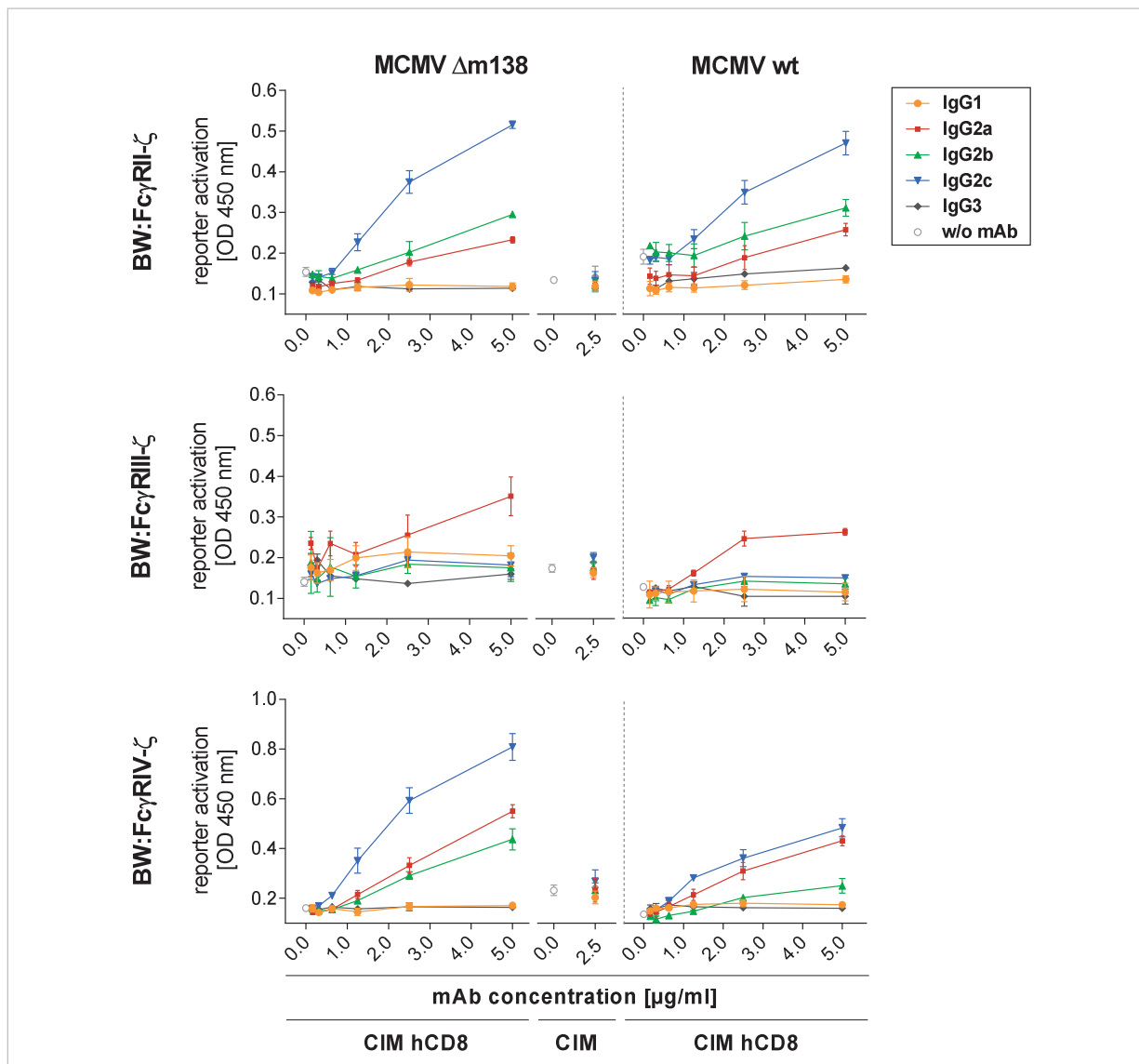


FIGURE 2.36.B Influence of MCMV and MCMV $\Delta m138$ infection on the selective IgG subclass dependent BW:Fc γ R– ζ activation pattern *in vitro*. Results with MCMV and MCMV $\Delta m138$ infected targets cells from Figure 36.A. with enlarged y-axis.

SUMMARY

- The surface expression of hCD8 of the hCD8 transduced mouse fibroblast cell lines was slightly diminished after MCMV infection and the hCD8 expression level correlated inversely with the duration of the MCMV infection.
- Only the magnitude of BW:Fc γ RIV– ζ activation was slightly reduced on MCMV wt infected target cells in comparison to the $\Delta m138$ mutant (reproduction needed).

The next step will be the evaluation of the protective capabilities of the OKT8 IgG subclass switch variants in MCMV hCD8 infection *in vivo*. Unfortunately, the production of sufficient amounts of recombinant IgG was difficult only allowing the performance of a preliminary first experiment (data not shown). Nevertheless, the predictive value of *in vitro* Fc γ R activation assay was demonstrated in the model of influenza A infection with non-neutralizing M2e specific IgGs that are dependent on Fc γ R activation *in vivo*. The *in vivo* protective capabilities of these mAbs correlated very well with the reporter cell data (cooperation with X. Saelens, Ghent) (6.7.).

2.9. *In vitro* FcγR activation capacities are equal for BALB/c and C57BL/6 derived FcγRIII

2.9.1. Comparison of the extracellular domains of the FcγRs derived from C57BL/6 and BALB/c mice

Considering the fact that BALB/c and C57BL/6 related mouse strains encode different IgG subclasses (IgG2a vs IgG2c), the strains might also reveal adaptive differences in their FcγRs. Consequently, the protein sequences of the IgG binding domain, i.e. the extracellular domain of the FcγR alpha chains, were compared (Table 2.2.). The extracellular domain is responsible for the IgG binding (1.2.3.4.) and the cloned domains for the FcγR-CD3ζ chimeras exhibit identical sequences to the NCBI Reference Sequences (Ref_Seq). The sequence comparison was performed with available data from different databases and BLAST.

The sequence of the extracellular domains from both mouse strains was identical for FcγRI and FcγRII, respectively. No sequence was available for FcγRIV derived from BALB/c. Therefore, cDNA from BALB/c splenocytes was cloned. Sequencing of the extracellular demonstrated no differences to C57BL/6. The sequence for FcγRIV found in the UniProt database contains an amino acid substitution in the D2 domain. However, this sequence is categorized unreviewed. In addition, the sequence obtained here for the generation of the BW:FcγRIV-ζ reporter cells was identical with the Ref_Seq sequence. For these reasons, the difference in the UniProt reported sequences was not further investigated.

	Protein	strain	extracel. domain
FcγRI	NP_034316.1 (Ref_Seq); BAC28504.1; AAD34918.1	C57BL/6J; C57BL/6ByJ	identical
	AAD34919.1	BALB/cByJ	
	P26151 (Uniprot)		
FcγRII	NP_001070657.1 (Ref_Seq); NP_034317.1 (Ref_Seq); BAE42388.1; BAE29704.1; BAC38062.1	C57BL/6J	identical
	AAA37289.1	BALB/c	
	P08101 (Uniprot)		
FcγRIII	NP_034318.2 (Ref_Seq); BAE30502.1; BAE31560.1; AAG28520.1; BAC36696.1; AAX13974.1; BAE35482.1	C57BL/6J	identical
	BAE30695.1; BAE31949.1; BAE32004.1	C57BL/6J	218 W/C
	AAX13976.1	BALB/c	79W/G; 80S/R; 88S/A
	P08508 (Uniprot)		
FcγRIV	NP_653142.2 (Ref_Seq); BAC36381.1; A0A0B4J1G0 (Uniprot)	C57BL/6J; mixed	identical
	Q8R477 (Uniprot)*	C57BL	157L/P
	Cloned from BALB/c splenocytes	BALB/c	identical

TABLE 2.2. Comparison of the amino acid sequence of the FcγR extracellular domain from C57BL and BALB/c mouse strains (excluding signal peptide), sources: NCBI gene, Uniprot, own cloning. * unreviewed sequence

FcγRIII is the receptor with the most prominent difference for IgG2a and IgG2c activation. Comparison of the FcγRIII sequence revealed three amino acid substitutions in the middle of the first Ig like domain D1 (Figure 2.37): the hydrophobic and aromatic amino acid tryptophan was substituted by glycine, the simplest amino acid existing. Furthermore, two serines, which are uncharged, are exchanged once by an arginine, which has a long and polar side chain, and an alanine, which lacks a hydroxyl group in comparison to serine. Therefore, a new reporter cell line was generated expressing FcγRIII-CD3zeta (BALB/c). Their generation is described in 4.7.1.3. The existing cell line had the sequence of C57BL/6 FcγRIII (4.7.1.1.). In addition, one amino acid substitution in another set of sequences is found in comparison the Ref_Seq sequence: a tryptophan is replaced by a cysteine. According to the predication software for protein domain (SMART), this position represents the last amino acid before

the transmembrane region. Consequently, it is unlikely to be involved in IgG binding and consequently this difference was not further investigated.

Some of the sequences are annotated with a shorter or longer signal peptide for FcγRII and FcγRIII. Since the signal peptide is cleaved during the translation, these differences have no obvious consequences for the function of the translated protein.

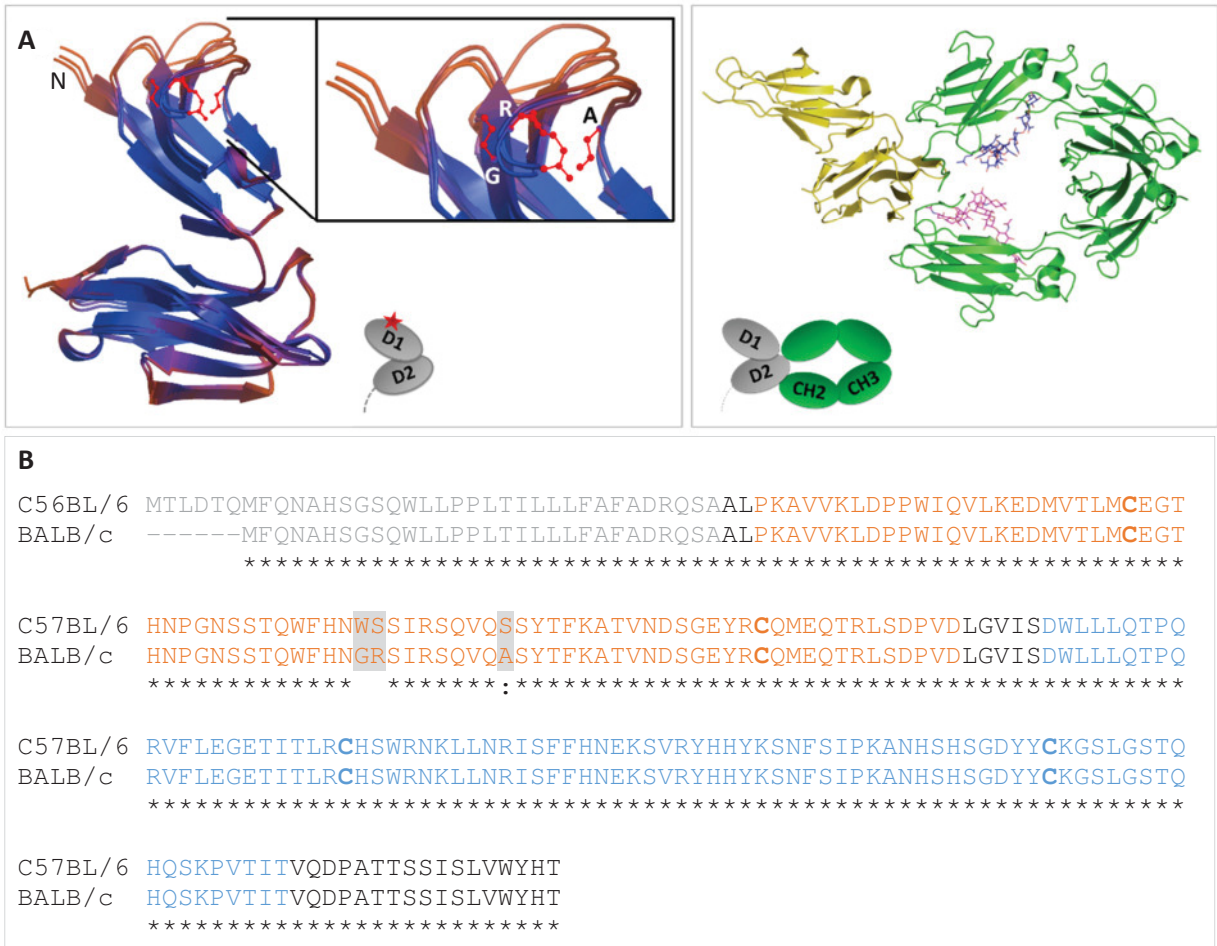


FIGURE 2.37. Extracellular domain of FcγRIII. A. Modeling of FcγRIII BALB/c extracellular domain with substituted AA (red) (SWISS Model: human FcγRIII as template: 2fcb.1.A; 1fcg.1.A; 1h9v.1.A.; AstexViewer; Crytal structure of human FcγRIII with IgG1 (PDBe 1e4k). B. Sequence of the extracellular domain of FcγRIII including the signal peptide. C57BL/6: NP_034318.2; BALB/c: P08508; annotations according to P08508; grey: signal peptide; orange: Ig like domain I; blue: Ig like domain II; bold: intra-molecular cysteine bonds the Ig like domain; alignment with Clustal Omega, * identical AA, : AA with strongly similar properties, ;grey: mismatches.

SUMMARY

- Comparing the extracellular domain of the FcγRs alleles from BALB/c and C57BL/6 mice, three amino acid polymorphisms were found in the first Ig like domain of FcγRIII.

2.9.2. IgG subclass dependent Fc binding of BW:FcγRIII–ζ BALB/c vs. C57BL/6

First, the Fc binding capabilities of the different IgG subclasses to FcγRIII from BALB/c vs. C57BL/6 was compared by flow cytometry (Figure 2.38). Therefore, two different aliquots of BW:FcγRIII–ζ C57BL/6 (B6) and three different subcloned cell lines of BW:FcγRIII–ζ BALB/c (BALB) were incubated with a biotinylated IgG subclass collection (Genetex). A representative staining is shown in Figure 2.38A and the statistical analysis in 2.56B. The FcγRIII–ζ expression of all BW:FcγRIII–ζ cell lines was comparable as well as binding of the graded concentration of mouse serum or the distinct IgG subclasses. A higher

concentration of IgG2c was applied since IgG2c is bound weakly by FcγRIII. It seems that BW:FcγRIII–ζ BALB/c might bind IgG2c a little bit stronger. If the stronger binding of IgG2c translates in a higher activation of the BW:FcγRIII–ζ BALB/c was analysed next.

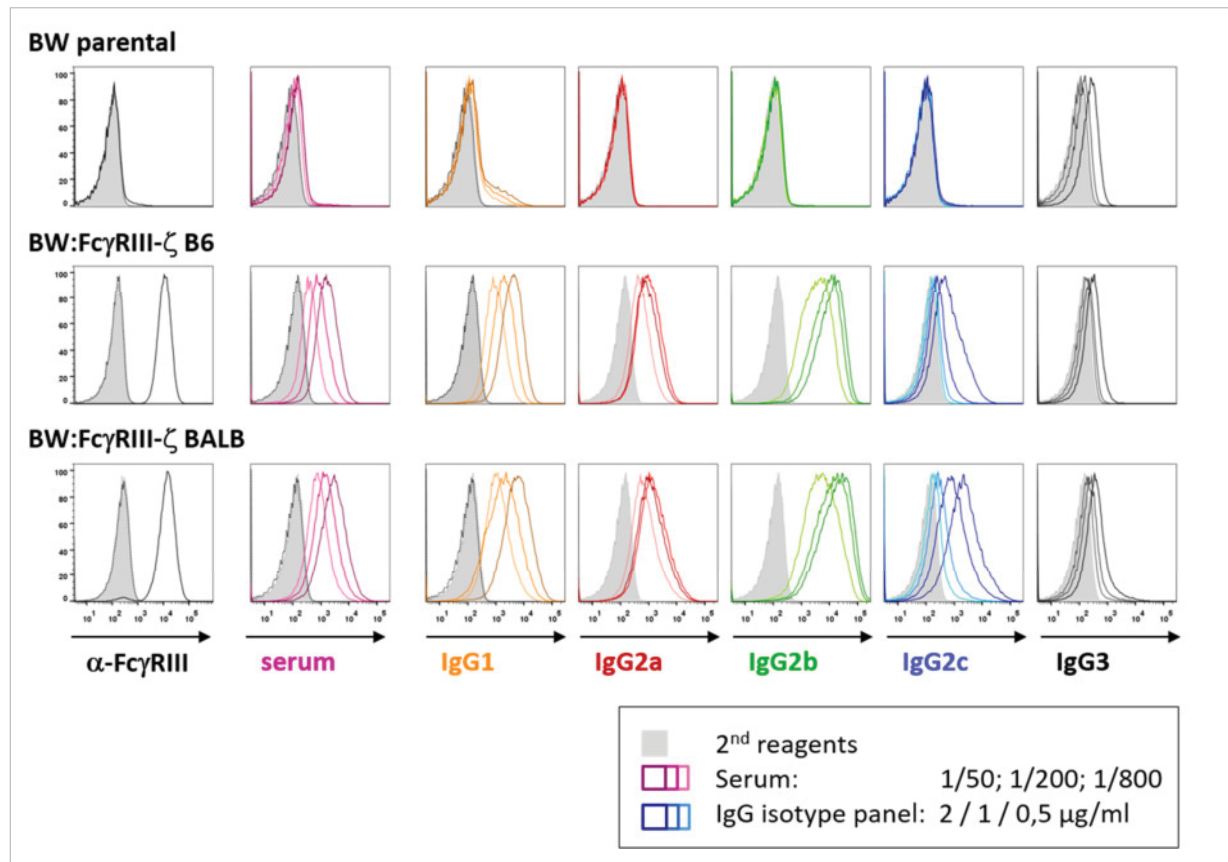


FIGURE 2.38A. BW:FcγRIII–ζ with the extracellular domain of C57BL/6 (B6) or BALB/c bind different IgG subclasses similarly. 2×10^5 cells were stained with graded dilutions (2; 1; 0,5 $\mu\text{g/ml}$) of the biotinylated IgG isotype panel from Genetex and detected with Streptavidin-APC. As controls, FcγRIII was stained with $\alpha\text{-Fc}\gamma\text{RIII-PE}$ and graded dilutions of naïve BALB/c derived mouse serum (1/50; 1/200; 1/800) which were detected with goat anti mouse Cy5. Grey solid: 2nd reagent or isotype stained; back dotted line: unstained, line: indicated staining. 6×10^4 cells were measured by flow cytometry (BD FACS Canto II, FACS Diva Software) and analysed with FlowJo (Tree Star Inc.).

SUMMARY

- BW:FcγRIII–ζ possessing the sequence of C57BL/6 or BALB/c displayed comparable binding of mouse serum and the distinct IgG subclasses.
- BW:FcγRIII–ζ BALB/c might bind IgG2c slightly stronger.

2.9.3. IgG subclass dependent *in vitro* FcγR activation of BW:FcγRIII–ζ BALB/c vs. C57BL/6

The *in vitro* FcγRIII activation capacities of the different recombinant OKT8 mAbs in dependency of the origin of the FcγRIII extracellular domain were tested (Figure 2.39). Therefore, HeLa hCD8 cells were opsonized with graded concentration of recombinant anti-hCD8 OKT8 mAbs produced in P3X or HEK293T cells and co-cultivated with two different aliquots of BW:FcγRIII–ζ C57BL/6 (A1, A2) and two different subcloned cell lines of BW:FcγRIII–ζ BALB (SC1, SC2). The magnitude of the signal, the IL-2 readout, cannot be compared between the cell lines because this is a function of the FcγRIII–ζ expression level, which might differ between cell lines, subcloned cell lines, and aliquots. Instead, the hierarchy of the FcγRIII activation by the different IgG subclasses is of high interest. The IgG subclass

dependent activation of BW:FcγRIII C57BL/6 (Figure 2.27 and Figure 2.30) was reproduced: IgG2a > IgG1 > IgG2c = IgG2b for P3X and IgG2a >> IgG2c > IgG2b>> IgG1 for HEK293T derived OKT8 mAbs. The hierarchy of BW:FcγRIII–ζ BALB/c activation was comparable for the recombinant OKT8 mAbs derived from HEK293T cells, whereby the IgG2c subclass seemed to be slightly more potent in comparison than for BW:FcγRIII C57BL/6. The same tendency was observable for the recombinant OKT8 mAbs produced in P3X. All subclasses demonstrated a comparable activation hierarchy for BW:FcγRIII C57BL/6 and BALB/c whereas there might be slight differences for the IgG2c subclass but also between the two BW:FcγRIII BALB/c subcloned cell lines (SC1, SC2). Testing of higher concentration would be desirable but this was not possible due to the limited amounts of the recombinant OKT8 mAbs.

SUMMARY

- *The FcγRIII polymorphism located in the first Ig like domain of FcγRIII in C57BL/6 and BALB/c might have a minor effect only on IgG2c but not the other IgG subclasses.*

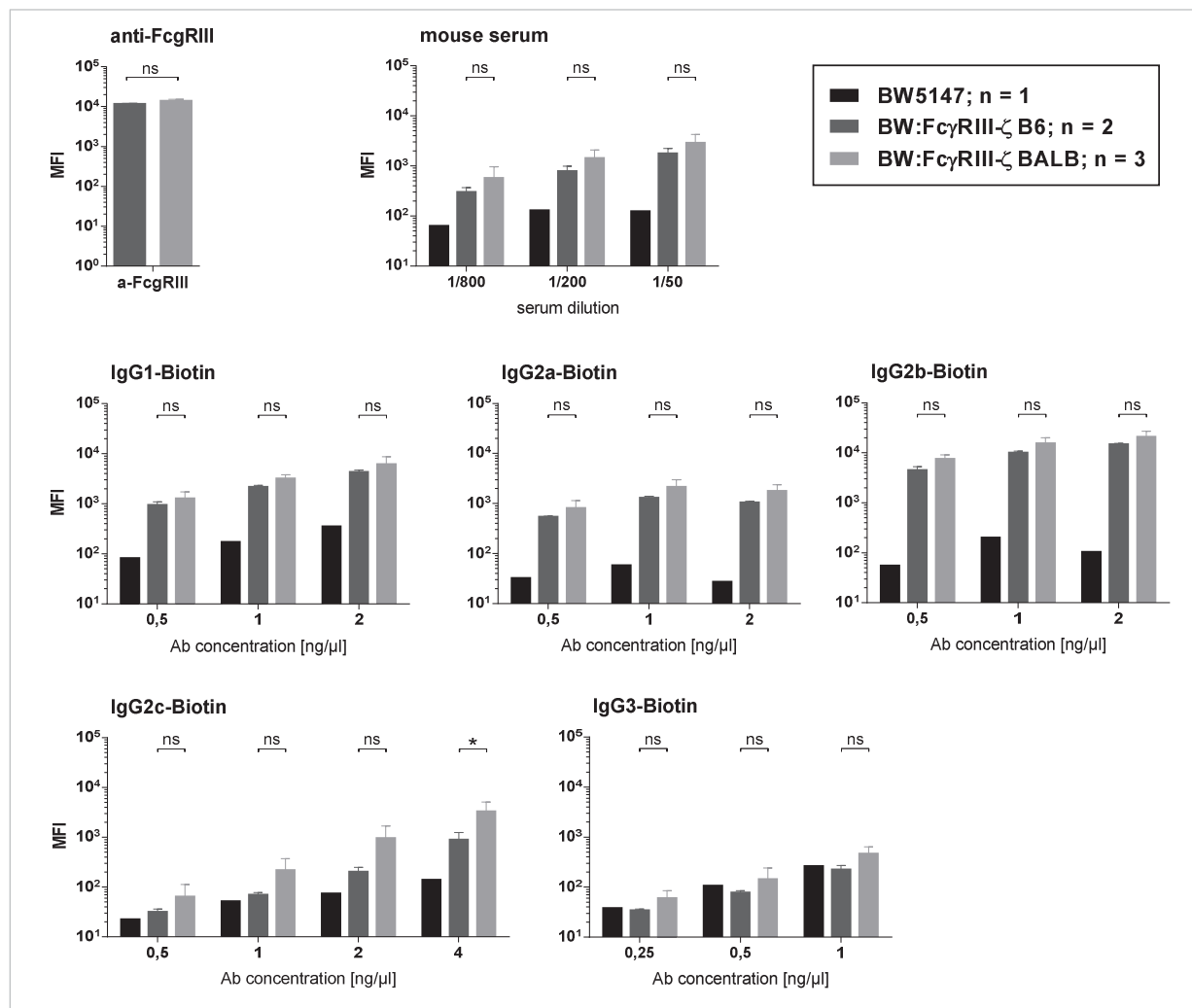


FIGURE 2.38B. BW:FcγRIII–ζ with the extracellular domain of C57BL/6 (B6) or BALB/c bind different IgG subclasses similarly – statistical analysis. For the statistical analysis of the mean fluorescence intensity (MFI), isotype or 2nd reagent stained controls were subtracted. Mean values with SD are shown. Two-way ANOVA was applied and the students t-test for the anti-FcγRIII staining. * p < 0,05.

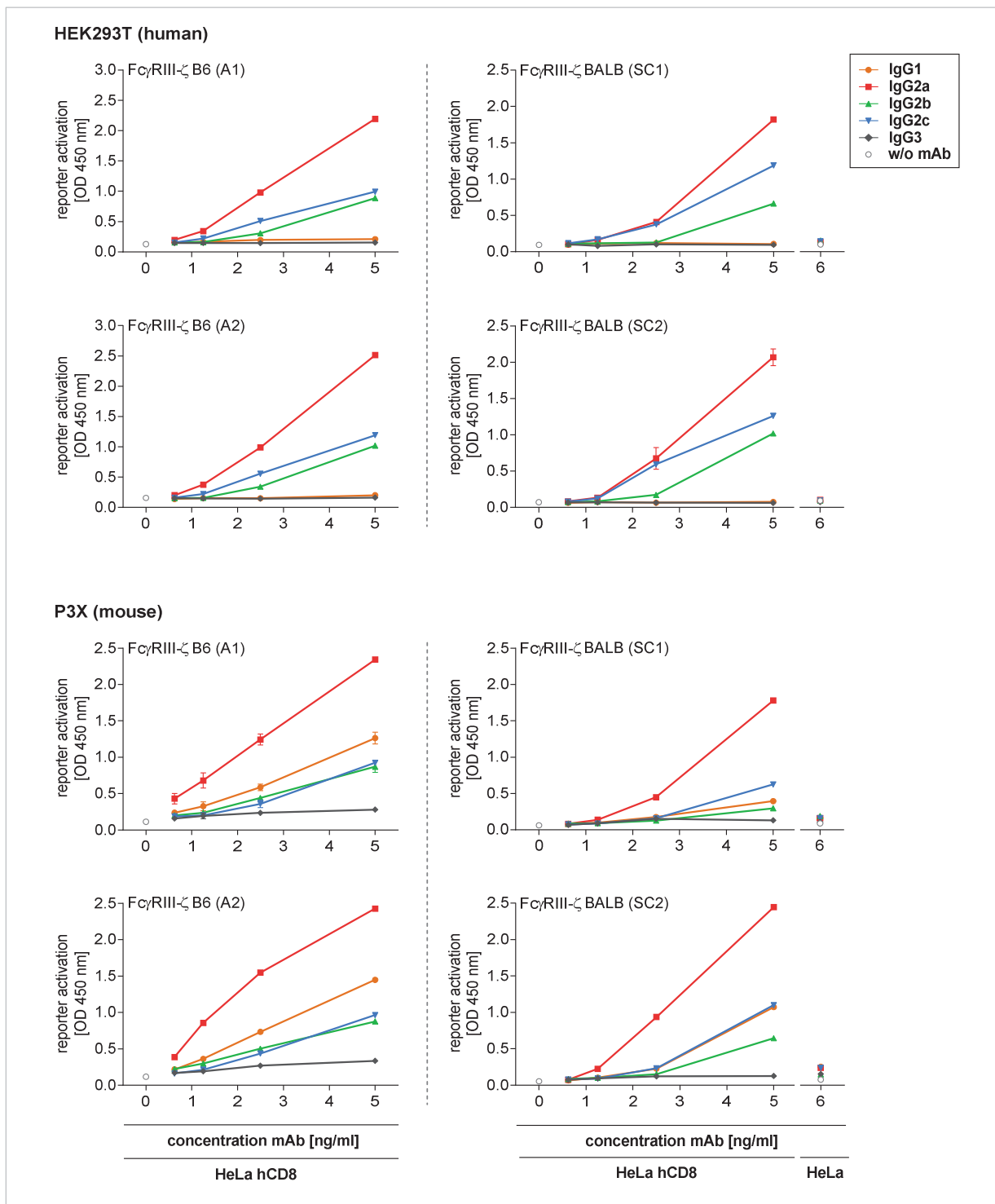


FIGURE 2.39. Comparison of the in vitro activation of FcγRIII composed of the extracellular domain from BALB/c or C57BL/6 by recombinant OKT8 mAbs. HeLa hCD8 or HeLa cells were opsonized with graded concentration of recombinant anti-hCD8 mAbs (OKT8) produced in P3X or HEK293T cells and co-cultivated with 2×10^5 cells of two different aliquots of BW:FcγRIII-ζ B6 (C57BL/6 derived; A1, A2) and two different subcloned cell lines of BW:FcγRIII-ζ BALB (SC1, SC2). Readout is the IL-2 quantification by sandwich ELISA. Means with SD are shown (GraphPad Prism).

3. DISCUSSION

Focusing solely on virion neutralization in the past, only lately the importance of cellular mediated FcγR dependent IgG effector mechanisms for immune control of (virus) infections and antibody-based therapies was realized. Investigating the impact of FcγR in primary MCMV infection using different mouse strains deficient in all or a single activating FcγRs revealed that FcγRs contribute to the immune control of primary MCMV infection in the SG (3.1.1.). However, the absence of one FcγR was compensated by the remaining ones (3.1.2.). This suggests that antibodies participate in the immune control of MCMV primary infection contrasting earlier studies that concluded from studying antibody deficient mice that antibodies exert only a role in the limitation of recurrent infections (Jonjic et al., 1994 and 1998) (3.1.3.). Possible immune cell populations exerting FcγR effector functions in the SG might be NK cells and macrophages because these populations were reduced at different time points post infection in the SG of FcγR deficient mice (3.1.4.).

Next, IgG subclass dependent activation pattern of the individual FcγRs were systematically evaluated in order to optimize IgG based therapies. To this end, a set of recombinant subclass switched IgGs were generated and a reporter cell based assay was established to analyse and compare FcγR activation capabilities of these IgG switch variants. The *in vitro* FcγR activation capabilities of the IgG subclass switch variants revealed unique IgG subclass dependent activation pattern for each of the FcγRs (3.2.1.). Production of the recombinant IgG switch variants in different cell lines (of mouse, human, and hamster origin) had a great influence on their FcγR activation capabilities, probably due to their differential (species and cell type specific) composition of the Fc glycan at position Asn297 (3.2.5.). Some subclasses were more affected than others were. Therefore, the subclass and Fc glycan composition affect the FcγR activation capabilities of IgG antibodies. Most laboratory inbred mouse strains only possess IgG2a or IgG2c, therefore a functional comparison of these subclasses was of special interest and revealed that they are functionally distinct in their FcγR activation capabilities (3.2.3.). Combined with the fact that they are also differentially induced during MCMV infection (Androsiac, 2012), this could have wide implications for the evaluation of FcγR dependent IgG effector functions in different transgenic mouse models of infection and autoimmunity. Optimizing an IgG based therapy against CMV has to take its FcγR-related immune evasive mechanism into account (3.3.2.). The IgG subclass hierarchy for the activation of respective FcγRs was not significantly altered but the overall magnitude of activation was greatly diminished on MCMV infected target cells when compared with stable hCD8 expressing target cells (3.2.6.).

3.1. Impact of FcγRs for the immune control of MCMV *in vivo*

3.1.1. Activating FcγRs contribute to the control of primary MCMV infection in the SG

The relevance of FcγRs mediated antibody effector functions during the course of the primary MCMV infection was evaluated in FcRγ-KO mice lacking all FcγRs. Mice deficient in the accessory gamma chain lack the expression of all activating FcγRs and revealed an 10 to 100 fold increased and prolonged virus replication in the SG two we

eks post infection and by trend increased viral loads in the other organs. To verify that the loss of virus control was caused by the absence of the FcγRs and not due to a diminished antibody response, the

total MCMV specific and MCMV neutralizing antibodies titers were quantified and even elevated levels were observed in Fcγ-KO mice. The increased viral replication leading to increased amounts of antigen might be causal for higher MCMV-specific and total antibody titers in Fcγ-KO mice. It was reported that the number of MCMV-specific IgG secreting long-lived plasma cells and consequently the magnitude of the antibody response are dependent on the MCMV inoculum dose (Welten et al., 2016). Along this line, an increased percentage of B cells (by trend) was detected 28 dpi in the SG of Fcγ-KO mice. Additionally, their activation marker CD86 (Suvas et al., 2002) was elevated. The deletion of the gamma chain is unlikely to alter directly the B cell activation state because B cells only express the inhibitor FcγRIIB, which is still present in Fcγ-KO mice. Likewise, the loss of the Fcγ does not alter maturation of the B cell response (Vora et al., 1997). The higher amount of neutralizing antibodies might even partially mask the impaired virus control caused by the absence of FcγRs.

However, the gamma chain participates also in other signaling pathways e.g. in NK cells and macrophages (1.2.4.5.). Nevertheless, the observed phenotype is most likely caused by the absence of FcγRs because the loss of virus control in the SG was observed upon two weeks post infection when virus specific IgG serum concentration reaches sufficient high levels to contribute to the immune control. The loss of virus control due to defective NK cells or macrophages would have been obvious very early in infection and presumably in multiple organs because NK cells contribute to the first line of defence against MCMV immediately after infection (1.3.4.5.a; Voigt et al., 2003).

The Fcγ is associated with the mouse IgE high affinity receptor (FcεRI), which is expressed on mast cells and basophils and during infection on DCs and neutrophils (Bruhn et al., 2015). The observed phenotype in Fcγ-KO mice is highly unlikely to be caused by the absence of FcεRI in these mice. Activation of FcεRI by IgE is mainly involved in the induction of allergic response and in the antimicrobial and antiparasitic defence. IgE is induced by T_H2 CD4 T cell responses whereas viruses generally elicit T_H1. Accordingly, IgE should not play a role in MCMV infection. In MCMV infection, mast cells are infected and play a role in recruiting immune cells to control pulmonary infection but independently of FcεRI / IgE (Podlech et al., 2015; Ebert et al., 2014; Becker et al., 2015).

In immunocompromised mice, deletion of the Fcγ (Fcγ x RAG1-KO) revealed that activating FcγRs are strongly involved in the protection by antibodies (Bootz, 2014). Transfer of immune serum exerted less protection than in control mice indicating a superior role of activating FcγR mediated effector functions and a minor participation of neutralization (in lungs, spleen, and especially in SG).

To confirm the partial loss of MCMV control in the SG during primary MCMV infection, the use of a triple Fcγ-KO mouse, which lacks the alpha chains of all activating FcγRs, would be an ideal approach. Nevertheless, the Fcγ-KO model strongly suggests that FcγRs and therefore non-neutralizing antibodies participate in the control of primary MCMV infection in the SG.

3.1.2. Redundant function of FcγRs

To dissect the importance of the individual FcγRs in controlling MCMV, knockout mice lacking a single FcγR due to the deletion of the alpha chain were evaluated. However, FcγRI-KO, FcγRIII-KO, and FcγRIV-KO mice control MCMV comparable to wildtype and / or heterozygous mice indicating that FcγRs might have overlapping functions and that the absence of a single activating FcγRs is compensated by the other two remaining FcγRs. Additionally, it has been noticed that the deletion of one FcγR affects the expression level of the other one(s). FcγRIII- but not FcγRI-KO mice exhibit an increased expression of FcγRIV (Nimmerjahn et al, 2010, Syed et al., 2009; Jönsson et al, 2011). This

might partially compensate the loss and mask the role of FcγRIII in these knockout mice. Similarly, FcγRIV knock out resulted in a slight up regulation of FcγRIII on neutrophils (Nimmerjahn et al., 2010). An explanation might be the competition for the accessory Fcγ chain, which is necessary for FcγR surface expression, when these FcγRs are coexpressed. FcγRIII and FcγRIV are coexpressed on neutrophils, monocytes, and macrophages. Moreover, single FcγR-KO mice on the RAG1-background also demonstrated a redundancy of FcγRs in the setting of antibody therapy with MCMV immune serum containing high amounts of virus specific antibodies of the IgG2c subclass (Bootz, 2014). Additionally, no difference in viral loads was observed for RAG1 x FcγRI / IV-KO indicating that FcγRIII might be dispensable.

Functional redundancy or overlapping roles of FcγRs are also observed in models of autoimmune diseases and in antibody-based therapies of cancer and virus infections (Boross et al., 2006; Albanesi et al., 2012; Otten et al., 2012; Jakus et al., 2008). Studies with FcγR deficient mice or FcγR inhibition revealed that the absence of one FcγR is mostly compensated although to a varying degree. The degree of compensation is dependent on the involved effector cells i.e. their FcγR expression profile and type of antibodies studied in the particular infection / disease model. E.g. IgG2a binds to all activating FcγRs whereby IgG1 only relies on FcγRIII (Nimmerjahn et al., 2005) resulting in a dependence of IgG1 but not IgG2a on FcγRIII expression *in vivo* (6.7.). MCMV infection induces a polyclonal antiviral antibody response with IgG2b and IgG2c being the predominant subclasses in C57BL/6 mice (Androsiac, 2012; Welten et al., 2016), which predominant engage FcγRIII/IV and FcγRI/IV, respectively. Furthermore, if monocytes / macrophages are the main effector cell mediating the IgG effector functions in MCMV control, deletion of one FcγR is well compensated because these cell types express all FcγRs and the remaining FcγRs are still engaged by either IgG2b and / or IgG2c. The next step for defining the impact of the single FcγRs in primary MCMV infection would be the evaluation of double knock out mice, which express only one activating FcγR. Comparing double deficient mice with the Fcγ- or triple-FcγR-KO mouse would reveal the gain of function of the prevailing FcγR.

3.1.3. Role of antiviral antibody response in primary MCMV infection, recurrent infection, and latency

To date, it is believed that antibodies don't play a role in the control of primary MCMV infection but limit recurrent infection and facilitate the maintenance of latency as suggested by studies in B cell deficient mice (μ chain-KO) (Jonjic et al, 1994; Polić et al., 1998). However, FcγR-KO mice control primary infection of the virus less efficient in the SG leading to a higher viral load and delayed clearance. B cell deficiency leads to a complete absence of antibodies and therefore the loss of immune control should be even more pronounced in B cell deficient mice than the FcγR-KO mice, where other antibody mediated effector functions like neutralization are still present. However, the B cell deficient mice in the study by Jonjic et al. were infected with wild type MCMV (Smith strain) into the foot pad whereas FcγR-KO mice received MCMV deleted of *m157* intraperitoneal (i.p.). Since both mouse strains are on C57BL/6 background, wild type MCMV is controlled rapidly by Ly49H NK cells and reaches lower titers than the *m157* deleted virus including the SG. The reduced virus replication in this model might lead to an underestimation of the role of antibodies for the virus control (Bubić et al, 2004; Corbett et al., 2011). The loss of immune control in the SG in primary MCMV infection found in FcγR-KO mice was not recapitulated with mice deficient for a single (activating) FcγR. As discussed,

FcγR functions seem to be redundant in MCMV primary infection and FcγR double deficient mice could reveal the gain of function of the individual activating FcγRs. Taking into account that antibodies are even more important for limiting recurrent virus, experimental setups for reactivation or superinfection might reveal even a higher contribution of FcγRs for the protection. Thereby high concentrations of virus specific affinity matured antibodies are already present at the time point of (re)infection in contrast to the primary infection in which high antibody concentrations need time to develop. Another option is the passive transfer of antibodies prior infection allowing investigating the quality and quantity of antibodies in correlation to their protective capacities. In this context, the IgG subclass composition of the antiviral antibodies might play a role. Relating to this point, the here analysed FcγR-KO mice are on C56BL/6 background, which possess the IgG2c gene instead of IgG2a. Since IgG2c is a worse activator of FcγRIII in comparison to IgG2a (2.6.; 2.7.), the evaluation of FcγR- and FcγRIII-KO mice on BALB/c background could reveal further insight in the role of FcγRIII and its IgG subclass dependent role in primary MCMV infection.

3.1.4. Immune cell populations possibly exerting FcγR dependent control of MCMV in the SG

FcγR-KO mice revealed an organ-dependent loss of MCMV control in the SG. Control of MCMV is exerted by multiple mechanisms (1.3.4.5.a) and deletion of one might be compensated fully or partially by other mechanisms. However, the SG is a site of diminished immune surveillance, i.e. immunoprivileged. Thus, the control by antibodies might be more relevant in SG than in other organs. Accordingly, the importance of antibody control is more pronounced in immunocompromised mice (RAG1 x FcγR-KO: Bootz, 2014; CD4-KO or MHC II-KO: Walton et al., 2011).

The next goal was the identification of the immune cell population(s) participating in the FcγR mediated and antibody dependent control of MCMV primary infection in the SG. First hints were gained by comparing the common immune cell populations in FcγR-KO vs. FcγR-HET mice. Surprisingly, only small differences in immune cell population were observed. In general, a slightly elevated level of CD3 positive cells (T cells) was present in the SG of FcγR-KO mice. Since T cells don't express FcγRs, the local expansion and / or recruitment of CD3 negative FcγR bearing cells might be slightly hampered in absence of FcγR on innate immune cells. The ratios of CD4 and CD8 T cells were comparable between KO and HET-mice. The CD4 T cells are the main effector cell type exerting antiviral functions. It would be of interest to compare the amount of virus specific CD4 T cells and their functionality because FcγRs facilitate antigen presentation of APCs and consequently their absence could result in slower and lower priming of T cells (Regnaut et al., 1999).

Moreover, slight alterations in two subsets were detectable: the level of NK cells at 14 dpi and the level of macrophages at 28 dpi were reduced in FcγR-KO mice. As described above, SG resident NK cells are phenotypically different and might be functionally impaired and peripheral NKs are not recruited to the SG during MCMV infection. Nevertheless, it was shown that NK cells preserve organ integrity and function and regulate the innate inflammatory response within the glands (Carroll et al., 2012). MCMV specific IgG antibodies only have a moderate concentration at 14 dpi and in infected mice on C57BL/6 background they are of the IgG2b and IgG2c subclass (Androsiac, 2012), which activate FcγRIII weakly compared to IgG2a (2.6.; 2.7.), which is absent in these mouse strains. Likewise, MCMV control is not reduced in the SG of FcγRIII-KO (2.1.2.) or RAG1 x FcγRIII-KO mice (Bootz, 2014). Therefore further investigations have to be performed to define if the absence of FcγRs have direct (e.g. loss of ADCC)

and / or indirect (e.g. cell activation) effects on the NK cells in the SGs. Otherwise, the reduced number might be a result of the FcγR deficiency unrelated to the loss of FcγR expression.

Macrophages play a dual role in MCMV infection. On the one hand, they are targets of infection and on the other hand, they can phagocytose virions and provide antiviral effects in cis and trans e.g. by limiting virus replication in the macrophage itself, secretion of cytokines, and exerting APC functions (Hengel et al, 2000; Hanson et al., 1999; Hamano et al., 1998). These cells express all FcγRs to high levels (Gulliams et al., 2014). Thus, macrophages might play a role in control of acute infection by taking up infectious virus and protecting more permissive cells from being infected (Hanson et al., 1999, Heide et al, 1995). Furthermore, monocyte and macrophage subsets are the main effector cells for FcγR mediated IgG dependent target cell depletion *in vivo* (Gordan et al., 2015). If activation by FcγRs is missing, ADCC is diminished and secretion of proinflammatory and antiviral substances might be reduced. Additionally, the intracellular virus might not be efficiently eliminated e.g. by ROS and virus replication leads to destruction of the cell (macrophage). Moreover, SG resident APCs have a macrophage like phenotype and are probably included in the overall macrophage population detected here. For these local APCs, it was speculated that they are not directly infected because of the absence of MHC I antigen presentation (Thom et al., 2014; Walton et al., 2011). The inability of FcγRs mediated phagocytosis and consequently antigen uptake or reduced amounts of APCs could lead to diminished priming of CD4 T cells and causing thereby indirectly the elevated viral load. Therefore, it has to be clarified if the (partial) loss of virus control in FcγR–KO mice is caused by the impairment of macrophages and APCs (as a direct consequence of the FcγR deficiency) and / or by inefficient priming and activation of CD4 T cells (as an indirect consequence).

3.2. Optimization of IgG based therapies: IgG subclass dependent activation of FcγRs

3.2.1. Unique FcγR activation pattern of each IgG subclass

Each of the FcγRs displayed a unique IgG subclasses dependent activation pattern seen in the *in vitro* FcγR activation assay using HeLa hCD8 target cells opsonized with the recombinant OKT8 mAbs IgG subclasses. Comparing the *in vitro* FcγR activation with the recombinant OKT8 mAbs produced in the murine P3X myeloma cell line to the binding affinities of the FcγRs to the monomeric IgG measured by flow cytometry revealed that the FcγRs, which bound a certain subclass, were also activated by those. FcγRI was only activated by IgG2a and IgG2c, FcγRIV was engaged by IgG2b in addition to IgG2a and IgG2c, and FcγRII and FcγRIII were triggered by all IgG subclasses except by IgG3. However, the magnitude of activation did not often correlate with the binding data and binding affinities (SPR measurements) reported in the literature. The weak binding of IgG2c to FcγRIII correlated with a weak activation of FcγRIII in the *in vitro* assay. In contrast, the affinity to FcγRIII measured by SPR for a HEK293T derived IgG2c was not reduced compared to the other subclasses (Nimmerjahn et al., 2005a and 2005b). FcγR binding and FcγR activation differed strongly for the IgG1 and IgG2b subclasses. The binding affinities (SPR) of the monomeric IgG in the literature correlate better with the binding data obtained with the biotinylated IgG subclass panel (measured by flow cytometry) than the *in vitro* FcγR activation assay with the P3X derived recombinant OKT8 mAbs. This might not be surprising since the mAbs in both assay (and in the literature) were of different origin. Even the recombinant OKT8 mAbs produced in different cell lines led to alter *in vitro* FcγR activation for the same subclass due to a producer cell specific Fc glycan composition (2.7.). The FcγR activation capabilities of IgG1 was strongly

dependent on its source (and consequently its glycan composition), e.g. IgG1 derived from CHO cells displayed a strong activation of FcγRIII in contrast to IgG1 derived from P3X (2.6.; 2.7.). However, IgG2b mediated FcγR activation was surprisingly weak and even absent if IgG2b was produced in CHO cells. No amino acid polymorphism in the anticipated FcγRs binding sites of IgG2b subclass was observed (2.4.1.), but the recombinant OKT8 mAb of the IgG2b subclasses possess a less frequent amino acid polymorphism in the C_H2 domain in comparison to the most abundant database sequence (2.4.1.). No functional comparisons of these allotypes were made for mouse. However, human IgG allotypes and some polymorphism were associated with altered FcγR activation capabilities. Another or an additional explanation is that (monomeric) binding of IgG does not necessarily correlate with activation by IgG-immune complexes as discussed above (2.2.).

One further factor influencing the activation capabilities of antibodies might be their affinity to the epitope, accessibility of the epitope, and / or epitope density. The epitope specificity has a great influence on the potential of antibodies to mediate Fc dependent effector functions. As an example, HIV envelope specific IgG2a mAbs binding to the same antigen but with different epitopes specificities displayed dissimilar protective capabilities *in vivo*, which did not correlate with their antigen affinity nor neutralization capability. These facts suggest that the dissimilar FcγR activation capabilities depending on the epitope specificity (Bournaszos et al., 2014). Similarly, different anti-CD20 mAbs of the IgG2b subclass displayed different *in vivo* activity demonstrating heterogeneity between individual mAb of the same subclass (Uchida et al., 2004). Furthermore, the affinity (amount of bound mAbs) did not correlate with their effectiveness implying that the subclass is a more critical factor (Uchida et al., 2004). Subclass switch variants of the IgG1 subclass were less protective *in vivo* than their IgG2a counterparts and protectively did not correlate with antigen affinity nor neutralization as well demonstrating a dependence on the IgG subclass and epitope specificity for Fc mediated effector functions (Bournaszos et al., 2014). Therefore, the inferior FcγR activation of the recombinant OKT8 IgG2b mAb might be due to its epitope specificity (OKT8) in comparison to other IgG2b antibodies, which are reported in the literature to trigger efficiently FcγRs.

3.2.2. IgG subclass dependant FcγR activation *in vivo*

As mentioned (2.8.3.), the *in vivo* performance of the recombinant OKT8 mAbs could not be determined in this study because sufficient amounts of the mAbs could not be produced. Nevertheless, numerous *in vivo* studies investigating the role of FcγRs and IgG subclasses (also IgG subclass switch variants) for the defence against infection, therapy of cancer, and autoimmune diseases exist. In general, the IgG subclass in combination with the experimental system and thus the type of immune cell(s) involved (FcγR expression profile, type of FcγR mediated effector functions) determines which FcγR(s) are preferentially engaged. Moreover, IgG subclass dependent engagement of FcγRIIB is not easy to assess *in vivo* due to its inhibitory function.

IgG1

The only IgG subclass depending solely on one activating FcγR is IgG1. A dependency of the IgG1 subclass on FcγRIII has been shown in multiple experimental models *in vivo* (e.g. Nimmerjahn et al., 2005a and 2005b; Fossati-Jimack et al., 2000; Hazenbos et al., 1998). These *in vivo* results are in accordance with the binding affinities and the *in vitro* FcγR activation assay demonstrating that FcγRIII is the only activating FcγR triggered by IgG1 (in addition to the inhibitory FcγRIIB). Generally, IgG1 is less effective than IgG2a and IgG2c due to its restricted FcγR activation capabilities *in vivo* (Abbound et

al., 2010; Kaneko et al., 2006; Nimmerjahn et al., 2005; exceptions: Fossati-Jimack et al., 2000; Hamaguchi et al., 2006) or it was not at all effective (Nimmerjahn et al., 2005; Girogini et al., 2008).

IgG2a

IgG2a is the only subclass, which can efficiently trigger all FcγRs *in vitro*. In vivo, the situation is complex: In a model of autoimmune hemolytic anemia, a mild form was induced by low concentration of IgG2a dependent on FcγRIII, but FcγRI and FcγRIV contributed to the development of severe anemia by high antibody concentrations (Baudino et al., 2008; Fossati-Jimack et al., 2000). Metastatic lung melanoma was reduced by IgG2a via FcγRIII and FcγRI (TA99 hybridoma; Albanesi et al., 2012). On the other hand, FcγRIII and FcγRIV are required for acute glomerular inflammation induced by IgG2a (Giorgini et al., 2008). Mostly, FcγRI does not play a central role for IgG2a mediated effector functions but contributes (Ioan-Facsinay et al., 2002; Barnes et al., 2002) or is even dispensable (Giorgini et al., 2008).

IgG2c

Studies comparing the efficiency of IgG switch variants in different experimental systems (B cell, metastatic melanoma, platelet depletion) showed an efficient engagement of FcγRIV, a varying contribution of FcγRI (Hamaguchi et al., 2006; Minard-Colin et al., 2015; Nimmerjahn et al., 2005 and 2010; Koa et al., 2015), and neglectable involvement of FcγRIII reflecting the low *in vitro* FcγRIII activation of IgG2c.

IgG2b

IgG2b is dependent on FcγRIV and FcγRIII *in vivo* and independent of FcγRI in accordance with the results of the *in vitro* FcγR activation assay. In some experimental systems, IgG2b activity is crucially dependent on FcγRIV (B cell depletion/anti-CD20: Hamaguchi et al., 2006; metastatic melanoma/TA99 and plateletdepletion/6A6: Nimmerjahn 2005;) and in others on FcγRIV and FcγRIII (autoimmune haemolytic anemia: Baudino et al., 2008; glomerular inflammation: Giorgini et al., 2008). IgG2b performs in general worse *in vivo* even though the binding affinities of IgG2b are equal to IgG2a/c for FcγRIII and FcγRIV. This might be explained (1) by the additional engagement of the high affine FcγRI by IgG2a/c or (2) by a weak FcγR activation by IgG2b as reflected in the *in vitro* FcγR activation assay in contrast to the binding affinities.

IgG3

As expected, IgG3 is largely inactive *in vivo* with regard to FcγR dependent functions (but IgG3 can mediate Fab or complement mediated effector functions) because it does not bind or engage any FcγRs (Hamaguchi et al., 2006, Nimmerjahn et al., 2005; Fossati-Jimack et al., 2000).

3.2.3. IgG2c substitutes genetically for IgG2a in certain mouse strains but is functionally different

Of special interest is the functional difference between the subclasses IgG2a and IgG2c. Most laboratory inbred mouse strains only possess one of these two subclasses and the potential disparity of them is a matter of controversial current debate because it has a wide impact on immunological data generated in different mouse strains.

The *in vitro* FcγR activation capabilities for the recombinant OKT8 IgG2c mAbs were strongly dependent on the producing cell line (Fc glycan composition) in contrast to IgG2a. P3X derived IgG2c was equal or slightly inferior to IgG2a, HEK293T derived IgG2c was superior, and CHO derived IgG2c strongly inferior compared with their respective IgG2a counterparts. The activation of FcγRIII was surprisingly weak by IgG2c independent of the producing cell line. Similarly, immune sera from MCMV

infected C57BL/6 mice were worse in activation of FcγRIII in contrast to sera from infected BALB/c mice (Androsiac, 2012). In BALB/c mice, the predominant MCMV specific IgG subclass is IgG2a but instead IgG2b and IgG2c are present in similar concentrations in C57BL/6 (Androsiac, 2012; Welten et al., 2016). Concentration, virus neutralization capacity, and avidity maturation were comparable for MCMV specific antibodies in both mouse strains (Androsiac, 2012). This implies that IgG2c (and IgG2b) are inferior activators of FcγRIII than IgG2a. These results suggest that IgG2c substitutes genetically for IgG2a in certain mouse strains, but appears functionally different. Given the fact that most transgenic mouse strains are on C57BL background, this genetic difference has high implications for investigating antibody mediated autoimmune diseases or vaccinations in the mouse model.

Most studies comparing IgG2a and IgG2c focused only on the differences on the genetic and protein level. Only a few studies performed functional evaluations: IgG2a and IgG2c elute at different pH values from Protein A sepharose (Seppälä et al., 1981). Furthermore, the Igh-1-linked genes influenced the subclass distribution but not the affinity of antibodies induced by contact sensitization (László et al., 1985) and as seen in MCMV infection (Androsiac, 2012). Unfortunately, no comparative studies of IgG2a and IgG2c were done by others, but the IgG2c subclass demonstrated its role in protection against cancer and beta-amyloid in Alzheimer disease (Lambert et al., 2004; Petrushina et al., 2003; Hamaguchi et al., 2006).

3.2.4. FcγR polymorphisms and their relevance for the affinity to IgG

Despite the difference in the IgG genes concerning IgG2a and IgG2c (3.2.4.; 1.1.3.), other IgG alleles (of a subclass) show only minor polymorphisms so that a strong difference of FcγRs activation is unlikely (2.1.2.). However, polymorphisms in human FcγRs genes are known of which two greatly affect the affinity to human IgG subclasses and consequently influence the prevalence or severity of autoimmune diseases or infections and the success of mAb based tumor therapies (Bruhns et al., 2009).

A few polymorphisms for mouse FcγRs have been identified. The protein sequence of the FcγRs from the strains BALB/c and C57BL/6 were compared in this study to assess if the FcγRs have adapted to the IgG subclasses present in the respective mouse strains. No differences in the protein sequence of the extracellular domain were found for FcγRI, FcγRII, and FcγRIV. Three amino acid substitutions were detected in the D1 domain of FcγRIII; the FcγR, which displays the biggest difference for the activation by IgG2a compared to IgG2c. These mutations are located at a site, which is not directly involved in IgG binding. The FcγRIII-ζs composed of the extracellular domain of BALB/c or C57BL/6 bound similarly to the IgG subclass panel expect that FcγRIII-ζ of BALB/c bound IgG2c slightly better. The same tendency was observed in the *in vitro* FcγR activation assay with recombinant mAb derived HEK293T cells and P3X myeloma. However, the slightly better activation of BALB/c derived FcγRIII by IgG2c has no biological relevance, because BALB/c mice do not possess IgG2c.

These polymorphism of the FcγRIII was observed before together with a further variant varying by one amino acid from the C57BL/6 (82V/I) and consequently by four amino acids from the BALB/c allele in the extracellular domain. Furthermore, two positions in the cytoplasmic tail differ. In an actively and passively induced arthritis, increase in disease induction and severity was observed for the third variant in comparison to the BALB/c allele (Andren et al., 2005). For FcγRI two groups exist, alleles similar to BALB/c or NOD mice (Gavin et al., 2000). NOD mice possess an FcγRI allele, which differs at several positions (substitution, deletion) displaying a broadened specificity binding IgG2b and IgG3

with high affinity in addition to IgG2a (Gavin et al., 1996 and 1998). For FcγRIIB two alleles were defined (Ly-17.1 and Ly-17.2) possessing four amino acid substitutions, but no functional comparison of the two alleles were made (Slingsby et al., 1997). Therefore, polymorphisms have to be taken into account for the evaluation and choice of therapeutic mAbs especially in the human system.

3.2.5. The IgG subclass dependent capability to trigger distinct FcγRs is modified by the Fc glycan composition

Numerous studies investigated the relationship of Fc glycan composition and its impact on effector functions *in vitro* and *in vivo* (1.2.3.5.). Most recombinant mAbs are of the human IgG1 subclass and consequently, the interplay of producing cell line, glycan composition, and effector functions was mainly evaluated for this subclass (e.g. Lifely et al., 1995). Here, the *in vitro* FcγR activation capabilities of all mouse IgG subclasses produced in three cell lines originating from different species were systematically compared for the first time. Murine recombinant OKT8 mAbs (IgG1, IgG2a, IgG2b, IgG2c, IgG3) were produced in HEK293T, CHO, and the murine myeloma cell line P3X resulting the identical protein sequence of a particular subclass but equipped with different Fc glycoforms. Each IgG subclass displayed a specific pattern of FcγR activation capabilities, which was greatly influenced by the producing cell line. The cell line defines the Fc glycan composition. Some subclasses, like IgG1 and IgG2c, seemed to be more influenced by the cell line they were produced in than other subclasses, like IgG2a. All FcγRs were sensitive to changes in the Fc glycoforms and FcγRIIB seemed to be the slightly more affected than the other ones. Another hint that the properties of IgG1 are rather dependent on the Fc glycan is that the IgG1 produced in CHO cells eluted at a different (less acidic) pH from the Protein G chromatography column than all other recombinant mAbs from any cell line. The fact that the IgG subclasses are differently affected by alterations of the glycan was also shown in different experimental systems (B cell, melanoma, and cell platelet deletion) using recombinant subclass switch mAbs (Albert et al., 2008; Kao et al. 2015; Ito et al., 2014). E.g. enzymatic removal of the majority of the Fc glycan abrogated the *in vivo* activity of IgG1 and IgG2b but not of IgG2c* platelet specific mAbs in the model of antibody induced thrombocytopenia (clone 6A6, produced in HEK293T cells) (Albert et al., 2008). [* In older publications, 6A6 IgG2c (Kao et al., 2015) was misleadingly assigned as “6A6-IgG2a” but it was described as C57BL/6 IgG subclass switch variants (Nimmerjahn et al., 2005; Albert et al., 2008)]. In accordance with the results obtained with the OKT8 mAbs, it was shown that the *in vivo* activity of IgG1 but not of IgG2a anti-erythrocyte autoantibodies is modulated by the glycan composition. Agalactosylation enhanced the FcγR dependent depletion of red blood cells by IgG1 but not IgG2a (Ito et al., 2014).

Unfortunately, the glycan profiles of the different IgGs could not be identified in this study due to limitation of the amount, so that no direct structure-function correlation is possible yet. Since the glycoforms is dependent on the species, the cell type, the IgG subclass, and eventually the culturing conditions no suitable conclusion can be drawn from the literature concerning the glycan composition of the recombinant OKT8 mAbs.

Taken together, it is tempting to speculate that the protein sequence, i.e. the subclass, determines if an IgG-FcγR interaction is possible and that the glycan modifies the affinity whereby it also can hinder the binding.

3.2.6. MCMV mediated alteration of the IgG subclasses dependent FcγR activation

CMV exerts various immune evasion mechanism. In order to optimize an IgG based therapy against CMV, the IgG subclass dependent FcγR activation was evaluated using MCMV infected target cells. The pattern of IgG subclass dependent FcγR activation was not significantly changed but the magnitude of activation seemed to be diminished when comparing MCMV hCD8 infected target cells to HeLa hCD8 targets. However, in some cases IgG2a seemed to be slightly more affected than the other subclasses. This inhibition of FcγR activation is most likely caused by MCMV encoded viral FcγRs like m138. For HCMV, the drastic inhibition of cellular FcγRs by vFcγRs was demonstrated (Corrales-Aguilar et al., 2008, 2013, and 2014; Mercé Maldonado, 2011).

The FcγR inhibition was independent from the producing cell (and consequently the Fc glycan composition) of the antibodies suggesting that the vFcγRs possess a differential binding site, e.g. the C_H2 - C_H3 interdomain, than the cellular FcγRs as shown for other vFcγRs (1.2.3.4.; Armour et al., 2002; Sprague et al., 2008).

The only characterized MCMV encoded vFcγR, m138, binds IgG2a and IgG2b (Bigl, 2010). However, flow cytometry analysis and immunoprecipitation (2.8.3.) indicate that at least one more MCMV encoded vFcγR exists. For example, flow cytometry analysis of IgG-Fc binding to infected cells revealed residual binding by the MCMV Δm138 mutant (Lenac et al., 2006) and even no difference between MCMV wildtype and MCMV Δm138 on an infected DC cell line (Mintern et al., 2006).

To characterize the magnitude of inhibition exerted by MCMV, the comparison of the *in vitro* FcγR activation on HeLa hCD8 to MCMV hCD8 infected fibroblasts is not appropriate, because the antigen amount might be dissimilar resulting in different FcγR-ζ activation levels independent from the expression of inhibitory vFcγRs. For a valid quantification of the inhibitory effect of MCMV vFcγR(s), the ectopic hCD8 antigen was expressed in a MCMV susceptible fibroblast cell line allowing the comparison of MCMV infected and non-infected cells. Unfortunately, the hCD8 expression level of the generated cell lines were negatively affected by MCMV infection and the reduction of the hCD8 surface expression was proportional to the duration of infection. This hampered a valid quantification of the inhibitory effect of the MCMV vFcγRs comparing infected to non-infected cells. However, the *in vitro* FcγR activation was almost completely inhibited on MCMV infected hCD8 expressing fibroblasts in contrast to naïve cells indicating that the viral mediated inhibition is the major cause besides the small reduction of hCD8 expression. An option is the comparison of different MCMV ΔvFcγR mutants in order to avoid different hCD8 expression. Surprisingly, the MCMV Δm138 infection led to comparable weak FcγR-ζ activation as the wild type virus. These findings also argue for further vFcγR(s) encoded by MCMV as discussed before. The additional vFcγR(s) expressed by MCMV Δm138 could cause the strong inhibition of the FcγRs-ζ. In this setting, m138 does not seem to play a superior role for the FcγR-ζ inhibition. The fact that m138 has more prominent functions concerning the downregulation of activating NK cell and T cell costimulatory ligands on infected cells (Mintern et al., 2006; Arapović et al., 2009; Lenac et al., 2006) might indicate an inferior role for m138 as vFcγRs.

The inhibition of the FcγR-ζ was stronger on the hCD8 expressing fibroblasts infected with MCMV than on fibroblasts infected with the MCMV hCD8 virus. This might be caused by the different surface amounts of hCD8 in these two different settings. It can be assumed that viral glycoproteins like gB are not so highly expressed on the cell surface like hCD8 because MCMV buds from inner membranes and not the plasma membrane.

The identification and the characterization of all MCMV encoded viral FcγRs by loss and gain of function approaches is of high interest in order to optimize an IgG based therapy.

3.3. Perspective

3.3.1. Predictive value of the *in vitro* FcγR activation assay

The identification of immune biomarkers that provide protection against infection or disease is an important task to improve prevention (vaccination) and / or therapy. These immune markers are called “correlates of protection” and are divided in non-mechanistic markers, which correlate with protection (e.g. important for quantification if someone is protected after vaccination), and mechanistic markers as causal component(s) for the protection (Plotkin et al., 2012). The *in vitro* FcγR activation assay could serve as a valuable tool to evaluate the quality of the induced antibodies in response to a vaccine approach (Storcksdieck et al., 2015). To protect against viral infections in the mouse model, it is desirable to induce a T_H1 prone immune response with high titers of antibodies of the IgG2a subclass.

For influenza, antibodies are an important mechanistic correlate of protection (Plotkin, 2013). The degree of protection of non-neutralizing anti-M2e mAbs from lethal influenza infection of wild type and different FcγR-KO mouse strains correlated remarkably with their *in vitro* FcγR activation capabilities (6.7.). Thus, if one mechanistic correlate of protection is FcγR activation, the *in vitro* FcγR activation assay has a predictive value for their performance *in vivo*. Nevertheless, the predictive value of the FcγR activation assay might differ for different infection / disease models. Additionally, if an antibody is able to efficiently engage several activating FcγRs *in vitro*, it is dependent on the infection / disease model and the immune cell type(s) predominantly involved, which FcγR(s) is / are preferentially engaged and exert the effector functions of this antibody (subclass) *in vivo*. Thus, the proportional participation of a single FcγRs might not be completely predictable by the *in vitro* FcγR activation assay. Furthermore, the ratio of activating to inhibitory FcγR engagement is not quantifiable. For that purpose, the A/I ratio (ratio of IgG binding to activating and inhibitory FcγR) was emphasized as predictive tool for the activity of antibodies and dependence of particular FcγRs *in vivo* (Nimmerjahn et al., 2005, 2006, and 2015). However, this value takes only the binding affinity of monomeric IgG to FcγRs into account independent of the antigen.

Nevertheless, comparing different antibodies or antibody samples for their *in vitro* FcγR activation capacities can provide important insights into their efficacy and possible mode of action. Furthermore, potential of therapeutic mAb candidates can be evaluated *in vitro* guiding their molecular optimization (3.3.2.) and preselection for *in vivo* evaluation.

3.3.2. The past and the future of an IgG based therapy against HCMV

Clinical trials could not reliably provide evidence in favour of a beneficial effect of hyperimmunoglobulin therapy against HCMV transmission and disease. However, hyperimmunoglobulin preparations, administration protocols, and parameters to evaluate efficiency were not standardized hampering a valid evaluation. Dosing and schedules have to provide constant levels of CMV specific antibody in the blood and their half-life might be shorter due to their consumption during CMV infection than that of non-CMV specific antibodies. Selection of donors for the preparation of IVIG

does not provide information about their biological efficacy. Conventional ELISA systems specifically select for serum donors with high titers of antibodies against internal viral proteins. These antibodies are expected to mediate limited neutralizing (Barahona Afonso et al., 2016) and Fc dependent effector mechanisms like ADCC. In addition, vFcγRs might contribute to the disappointing performance of hyperimmunoglobulin prophylaxis and therapy against HCMV in clinical trials (1.4.3.1.; Budt et al., 2004).

The key for optimized therapeutic mAbs will be the combination of desired and elimination of undesired functions. For an improved therapy by rational designed antibodies, the optimization of the Fab (antigen binding) and Fc mediated effector functions (immune cell activation, half-life) are of great relevance for the efficacy of a therapeutic antibody. This optimization has to include the choice of the antigen(s) / epitope(s), the affinity, the IgG subclass, and the Fc glycan composition.

On the one hand, optimal IgG epitopes have to be identified. Therefore, understanding of the detailed and cell type specific mechanisms of entry and dissemination will provide insights if targeting epitopes on infected cells (by FcγR engagement) or virions (by neutralizing antibodies) or both will be most effective for controlling the virus. A combination of mAbs targeting different viral antigens might be required. The importance of neutralization for controlling CMV is debated (Wirtz et al., 2008; Farrell et al., 1990). Mostly, the virus disseminates in a cell-associated fashion via infected endothelial cells or myeloid cells or by cell-to-cell contact. Therefore, activation of cell mediated IgG effector mechanisms via FcγRs are of special interest.

Besides the targeted antigens, the IgG molecule itself has to be optimized to avoid engagement of the vFcγRs and inhibitory host FcγRs while optimizing binding to activating FcγRs and the FcRn for optimal triggering of effector functions and half-life. The efficiency of the therapeutic antibody against herpesviruses will presumably benefit crucially from prevention of vFcγR binding. The choice of an IgG subclass in combination with amino acid mutations allows for the modulation of Fc mediated effector functions (FcγRs, FcRn, complement, vFcγRs). Furthermore, the Fc glycan composition can be manipulated by the choice of the expression system and knock in or out of glycosyltransferases. Enzymatic modification of antibodies' glycan *in vitro* or *in vivo* are currently evaluated. The effect of the manipulation of the Fc glycan composition and the Fc amino acid sequence cannot be predicated beforehand. Nevertheless, considering the FcγR activation, the *in vitro* FcγR activation assay demonstrated a predictive value for the efficiency of non-neutralizing antibodies *in vivo*. Thus, this assay could guide the molecular optimization and design of therapeutic antibodies (3.3.1.; Corrales-Aguilar et al., 2013).

4. Experimental procedures

4.1. Molecular biological methods with nucleic acids

4.1.1. Molecular cloning

Molecular cloning describes a set of methods to generate recombinant DNA. A gene of interest is introduced into a plasmid, which is amplified in *E.coli* and the re-isolated plasmid is used to express the gene of interest in transfected cells. The plasmid contains sequence elements for the replication in its host species (origin of replication), a selection marker (antibiotic resistance gene) and a site consisting of a set of unique restriction recognition sites (multiple cloning site) to allow the insertion of the gene of interest. An expression vector is a plasmid, which also possesses sequence elements for the expression of the gene(s) of interest in target cells, typically mammalian cells, i.e. promotor, polyadenylation site (polyA), translation initiation sequence, etc.

A representative workflow is the isolation of mRNA (4.1.3.) with subsequent cDNA generation by RT-PCR (4.1.4.4.). Alternatively, the gene of interest is amplified from a donor plasmid by PCR (4.1.4.1.). Commonly, restriction recognitions sites are added to the ends of the PCR product with help of the primers to facilitate the insertion into the target vector. The PCR product is controlled in an agarose gel electrophoresis (4.1.6.), purified (4.1.7.) and digested (4.1.5.) with the same restriction endonuclease(s) like the target plasmid/vector. If only one restriction endonuclease is used, the vector has to be dephosphorylated (4.1.8.). Next, the digested and purified PCR product and vector are mixed and the compatible ends are ligated (4.1.9.). The ligation product is transformed into bacteria and the transfectants are selected applying an antibiotic to the LB agar plate (4.1.11.). Afterwards, the plasmid / vector is re-isolated from individual colonies (4.1.12.), controlled by digestion (4.1.5.) and sequenced (4.1.14). Using only one restriction endonuclease for the insertion, the orientation of insert has to be determined as well (4.1.13). Subsequently the vector can be transfected into target cells to express the gene of interest (4.3.4.). The distinct methods are described in further detail in the corresponding paragraphs.

4.1.2. Concentration of nucleic acids

The concentration of nucleic acids in aqueous solutions was determined by the absorption at wavelength of 260 nm in a micro-volume spectrophotometer (Nanodrop, Peqlab or Biophotometer, Eppendorf). The Beer-Lambert law relates the absorption (A) to the product of the concentration (c), the light path length (l), and an absorption coefficient (ϵ): $A = \epsilon \cdot c \cdot l$. The absorption coefficient is specific for every substance. The average extinction coefficient for double-stranded DNA is $0.020 \mu\text{g} \cdot \text{ml}^{-1} \cdot \text{cm}^{-1}$ and for single-stranded RNA $0.025 \mu\text{g} \cdot \text{ml}^{-1} \cdot \text{cm}^{-1}$ at 260 nm.

4.1.3. RNA isolation and DNA digestion

RNA was isolated to generate cDNA for cloning. The isolation was performed with the RNeasy Kit including the Qiagen Shredder (Qiagen) according to the manufacturer's instructions. Subsequently, RNA concentration was determined (4.1.2.) and a DNA digestion was performed to eliminate possible genomic DNA contaminants. Therefore, 1 μl of DNase I (Roche) was added to 1 μg of RNA in a final volume of 10 μl and incubated at 22°C for 15 min. By incubating the sample at 70°C for 15 min, the DNase was inactivated and in parallel secondary structures of the RNA were dissolved. Afterwards a RT-PCR (4.1.4.4.) or a 5'RACE (4.1.4.5.) was performed.

4.1.4. Methods based on the polymerase chain reaction (PCR)

4.1.4.1. Polymerase chain reaction (PCR)

A polymerase chain reaction (PCR) allows the *in vitro* amplification of a distinct DNA sequence. The specificity is defined by two short single-stranded oligonucleotides (primer), which hybridize at both ends of a defined sequence. A thermostable DNA polymerase generates a copy by adding single nucleotides (dNTPs) to the 3' end of the primer complementary to the sequence of the template DNA. By repeating cycles of template denaturation, primer annealing and elongation an exponential amplification of the DNA fragment is achieved as the template itself as amplified as well.

step		cycles	Standard polymerases		high-fidelity polymerases	
			temperature	duration	temperature	duration
1	Initial denaturation of plasmid		95°C	120 s	98°C	30 s
2	Denaturation of PCR products	Repetition of 2-4 for approx. 30 times	95°C	15-30 s	98°C	5-10 s
3	Primer annealing		50-68/72°C	15-30 s	50-72°C	10-30 s
4	Elongation		68-72°C	60 s/kb	72°C	15-30 s/kb
5	Finale Elongation		68-72°C	7-10 min	72°C	7-10 min
6	Storage		4°C	∞	4°C	∞

TABLE 4.1. Standard PCR Program

Component	Final concentration
Reaction buffer (with MgCl ₂)	1x
dNTPs	200 – 500 µM each
Forward primer	0,2 - 0,5 µM
Reverse primer	0,2 - 0,5 µM
Polymerase	0,025 U/µl
Template DNA	
- low complexity DNA (e.g. plasmid)	1 pg – 1 ng
- high complexity DNA (e.g. genomic DNA)	1 ng – 1 µg
DMSO (optional, e.g. for GC-rich templates)	(3%)
H ₂ O	ad 20 or 50 µl

TABLE 4.2. Standard PCR conditions

A standard 3-step PCR program is shown in Table 4.1. The temperature and duration of the distinct steps are dependent on the polymerase, the template, and the primers. The annealing temperature influences the specificity and sensitivity of the PCR and it is dependent on the melting temperature (T_M) of the primer pair (4.1.4.2.). The recommended annealing temperature is ~5 °C below the T_M for standard polymerases, whereas ~3°C above the lower T_M of the primer pair for high-fidelity polymerases. The standard conditions for a PCR reaction are listed in Table 4.2. DMSO can be added to optimize the PCR specificity and/or yield. The variable parameters for each PCR were chosen according to the manufactures recommendations of the utilized polymerase. A standard polymerase, e.g. Taq, was used for the amplification of short DNA sequences, whereas a high-fidelity polymerase, e.g. Phusion, was utilized for long DNA sequences and difficult templates. A high-fidelity polymerase possess a 3'-5' exonuclease activity, which allows the exchange of an incorrect base pair (proofreading).

4.1.4.2. Primer design

A primer is a sequence specific oligonucleotide, which hybridize to the complementary DNA sequence and serves as starting point for DNA synthesis. A primer pair, a forward and reverse primer, binding to

the sense and antisense DNA strand respectively, determines the DNA fragment amplification by PCR. The length and sequence of the primer pair defines the specificity of the PCR and influences the annealing temperature, which is dependent on the melting temperature (T_M) for the primer. The T_M can be estimated based on the nucleotide sequence and buffer conditions (Formula 4.1.; Wallach et al., 1979). Optimal characteristics are a length of 18-35 bp, a G/C content of 40 – 60%, and a melting temperature of 50 - 75°C, whereat both primers of a primer pair should have similar T_M ($\Delta T_M < 5^\circ\text{C}$). Further requirements are a high specificity of the 3' end, i.e. 2-3 GC nts, no secondary structures, and no complementary sequences within the primer or primer pair. Primers were ordered at Eurofins MWG-Biotech or Integrated DNA Technologies (IDT).

$$T_M[^\circ\text{C}] = 64,9 + 41 \cdot \frac{\text{number of G and C nucleotides} - 16,4}{\text{total number of nucleotides}}$$

FORMULA 4.1. Wallace formula to calculate T_m for oligonucleotides with nt > 13 (Wallace et al., 1979).

4.1.4.3. PCR mediated in vitro mutagenesis

Different types of site-directed mutagenesis, i.e. point mutations, substitutions, insertion, and deletion, can be realized by modifying the primer sequences for a PCR.

a) Addition of recognition sites for restriction enzymes

The most common modification is the addition of recognition sites for restriction endonucleases at the 5' end of the primer facilitating the insertion of the PCR product into a certain plasmid (4.1.5.). In addition, about three nucleotides have to be added to the end of the recognition site to ensure efficient binding and cleavage of the restricting endonucleases.

b) Point mutations

For the insertion of point mutations, i.e. substitution of a few nucleotides, the desired mutation is integrated into the middle of primer sequence. The mismatches reduce the T_M of the primer by 1°C per percent of mismatches. The complete vector sequence is amplified in a PCR reaction with a complementary primer pair and the parental plasmid is digested with *DpnI*. The newly synthesized plasmids are not methylated and therefore not targeted by the *DpnI* digest. In this work, the QuickChange II XL Site-Directed Mutagenesis Kit (Aligent) was used according to the manufacturer's instructions with the exception that the DNA was predicated with 0,8% (v/v) volume Isopropanol, washed with 70% EtOH, and resuspended in H₂O before the *DpnI* digest was performed.

c) Fusion of two sequences by overlap extension PCR

Two DNA sequences can be combined without the insertion of a recognition site for restriction endonucleases with a so-called overlap extension PCR. First, two individual PCR products are generated, whereat an overlapping sequence of about 18- 20 nt is added to the primers at the ends to be joined. Subsequently, the sequences are fused by using both PCR products as templates in a further PCR with the primers for the far ends. Thereby the complementary sequences of both PCR products hybridize and serve as primers as well.

4.1.4.4. Reverse transcription PCR (RT-PCR)

To clone a gene, the complementary DNA sequence (cDNA) of the RNA is commonly used, because it doesn't contain any intronic sequences. The cDNA is generated with a reverse transcriptase, which is a

RNA dependent DNA polymerase, and a 3' primer. Additionally, the reverse transcriptase exhibits a RNase H activity that digest the RNA strand within the RNA:DNA hybrid. Subsequent the cDNA synthesis, it is amplified in a PCR.

Here, the *OneStep RT-PCR Kit* (Qiagen) was used. After reverse transcription for 30 min at 50°C, the reaction mixture was heated to 95°C for 15 minutes to activate the DNA polymerase and simultaneously inactivate the reverse transcriptase, allowing both reactions to take place in the same reaction mixture in succession. The isolation of template RNA is described in 4.1.3., the compounds of the reaction mixture are listed in the manufacturer's instructions, and the scheme of a suitable PCR program is described in 4.1.4.1.

4.1.4.5. Rapid amplification of 5' unknown cDNA ends (5'RACE)

A 5'RACE allows the amplification and identification of a 5' unknown end of an mRNA template, when a small region of the 3' sequence is known. The method is illustrated in Figure 4.1. First, the cDNA is synthesized by RT-PCR using isolated mRNA and a 3' primer (*gene specific primer 1*, GSP1) that recognizes a known sequence in the gene of interest. Alternatively, an Oligo(dT) primer, which consists of 12 - 18 thymine nucleotides and hybridizes to the poly(A) tail of eukaryotic mRNA, can be used. Subsequently, a tail of identical nucleotides, which serves as binding site for an anchor primer, is added to the 3' end. Following, the template is amplified by PCR using an anchor primer and a second, a nested 3' gene specific primer (GSP2). Both primers contain a 5' recognition sites for endonucleases to allow further cloning. Finally, the PCR product is inserted into a plasmid and sequenced.

The choice of nucleotide for tailing is important, because homopolymeric sequence leads to atypical melting temperatures and exhibit low specificity. To overcome these problems, deoxyinosine (dI), which is capable to interact with all four bases with different affinities, is incorporated in the anchor primer. As a result, poly(C)tailed cDNA can be robustly amplified using an optimized anchor primer, which contains a 16mer of dGs and dIs.

The isolation of template RNA is described in 4.1.3. The cDNA synthesis was performed with the SuperScript II Reverse Transcriptase (Invitrogen). The compounds of the reaction are listed in Table 4.3. and reaction mixture was incubated at 42°C for 60 min followed by an inactivation and DNA:RNA hydride denaturation for 15 min at 70°C. Because the utilized reverse transcriptase exhibits an inefficient RNase H activity, a RNA digestion was performed by adding RNase A, which degrades single-stranded RNA (final concentration 0,1 mg/ml; Fermentas) and 1 µl RNase H, which degrades the RNA strand in RNA-DNA hybrids (1 U, Fermentas) for 30 min at 37°C. The DNA was purified by the QIAquick PCR Purification Kit (Qiagen) and eluted in 30 µl H₂O. Subsequent C-nucleotides were added to the 3' end of the cDNA (C-tailing) with the help of a Terminal Deoxynucleotide Transferase (TdT, Invitrogen). The TdT is a DNA polymerase which adds dNTPs to the 3' end of DNA templates and which can be inhibited by RNA contaminations. The reaction buffer (1x final concentration), dCTPs (200 µM final concentration), and 16,5 µl of purified cDNA were mixed, incubated 3 min at 95°C to dissolve the secondary structures of the ssDNA and chilled for 1 min on ice. Then, 1 µl of the TdT was added, the reaction mixture was incubated at 37°C for 10 min, and inactivated by heating to 65°C for 10 min. Next, a PCR was performed with a high-fidelity polymerase, the anchor primer, a 3' gene specific primer, and different amounts of template. The PCR was done with a touch down program, in which a first set of cycles were performed at a high annealing temperature to grantee a high specificity, while the annealing temperature was lowered during the second set of cycles to increase the efficiency (Table

4.4.). Afterwards the PCR fragments were controlled for size with an agarose gel electrophoresis (4.1.6.) and inserted into a plasmid by TOPO cloning (4.1.10) for sequencing.

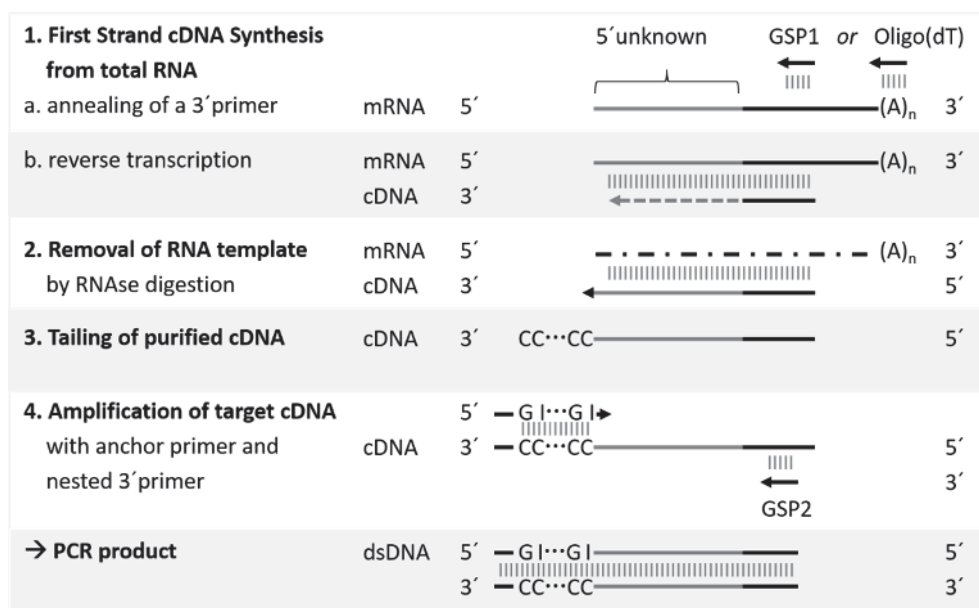


FIGURE 4.1. Scheme of 5' RACE. GSP: gene specific primer ; (A)_n: polyadenylation site

Compound	Final concentration
5x First Strand Buffer	1x
3' Primer (GSP1 or Oligo-dT)	0,2 µM or 0,5 µg
DTT	10 mM
dNTPs	500 µM
Reverse transcriptase (SSCII)	200 U
RNA after DNA digestion (11 µl)	1 µg

TABLE 4.3. cDNA synthesis reaction mix (20 µl)

step	cycles	temperature	duration
1	Initial denaturation	98°C	30 s
2	Denaturation of PCR products	98°C	10 s
3	Primer annealing	64°C	20 s
4	Elongation	72°C	20 s
5	Denaturation of PCR products	98°C	10 s
6	Primer annealing	43°C	20 s
7	Elongation	72°C	20 s
8	Finale Elongation	72°C	10 min
9	Storage	4°C	∞

TABLE 4.4. Touch down PCR program for a high fidelity polymerase

4.1.5. Generation of DNA fragments with restriction endonucleases

Prokaryotes possess restriction enzymes as a defence mechanism against foreign DNA. Type II enzymes cut double stranded DNA at a defined position within or close to a recognition site, which mostly is a 4-8 bp long palindromic sequence. Thereby overhangs of a few nucleotides (cohesive or sticky ends) or, less common, blunt ends are generated. This DNA cleavage is used to control a plasmid preparation (analytical digestion) or for molecular cloning (preparative digestion); e.g. to insert a DNA fragment into a plasmid by digesting both creating complementary ends which can be subsequently ligated (4.1.9.). Enzymes from NEB were used according to the manufacturer's instructions (Table 4.5.). In rare cases, when a non-unique restriction recognition site had to be used for molecular

cloning, a partial digest was performed. Therefore, suboptimal reaction parameters were chosen: suboptimal reaction buffer, drastically shortened incubation time, and a temperature decrease to 4°C.

compound	analytical digestion	preparative digestion
Buffer	1x	1x
BSA (enzyme specific)	1x	1x
Restriction endonuclease	2,5 U	10-20 U
DNA	1,5 µg	2-5 µg
H ₂ O	ad 10 µl	ad 50 µl
Incubation time at 37°C	1 h	2 – 16 h

TABLE 4.5. Reaction mixture for analytical and preparative digestion with restriction endonucleases.

4.1.6. Agarose gel electrophoresis

The separation of DNA fragment by size is accomplished by horizontal agarose gel electrophoresis. DNA molecules are negatively charged due to the phosphate groups of their molecule backbone. Consequently, DNA migrate in the electronic field toward the anode and it can be separated by size in porous agarose gel.

Depending on the size of the DNA fragments, 0,8 - 2% (w/v) agarose was dissolved in 1x TAE by boiling. After addition of ethidium bromide (0,5 µg/ml final concentration), the solution was poured into the electrophoresis chamber and the comb was inserted to form the sample wells. The polymerized gel was covered with 1x TAE and the samples, which were diluted in 6x sample buffer, were loaded. To determine the size, a DNA marker was loaded as well. The electrophoresis was performed at a voltage of 100 -120 V until the desired degree of separation was achieved. The ethidium bromide intercalates into the DNA allowing visualizing the DNA in UV light.

4.1.7. Purification of DNA fragments

To purify DNA fragments after PCR or a preparative digestion, the QIAquick PCR Purification Kit (Qiagen) or for extraction of a specific band from agarose gel the QIAquick®Gel Extraction Kit (Qiagen) was used according to the manufacturer's instructions.

4.1.8. Dephosphorylating of linearized plasmids

After a preparative digestion (4.1.5.) of a plasmid with only one restriction endonuclease, the 5'phosphat groups of the generated ends were eliminated by the alkaline phosphatase to prevent relegation of the plasmid backbone without an insert during the subsequent ligation step (4.1.9.). The linearized plasmid was purified (4.1.7.) and dephosphorylated with the CIP (NEB) according to the manufacturer's instructions.

4.1.9. Ligation of DNA fragments

A DNA ligase catalyses the formation of a phosphodiester bonds between 5' phosphate and neighbouring 3' hydroxyl termini of double stranded DNA fragments under ATP consumption.

The insertion of DNA fragments into linearized plasmids was performed with the T4 ligase from Invitrogen / Life Technology according to the manual containing specific protocols for the ligation of fragments with of cohesive or blunt ends. The molar ratio of vector to insert was 1:3.

4.1.10. TOPO-TA-Cloning

The TOPO-TA-Cloning Kit allows the direct insertion of PCR fragments into a vector. It contains a linearized vector whose ends are covalently linked to DNA topoisomerase I (vaccinia virus) and possesses the enzyme recognition site followed by a single 3'T overhang. The PCR product was synthesized with a DNA polymerase exhibiting a terminal transferase activity, which generate 3'A overhangs. Using DNA polymerase with proofreading (exonuclease activity), a separate A-tailing was performed in succession of the PCR. The A-overhangs hybridize with the T overhang of the vector and they are ligated by and under release of the topoisomerase.

4.1.11. Transformation of *E.coli*

A transformation describes the introduction of a naked exogenous DNA, i.e. a plasmid, into a prokaryotic cell by chemical or physical methods.

4.1.11.1. Transformation of chemically competent *E.coli*

First, the bacteria are treated with divalent cations under cold conditions to shield the negative charge of the anionic cell membrane allowing the negatively charged DNA to adhere to the bacterium. In addition, it is suggested that the cell membrane integrity changes as well. A heat shock enables the DNA to enter the cells through the transiently disrupted cell membrane. However, the exact mechanism is still under debate.

a) Generation of chemical competent *E.coli*

The *E.coli* stain XL2 blue was used and all steps are performed on ice. 100 ml LB medium was inoculated with 1-2 ml of an *E.coli* overnight culture and grown at 37°C and 300 rpm to an optical density of $A_{595\text{ nm}} = 0,4 - 0,5$. This ensured that the bacteria were in the exponential grow phase. The bacteria are incubated in 3 different salt solution and pelleted in-between (4000 rpm, 10 min, 4°C): 1. 50 ml 0,1 M $MgCl_2$ for 20-30 min; 2. 50 ml 0,04 M $CaCl_2$ for 10 min, and 3. 2 ml 0,05 M $CaCl_2$ 15% Glycerol for 20 min. Afterwards they are the aliquoted and stored at -80°C.

b) Transformation with heat shock

50 µl chemically competent bacteria were thawed on ice, mixed with the ligated plasmids (4.1.9.) and incubated for 20 min on ice, which allows the plasmid to adhere to the cell surface. For a retransformation of a known plasmid, 0,1 - 1 ng were used. A heat shock was applied for 40 s at 42°C and the mixture was cooled down for 2 min on ice. To allow the expression of the plasmid encoded antibiotic resistance, the bacteria were resuspended in 200 µl LB medium and cultured for 1 hat 37°C and 800 rpm. The majorly of the LB medium was discarded after centrifugation (5000 rpm, 1 min, RT) and the pelleted bacteria were resuspended, plated on a LB agar plate with the antibiotic for selection of transformants, and incubated at 37°C overnight. Afterwards the plasmid was re-isolated (4.1.12.) and analysed (4.1.5.; 4.1.14).

4.1.11.2. Transformation with electroporation (BACmid)

The electroporation is more efficient and more tolerant against large charged molecules than chemical transformation and is used for the transformation of BACmids. Applying an electric pulse with defined parameters, the membrane integrity is disturbed causing the formation of transient pores. In addition, the membrane potential is increased, which facilitated the uptake of the negative charged DNA.

50 µl electrocompetent bacteria (in a conductive solution, generation not described) are thawed on ice, mixed with the nucleic acid (50 ng) and transferred to a chilled electroporation cuvette (0,2 cm, *E.coli* Pulser Cuvette, Bio-Rad). The electric pulse is generated by an electroporator (Genepulser II, Bio-Rad) and the standard parameters for prokaryotic cells (2,5 kV, 200 Ω, 25 µF, 5 ms) were applied. Because the pulse disturbs the membrane integrity, it is important to resuspend the bacteria immediately in 1 ml LB medium. To allow the expression of the encoded antibiotic resistance(s), they were cultured at 800 rpm for 1 h at 37°C or 2 h at 30°C if temperature sensitive plasmid is transformed or present in the bacteria (4.1.15.). The majority of the LB medium is discarded after centrifugation (5000 rpm, 1 min, RT) and the pelleted bacteria are resuspended, plated on a LB agar plate with the antibiotic for selection of transformants, and incubated overnight at 37°C or 42°C respectively (see 4.1.15.).

4.1.12. Isolation of DNA from bacteria

To amplify plasmids, *E.coli* were transformed (4.1.11.), grown over night in LB medium with an according antibiotic, and the plasmids were re-extracted by alkaline lysis and purified by anion exchange chromatography. A plasmid isolation in an analytical scale was done with the Mini Kit from single colonies with the objective to subsequently check the recombinant plasmid of correctness (4.1.5.; 4.1.14). The Midi DNA preparation Kit was utilized for the isolation of preparative amounts, e.g. for transfection. The kits were obtained from Qiagen or Machery-Nagel. The BACmids isolation was done with the NucleoBond Kit (AX100, Macherey-Nagel). All kits were applied according to the manufacturer's instructing.

4.1.13. Determination of the orientation of an insert in a plasmid

If a DNA fragment is inserted into a plasmid by the usage of only one restriction endonuclease (4.1.5.) or using TOPO-TA cloning (4.1.10.), it can be present in both orientations: *sense* (5'→3') or *antisense* (3'→5'). The orientation in *sense* is crucial for the expression of the insert and can be determined by restriction analysis (4.1.5.) or PCR (4.1.4.1.). For the restriction analysis, a recognition site has to be present in the insert and the plasmid, so that different fragment sizes are generated dependent on the orientation. The other possibility is to perform two PCRs per clone with a forward primer binding to the insert combined with a forward primer upstream of the insert or reverse primer downstream of the insert, whereas only the second combination leads to PCR product if the insert is in *sense* direction.

4.1.14. Sequencing

If a DNA fragment is amplified or modified by PCR before its insertion into a plasmid, the sequence has to be controlled, because DNA polymerases exhibit a certain error rate. The sequencing was done at GATC Biotech. All generated plasmid were controlled by sequencing.

4.1.15. Generation of recombinant MCMV by BACmid mutagenesis

The MCMV genome size (230 kp) does not allow conventional cloning. To be able to maintain and modify the herpesviral genome in *E.coli*, it was converted to a BACmid (Messerle et al., 1997). A BACmid is a bacterial artificial chromosome, a large circular single-copy episome, which was developed from the single-copy F (fertility) plasmid naturally occurring in *E.coli*, hence containing functional segments for its replication and horizontal transfer. After modification of the BACmid sequence in *E.coli* by different possible recombination strategies, the recombinant virus is reconstituted by transfection of the isolated BACmid into permissive cells (Brune et al., 2000; Figure 4.2.).

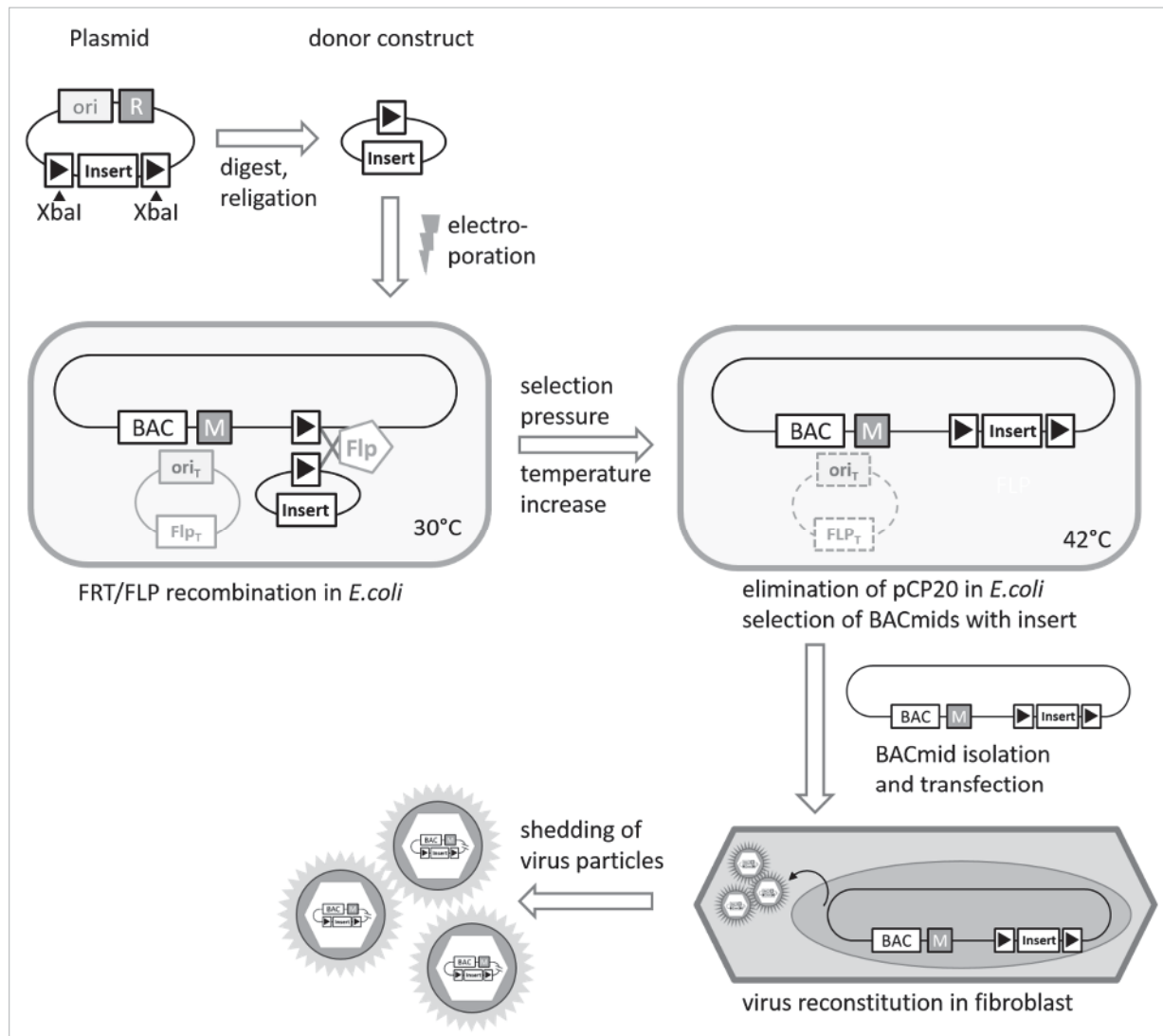


FIGURE 4.2. Generation of recombinant CMV virus particles by BACmid mutagenesis via site-specific recombination (FRT/FLP). The insert contains the gene of interest, a selection marker, and it is flanked by two FRT sites. A donor construct with the insert and one FRT site is generated by *XbaI* digest and religation. This donor construct is electroporated into *E. coli* expressing a FLP recombinase from a temperature sensitive plasmid (pCP20). The insert is recombined with the BACmid at 30°C. Then, the FLP expressing plasmid is eliminated by increasing the temperature and BACmids with insert are selected by antibiotics. The BACmid is re-isolated from *E. coli*. After transfection of the BACmid into fibroblasts, virus particles are produced and shed into the supernatant. These particles are infectious and can be amplified in tissue culture by infection of new target cells.

Here, the insertion of a gene of interest was realized by site-specific recombination via the FRT/FLP system (FRT: flippase recognition target; FLP: flippase, a recombinase; origin: *Saccharomyces*

cerevisiae). The FLP recombinase recombines a pair of short target sequences, whereby one FRT site has to be present in the donor construct with the gene of interest and the other one in the BACmid (Figure 4.2.). To control the expression of the recombinase in *E.coli*, the promoter of the FLP gene as well as the origin of replication (ori) are temperature-sensitive ("suicide plasmid" pCP20, Cherepanov et al., 1995). The BACmid mutagenesis was performed in the recombinase deficient *E.coli* strain DH10B to assure the stability of the genome sequence.

To create the donor construct, a plasmid that possesses the gene of interest together with a selection marker flanked two FRT sites was generated using the conventional molecular cloning methods described in this chapter (4.1.). Via the *Xba*I recognition site, that is present in both FRT sites, the plasmid was cut (4.1.5.) and subsequently the gene of interest containing fragment was re-ligated (4.1.9.), generating a circular DNA fragment only possessing the gene of interest, the selection marker, and one FRT site (donor construct). This construct was dialyzed (4.2.7.5.) and transformed into electrocompetent *E.coli* strain DH10B, which already contained the BACmid and the pCP20 plasmid, by electroporation (4.1.11.2.). During the subsequent incubation for 2h at 30°C the FRT/FLP recombination was occurring. Afterwards, the bacteria were grown overnight at 42°C on LB agar selecting for the BACmids possessing the insert. At 42°C, the pCP20 plasmid is not replicated nor is the FLP expressed. To ensure the selection, the colonies were grown a second time on a new LB agar plate under selection overnight at 42°C. Subsequently, the BACmid was isolated from overnight cultures from individual colonies grown at 37°C (4.1.12.), control digested (4.1.5.) and checked by southern blot (4.1.17.). Correct BACmids were transfected into MEF (4.3.4.). The reconstituted virus was propagated for at least five passages, so that the BAC cassette was eliminated by recombination events in the infected cell (Wagner et al., 1999). The gene expression of the inserted gene(s), the purity of the virus preparation, and the *in vitro* growth kinetics were analysed.

4.1.16. Cryopreservation of bacteria

For long-term storage of transformed bacteria, bacteria from a fresh overnight culture were mixed 1:1 with glycerol and stored at -80°C.

4.1.17. Southern Blot

A specific DNA sequence within a DNA sample is detectable by a Southern Blot. Therefore, the DNA is digested into smaller fragments, which are separated by size in a gel electrophoresis, transferred to a nylon membrane by capillary forces and charge interactions, and fixated by UV light. A particular DNA fragment is detected through the hybridization with a labelled DNA probe exhibiting the complementary target sequence. The probe was labelled with Digoxigenin (DIG), which was detected with an anti-DIG antibody coupled to an alkaline phosphatase (AP) enabling the detection by a chemiluminescent reaction. This method was applied to control the site-specific insertion of genes into the MCMV BACmid.

For the generation of the probe, the DIG High Prime (Roche) was used according to the manual, whereat DIG coupled dUTP nucleotides are incorporated in newly synthesised sequence specific DNA fragments using random primers. One µg of plasmid was used as template to generate the probes, which were stored at -20°C.

The DNA sample (1 µg) was digested by restriction endonuclease(s) over night (4.1.5.). The DNA fragments were separated by gel electrophoresis (4.1.6.) in a 0,5% agarose gel in 0,5% TBE for 2-3 h at 100 - 120 V. Prior to blotting, large DNA fragments were broken down by acidic treatment, which causes the removal of purines from the DNA backbone by hydrolysis. Therefore, the gel was incubated in 250 mM HCl and washed with dH₂O. To separate the DNA stands, the gel was treated two times for 15 min with denaturation buffer (0,5 M NaOH; 0,5 M NaCl), washed with dH₂O, treated two times for 15 min with neutralization buffer (0,5 M Tris/HCl; 1 M NaCl, pH 7,5), and washed again.

For the DNA transfer, the agarose gel and a hydrated nylon membrane (Nylon membrane positively charged, Roche) were equilibrated in 20x sodium citrate standard buffer (SSC). The Turbo-Blot-Apparatus (Schleicher & Schuell) was used according to the instructions and the DNA was covalently bound to the membrane by UV light (UV-Crosslinker CL-1000, UVP). After washing with dH₂O for two times, the membrane was incubated with hybridization buffer for 2 h at 42°C under rotation. In this step, the free binding sites of the membrane are saturated preventing unspecific binding of the probe later on. The hybridization buffer was prepared with *DIG Easy Hyb Granules* (Roche) according to the manufacture's descriptions. For the hybridization, the DIG labelled probe was thawed, denatured for 5-10 min at 98°C, diluted in hybridization buffer, and incubated with the membrane over night at 42°C under rotation. The membrane was washed with different buffers to remove unspecific bound probe: dH₂O; two times with stringent wash buffer I, two times for 20 min at 68°C with stringent wash buffer II, and 2 times with dH₂O.

For detection, the membrane was washed with maleic acid buffer and blocked in 1x blocking reagent (Roche; diluted in maleic acid buffer) for 30 min. Subsequent, the probe was detected with an anti-DIG antibody (anti-DIG AP, Roche) by incubation with ~ 40 mU/ml final concentration in 1x blocking reagent / maleic acid buffer for 30 min. Unbound antibody was removed by washing three times for 10 min with maleic acid buffer and the membrane was equilibrated for 5 min in AP buffer (0,1 M Tris/HCl, 0,1 M NaCl, pH 9,5). The dried membrane was incubated with the substrate (CDP Star, Roche) in the dark for 5 min and the chemiluminescence was visualized on an Amersham Hyperfilm.

After a stripping procedure, the membrane can be detected with another probe. Therefore the membrane was rehydrated with H₂O and incubated two time for 10 min with stripping solution at 42°C in the hybridization tube under rotation, followed by two incubations 10 min with 2x SSC, and finally two incubations for 10 min with H₂O. The protocol was continued at the incubation step with hybridization buffer for 2 h.

4.2. Protein biochemical methods

4.2.1. Determining Protein Concentrations

4.2.1.1. Absorption

The concentration of purified proteins was determined by the absorption at wavelength of 280 nm in a micro-volume spectrophotometer (Nanodrop, Peqlab or Biophotometer, Eppendorf). Aromatic amino acids and Cys-Cys disulphide bonds are responsible for the absorption at 280 nm. Consequently, the protein's amino acid composition influences the absorption coefficient, which is needed to calculate the protein concentration with the Beer-Lambert law (4.1.2.). The average extinction coefficient for IgG it is 1,37 mg · ml⁻¹ · cm⁻¹.

4.2.1.2. Bradford

The protein concentration is determined by a colorimetric reaction. The absorbance of the dye Coomassie Brilliant Blue G-250 changes when it binds to the proteins in a sample. The increase in absorbance at 595 nm is proportional to the amount of the bound dye and consequently the concentration of the protein.

The sample was diluted 1/200 to 1/1000 in the Bradford Solution and the absorption was determined at a wavelength of 595 nm in a spectrophotometer (UV-VIS Spectrophotometer UVmini 1240, Shimadzu).

4.2.2. Lysates for SDS PAGE and Western Blot

The cells were washed with PBS, scraped or detached by Accutase (Sigma-Aldrich) from the tissue culture vessel pelleted (5000 rpm, 1 min, 4°C), and washed twice with cold PBS (4000 rpm, 2 min, 4°C). The pelleted cells are resuspended in lysis buffer (from Luciferase Reporter Gene Assay, Roche) and frozen at -20°C. After thawing on ice, the debris is pelleted (13000 rpm, 30 min, 4°C), and the supernatant is mixed with sample buffer and heated for 5 min to 95°C. To compare different samples in a semi-quantitative Western Blot, the protein concentration of the supernatant is determined by Bradford (4.2.1.2.) and adjusted before the sample buffer is added.

4.2.3. SDS PAGE – Separation of proteins by molecular weight

In a SDS PAGE (sodium dodecyl sulfate polyacrylamide gel electrophoresis), proteins are separated in a porous gel (polyacrylamide) by an electric field according to their molecular weight (Laemmli, 1970). Therefore, the proteins have to be unfolded (denatured) and coated with negative charge, which is achieved by heating the samples in presence of a reducing agent (beta-mercaptoethanol, DTT) and SDS, an anionic detergent. SDS binds to the proteins, thereby imprinting its charge so that the intrinsic charge of the protein is negligible and the molecular weight is the only parameter for the separation in the PAGE. The discontinuous gel consists of a stacking and a resolving gel. In the stacking gel, the samples are concentrated due to the ionic composition in combination with its specific pH and the large pores (low acrylamide percentage) in the electric field. The polymerization is a radical reaction, whereby APS (Ammonium persulfate) initiates the reaction by releasing free radicals and TEMED (N, N, N', N'-tetramethylethylenediamine) stabilizes the radicals leading to a continuous cross-link of the acrylamide / bisacrylamide mixture. The percentage of the polyacrylamide and TEMED in the separation gel defines the pore size and therefore the separable molecular weight range.

First, the separation gel was poured in the gel chamber (two glass plates) and overlaid with Isopropanol to prevent the formation of a meniscus. After polymerization, the isopropanol was removed, the stacking gel was poured and a comb inserted to form the samples wells. The compounds of the gel are listed in 5.5. The gel chamber containing the polymerized gel was inserted into the electrophoresis chamber and running buffer (1x Laemmli) was added into both reservoirs. The comb was removed and the wells were washed with running buffer. The samples were mixed with sample buffer, heated at 95°C for 5 min, and shortly centrifuged before they were loaded. In order to load the same volume per lane, the volume of the samples was always adjusted with an appropriate buffer in advance. A protein size marker (Kaleidoscope Prestained Standards) was loaded as well. According to the size of the gel, a current of 20-30 mA was applied per gel for 1-3 h until the running front, which is

visible due to a blue dye in the sample buffer, has reached the end for the gel. The separated samples were analysed by Coomassie staining (4.2.3.) or Western Blot (4.2.4.).

4.2.4. Protein staining with colloidal Coomassie

Coomassie brilliant blue is an anionic dye, which non-specifically binds to proteins and visualizes them as blue bands. A colloidal staining solution (5.5.) was used, which fixes the protein in the gel (phosphoric acid and ethanol) and simultaneously stains them. To remove the SDS, the gel was washed twice for 10 min in water and it was incubated for at least 3 h with the Coomassie solution. Excess dye was removed by washing with 10% EtOH or water. Otherwise, the InstantBlue (Expedeon, UK), with a detection limit of 5 ng BSA, was used according to the manufacturer's instructions. All incubation steps were performed on a rocking shaker.

4.2.5. Western Blot - Detection of specific proteins

Western Blotting allows the specific and semi-quantitative detection of proteins. Therefore, the proteins are separated by their molecular weight in a SDS PAGE. The separated proteins are transferred to a membrane by applying an electric field (Gershoni et al., 1983). Then, the proteins are specifically detected by a primary antibody. The primary antibody is recognized by a secondary, peroxidase (from horseradish, POD) conjugated antibody. The POD catalyses the oxidation of luminol, which is associated with the emission of light (chemiluminescence) allowing visualizing the protein band.

After a SDS PAGE (4.2.3.), the proteins were transferred to a nitrocellulose membrane by applying an electric field under semi dry conditions. All compounds were equilibrated in blotting buffer and arranged as follows in the blotting apparatus (Fastblot, Biometra): Anode (+) > 3x filter paper (Whatman) > membrane > resolving gel > 3x filter paper (Whatman) > Cathode (-). The transfer was accomplished using a voltage of 14 - 16 V for 60 - 75 min. Subsequently, the membrane was incubated with blocking solution (5% skimmed milk powder/TBST) for at least 1 h at RT or overnight at 4°C to saturate their free binding site. Then, the primary antibody was incubated for 1 h at RT followed by the secondary antibody, which was incubated for at least 30 min at RT or overnight at 4 °C. The antibodies were diluted in a solution of 2,5% skimmed milk powder in TBST. In-between the incubation step, the membrane was washed three times for 10 min with TBST and all steps were performed on a rocking shaker. After drying of the membrane with Whatmann paper, it was incubated for 2 min with an ECL substrate solution (A+B=1:1 mixture), dried again and protected with a foil. The chemiluminescence was detected with by film (Biomax MR, Kodak; Amersham Hyperfilm ECL, GE Healthcare).

After a stripping procedure, the membrane can be detected with another antibody. Therefore, the membrane was washed two times for 5 - 10 min with TBST and H₂O. Subsequently the membrane was incubated for 10 to 30 min with the stripping solution (Reblot Plus Stripping Solution, Millipore) and washed two times for 5 - 10 min with H₂O and TBST. The protocol was continued at the incubation step with the blocking solution.

4.2.6. Native PAGE - Detection of native proteins and complex

In a native PAGE (also named CN-PAGE, colourless native PAGE) the proteins are separated according to their molecular weight, shape, and charge or more exact the isoelectric point (pI). Consequently, the pH of the buffer may influence the running behaviour of the proteins as well. As native PAGE is non-reducing nor denaturing and sodium deoxycholate is a mild detergent, protein complexes or multimers can be detected.

The overall protocol is similar to the SDS PAGE (4.2.3.). The gel was produced as described in 4.2.3., whereby SDS was substituted by H₂O. The glass plates have to be free of tensides as well. The samples were mixed with a native sample and not heated. The gel was pre-run for 30 min at 45 mA at 4°C and separate running buffers for the anode and the cathode were used. After loading the samples, the gel was run with 20 mA at 4°C until the desired degree of separation was achieved. The gel was directly stained with colloidal Coomassie (4.2.4.), without washing beforehand.

4.2.7. Antibody purification

Antibody purification is based on the affinity chromatographic capture (4.2.7.2.) from an antibody source, like tissue culture supernatant of mAbs secreting cells (4.2.7.1.). For a small-scale, the eluted IgG were dialysed against PBS (4.2.7.5.) and analysed by size exclusion chromatography (4.2.7.3.). For a larger production scale, a size exclusion chromatography (preparative scale) was done in succession to the affinity chromatography. If necessary, the samples were concentrated by ultrafiltration (4.2.7.4.). Additionally, the produced antibodies were controlled by Western Blot (4.2.5.) and native page (4.2.6.) before the usage in functional assays (4.5.2.; 4.5.3.) or *in vivo* experiments. The single methods are described in further details in the corresponding paragraphs.

4.2.7.1. Production of monoclonal antibody containing tissue culture supernatant

The production of monoclonal antibodies (mAbs) is achieved by generation mAb secreting cell lines like hybridoma cell lines (1.1.7.1.) or by the transduction a cell line with the cloned heavy and light genes, as done in this study.

The antibody producing cell lines were cultivated in complete RPMI media with decreasing amounts FCS down to 2-3% FCS. Afterwards, the cells suspension was diluted 1/5 – 1/7 with complete RPMI with 0,5 - 1% FCS and cultured for 7 - 14 days until the majority of the cells had died. The cells were pelleted (4000 rpm, 10-30 min, RT) and the supernatant was sterile filtered (Nalgene Rapid-Flow Sterile PES 0,45 µm, Thermo Scientific). The pH was adjusted to pH 7 if necessary and the supernatant was stored shortly at 4°C before antibody purification by Protein G affinity chromatography.

4.2.7.2. Protein G affinity chromatography

Affinity chromatography bases on a specific and reversible protein-protein interaction and allows the concentration and purification of a protein of interest (analyte) from a complex mixture. The binding partner is immobilized on a column matrix (ligand) and captures the analyte, which is applied under binding conditions in a constant flow. Unbound material is washed away and the bound analyte is recovered by specific elution with a competitive binding partner or by nonspecific elution via a change of the buffer condition to those releasing the ligand-analyte-interaction like the pH, ionic strength or polarity. For the antibody purification, two Fc binding proteins (Protein A or G) are commonly used. Protein G is derived from *Group G streptococci* and genetically modified, so that it lacks the albumin-

binding region and possesses two Fc binding domains, which bind to the C_H2-C_H3 interface of all human and mouse IgG subclasses (with different affinities). In addition, a low affinity-binding site can bind to the Fab region (CH domain) of many antibodies. The elution is achieved under acidic conditions (pH 2,5 - 3), which temporary change the tertiary structure of antibody and which have to be neutralized immediately after elution to restore the correct folding and therefore to maintain the function of the antibody.

An ÄKTA basic or basic/purifier system and HiTrap Protein G HP columns (1 ml, GE Healthcare Life Science) were used and the protein concentration (absorption at 280 nm), the pH, and the system pressure were monitored. The column was equilibrated with at least 10 column volumes of PBS using a flow rate of 0,7 ml/min. Approximately 1 - 1,5 L of tissue culture supernatant (4.2.7.1.) were applied to the column with a sample pump using a flow rate of 1 ml/min. PBS wash steps of 10 column volumes were executed after the application of every 100 ml of supernatant. After the final wash step (10 column volumes), the antibody was eluted with 0,1 M Glycin-HCl (pH 2,7), 700 µl fraction were collected and immediately neutralized with 1 M Tris-HCl (pH 9.0). The protein concentration was measured (4.2.1.1.) and selected fractions were pooled. The purification was done at 4°C, 10°C, or RT.

4.2.7.3. Size exclusion chromatography (SEC)

The size exclusion chromatography separates molecules by size and bases on the retention of molecules within the column matrix in contrast to other chromatographic methods, which are dependent on specific interactions. The matrix consists of inert, porous spherical particles, which are filled with buffer (stationary phase). The stationary phase is in equilibrium with the mobile phase. Molecules smaller than the pore size are retained, whereby the duration is inversely proportional to their size. Larger molecules pass through the column at the same flow rate as the buffer and consequently they are eluted with the void volume. The sample volume significantly influences the resolution (peak width).

An ÄKTA basic/purifier system (GE Healthcare Life Science) was used with PBS (Gibco) as running buffer with a flow rate of 0,7 ml/min. For the analytical scale, the column Superdex 200 10/300 GL (GE healthcare) was loaded with 0,1 - 0,5 ml sample. For the preparative scale, the Superdex 200 HiLoad 16/600 Prep Grade (GE healthcare) was loaded with max. 4 ml sample. The sample, which was the Protein G affinity chromatography eluate, was concentrated by ultrafiltration and sterile filtrated (4.2.7.4.) beforehand. A molecular weight standard served as a marker (data not shown). Fractions were collected and the protein concentration was determined (4.2.1.). Fractions with high IgG concentration were pooled and analysed in a native page.

4.2.7.4. Concentration by Ultrafiltration

This filtration method bases on a semipermeable membrane with pores of a distinct size, which defined the molecular weight cutoff (MWCO). Applying pressure (e.g. by centrifugation), buffer and molecules smaller than MWCO pass the membrane, whereat larger molecules are retained and thereby concentrated in the reservoir. The membrane retention a protein depends of on the molecular weight (MW) and the shape and the MWCO typically refers to the smallest MW of a standard molecule that will not effectively pass the membrane, so that molecules with the MW ~ MWCO will only be partially retained. Thus, it is recommended to choose the MWCO at least two fold smaller than the MW of the protein.

Here, the 50K Amicon® Ultra 4 mL Centrifugal Filters (Millipore) were used for the concentration of IgGs with minimal centrifugation times of 5 -15 min depending on the volume in a swinging-bucket rotor at 3900 rpm and RT.

4.2.7.5. Buffer exchange by dialysis

Similar to the ultrafiltration, the dialysis bases on the separation of molecules by their MW using a semi-permeable membrane with a defined pore size (MWCO). The buffer exchange, or more exactly, the out dilution of compounds with $MW \leq MWCO$ in the sample, is dependent on differential diffusion of the molecules. The sample is filled in dialysis tubing (large scale) or as drop on a dialysis membrane (small scale) and incubated with a large volume of buffer, which defines the final concentration of the molecules $MW \leq MWCO$ in both solutions once the equilibrium is reached.

During the process of antibody purification the eluted IgGs from the Protein G affinity chromatography were dialyzed against PBS (Gibco) and subsequently sterile filtrated (0,45 µm sterile Acrodisc Supor membrane, PALL Life Science) when no SEC was done in succession. The Spectra/Por (MWCO 20k, CE, sterile, 16 mm, Roth) was used according to the instructions. For transformation of *E.coli* by electroporation (4.1.11.2.), the DNA has to be in a salt free solution. Therefore, the “drop dialysis” technique from Millipore (V-series membrane) was applied following the manufacturer’s instructions.

4.2.8. Immunoprecipitation of protein complexes

An immunoprecipitation of metabolically labelled proteins allows the isolation of specific proteins and their interaction partner from a cell lysate by specific antibodies. For labelling, ³⁵S- labelled amino acids, namely, methionine and cysteine, were used. The starvation medium lacks these amino acids so that ³⁵S labelled methionine and cysteine are incorporated into all newly synthesised proteins. These proteins are separated by size in a SDS-PAGE and visualised on an autoradiography film.

MEF cells were seeded in 6-well plates and infected with MCMV with MOI 2 the next day. Generally, one well was used per sample. After 2 days, the infected cells were washed with PBS and incubated with 700 µl/well starvation medium supplemented with ~150 µCi L-[³⁵S]-methionine and L-[³⁵S]-cysteine for 2 h at 37°C. Samples were washed three times with cold PBS and lysed for 20 - 30 min with 700 µl/well IP lysis buffer on ice. Cells and cell lysate were transferred into a 1,5 ml tube and the cell debris was pelleted (13 000 rpm, 30 min, 4°C). The supernatant was transferred to a new 1,5 ml tube and incubated with the specific antibody (typically 0,5 - 10 µg) at 4°C under rotation in an overhead mixer. After one hour, Protein G sepharose (PGS) was added and incubated at 4 °C under rotation for 1 – 1,5 h. Previously, the PGS was washed and resuspended in buffer IP-B. PGS was always pipetted with cut tips. Next, the PGS was washed two times with Buffer IP-B, once with buffer IP-C, and once with buffer IP-D. In-between, the PGS was pelleted at 13 000 rpm, 20s, 4°C and the supernatant was aspirated. After the last washing step, the complete liquid was removed and the dry sample was resuspended in IP sample buffer. Alternatively, the sample was resuspended in 30 µl PNG buffer for the deglycosylation. After denaturation at 95°C for 5 min, the samples was cooled down on ice, and 6 µl beta-Mercaptoethanol and 2 µl PNGase F was added and incubated overnight. Samples, which were not deglycosylated, were frozen at -20°C.

Samples were resuspended in 16 µl IP sample buffer, proteins were desaturated 5 min at 95°C, and added in pockets (without PGS). Samples were separated by a discontinuous SDS-PAGE with 8 - 11,5% polyacrylamide. The gel apparatus was designed in our laboratory. It is a vertical gel system with a

separating gel of about 22 cm length. First, the separating gel was poured between two glass plates using a mixing chamber for the gradient. The separating gel was overlaid with 0,2% SDS during its polymerisation. Afterwards the stacking gel was poured and the comb inserted. The composition of the IP gel was identical to the conventional SDS-PAGE with the exception that the higher concentrated separating gel contained 15% (w/v) sucrose and only 0,03% (w/v) APS was used. The gel was run with IP running buffer for about 17 h with 20 mA. The proteins in the separating gel were fixated in 40% (v/v) MeOH and 10% (v/v) glacial acetic acid for 1 h with gentle shaking and washed two times with H₂O. Next, the gel was transferred to a wet Whatman paper and overlaid with foil. It was dried for 2h, 80°C in a vacuum dryer. The dried gel was exposed to an autoradiography film in a film cassette. The exposure time of the film is dependent on expression level and labelling time of the specific protein. For vFcγR, the first exposure time of about one week and a second exposure about of 2 - 3 weeks.

4.3. Cytological methods

4.3.1. Cultivation of eukaryotic cells

Cultivated cells are of either primary origin or an immortalized cell line. Primary cells have a limited survival capacity in contrast to cell lines, which are immortalized due oncogenic mutations or the presence of a viral anti-apoptotic protein.

Adherent cell lines are cultured in DMEM supplemented with 10% FCS, 1% Penicillin, and 1% Streptavidin (complete DMEM). When 90 - 100% confluence is reached, cells were washed with PBS, incubated with trypsin at 37°C for several minutes until all cells were detached, resuspended in medium (37°C), and a fraction was transferred to a new flask with the appropriate volume of fresh medium.

The suspension cell lines are grown in RPMI Glutamax with 10% FCS, 1% Penicillin, 1% Streptavidin, 1 mM sodium pyruvate and 50 µM beta-Mercaptoethanol as additives (complete RPMI). The confluent cell suspension is resuspended to separate cell clumps and a fraction is transferred to a new flask with the appropriate volume of new medium (37°C). The cells are kept at 37°C, 5% CO₂ and 95% humidity. The complement in FCS was inactivated for 30 min at 56°C.

4.3.2. Cryopreservation of eukaryotic cells

Eukaryotic cells can be frozen in 10% DMSO by slowly decreasing the temperature, which prevents the crystallization of water and therefore cell lysis, and stored in liquid nitrogen (-196°C), a temperature where no biological process is taking place.

The cells are detached and/or resuspended, washed in PBS, and pelleted (1000 rpm, RT, 5 min). Adherent cells are resuspended in 50 % complete DMEM, 40% FCS, and 10% DMSO, whereas the suspension cells are frozen in 90% FCS and 10% DMSO. The cells were cooled down in a Cryobox filled with 2-Propanol at -80°C, which leads to a temperature decrease of approximate 1°C per minute. The next day the frozen vials were transferred to the liquid nitrogen tank for long-term storage. Thawing was executed in a 37°C water bath, cells were diluted in 10 ml medium (37°C), centrifuged and the DMSO containing supernatant was removed, and the cells were resuspended in fresh medium. Since a prolonged contact with DMSO at RT is toxic for the cells, all procedures were performed in an appropriate period.

4.3.3. Preparation of primary Mouse Embryonal Fibroblasts (MEF)

Primary MEF are still the best target cell for MCMV infection although different immortalized variants are available, but these are not suitable for all applications. MEF were generated as described in Brune et al., 2001. Day 15 - 17 pregnant mice were euthanized by cervical dislocation, the foetuses were taken out and placed into PBS. Liver and gut were removed, the remaining tissue was washed in PBS, and cut into small pieces in the minimal volume of PBS. The tissue pieces are pooled and carefully washed by adding PBS ad 50 ml in a (or several) 50 ml tube(s). The tissue pieces are sedimented by allowing the tube(s) to stand for five minutes and subsequent one third of the PBS was removed. The washing was repeated until the supernatant was clear. The supernatant was removed so that the tissue was covered by about 5 ml of PBS. To obtain a single cell suspension, mechanical tension by glass beads is applied together with enzymatic digestion of the connective tissue by trypsin and released DNA by DNase I. Therefore, the tissue was transferred into an Erlenmeyer flask with two layers of glass beads and filled up with PBS / Trypsin so that the beads are slightly covered with liquid (final volume of about 25 ml per Erlenmeyer flask; with final concentration of trypsin of 0,6%). The mixture was stirred slowly for 30 min at 37°C before 5 ml of trypsin (2,5%, Gibco) and 500 µg of DNase I (Roche) were added and stirred for another 30 min. Afterward, the cell suspension was transferred into 50 ml tubes and the glass beads were washed with PBS; the PBS was added to the cell suspension. The cells were pelleted 10 min, 800 rpm, RT. Two thirds of the supernatant were removed and the pellet was resuspended in complete DMEM. Tissue clumps were sedimented and the supernatant was transferred into tissue culture flask (175 cm²) with a final volume of 60 - 90 ml medium per flask. The amount of cells per flask are important for the fitness and survival of the cells and it has to be taken into account, that not all prepared cells are fibroblasts, consequently a fraction of cells do not adhere. They were removed by a medium exchange after 4 - 6 hours of culturing (= passage 0). Typically, cells from about five foetuses were plated per 175 cm² flask. If the cells were confluent after one day, they are expanded 1/10. If they were confluent after two days, they are expanded 1/4. The MEF are frozen as described in 4.3.2. (= passage 1). After thawing, the MEF were expanded two times ~1/3 and passage 3 was used for the experiments.

4.3.4. Transient transfection of eukaryotic cells

Transfection describes the introduction of naked exogenous DNA into eukaryotic cells by chemical or physical methods. The target cells were seeded one day prior transfection into a well (10cm²) of a 6 well plate so that they reached 70% confluency the next day. The transfection was performed with Superfect (Qiagen), a branched protein that binds to the natively charged DNA and to the cell surface facilitating the uptake of the complex by endocytosis.

4.3.5. Generation of stable cell lines

4.3.5.1. Stable transfection

The cells are transfected as described in 4.3.4. and selected by adding the antibiotic, which is encoded on the transfected vector. The duration of the selection and the concentration is dependent on the particular antibiotic and the cell type. For the cultivation, the antibiotic concentration is reduced but it has to be applied constantly to prevent the loss of the transfected vector.

4.3.5.2. Lentiviral transduction

Transduction describes the infection of target cells with viral vectors. In contrast to (stable) transfection, the lentiviral transduction has the advantages that the gene is integrated into the genome leading to a stable expression also without constant selection pressure. Furthermore, various cell types can be efficiently transduced in contrast to transfection.

Lentiviral particles are produced by transfection of a producer cell line (e.g. HEK293T) with three trans-complementing vectors encoding diverse compounds that are needed for the formation of infectious but replication deficient vector particles: (i) the pseudotyping vector commonly encoding the G protein of the Vesicular Stomatitis Virus (VSV-G) because of its broad cell tropism, (ii) the packaging vector encoding HIV derived enzymes (*pol*), structural proteins (*gag*), and necessary accessory proteins (*tat*, *rev*), (iii) the transfer vector contains the HIV encapsidation signals (Ψ), the gene of interest controlled by a promoter, the *rev*-response element (RRE), and an selection marker. This sequence is flanked by the HIV genome ends (LTRs, long terminal repeats) that facilitates its packaging into the virions (together with the viral enzymes). The target cell line is infected with the vector particles and after two to three days, viral gene expression is detectable. The lentiviral system works by reverse transcription of the LTRs flanked RNA into double-stranded DNA, which is then inserted into the host genomic DNA by non-homologous recombination, which is essentially a random process but favouring sites of gene expression because of the non-condensed structure of the DNA (Ramezani et al., 2002). This system is called 2nd generation and assures the biosafety by the physical separation of different compounds and by using a modified and therefore transcriptional inactive 3'LTR (e.g. deletion of U3).

The HEK293T cells were seeded in cell culture dished (diameter 10 cm) so that 70% confluence are reached the next day. Prior to transfection, the medium was exchanged with 4 ml fresh complete DMEM. The transfection agent polyethylenimine (PEI) was mixed in a final concentration of 22,5 $\mu\text{g/ml}$ with 6 μg of the packaging, the envelope, and the transfer plasmid in a total volume of 2 ml DMEM. PEI is a stable cationic polymer, which condenses DNA into positively charged particles that bind to the anionic cell surfaces and that are endocytosed by the cells. After 15 min of incubation at RT, the mixture was added to the HEK293T cells. The next day, the medium was exchanged with 7 - 10 ml fresh compete medium. Two days after transfection, the vector particle containing supernatant was harvest, centrifuged (1500 rpm, 5 min, RT), and sterile filtrated (0,45 μm). Polybrene was added to a final concentration of 4 $\mu\text{g/ml}$. It is a positively charged large polymer facilitating the infection by reducing the electrostatic repulsion of overall negative charge membranes creating attraction among the virus particles and the virus particles to the cells (Davis et al., 2004). A fraction of the infectious supernatant was added to the target cells, whereby the MOI should not exceed one. To improve further the infection, the supernatant was centrifuged on the adherent target cells layer for 2 h at 2000 rpm and RT. Instead, suspension cells were rotated in the supernatant at 37°C for 2 h. Afterwards, fresh medium was added. The next day, the medium was exchanged and the cells were transferred to a bigger flask if needed. The selection was started two to four days after transduction to grantee a sufficient expression of the selection marker. The duration of the selection and concentration of the antibiotic is dependent on the cell line and antibiotic and was empirically tested beforehand. The expression of the gene of interests and the completeness of the selection was verified by flow cytometry and / or western blot.

4.4. Virological methods

4.4.1. Infection of cells with MCMV

The multiplicity of infection (MOI) describes the ratio of infectious particles per target cell. At MOI of one as much virus particles as cells are applied. However, the probability that a certain amount of cells is infected is dependent on the statistical Poisson distribution. As remark, the virus titer is attributed to the cell type, which was used for the titration and may differ for another cell type.

Target cells are seeded one day prior infection. The virus stock is thawed, diluted in complete DMEM, and added to the cells. Using tissue culture plates, the infection is enhanced by centrifugation 2000 rpm, RT, 30 min. If an unpurified stock is used, the medium is exchanged 2 hours after centrifugation. Dependent on the experimental requirement, the cells are cultivated for 1 - 3 days. One day after infection, a cytopathic effect (CPE) which describes the morphological changes due to the infection is observable. MCMV infected cells round up, are enlarged, and form syncytia, whereat neighbouring cell fuse together. In addition, nuclear or cytoplasmic inclusion bodies appear.

4.4.2. *In vitro* Amplification of MCMV and Purification of a virus stock

After the reconstitution of a recombinant virus from its BAC (4.1.15.), a first stock (prime stock) was generated. All working stocks for *in vitro* and *in vivo* experiments were inoculated with this prime stock to prevent genetic alterations of the recombinant virus over time by multiple passaging.

First, an inoculum for the working stock was produced by infecting a 175 cm² flask of mouse fibroblasts (MEF, CIM, BIM) with the MCMV prime stock (4.4.1.). When all cells were infected after one to a few days, the supernatant and the cells were harvested after two additional days of culturing to ensure the finalization of the replication cycle. The cells were dounced in a small volume of the supernatant, mixed with the supernatant, aliquoted, and stored at -80°C. The virus titer was determined without centrifugal enhancement (4.4.3.). 25 - 35 175 cm² flasks were infected with an MOI of about 0,01, so that the virus production will peak after completing two replication cycles after 4 - 6 days. It is important during that the media is not turning too acidic during culturing, because an acidic pH leads to diminished virus titers. The pH was monitored by the medium colour and fresh medium was added or partially exchanged (dependent on the progress of the replication cycle) when the colour turned from orange to yellow. After 4 - 6 days, the supernatant was collected and the cells and cell debris were pelleted at 6300 rpm, 20 min, 4°C (Beckman J2-21, Rotor JA-10). The supernatant was transferred to new centrifugation bottles and the virus was pelleted 4°C, 3 h, 13 000 rpm (Beckman, rotor JA-16.250). The supernatant was discarded except for a small volume covering the pellets. By incubation for a few hours, the remaining supernatant loosened up the pellet. Afterwards, the pellet was resuspended and dounced in a frozen douncer and it was further purified by ultracentrifugation on a cushion of 15 - 20 ml of 15% sucrose in VSB with 20 000 rpm, 1,5 h, 4°C (Beckman L-70K ZU, Rotor SW 32 Ti). After discarding the supernatant, the pellet was covered with 1 - 1,5 ml VSB for several hours to loosen up the pellet again, resuspended, and dounced until the solution was homogenous. Aliquots were stored at -80°C. All steps of the virus purification were performed on ice and under sterile conditions.

4.4.3. Quantification of MCMV virus titer

The virus titer is the number of infectious, more precise replication competent, particles in a certain volume or organ and it is indicated as plaque forming unit (PFU). As remark, a CMV virus stock contains also non-replication competent particles e.g. without genome or even without the whole capsid (dense bodies). The classical determination of the virus titer bases on counting virus plaques. Recent developed methods relay on the activity of a reporter gene encoded by a recombinant MCMV. Most commonly, GFP or Luciferase are used. In this work, the classical plaque titration and a Luciferase based methods were applied.

4.4.3.1. Plaque titration of virus stocks

A plaque is a hole in the cell monolayer surrounded by infected cells, which show a CPE in case for MCMV. A plaque is caused by an infectious virus particle. The formation of a plaque is achieved by overlaying an infected target cell monolayer with a viscous nutrition medium, allowing the infected cell to spread the new virus progeny only to the neighbouring cells. The infected cells die and create a visible hole in the monolayer, which is growing with time. For MCMV, the first small plaques are visible within three days post infection. Usually the plaques are counted 4 - 6 days post infection.

MEF were seeded one day prior titration in a 48 well tissue culture plate. For purified or non-purified virus stocks, two different starting dilutions are prepared in complete DMEM (typically, 1/1000 and 1/10000 or 1/10 and 1/100 respectively). A 1/10 dilution series (55 µl + 500 µl) was performed directly on the plate with eight dilution steps and each dilution was determined in triplicates. In general, the infection was enhanced by centrifugation (2000 rpm, RT, 30 min). Two hours after centrifugation, the medium was aspirated and the cells were overlaid with approximately 500 µl / well methylcellulose. After four and five days, the plaques were counted under the microscope and the titer was calculated in PFU / ml.

4.4.3.2. Viral load in mouse organs

a) Generation of organ homogenate

To determine the viral load in mouse organs, these are snap frozen immediately after harvest in liquid nitrogen and stored at -80°C. Usually, half a spleen, half a lung, one of the two SG, and a small piece of the biggest liver lobe is taken. The organs were thawed on ice and homogenized by mashing it through a 75 µm cell strainer, which is placed in a 50 ml tube, with a syringe plunger on ice. The cell strainer is rinsed in-between and the organ is homogenized in a total volume of 2 ml chilled PBS / 5% FCS. The cell debris was pelleted (800 rpm, 10 min, 4°C), the supernatant was transferred in a 15 ml tube, and centrifuged again (3900 rpm, 2 min, 4°C). The supernatant from the last centrifugation (called homogenate) was used for the titration.

b) Plaque titration (see also 4.4.3.1.)

MEF were seeded one day prior titration in a 48 well tissue culture plate. The homogenate was further diluted ¼ in complete DMEM on ice. A 1/5 (500 µl + 125 µl) dilution series was performed directly on the plate. Each homogenate was titrated in a triplicate with 4 - 6 dilution steps. The infection was enhanced by centrifugation (2000 rpm, RT, 30 min). Two hours after centrifugation, the medium is aspirated and the cells are overlaid with approximately 500 µl / well methylcellulose. After four and

five days, the plaques were counted under the microscope and the viral load was calculated as PFU per gram organ. The weight of the organ was determined by subtraction of the weight of the cryotube with and without the organ.

c) Titer quantification by the luciferase activity

If a recombinant MCMV, which expresses a luciferase reporter gene, was used in a mouse experiment, the luciferase expressed in infected cells can be used to quantify

(i) the viral load in the organ (direct measurement of luciferase activity in the homogenate)

(ii) the produced virus progeny in the organ (by infecting new target cells but without dilution series).

Fibroblasts (CIM, BIM, or MEF) were seeded one day prior titration in a 24 well tissue culture plate so that their reach 80% confluence. 200 µl of homogenate were added to three wells and the infection was enhanced by centrifugation (2000 rpm RT, 30 min). Two hours after centrifugation, the medium was exchange to remove the homogenate, because it contains harmful substances for the cells. 24 hours after infection, the medium was aspirated and 100 µl lysis buffer (Luciferase Reporter Gene Assay, Roche) were added per well. Subsequently, the plates were frozen at 20°C to facilitate the lysis. After thawing, the plates were incubated on a shaking device for 10 min and 50 µl of the supernatant was transferred to a 96 well plate. The chemiluminescence was measured (Mithras LB 940, Berthold or Infinite M200, Tecan) by injection 100 µl of substrate (Luciferase Reporter Gene Assay, Roche) per well and a counting time of 10 s.

The unit of the chemiluminescence is RLU (relative light units). To correlate the measured RLU with PFU, a standard curve with the virus used for infecting the mice was done in parallel to the titration of the organ homogenates. Therefore, a 1/5 dilution series with 12 dilutions was prepared starting with $0,5 \cdot 10^6$ PFU / well. Mock cells are measured to obtain the background, which was subtracted from the RLU. The viral load was calculated as PFU per gram organ. The weight of the organ was determined by subtraction of the weight of the cryotube with and without the organ.

4.4.4. *In vitro* growth kinetics of recombinant MCMV viruses

The replication kinetics of newly generated, recombinant MCMV viruses were compared to an appropriated MCMV virus control to determine if the genome modification had an influence on the viral fitness. MEF were plated in 24 well plates one day prior and infected with MOI of 0,1 and 0,01 with centrifugal enhancement (4.4.1.). After 2h, the medium was exchanged. The cells were cultivated and every 24 h, the supernatant was collected and frozen at -80°C. After the collection of all samples, they were titrated in duplicates (4.4.3.).

4.4.5. Antibody neutralization test (plaque reduction test)

This method quantifies the neutralization capacity of antibody samples (1.1.5.1.).

4.4.5.1. Plaque reduction test

The technique bases on the virus titer determination by plaque titration (4.4.3.1.). One day prior, MEF were seeded in a 48 well plate. Before infecting the target cells, the virus was incubated with the antibody containing samples. 2 - 3 dilutions were determined in triplicates per antibody sample. Therefore, 600 - 700 PFU of MCMV was mixed with the antibody sample and incubated for 1h - 1,5 h at 37°C. Before, the complement is inactive in serum samples by heating them to 56°C for 30 min. The

virus-antibody-mixture was added to the first well and titration in a 1/5 dilution series with six dilution steps. The virus titer was determined as described in 4.4.3.1. The neutralization capacity of the sample was quantified by comparing the virus titer of samples treated with the antibodies and samples treated with a non-neutralizing control antibody.

4.4.5.2. Luciferase based reporter assay

This variation of the assay bases on the virus titer determination by luciferase reporter gene expression (4.4.3.). BIM or CIM are plated in 24 well plates on day prior. $3,5 \cdot 10^3$ PFU were mixed with the antibody samples and incubated as describes above. The virus titer was determined according to 4.4.3.2.

4.5. Immunological methods

4.5.1. Enzyme-linked immunosorbent assay (ELISA)

An ELISA quantifies a specific protein in a complex mixture with the help of specific antibodies and an enzymatic catalysed colorimetric reaction.

4.5.1.1. Direct and Sandwich ELISA

The protein of interest is immobilized on a solid phase (plate) non-specifically via adsorption to the surface or specifically by capture with a coated binding partner e.g. a specific antibody (capture antibody; Sandwich-ELISA). Unbound compounds are washed away and the protein is detected with a specific antibody (detection antibody), which is peroxidase (POD) conjugated. The POD causes the oxidation of a chromogenic substrate thereby converting it into a dye. This colorimetric reaction is stopped by addition of an acidic solution inducing the denaturation of the enzyme. The absorbance is proportional to the protein amount detected and the concentration can be determined with a standard curve (dilution series of the protein with known concentration). The signal can be further enhance by detecting an uncoupled detection antibody with an additional, POD coupled (polyclonal) antibody or by using a detection system of a biotinylated detection antibody and Streptavidin coupled POD. In this work, the concentration of total and MCMV specific IgG in mouse serum was determined by a direct ELISA, coating the serum or a lysate of MCMV infected cells respectively. Furthermore, the amount of IL-2, which represents the readout of the *in vitro* FcγR activation assay (4.5.2.), was measured with a Sandwich-ELISA.

The ELISA plate (96 well, Maxisorp, Nunc) was coated overnight at 4°C with mouse serum, cell lysate (4.5.1.2.) or a capture antibody diluted in EBB. The next day, the free binding sites on the plate were blocked with 100 µl 10% FCS / PBS-T per well for at least for 1 h at RT. The samples transferred to the plate and incubated for 2 - 3 hours at RT or overnight at 4°C. If mouse serum was coated, this step was skipped. Afterwards, the detection antibody was added for 60 min. If a biotinylated detection antibody was used, a subsequent incubation step with POD coupled Streptavidin for 30 min was performed. Finally, 50 µl substrate (1-Step™ Ultra TMB-ELISA Substrate Solution, Thermo) was added per well. The colorimetric reaction was stopped with 50 µl 1 M H₂SO₄ per well after 1 - 3 min. The absorbance was measured at 450 nm and corrected by subtracting the absorbance at the reference wavelength at 620 nm (Rainbow ELISA Reader, Tecan or Infinite M200, Tecan). Samples and antibodies

were diluted in 5%FCS / PBS-T. In-between the different incubation steps, the ELISA plate was washed 3 - 5 times with PBS-T. Generally, the samples were determined in triplicates.

4.5.1.2. Lysates for ELISA

Cells were removed from the tissue culture flask by incubation with Accutase (Sigma-Aldrich) or with a cell scraper, washed with PBS, centrifuged (1500 rpm, 5 min, RT), and the cell pellet was resuspended in about 1 ml cold PBS with protease inhibitor (Roche *Complete Protease Inhibitor Tablets*) per 175 cm². The cells were lysed by sonication (Branson Sonifier II 450). The cell debris was pellet (3900 rpm, 5 min, 4°C) and the supernatant was aliquot and stored at -20°C. The volume used for coating of one ELISA plate was titrated for every batch. The typical dilution was around 1/100.

4.5.2. *In vitro* FcγR activation assay and IL-2 sandwich ELISA

The principle of this assay is described in 2.2. and by Corrales-Aguilar et al., 2013. Briefly, the activation of the individual FcγRs by distinct antibodies or serum preparations can be quantitatively determined by co-cultivation of thymoma cell line expressing FcγR-CD3z chimaeras with immune complexes, typically antibody opsonized target cells. Crosslinking of these chimeric receptors leads to the activation of the TCR signalling cascade and consequently IL-2 is secreted into the tissue culture supernatant, which is quantified by an IL-2 sandwich ELISA and a measure for the magnitude of FcγR activation.

The target cells were seeded in a 96 well tissue culture plate. Either an antigen expressing cell line is used or fibroblasts were infected with MCMV for 1 - 3 days (4.4.1.). Antibody or serum dilutions were diluted in complete RPMI and were added together with $1 - 2 \cdot 10^5$ BW FcγR-ζ cells to the target cells and co-cultured overnight in a final volume of 200 μl per well. The next day 100 μl of PBS-T was added per well to lyse the cells. 150 μl per well were transferred on a prepared ELISA plate. The Sandwich-ELISA was performed as described in 4.5.1.1. with an anti-IL-2 capture antibody (clone JES6-1A12, BD Pharmingen), a biotinylated anti-IL2 detection antibody (clone JES6-5H4, BD Pharmingen), and the POD coupled Streptavidin (Dianova / Jackson ImmunoResearch).

4.5.3. Flow Cytometry

Flow cytometry is a laser-based technology, which characterizes single cells in a fluid by relative size, relative granularity, and relative fluorescence intensity. Multiple molecules on (extracellular) or inside (intracellular) one single cell can be analysed simultaneously via their staining by specific antibodies labelled with distinct fluorophores. From a few hundred up to a few thousand of cells are measured per second. If a cell passes through the laser light, light is scattered by the cell body and the fluorophores are excited by a defined wavelength. The intensity of the emission at a characteristic wavelength for a distinct fluorophore is a relative quantification for the amount of stained molecule expressed by the cell. While the forward-scattered light (FSC) is proportional to cell-surface area or size, the side-scattered light (SSC) is proportional to cell granularity or internal complexity. The association of FSC and SSC allows the differentiation of cell types in a heterogeneous cell population and whole cells from cell debris. A BD Canto II with FACS Diva software was used and fluorophore compensation was performed for multicolour staining if the fluorophores exhibit partially overlapping emission spectra.

4.5.3.1. Generation of single cell suspension for flow cytometry

The procedure is dependent on the cell line. If not stated differently, the centrifugation steps were performed at 1300 rpm, 5 min, and 4°C.

a) Cell preparation of tissue culture cells

Adherent cells were washed with PBS, detached with Accutase (Sigma-Aldrich) or cell dissociation solution (Sigma-Aldrich), and washed again. Suspension cells were washed with PBS. The cells were pelleted, resuspended in FC buffer and eventually counted.

b) Isolation of primary immune cells

(i) Whole Blood

The isolation of mononuclear cells from human peripheral blood (PBMCs) was accomplished by density gradient centrifugation. PBMCs have a lower density than erythrocytes and polymorphonuclear leukocytes (granulocytes). Thus, they can be isolated by centrifugation on an isoosmotic medium with a higher density (Lymphoprep, Axis Shield), which allows the PBMCs to retain at the sample / medium interface while the erythrocytes and granulocytes are sedimented.

Blood was collected into a tube containing anticoagulant (EDTA). The blood was mixed with PBS in a ratio 1:1 and layered on the same volume Lymphoprep (Axis Shield). The different layers according to their density were formed by centrifugation (20 min, 2000 rpm, RT, without breaks). After carefully discarding the serum, the lymphocytes were collected, washed with PBS, resuspended in FC buffer, placed on ice, and eventually counted.

(ii) Mouse spleen (lymphoid tissue)

The mechanical disruption of the spleen or other lymphoid tissue is generally sufficient to generate a single cell suspension. The spleen was harvested and homogenized with a plug of a 5 ml syringe through a 70 µm cell strainer which is placed in medium (RMPI-Glutamax, 10% FCS, 1% P/S). The cells were pelleted and the erythrocytes were lysed (BD Pharm Lysis Buffer, BD Pharming) according to the product instructions. Afterwards, the cells were pelleted and resuspended in medium, placed on ice, and counted.

(ii) Salivary glands (non-lymphoid tissue)

For non-lymphoid tissue mechanical dissociation and enzymatic digestion is recommended for optimal recovery of immune cells. Collagenase D digests the connective tissue, but retains the cell-surface proteins and DNase I is needed to digest the released DNA, which would otherwise agglutinate the cells.

The SG were harvested and fragmented with chirurgic scissors in a small volume of medium (RMPI-Glutamax, 5% FCS, 1% P/S). The samples were incubated in medium with 0,2 mg/ml Collagenase D and 0,1 mg/ml DNase I in a final volume of 6 ml at 37°C for 45 min with frequent resuspension by pipetting. The suspension was further homogenized with a plug of a 5 ml syringe through a 70 µm cell strainer and washed with PBS. To separate further the mononuclear cells, the suspension was layered on two volumes of Lymphoprep following the protocol above. Afterwards, the cells were washed twice with FC buffer with 2 mM EDTA and placed on ice. After the staining procedure (4.5.3.2.), the cells are filtered once more through a filter (Cell Tris 50 µm, Sysmex Partec) before they were measured by flow cytometry.

4.5.3.2. Extracellular staining of surface proteins for flow cytometry

All steps are performed on ice and centrifugation was carried out at 1300 rpm, 5 min, and 4°C. After preparing a single cell suspension (4.5.3.1.), $2 - 5 \cdot 10^5$ cells were seeded per well in a 96 well V-bottom plate. After centrifugation, the supernatant was discarded and the cells were incubated in 50 µl/well staining solution, which contained either the primary antibody, mouse serum, or a mixture directly labelled of primary antibodies, for at least 45 min. If immune cells were stained, a previous incubation step with Fc block for 15 min was added to prevent antigen unspecific binding of the antibodies via FcγRs. The standard dilution for primary antibody was 1/100. Then, the cells were washed two to three times with FC buffer. If unlabelled primary antibody or mouse serum was used, a second staining solution with a labelled detection antibody was added and incubated for at least 30 min. The dilution was dependent on the antibody and varied from 1/200 to 1/500. If a biotinylated detection antibody was used, a third incubation step with the fluorophore labelled streptavidin was performed for at least 30 min. Afterwards, the cells were washed twice and resuspended in 100 - 300 µl FC Buffer containing 3 µM DAPI. DAPI binds DNA and consequently stains dead cells only. Infectious samples were fixed in 3% PFA for 15 min at RT in addition. After fixation, cells were washed with FC buffer by centrifugation at 1500 rpm, 5 min, and 4°C. The cells are measured with a DB Canto II instrument (program FACS DIVA) and evaluated with FlowJo.

4.5.3.3. Intracellular staining of proteins for flow cytometry

If desired, surface proteins were stained first (4.5.3.2.) and cells were resuspended in FC buffer without DAPI. Next, the cells were fixed in 3% PFA for 15 min at RT and washed two times with FC buffer containing 0,05 – 0,1% (w/v) Saponin by centrifugation at 1500 rpm, 5 min, and 4°C. Saponin permeabilizes the cell membrane allowing the intracellular staining. The staining procedure and was performed the same way as for the surface proteins (4.5.3.2.) except that the FC buffer was supplemented with Saponin and the centrifugation was performed at 1500 rpm. The cells are measured with a DB Canto II instrument (program FACS DIVA) and evaluated with FlowJo.

4.6. In vivo experiments in the mouse model

4.6.1. Genotyping of mice strains

The genotype of a mouse strain was controlled routinely. After DNA isolation from the tip of the mouse tail, the gene deletion (or insertion) was detected by PCR. Typically, a common reverse primer is used together with two forward primers, one specific for the wild type sequence and the other for the deletion. Two bands indicate a heterozygote genotype for the specific gene and one band identifies a homozygote wild type or knockout mouse depending on the size of the band.

Therefore, the tip of the tail (0,5 cm) was taken and the tissue was digested by proteinase K (200 µg/ml final concentration) in 500 µl Laird's tail buffer over night at 56°C, 800 rpm. The debris was pelleted twice by centrifugation (13000 rpm, 10 min, RT). To precipitate the DNA, the supernatant was mixed with one volume isopropanol followed by inverting the reaction tube for several times. After centrifugation (13000 rpm, 10 min, RT), the DNA pellet was washed with 70% Ethanol, the supernatant was aspirated, and the pellet was dried at 37°C. After dissolving the DNA in 60 µl ddH₂O overnight, a PCR was performed (4.1.4.1.) and analysed by agarose gel electrophoresis (4.1.6). Alternatively, the DNA was purified with DNeasy Blood and Tissue Kit (Qiagen). For the PCR, the

Promega Master Mix was used, 1 µl of Tail DNA, 0,8 µM of each forward primer, 1,6 µM of the reverse primer, and ad 25 µl with H₂O.

4.6.2. Intraperitoneal injection of mice

Mice were injected intraperitoneally (i.p.) for infection with MCMV or IgG transfer. The mouse was restrained in one hand fixing the neck with the angle of index finger and thumb, the tail with the little finger, and one leg with the ring finger. The mouse was tipped slightly headfirst and the needle of the syringe was inserted into the lower part of the abdomen in cranial direction. The volume was released and the syringe was pulled out after a short pause.

4.6.3. Blood collection and serum preparation

4.6.3.1. Repeated blood collection from the orbital sinus under narcosis

The total blood volume of a mouse is about 7 - 8% of its body weight. Maximal 7,5% of the blood volume can be withdrawn from the retro-orbital venous per week with a recovery time of two weeks per eye. The mouse was anesthetized by inhalation of evaporated Isoflurane and placed on the side. The skin above and below the eye was pulled outwards with the index finder and thump, so that the eyeball was protruding. The orbital sinus was incised with a thin glass capillary (Micro-Haematocrit Capillary) by inserting the capillary in the left or right corner of the eye and applying a short-time gentle pressure plus rotation. Releasing the pressure, the capillary was filled with blood by the capillary forces. The blood was transferred immediately to a reaction tube. Afterwards, the skin was released and the eyeball was pressed gently to stop the bleeding. After 15 min, the coagulated compounds were pelleted (by 10 min, 10 000 rpm, 10°C), the supernatant (serum) was transferred in a new tube, and stored at 4°C or for long-term storage at -20°C.

4.6.3.2. Total blood collection from the heart under thoracotomy

The mouse was anesthetized and subsequently euthanized by CO₂ inhalation. After moisturizing with 70% EtOH, the mouse was fixed on an operating board on its back, the skin was opened and pulled to the sites exposing the thorax. The thorax was opened by cutting the sternum above the xiphoid process and extending the cut parallel to the sternum on both sites allowing the cut thoracic wall to be pulled upwards and revealing the beading heart while leaving the diaphragm intact. The venous blood was slowly withdrawn from the right ventricle with a 26G needle and it was transferred into a tube after removing the needle from the syringe to avoid hemolysis. After 30 min, the coagulated compounds were pelleted (10 min, 10 000 rpm, 10°C) and the serum was transferred into a new tube. After a further centrifugation (2-5 min, 14 000 rpm, 10°C), the serum was stored at 4°C or for long-term storage at -20°C.

4.6.4. Harvest of mouse organs

For the determination of the viral load, the mouse was euthanized by cervical dislocation or by CO₂ inhalation, if the blood was collected as well. After moisturizing with 70% EtOH, the mouse was fixed on an operating board on its back, the skin was opened and pulled to the sites. First, the SG (sublingual gland and submandibular gland) were perpetrated. The thorax was opened to obtain the lung. Afterwards the abdomen was opened and the spleen and the liver (a piece of the middle of the

biggest lobe) were perpetrated. Immediately, every the organ was transferred into cryotubes and snap frozen in liquid nitrogen. The organs were stored at -80°C until the titration (4.4.3.2.)

4.7. Miscellanea

4.7.1. Generation and characterization of BW:FcγR-ζ reporter cell lines

4.7.1.1. Cloning of FcγR-ζ constructs and generation of BW:FcγR-ζ reporter cell lines

The cloning of the mouse FcγR-ζ constructs was performed according to Corrales-Aguilar et al., 2013 and Storcksdieck et al, 2015. Briefly, the chimera consisting of the extracellular domain of the FcγR and the transmembrane and intracellular domain of the CD3 zeta chain (CD3ζ) was constructed by overlap extension PCR. Therefore, the extracellular portion of the FcγRs was amplified from cDNA of mouse splenocytes (primer pair 5-FcγR-*SpeI* and 3-FcγR-zeta). In parallel, the desired domains of mouse CD3ζ chain (primer 5-Zeta-FcγR and 3-Zeta-*SpeI*) were amplified from a vector. Via the primers, a *SpeI* restriction recognition site as well as an overlapping region containing the sequence of the respectively other PCR product were added at the ends of the PCR products. In a third PCR reaction, both PCR products served as template. Pairing of their overlapping ends and PCR amplification using the outer primer (5-FcγR-*SpeI* and 3-Zeta-*SpeI*) “fused” both PCR products together. The latter PCR product was inserted via the *SpeI* restriction recognition sites into the lentiviral transfer vector puc2CLIPwo, which was previously digested with *NheI*. The orientation of the insert in the generated puc2CL6IP-mFcγRI-ζ, puc2CL6IP-mFcγRII-ζ, puc2CL6IP-mFcγRIII-ζ, and puc2CL6IP-mFcγRIV-ζ constructs was tested by a control digestion and the sequence of the insert was controlled by sequencing.

To transduce BW5147 cells, lentiviral particles were produced in HEK293T cells by co-transfection of plasmids coding for VSV-G (envelope plasmid), gagpol (packaging plasmid), and the transfer vector as described in 4.5.3.2. After infection of 0,5 x 10⁶ BW5147 cells with the lentiviral particles, Puromycin selection (1 ng/ml, Sigma-Aldrich) was applied for 10 days starting at day 5 - 6 because of the reduced cell growth after the transduction procedure. To ensure the complete selection, selection pressure was applied a second time for seven days after a recovery phase. The cell lines BW:FcγRI-ζ, BW:FcγRII-ζ, BW:FcγRIII-ζ, BW:FcγRIV-ζ, and later BW:FcγRIII-ζ (BALB/c) were generated.

4.7.1.2. FcγR-ζ surface expression and Fc binding capabilities of the BW:FcγR-ζ reporter cell lines

The stable BW:FcγR-ζ reporter cell lines were stained with FcγR specific mAbs revealing a high surface expression of the chimeric receptor. Furthermore, their IgG Fc binding capabilities were demonstrated by incubation with different concentration of naïve mouse serum derived from BALB/c mice (Figure 4. 3). A concentration dependent binding of IgGs (via their Fc) was detectable for all FcγR chimeras. As expected the high affinity receptor, FcγRI-ζ, bound significant more IgGs than the other FcγR-ζs.

4.7.1.3. Generation of BW:FcγRIII-ζ BALB reporter cells

To convert the FcγRIII C57BL/6 into the BALB/c sequence, three amino acids had to be exchanged. This was realized by an overlap extension PCR whereby the nucleotide substitutions were introduced via the primer sequences (primer pair 1: 5-*SpeI*-Balb-FIII, 3-Overl-FIII; primer pair 2': 5-Overl-FIII, 3-*SpeI*-FIII). The puc2CL6IP-mFcγRIII-ζ (C57BL/6) served as template and the final PCR product was inserted into puc2CLIPwo via *NheI* recognition sites of the vector and *SpeI* in the PCR product. BW5147 cells

were transduced and selected as described before. Complete selection was control by anti-FcγRIII staining in flow cytometry, which revealed a small population of none or very low level FcγRIII–ζ expressing cells. Consequently, the BW:FcγRIII–ζ BALB/c cell line was subcloned by limiting dilution allowing obtaining cell lines derived from only a few cells.

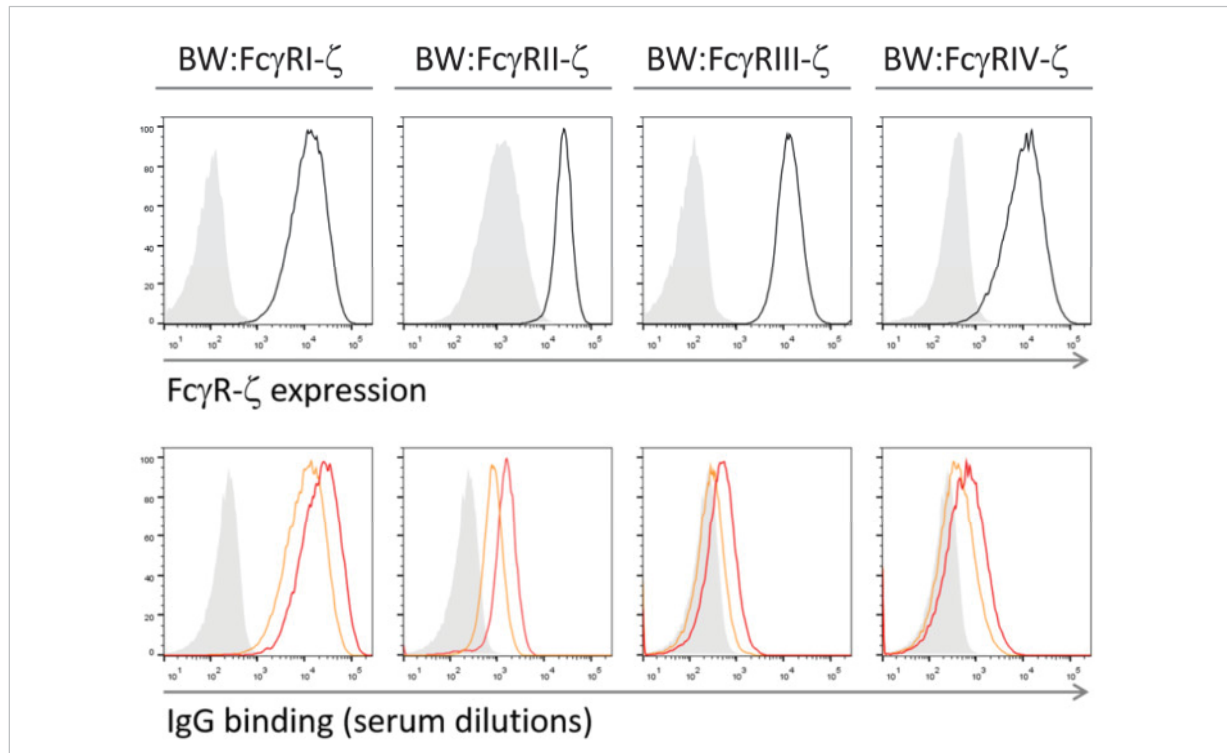


FIGURE 4.3. Transduced BW: FcγR–ζ demonstrate high levels of surface expression of the chimeric receptors and binding of mouse IgG. Parental BW5147 (grey solid) or transduced BW:FcγR–ζ (line) were stained with FcγR specific mAbs (black line) or AlexaFluor647 conjugated FcγRIV specific mAb (clone E9E, Nimmerjahn et al., 2005). Fc binding is shown by incubation with naive BALB/c serum dilutions (orange line: 1/500; red line: 1/200). Primary antibodies were detected with Cy5 conjugated goat anti mouse (Dianova). 2,5x 10⁴ living (DAPI negative) cells were measured by flow cytometry (BD FACS Canto II, FACS Diva software) and analysed with FlowJo (Tree Star Inc).

4.7.2. Generation and characterization of a recombinant MCMV hCD8 mutant

Because of the genome size of herpes viruses, conventional molecular cloning methods cannot be applied and the BACmid technology has to be applied. The method is described in detail in 4.1.1.5. Here, the insertion of the desired genes into the MCMV BACmid was accomplished by FRT/FLP recombination. First, a donor plasmid containing the desired insert was constructed.

4.7.2.1. Design of the insert

The hCD8 was chosen as ectopic antigen (2.3.1.). To ensure an early and strong expression, the hCD8 gene was expressed under the control of the HCMV major immediately early promoter (MIEP), which is commonly used in diverse expression vectors (Boshart et al., 1985). The luciferase Firefly reporter gene was inserted downstream of an internal ribosome entry site (IRES) to facilitate the quantification of infected cells as already established with MCMV Δm157 Luc. Additionally, Zeocin was chosen as selection marker. As a control, a recombinant mutant expressing hCD4 instead of the hCD8 was also generated (MCMV hCD4). These inserts have to be flanked by FRT sites and a scheme is shown in Figure 4.4.

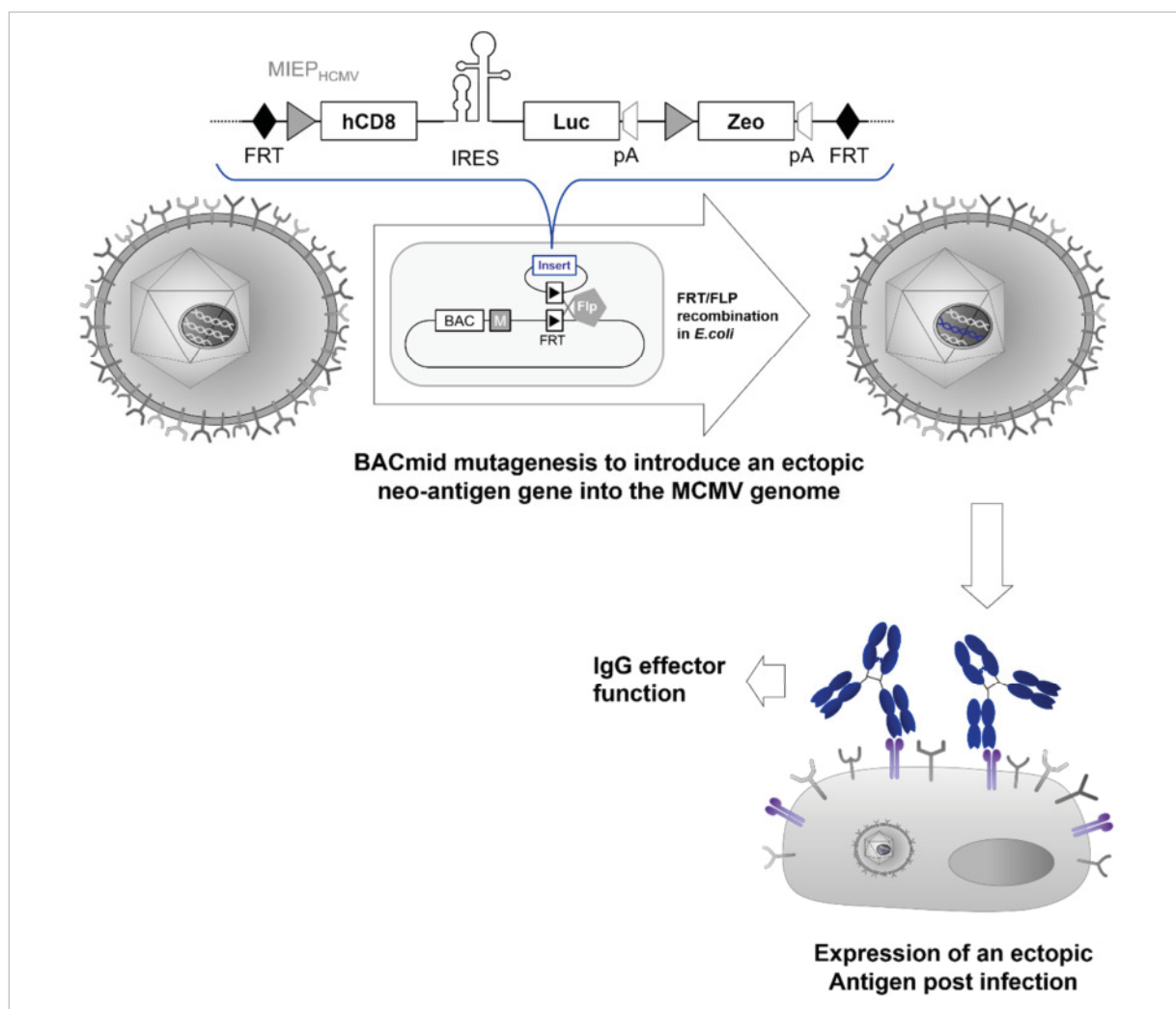


FIGURE 4.4. Scheme of the insert, which was integrated into the MCMV BACmid C3X Δ m157 FRT. The hCD8 gene is under the control of the HCMV MIEP. Downstream of the hCD8, the luciferase reporter gene is inserted and its transcription is driven by an IRES. Additionally, Zeocin is expressed under the promoter SV40/EM7 as selection marker. Both expression units are terminated by a polyadenylation site (pA). The construct is flanked by FRT sites.

4.7.2.2. Generation of the donor plasmids for the BACmid recombination via FRT/FLP: pFRTZ-MIEP-hCD8 / hCD4-IRES-Luc

To be able to insert all desired genetic elements, three steps were performed. First, the vector pIRES-Luc was generated by exchanging the eGFP gene in pIRES-eGFP with the luciferase reporter gene. The Firefly luciferase gene was amplified from the template pTA-Luc-m157FLK (kindly provided by Albert Zimmermann) by PCR with the primer 5-MscI-Luc and 3-Luc-NotI. To excise the GFP and to insert the gene into the pIRES vector, the restriction recognition sites *MscI* and *NotI* were used, whereby pIRES-eGFP was only partially digested with *MscI*.

Next, the ectopic antigen gene was inserted into the multiple cloning site (MSC) of pIRES-Luc (phCD8/4-IRES-Luc). Therefore, the restriction recognition sites *EcoRI* and *BamHI* of the vector pIRES-Luc and *EcoRI* and *BglIII*, an isoschizomer for *BamHI*, flanking the hCD8 / hCD4 gene were used. The hCD8 gene was amplified by PCR from the template pCMV6-XL5-hCD8 (Origene, SC111602, NM_001768) with the primer pair 5-EcoRI-hCD8 and 3-BglIII-hCD8. The hCD4 gene was amplified by PCR from cDNA of Jurkat cell with the primer pair 5-EcoRI-hCD4 and 3-BglIII-hCD4. The restriction recognition sites *BamHI* and *BglIII* were added via the primer to the hCD8 / hCD4 gene.

The last step was the generation of pFRTZ-MIEP-hCD8/hCD4-IRES-Luc by the exchange of the MIEP-IRES-eGFP cassette in pFRTZ-MIEP-IRES-eGFP with the MIEP-hCD8/hCD4-IRES-Luc cassette from phCD8/hCD4-IRES-Luc. This was accomplished via the restriction recognition sites *NotI* and *SnaBI*. This final vector contains the cassette FRT-MIEP_{HCMV}-hCD8/hCD4-IRES-Luc-polyA_{BGH} promoter_{SV40/EM7}-Zeocin-polyA_{SV40}-FRT sites (Figure 4.4.). All steps were controlled by sequencing. Furthermore, the functionality of the selection marker Zeocin was tested by growing the transformed bacteria in selection medium. The surface expression of the hCD8 and hCD4 on transfected HEK293T cells was confirmed by flow cytometry, and the functionality of the luciferase gene was verified by measuring the luciferase activity in lysates of transfected HEK293T cells according to 4.4.3.2.c (data not shown).

4.7.2.3. BACmid mutagenesis to generate C3X Δm157 MIEP hCD8/hCD4 IRES Luc

As location for the insertion of the expression cassette for ectopic antigen, the *m157* gene was chosen. This gene is commonly deleted in recombinant MCMV mutants to avoid an excessive NK cell response in C57BL/6 mice (2.1.; Bubić et al., 2004). Another advantage of the *m157* gene deletion is the increased cloning capacity. Although herpesviruses tolerate quite large insertions into their genome, an oversized genome affects negatively virus replication.

The FRT/FLP recombination was used to insert the desired expression cassette into the BACmid. Electrocompetent DH10B *E.coli*, which contained the C3X Δm157-FRT BACmid and pCP20 vector, were kindly provided by Albert Zimmermann. The C3X-Δm157-FRT BACmid was generated by Albert Zimmermann based on the C3X BACmid (Jordan et al., 2011) and according to the description in Walton et al 2008. The correct MCK-2 gene sequence was restored in the C3X BACmid in contrast to the original C3X BACmid. The C3X BACmid contains a point mutation, which leads to reduced viral titers in the SG *in vivo* (Jordan et al., 2011).

The BACmid mutagenesis via FRT/FLP recombination is described in 4.1.15. Briefly, 1 µg of the donor plasmid was digested with *XbaI*, which is present in the FRT sites. After religation, a construct with the expression cassette and one FRT site was obtained. Next, *E.coli* containing the BACmid and the FLP recombinase were transformed with this construct via electroporation. Recombination was allowed at 30°C. Afterwards the selection of the *E.coli*, which contain the BACmid with the expression cassette, was performed with Zeocin (gene is present in the insert) and Chloramphenicol (gene is present in the BAC cassette) twice. The selection was done at 42°C to eliminate the temperature sensitive recombinase encoding plasmid and therefore avoiding further recombination.

4.7.2.4. Control of the generated BACmid C3X Δm157 MIEP hCD8 / hCD4 IRES Luc

To control the BACmid mutagenesis, the BACmid was isolated and digested with the restriction endonuclease *XbaI* (4.1.5., Figure 4.5.). The wildtype BACmid C3X was used as control and its digestion resulted in 29 fragments whereas the new generated BACmids C3X Δm157 MIEP hCD8 / hCD4 IRES Luc (MCMV hCD8 / hCD4) produced 30 fragments, one fragment unique for the insert (MIEP hCD8 / hCD4 IRES Luc with ~6400 and ~7100 bp, respectively). In addition, a Southern Blot was performed detecting sequence-specific DNA fragments (4.1.17.). The insert was detected with the probe “MIEP-hCD4-IRES-Luc”. Due to the *m157* gene deletion in MCMV hCD8/hCD4, the wildtype and the generated BACmids differ in the two bands flanking the insert, which were detected with the probe “Luc-*m157*FLK”. In addition this probe detects the luciferase gene in the insert and stains the same unique band for the respectively BACmids like the first probe. The detected band patterns are in accordance with the

virtual gel predicting the resulting DNA fragments. Apparently, no unspecific recombination events have taken place.

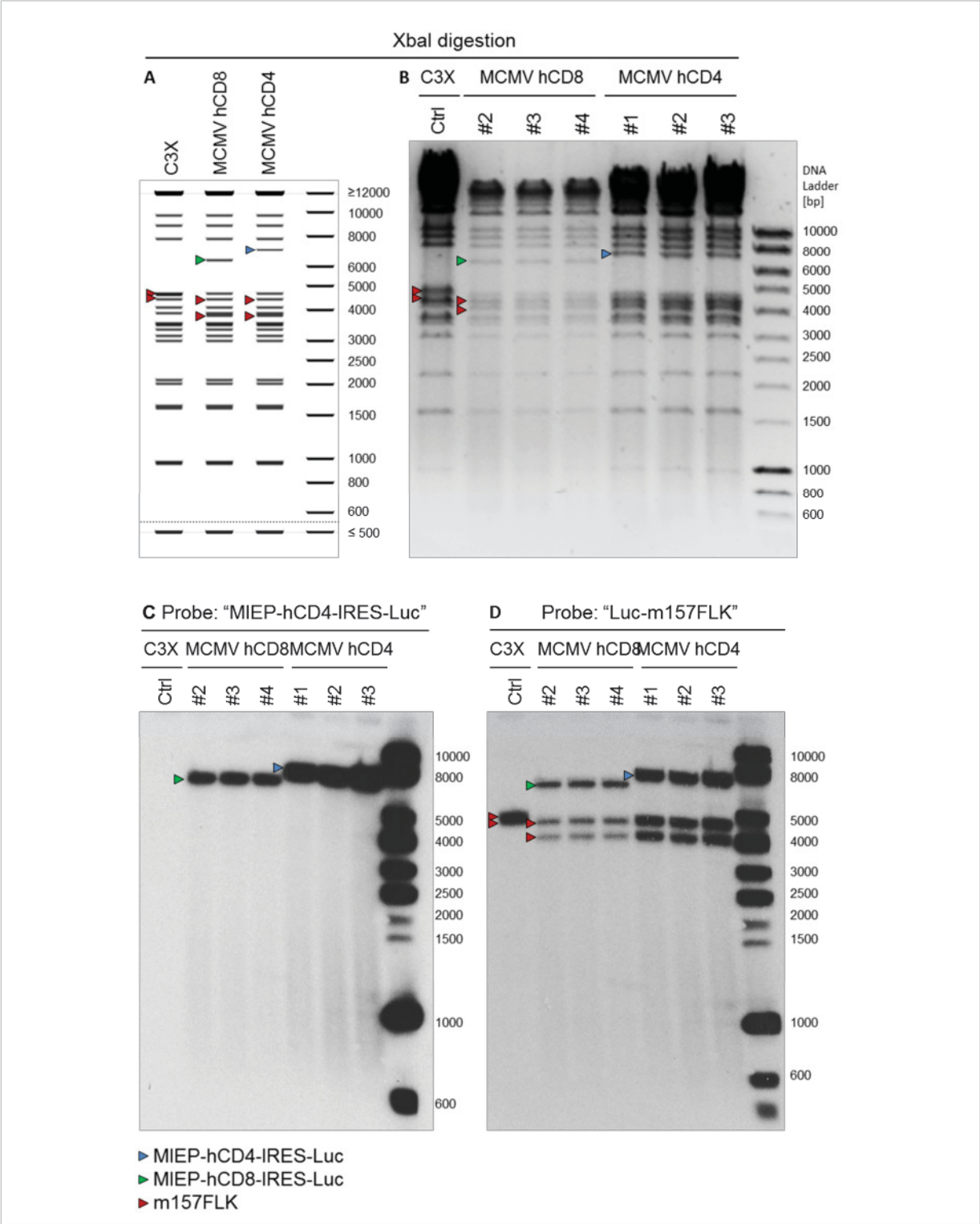


FIGURE 4.5. Restriction endonuclease digest and Southern Blot confirm the predicated DNA band pattern of the generated BACmids for MCMV hCD8 and MCMV hCD4. A. Virtual gel showing the DNA band pattern for the *XbaI* digestion of the C3X, MCMV hCD8, and MCMV hCD4 (Geneious R8). B-D. 1 µg of BACmid DNA was digested with *XbaI* and separated in a 0,5% agarose gel in 0,5% TAE running buffer at 120 V for 2,5h. B. Agarose gel before Southern blot analysis. C, D. Southern blot. Bands were detected sequence-specifically with the probe "MIEP-hCD4-IRES-Luc" (pFRTZ-MIEP-hCD4-IRES-Luc, C) and after stripping with the probe "Luc-m157FLK" (D).

4.7.2.5. Reconstitution of the MCMV hCD8 and MCMV hCD4 virus mutants

For the reconstitution of infectious virus, 2 - 3 μg of the BACmid were transfected into approx. 1×10^6 MEF. Plaques were visible displaying a CPE typically for MCMV after a couple of days. The viruses were passaged for seven times on MEF to eliminate the BAC cassette from the viral genome (Wagner et al., 1999). Finally, MCMV hCD8 and MCMV hCD4 were analysed by the following methods (5.3.2.5.a - e) whereby MCMV Δm157 Luc served as control. MCMV Δm157 Luc only possesses the Firefly luciferase reporter gene inserted via the FRT side into the parental BACmid C3X Δm157 FRT equally to the hCD8 / hCD4 expression cassette. MCMV Δm157 Luc is commonly used for *in vivo* experiments (5.1.). In addition, the expression of the luciferase gene in MCMV hCD8 and MCMV hCD4 infected fibroblasts (MEF) was verified (data not shown).

4.7.3. Generation of hCD8 expressing cell lines

hCD8 expressing cell lines were generated by lentiviral transduction. The hCD8 gene was amplified by PCR with the primer pair 5-EcoRI-hCD8 and 3-BglII-hCD8 from the template pCMV6-XL5-hCD8 (Origene, SC111602, NM001768) and inserted into pCRII-TOPO. Afterwards, the hCD8 gene was subcloned from pCRII-TOPO-hCD8 in to puc2CL6lpwo via *EcoRI* restriction recognition sites. The orientation and the sequence of the insert were controlled. Lentiviral particles were produced as described (4.5.3.2.). HeLa and three different fibroblast cell lines, namely CIM, BIM, and NIH3T3, were transduced and selected for hCD8 gene insertion by Puromycin (HeLa: 5 ng/ml; fibroblasts: 2,5 $\mu\text{g}/\text{ml}$) for about one week. Flow cytometry analysis of the newly generated cell lines demonstrated a high hCD8 expression (Figure 4.6.). The absence of non-hCD8 expressing cell confirmed the completeness of the selection. In summary, different cell lines expressing hCD8 were generated as tool for the analysis of the recombinant OKT8 mAbs.

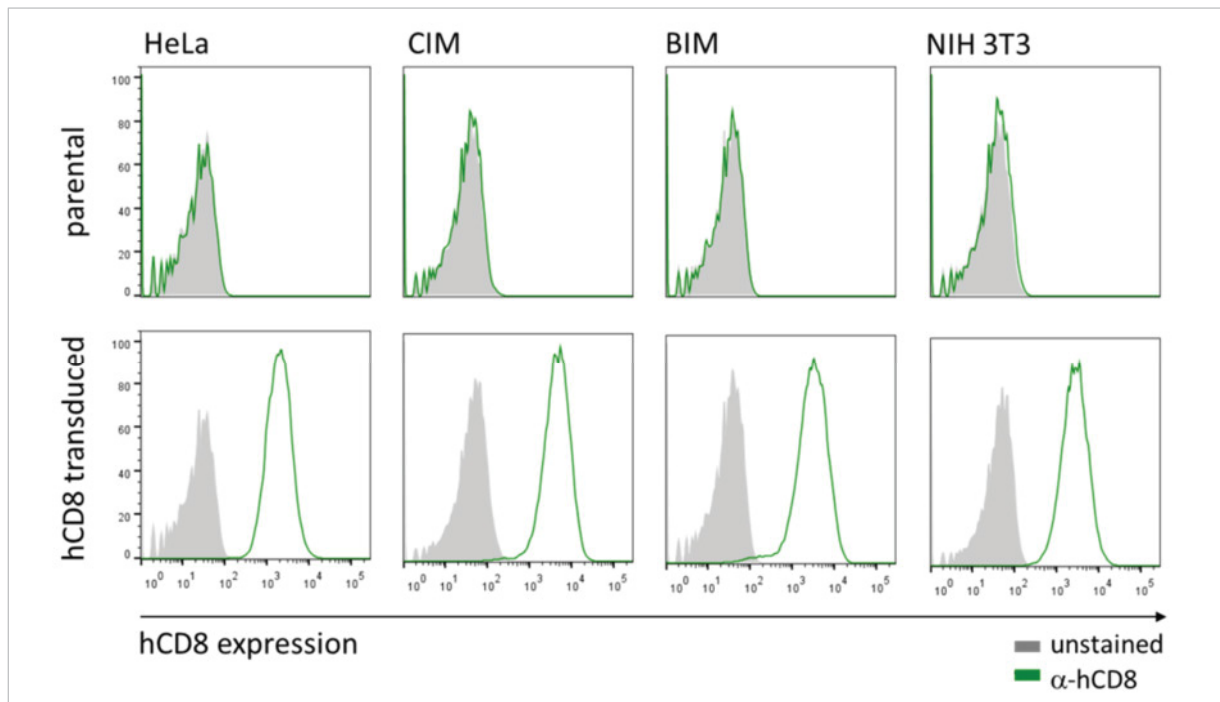


FIGURE 4.6. Verification of hCD8 surface expression of hCD8 transduced cell lines. After hCD8 transduction and selection of different cell lines, transduced and parental cell lines were stained with anti-hCD8-APC (OKT8-APC, green line) or mock stained (grey solid). 2×10^4 living cells were measured by flow cytometry (FACSCanto II BD, FACSDiva Software) and analysed by FlowJo (TriStar). Histograms of APC fluorescence intensity are shown in the single cell gate.

4.7.4. Generation and characterization of mAbs possessing identical variable regions but different IgG subclasses

Recombinant monoclonal antibodies possessing the same variable region but different IgG constant regions, i.e. the different IgG subclasses, were generated (Figure 4.7.). To this end, the variable regions (V_H , V_L) of a distinct mAb, OKT8 (2.3.1.), were identified and cloned into the expression vectors (pFUSE, InVivogen) containing the constant region of the heavy or light chain.

The first step was the identification of the V_H and V_L sequences of the desired antibody. Therefore, mRNA was isolated from a hybridoma cell line and reverse transcribed into cDNA using a 3' primer binding to the known constant region. A 5'RACE PCR (*rapid amplification of 5'unkown ends*) was performed and the PCR products (V_H and V_L) were sequenced (4.7.4.2.) and *in silico* analysed for N- and O-glycosylation sites (2.4.4.)

Next, V_H and V_L were inserted into the pFUSE expression vectors (4.7.4.3.). The pFUSE system consists of the vectors pFUSE-CHlg and pFUSE2-CLlg expressing the constant regions of the heavy (C_H) and light (C_L) chain, respectively. They contain a multiple cloning site (MCS) upstream of these constant regions to enable the cloning of the variable regions of a given monoclonal antibody. The expression vectors from InVivogen were used for mouse IgG1, IgG2a, IgG2b, IgG3 (pFUSE-CHlg-mG1, pFUSE-CHlg-mG2a, pFUSE-CHlg-mG2b, pFUSE-CHlg-mG3) and kappa light chain (pFUSE2-CLlg-mK). The expression vector for the IgG2c heavy chain was not available and therefore it was generated (pFUSE-CHlg-m2c-Ecor47III) (2.4.3.; 4.7.4.1.).

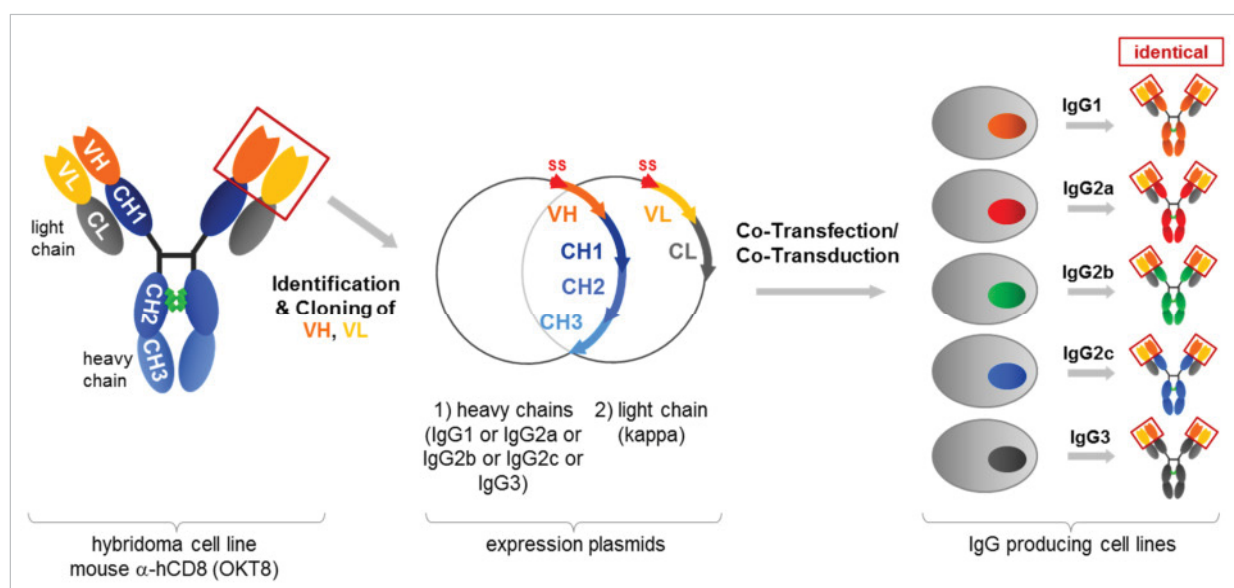


FIGURE 4.7. IgG structure and strategy for exchange of the constant regions of the heavy chain (C_{H1} - C_{H3}) and light chain (C_L). The sequence of the variable regions (V_L , V_H) are determined and cloned into expression vectors, that contain the constant region for a heavy chain subclass (IgG1, IgG2a, IgG2b, IgG2c, or IgG3) or the light chain (kappa). After co-transfection or co-transduction of mammalian cells the mAbs are expressed and secreted into the cell culture supernatant. (green: glycosylation, SS: signal sequence)

Co-transfection of mammalian cell lines with the recombinant pFUSE-CHlg and pFUSE-CLlg pair allowed the expression of monoclonal IgG antibodies in cell culture (4.7.4.3.). Selection markers were Blasticidin and Zeocin, for the LC and HC respectively, allowing selection in both bacteria as well in mammalian cells. Additionally, the IgG genes were subcloned from the pFUSE vectors into lentiviral transfer vectors allowing co-transducing cell lines as well (4.7.4.4.). The produced IgGs can be purified

from the tissue culture supernatant using affinity chromatography and further polishing steps. Here Protein G affinity chromatography was applied (4.7.4.6.).

4.7.4.1. Generation of an expression vector containing the IgG2c constant region

An expression vector with the IgG2c heavy chain was generated. First, the RNA was extracted from splenocytes of MCMV Δ m157 Luc infected C57BL/6 mice 14 days post infection and the cDNA was cloned into a TOPO-TA vector (pCRII-TOPO-IgG2cHC, primer 5-IgG2c, 3-IgG2c). The insert was sequenced and the according coding sequence was compared to sequences available in databases (Table 4.6.). The multiple alignments of chosen sequences is shown in Figure 2.20. The IgG2c HC was subcloned into the pFUSE-CHlg vector backbone from InVivogen to generate pFUSE-CHlg-m2c. Therefore, the IgG2a HC sequence was removed by a digestion of pFUSE-CHlg-m2a with *NheI* and a subsequent partial digestion with *MscI*. The IgG2c HC sequence was excised from the pCRII-TOPO-IgG2c HC with *NheI* and *MscI* and ligated into the pFUSE vector backbone. The inserted fragment was sequenced. To be able to insert the variable regions upstream of the constant region of the IgG2c HC by keeping the open reading frame of the gene, a blunt end restriction recognition site had to be generated at the start of the coding sequence for the constant region without altering the AA sequence (silent mutation). Analogous to the available pFUSE-CHlg-mG1/2a/2b/3 expression vectors (InVivogen), a *Eco47III* restriction recognition site was introduced by site directed mutagenesis (4.1.4.3.b) with the primer pair 5-IgG2c-Eco and 3-IgG2c-Eco. The IgG2c gene sequence of the resulting vector, pFUSE-CHlg-m2c-Eco47III, was controlled by sequencing.

Nr.	Database sources						strain	comment
	GI (Gene) /GI (Protein)	NCBI GenBank	NCBI RefSeq	NCBI Protein ID	Uniprot	MGI		
<u>1</u>							C57BL/6J	cloned
2	GI194444 /GI194445	J00479.1		AAA37906.1			C57BL/6	IGHG2C*01 (IMGT/Gene-DB)
3	-/ GI121049				P01864		C57BL/6	
<u>4</u>	GI78190277 /-	AC160982.5			A0A0A6YY53	2686979	C57BL/6J	Incorporated in NG005838
5	GI52991 /GI1334119	X16998		CAA34864.1			MAI	IGHG2C*02 (IMGT/Gene-DB)
<u>6</u>	GI1806127 /GI1806128	Y10606		CAA71613.1			NOD/Lt	IGHG2C*03 (IMGT/Gene-DB)
<u>7</u>	GI372099098 /-		NC000078.6 in Gene ID 404711				C57BL/6J	
<u>8</u>	GI121699722 /-		NG005838.1 in Gene ID 404711				C57BL/6	
<u>9</u>	GI12841780 /GI12841781	AK007918.1		BAB25349.1	Q9D8L4		C57BL/6J	
<u>10</u>	GI802199553 /GI802199554	LC037230.1		BAR42291.1	A0A0E4B366		hybridoma	
<u>11</u>	GI62028521 /GI62028520	AAH92061.1	Gene ID 111507*	BC092061.1	Q58E56	96442	Czech II	
0	GI51835 /GI1333984	V00798/ CAA24178.1		CAA24178.1	P01863		BALB/c	IgG2a

TABLE 4.6. IgG2c HC sequences in different databases. Underlined numbers: identical sequences (for comparison upon AKTTAPSVYPL...); *RefSeq in GenID111507: NC000078.6; NG005838.1 (same as in Gene ID404711); Databases: NCBI Protein, NCBI Genbank, NCBI Gene/RefSeq/Nucleotid, Uniprot, Blast Protein Ident 94-100%, MGI, IMGT/Gene-DB

4.7.4.2. Identification and cloning of unknown variable region of OKT8 hybridoma

To identify the variable regions of the OKT8 heavy and light chains a 5'RACE was performed. The method is described in detail in 4.1.4.5. Briefly, RNA was extracted from the OKT8 hybridoma cell line and cDNA was generated with 3' gene specific (GSP1) or an Oligo-dT primer. The 5' end was C-tailed.

Subsequently, the unknown sequence was amplified by PCR with an anchor primer which binds the 5'-tail and a 3'-gene specific primer, GSP1 or the nested GSP2. The 5'-anchor primer (5-AnchorP) contains restriction endonuclease recognition sites and the special anchor sequence. This sequence consists of a combination of dGs and dIs to overcome the disadvantages of high melting temperature and poor specificity of homopolymeric primer because the incorporated dIs base pair with all NT with varying affinities. The gene specific primer 3-GSP-HC is complementary to the 5'-part of constant region of the heavy chain of the IgG subclasses IgG2a and IgG2b. Accordingly, the gene specific primer for the light chain, 3-GSP-LC, binds to the 5'-part of the constant region of the kappa light chain. In a next step, the purified PCR products were inserted into a vector for sequencing, which was achieved here by TOPO cloning (pCRII-TOPO) (4.1.10.).

Best results were achieved in this case utilizing the Oligo-dT primer for cDNA synthesis and the anchor / GSP1 primer pair for the subsequent PCR with a high fidelity polymerase (Roche) in a touchdown PCR program. Sequencing of the pCRII-TOPO inserts was not trivial and required specialized protocols performed by the service provider (BMFZ at the HHU Düsseldorf or GATC, Germany) because of the poly-G sequence resulting from the anchor primer. For the identification of the OKT8-V_H and -V_L sequences, two and respectively three independent PCRs including the TOPO-TA cloning were performed and all sequenced clones (V_H n = 6; V_L n = 5) displayed the identical V_H / V_L sequence (Figure 4.8). Furthermore the V_L and V_H sequences were once more validated by sequencing of PCR products synthesised with a specific primer pairs which binds to the ends of the V regions (5-OKT8VH-EcoRI and 3-OKT8VH-BstUI; 5-OKT8VL-AgeI, 3-OKT8VL-BstAPI, see also 4.7.4.3.) using cDNA generated from newly extracted RNA.

4.7.4.3. Expression of the recombinant OKT8 mAbs in mammalian cells

a) Expression of the recombinant OKT8 mAbs in stably transfected adherent cell lines

(i) Generation of the OKT8 mAb expression vectors

To express recombinant OKT8 mAbs possessing different mouse IgG subclasses, the V_H and V_L sequences were inserted into the pFUSE vectors. The pFUSE system consists of the vectors pFUSE-CHlg and pFUSE2-CLlg expressing the constant regions of the heavy (C_H) and light (C_L) chains, respectively. A range of restriction endonucleases for the 5'-end is present in the MCS. The 5'-end of the variable region has to include the native ATG initiation codon, the signal sequence, and furthermore a Kozak translation initiation sequence upstream of the ATG to guarantee a proper initiation of translation in mammalian cells. In addition, the 3'-end has to be inserted by blunt-end cloning in order to preserve open reading frame of constant region.

To insert the sequence of the variable region of the OKT8 mAb heavy chain into the pFUSE expression vectors of the different IgG heavy chain subclasses, the OKT8-V_H sequences were amplified by PCR from pCRII-TOPO-OKT8VH (4.7.4.2.) with the primer pair 5-OKT8VH-EcoRI and 3-OKT8VH-BstUI. Thereby an *EcoRI* site and the Kozak consensus sequence was introduced at the 5'-end and a *BstUI* site at the 3'-end of the OKT8HC sequence. For the latter, by using a mismatched 3'-primer, the last nucleotide of the OKT8-V_H sequence was exchanged (A→G) creating the restriction site without altering the amino acid sequence. The PCR product was digested sequentially with *EcoRI* (37°C) and *BstUI* (60°C) and ligated into the different *EcoRI/Eco47III* digested pFUSE-CHlg-mG vectors generating pFUSE-CHlg-mG1-OKT8VH, pFUSE-CHlg-mG2a-OKT8VH, pFUSE-CHlg-mG2b-OKT8VH, pFUSE-CHlg-mG2c-OKT8VH, and pFUSE-CHlg-mG3-OKT8VH. To create to pFUSE-CLlg-mk-OKT8VL, the OKT8-V_L

sequence was amplified by PCR from pCRII-TOPO-OKT8VL (4.7.4.2.) with the primer pair 5-OKT8VL-AgeI/ and 3-OKT8VL-BstAPI introducing an *AgeI* site and the Kozak consensus sequence at the 5' end and adding the sequence of the 5' constant part with the *BstAPI* site at the 3' end of the OKT8-V_L sequence. The PCR product and the parental vector pFUSE-CLlg-mk were digested sequentially with *AgeI* (37°C) and *BstAPI* (60°C) and ligated. All inserts were sequenced.

A. Nucleotide sequences

>OKT8 V_L kappa C_L (cDNA)

ATGAGGTTCCAGGTTTCAGGTTCTGGGGCTCCTTCTGCTCTGGATATCAGGTGCCAGTGTGATGTCCAGATAAACCAGTCTCCAT
CTTTTCTTGTGCGTCTCCTGGAGAAACCATTACTATAAATTGCAGGACAAGTAGGAGTATTAGTCAATATTTAGCCTGGTATCA
AGAGAAACCTGGGAAAACCTAATAAGCTTCTTATCTACTCTGGATCCACTCTGCAATCTGGAATTCCATCAAGTTTCAGTGGCAGT
GGATCTGGTACAGATTTCACTCTCACCATCAGTGGCCTGGAGCCTGAAGATTTGCAATGTATTACTGTCAACAGCATAATGAAA
ACCCGCTCACGTTTCGGTCTGGGACCAAGCTGGAGCTGAGACGGGCAGATGTCTGCACCAACTGTATCCATCTTCCCACCATCCAG
TGAGCAGTTAACATCTGGAGGTGCCTCAGTCGTGTCTTCTGAACAACCTTCTACCCCAAAGACATCAATGTCAAGTGAAGATT
GATGGCAGTGAACGACAAAATGGCGTCTGAACAGTTGGACTGATCAGGACAGCAAAGACAGCACCTACAGCATGAGCAGCACCC
TCACGTTGACCAAGGACGAGTATGAACGACATAACAGCTATACCTGTGAGGCCACTCACAAGACATCAACTTACCCATTGTCAA
GAGCTTCAACAGGAATGAGTGTAG

>OKT8 V_H IgG2a C_H (cDNA)

ATGAAATGCAGCTGGGTTATCTTCTTCTGATGGCAGTCGTTACAGGGGTCAATTCAGAAGTTCAACTGCAGCAGTCTGGGGCAG
AGCTTGTGAAGCCAGGGGCCCTCAGTCAAGTTGCTCTGCACAGCTTCTGGCTTCAACATTAAAGACACCTATATACACTTCGTGAG
GCAGAGGCCCTGAACAGGGCCCTGGAGTGGATTGGAAGGATTGATCCTGCGAATGATAATACTTTATATGCCTCAAAGTTCAGGGC
AAGGCCACTATAACAGCAGACACATCATCAACACAGCCTACATGCACCTCTGCAGCCTGACATCTGGGGACACTGCCGTCTATT
ACTGTGGTAGAGGTTATGGTTACTACGTATTGACCACTGGGGCCAAGGCACCACTCTCACAGTCTCCTCAGCTAAAAACAACAGC
CCCATCGGTCTATCCACTGGCCCTGTGTGTGGAGATACAACCTGGCTCCTCGGTGACTCTAGGATGCCTGGTCAAGGGTTATTTT
CCTGAGCCAGTGACCTTGACCTGGAACCTCTGGATCCCTGTCCAGTGGTGTGCACACCTTCCCAGCTGTCTCTGCAGTCTGACCTCT
ACACCCTCAGCAGCTCAGTGAAGCTCGAGCAGCTGGCCAGCCAGTCCATCACCTGCAATGTGGCCACCCGGCAAGCAG
CACCAAGGTGGACAAGAAAATTGAGCCCAGAGGGCCCAATCAAGCCCTGTCTCCATGCAATGCCAGCAGCCTAACCTCTTG
GGTGGACCATCCGTCTTCTATCTTCCCTCCAAAGATCAAGGATGTACTCATGATCTCCCTGAGCCCCATAGTCACATGTGTGGTGG
TGGATGTGAGCGAGGATGACCCAGATGTCAGATCAGCTGGTTGTGAACAACCTGGAAGTACACACAGCTCAGACACAAACCCA
TAGAGAGGATTACAACAGTACTCTCCGGGTGGTCTCAGTGCCCTCCCCATCCAGCACCAGGACTGGATGAGTGGCAAGGAGTTCAA
TGCAAGGTCAACAACAAAGACCTCCAGCGCCCATCGAGAGAACCATCTCAAAACCCAAAGGGTCAGTAAGAGCTCCACAGGTAT
ATGTCTTGCCTCCACCAGAAGAAGAGATGACTAAGAAACAGGTCACTCTGACCTGCATGGTCACAGACTTCATGCCTGAAGACAT
TTACGTGGAGTGGACCAACACGGGAAAACAGAGCTAAACTACAAGAACTGAACCAGTCTGGACTCTGATGGTTCTTACTTC
ATGTACAGCAAGCTGAGAGTGGAAAAGAAGAACTGGGTGAAAAGAAATAGCTACTCCTGTTTCAAGTGGTCCACGAGGGTCTGCACA
ATCACACACGACTAAGAGCTTCTCCGGACTCCGGGTAATGA

B. Amino acid sequences

>OKT8 V_L kappa C_L (protein, 234 AA)

MR~~F~~QVQLG~~L~~LL~~L~~WISGA~~Q~~CDVQINQSPSFLAASPGETITINCR~~T~~SR~~S~~ISQYLAWYQE~~K~~PKTNKLL
IYSGSTLQSGIPSRFSGSGSTDF~~T~~LTISGLEPEDFAMYYCQQH~~N~~ENPLTFGAGTKLELRRADAAPT
VSIFPPSSEGLTSGGASVVCFLNNFYPKDINVKWKIDGSE~~R~~QNGVLNSWTDQDSKSTYSMSSTLT
TKDEYERHNSYTC~~E~~ATHK~~T~~STSPIVKSFNRNEC-

>OKT8 V_H IgG2a C_H (protein, 467 AA)

MKCSWVIFFLMAVVTGVNS~~E~~VQLQQSGAELVKPGASVKLSCTASGFN~~I~~KD~~T~~YIH~~F~~VRQRP~~E~~QGLEWIGRIDPANDNTLYASKFQ~~Q~~
KATITADTSSNTAYMHLCSLTSGD~~T~~AVYYCGRGYGYVFDHWGQGTTLTVSSAKTTAPSVYLPAPVCGD~~T~~TGSSVTLGCLVKGYF
PEPVTLTWNSGSLSSGVHTFPAVLQSDLYTLSSSVTVTSSTWPQSITCNVAHPASSTKVDK~~K~~IEPRGPTIKPCPPCKCPAPNLL
GGPSVFIFPPKIKDVLMSISLSPITVTCVVVDVSEDDPDVQISW~~F~~VNNVEVHTAQ~~T~~QTHREDYNSTLRVVSALPIQH~~Q~~DWMSGKEFK
CKVNNKDLPAPIERTISKPKGSRAPQVYVLPPEEEMTKQVTLTCMVTDFMPED~~I~~YVEWTNNGKTELNYKNTEPVLDSDGSYF
MYSKLRVEKKNWVERNSYSCSVVHEGLHNHHTTKSFRTPGK-

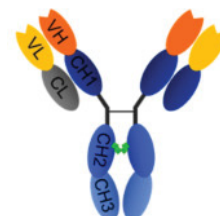


FIGURE 4.8. Identified sequences for OKT8 V_H and V_L by 5'RACE. A. nucleotide sequences of OKT8 V_L or V_H; underlined: C_L kappa or C_H IgG2a (constant region of mouse kappa light chain or IgG2a); ~~X~~ nucleotide substitution to generate a blunt end restriction site without altering the amino acid sequence (C_L: T→A creating *BstAPI*; C_H: C→T creating a *Eco47III*); B. protein sequences obtained by *in silico* translation of the nucleotide sequence with the ExPASy translate tool. OKT8 V_L or V_H; underlined: C_L kappa or C_H IgG2a; protein domain prediction with SMART (EMBL Heidelberg); red: signal peptide; yellow: V_L 30-110, organe: V_H 36-117; Ig or Ig-like domains: grey: C_L 149-224; dark blue: C_H1 159-229; medium blue: C_H2 276-351; light blue: C_H3 382-455

(ii) Production of the recombinant OKT8 mAbs in cell culture

Subsequently, the recombinant pFUSE-CHlg-mG1/2a/2b/2c/3-OKT8VH and pFUSE2-CLlg-mk-OKT8VL vector pairs were transfected into mammalian cell lines. The cell lines commonly used for antibody

production are CHO (Chinese hamster ovary) or HEK293T (human embryo kidney, HEK293T with SV40 large T antigen, here referred to as HEK293T) and they were utilized in this work to generate stable transfectants.

HEK293T cells or CHO cells were transfected with pFUSE-CHlg-mG1/2a/2b/2c/3-OKT8VH and pFUSE-CLlg-mk-OKT8VL in the ratio 2:3 according and kept in complete RMPI (4.3.5.1.). The pFUSE-CHlg vectors contain a resistance gene for Zeocin and the pFUSE-CLlg for Blasticidin. For CHO cells, 10 µg/ml Blasticidin and 133 µg/ml Zeocin were applied for 2,5 weeks starting one day past transfection. Afterwards the amount was reduced for culturing to 5 and 50 µg/ml respectively. For HEK293T cells, the selection was performed with 13,3 µg/ml Blasticidin and 133 µg/ml Zeocin and the amount was reduced successive within two weeks to 5 µg/ml Blasticidin and 50 µg/ml Zeocin for culturing. The required concentration for the selection of HEK293T and CHO with Blasticidin and Zeocin were empirically tested beforehand. Nevertheless, a non-transfected control was also treated in parallel to the transfected cells, which were eliminated after approximately one week for both cell lines.

To produce recombinant OKT8 mAbs containing tissue culture supernatant the stably transfected HEK293T and CHO OKT8 cell lines were cultured with complete RPMI medium. First, a small volume of supernatant was produced to verify the production and antigen binding of the recombinant OKT8 mAbs. Afterwards a larger volume was produced by collecting the cell culture supernatant after several days of cultivation. The recombinant mAbs were controlled (4.7.4.4.) and purified by affinity chromatography (4.7.4.5.)

4.7.4.4. Expression of recombinant OKT8 mAbs in a transduced murine myeloma cell

a) Generation of the OKT8 mAb transfer vectors

To generate the lentiviral transfer vectors, the gene for the OKT8 heavy chain genes ($V_H + C_H$, different subclasses) were excised from the pFUSE-CHlg-m2a/2b/2c/3-OKT8VH with the restriction endonucleases *EcoRI* and *MscI*. An *MscI* restriction recognition site is present in the constant region of the IgG1 subclass. As a result, the vector pFUSE-CHlg-m1-OKT8VH was digested completely with *EcoRI* first and subsequent partially digested with *MscI*. The DNA fragments were ligated into the vector puc2CL6IPwo (\rightarrow puc2CL6IP-m1/2a/2b/2c/3-OKT8HC). To this end, the vector was digested beforehand with *BamHI* and the sticky ends were filled up to blunt ends with a proof reading DNA polymerase (5 min, 72°C), and subsequent the vector backbone was digested with *EcoRI* to generate compatible ends to the insert.

The gene for the OKT8 light chain ($V_L + C_L$) was amplified with the primer pair 5-XhoI-8VL and 3-BglII-8VL from the template pFUSE-CLlg-mk-OKT8VL and it was ligated into pCRII vector (pCRII-mk-OKT8VL). The OKT8 light chain was excised from pCRII-mk-OKT8VL with *XhoI* and *BglII*. Subsequently it was inserted into the transfer vector puc2CL6INwo (\rightarrow puc2CL6IN-mk-OKT8LC), which was digested with *XhoI* and *BamHI*. As side note, *BamHI* is an isochizomer of *BglII*. Puc2CL6IPwo and puc2CL6INwo possess Puromycin or Neomycin gene as selection marker, respectively. All inserts were controlled by sequencing.

b) Production of the recombinant OKT8 mAbs in cell culture

To produce the recombinant OKT8 mAbs in the P3X myeloma cell line, the cells were first transduced with the OKT8 LC gene (puc2CL6IN-mk-OKT8LC) (4.5.3.2.). Selection was performed with G418 / Geneticin, which is an analogue of neomycin, in a final concentration of 500 µg/ml in complete RPMI medium for at least one week. Non-transduced P3X cells were eradicated after 5 days of G418 treatment. In parallel, the GFP containing transfer vector (pcu2CL6leGwo) was utilized as control and a

weak fluorescence was detectable in a great portion of cells 3 days after transfection. Subsequently, the OKT8LC transduced and selected cells were transduced with OKT8HC genes exhibiting the different IgG subclasses (puc2Cl6IP-m1/2a/2b/2c/3-OKT8HC). This second transduction led to a loss of a great cell amount without applying selection pressure. Therefore, the cell population was expanded for about two weeks before starting the selection. The selection was achieved with a beforehand empirically tested concentration of 2,5 µg/ml Puromycin in complete RPMI medium and it was applied for about a week. P3X cells only transduced with OKT8LC were eliminated after two to three days of Puromycin treatment. As note, the parallel transduction of the heavy and light chain was tested as well. In this case, it was less efficient than the subsequent transduction of both genes.

To produce recombinant OKT8 mAbs containing cell culture supernatant, the transduced P3X OKT8 cell lines were cultured with successively decreasing the FCS supplement to 1%. First, a small volume of supernatant was produced to verify the production and antigen binding of the recombinant OKT8 mAbs. Afterwards larger volumes of supernatant were produced cultivating the cells lines for 7 to 14 days (4.2.7.1.). The recombinant mAbs were controlled (4.7.4.4.) and purified by affinity chromatography (4.7.4.5.)

4.7.4.5. Characterization and Purification recombinant OKT8 mAbs

a) Expression and secretion of the recombinant OKT8 mAbs

To control the expression and secretion of the recombinant OKT8 mAbs, a Western Blot was performed detecting the IgGs in the cell lysates and supernatants of the stable transfected cells with a POD coupled polyclonal goat anti mouse antibody (Figure 4.9.). The OKT8 hybridoma supernatant served as control. The IgG heavy chain was detectable in all samples derived from the different stable transfected HEK293T cell lines. The light chain was clearly visible in the cell lysates and only very weakly in the supernatant samples probably due to the lower IgG concentration in the supernatant. The IgG3 subclass was hardly detectable with the used polyclonal goat anti mouse antibody preparation. Most likely, this was a result of the production method of the anti-IgG serum. In general, goats are immunized with mouse IgG purified from serum, which contains only in minor amounts IgG3 and therefore the detection of IgG3 relies largely on the cross-reactivity with antibodies against the other mouse IgG subclasses. Nevertheless, stably transfected HEK293T and CHO cells (data not shown) expressed and secreted the recombinant OKT8 mAbs.

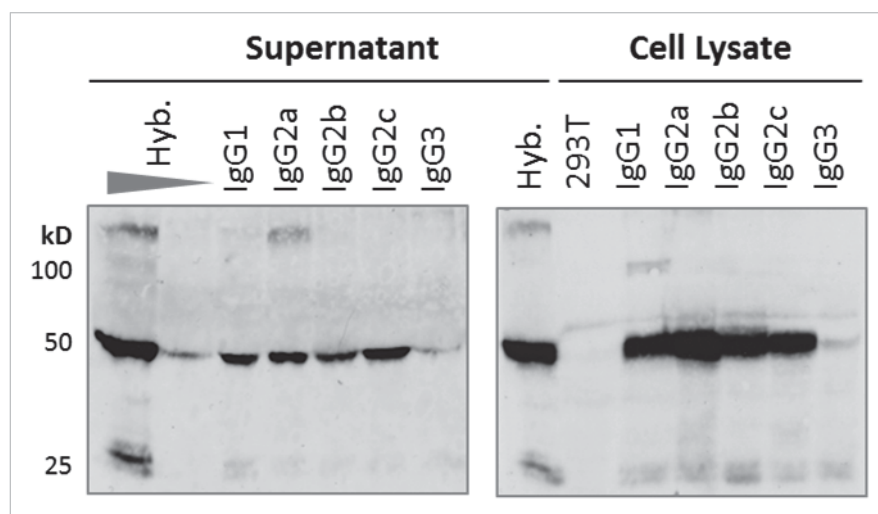


FIGURE 4.9. Expression and secretion of recombinant OKT8 mAbs produced in stably transfected HEK293T cells (Western Blot). IgGs in 20 µl tissue culture supernatant and cell lysates of approx. 500 000 cells per lane were separated in a 10% SDS PAGE and detected with goat anti mouse-POD. OKT8 hybridoma supernatant (1 µl) and a 1/10 dilution served as control (Hyb.).

b) Antigen binding of the recombinant OKT8 mAbs

After verifying the production of the recombinant OKT8 subclass switched mAbs, the binding specificity for its antigen had to be demonstrated. To this end, MCMV hCD8 infected MEF were stained with cell culture supernatant from stably transfected HEK293T and CHO cells (Figure 4.10). Human CD8 antigen expression was controlled by staining with OKT8-APC. For all tested IgG subclasses produced in either HEK293T or CHO cells recombinant OKT8 mAb binding is detectable to MCMV hCD8 infected MEF in contrast to MCMV hCD4 infected MEF or mock cells in flow cytometry.

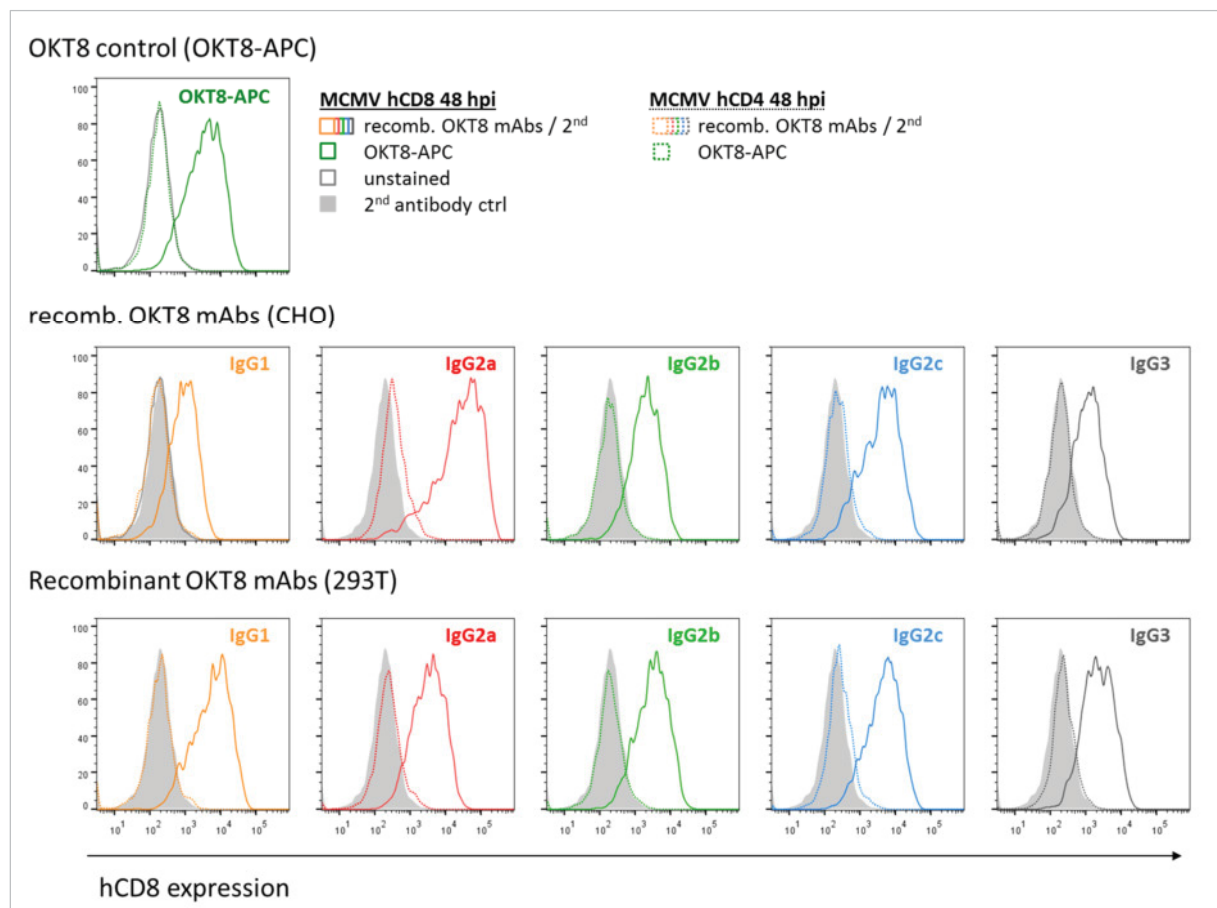


FIGURE 4.10. The recombinant OKT8 mAbs produced in stably transfected HEK293T and CHO cells bind to their antigen. Fibroblasts (BIM) were infected with MOI 2 of MCMV hCD8 or as control with MCMV hCD4 for 48 h. The infected cells were incubated with 50 μ l of tissue culture supernatant and the bound IgG was detected with Cy5 coupled goat anti mouse. As control served the directly labelled and commercially available OKT8-APC. Approx. $1,2 \times 10^4$ cells were measured by flow cytometry (BD FACS Canto II, FACS Diva software) and analysed with FlowJo (Tree Star Inc). The Cy5 signal of living cells (DAPI negative) cells is shown.

The binding ability of recombinant OKT8 IgG subclasses produced in transduced P3X cells was proven by staining hCD8 transduced HeLa (HeLa hCD8) cells with the respective supernatants. As expected, for all subclasses binding to HeLa hCD8 cells was detectable but not to HeLa cells, which do not express hCD8 (Figure 4.11). Supernatant derived from the parental P3X myeloma cell failed to stain HeLa or HeLa hCD8.

The fluorescence intensity of the peaks does not represent the affinity of the recombinant OKT8 mAbs because the mAb concentration in the tested supernatants was not adjusted. The secondary antibody, which is a fluorophore labelled polyclonal goat anti mouse preparation, adds a bias by detecting the distinct subclasses with different preferences due to its production method as described above. However, IgG3 is detectable more reliably in flow cytometry because the whole molecule is intact. It

can be bound by anti-light chain antibodies from the polyclonal anti-serum in contrast to Western Blot where heavy and lights are separated. In summary, all generated recombinant OKT8 mAbs bind to their antigen.

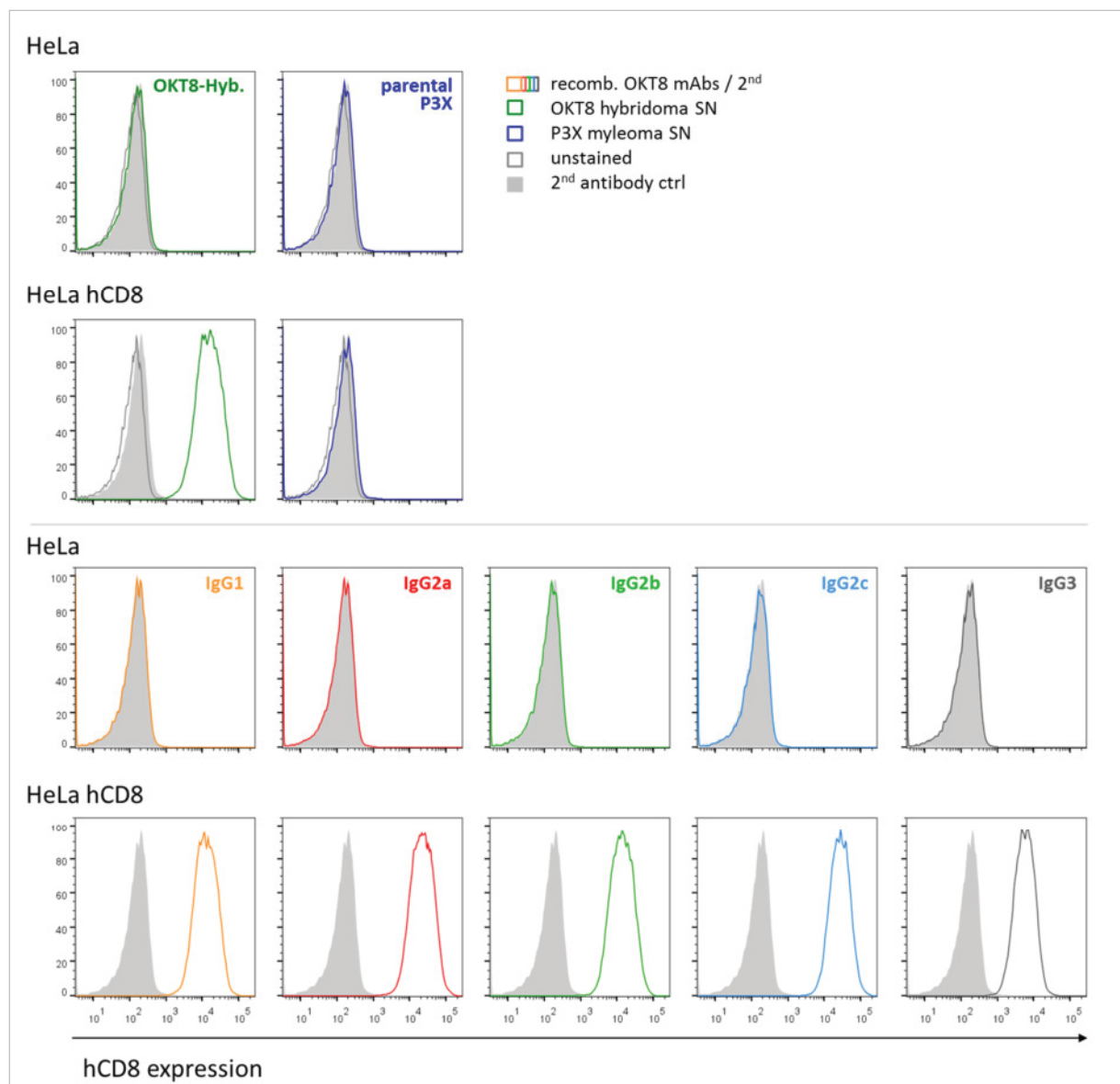


FIGURE 4.11. The recombinant OKT8 mAbs produced in transduced P3X cells bind to their antigen. HeLa and HeLa hCD8 cells were incubated with 50 μ l of tissue culture supernatant and the bound IgG was detected with Cy5 coupled goat anti mouse. The OKT8 hybridoma supernatant was diluted 1/400. 4×10^4 cells were measured by flow cytometry (FACS Canto II; FACS Diva software, BD) and analysed with FLOWJo (Tree Star Inc, USA). The Cy5 signal of living cells (DAPI negative) and single cells is shown.

4.7.4.6. Purification of the recombinant OKT8 mAbs by Protein G affinity chromatography

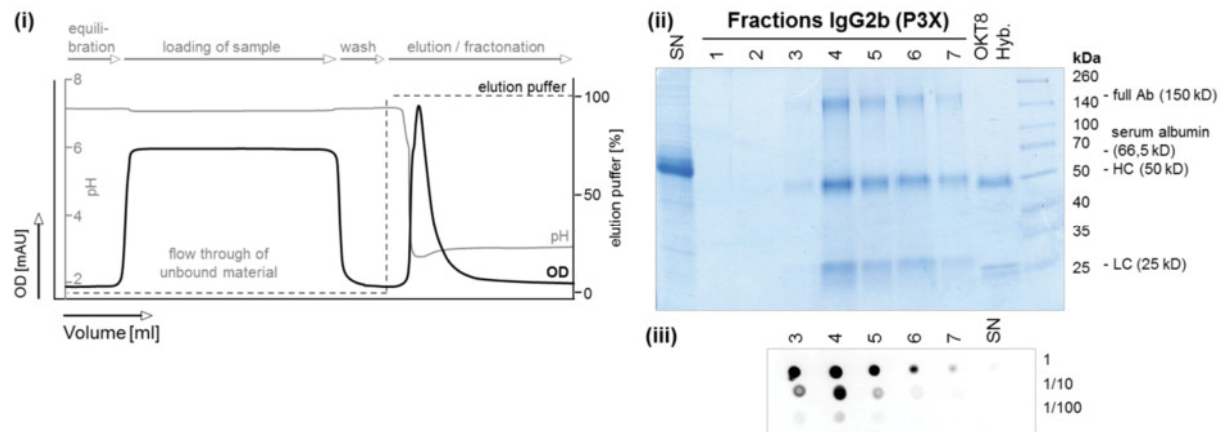
For functional analysis, the recombinant mAbs had to be purified and concentrated. Therefore, IgGs from cell culture supernatants were purified by Protein G affinity chromatography. Protein G is superior to Protein A in binding reliably to all mouse IgG subclasses. The Protein G Hi Trap 1 ml column and an ÄKTA basic or ÄKTA basic/purifier system (Unicorn Software; GE Healthcare) were utilized. The purification is described in 4.2.7.2. Briefly, after equilibration of the column, the mAb containing supernatant was applied, unbound material was washed off, and the bound mAbs were eluted by lowering the pH value. The eluate was collected in fractions, which were neutralized immediately to ensure the integrity of the IgG molecules. A schematic elution profile as well as an analysis of the

eluted fractions by Coomassie stained SDS PAGE and Dot Blot are shown in Figure 4.12A. The fractions with the highest IgG amount were pooled and dialyzed against PBS. These were fraction No. 3 and 4 for P3X derived recombinant OKT8 mAbs and fractions No. 4 and 5 were pooled from the HEK293T and CHO cell lines. In contrast, the highest concentration was present in the 3rd fraction for the IgG1 subclass derived from CHO cells. The purified recombinant OKT8 mAbs were visualized by Coomassie stained SDS PAGE and Western Blot (Figure 4.12B). Utilizing moderate amounts of beta-mercaptoethanol, only a portion of the antibody molecules are reduced and separated in their subunits (heavy and light chain) in the Coomassie stained SDS PAGE. The IgG3 subclass is detectable in Western Blot because a higher amount of protein was loaded in comparison to Figure 4.9. However, the band is still weaker in contrast to the Coomassie gel verifying a disadvantage for the IgG3 detection with the goat anti mouse POD. In Figure 4.12C, all purified recombinant antibodies were analysed and show the expected molecular weights for the full IgG molecule, the heavy, and the light chain. All recombinant OKT8 mAbs were successfully purified.

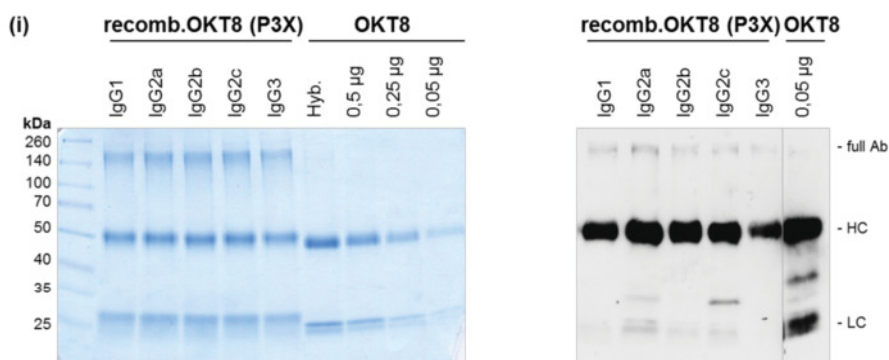
4.7.5. *In vitro* FcγR activation assay on influenza infected target cells

The *in vitro* FcγR activation assay was performed with MDCK cells infected with MOI 5 of H1N1 (strain RP8: A/Puerto Rico/8/1934). One hour after infection, the unbound virus was removed by washing and subsequently the infected cells were opsonized with graded concentrations of antibodies and co-cultivated with the BW:FcγR-ζ reporter cells overnight. The RP8 virus (A/Puerto Rico/8/1934), the MDCK cells, and the immune serum (C57BL/6 Mx^{-/-}, RP8, 16 dpi) were kindly provided by Prof. Peter Stäheli (Institute for Virology, Medical Center Freiburg). Silvie van den Hoecke and Xavier Saelens kindly provided the mAb37, mAb65, a further anti-M2e IgG1 mAb (mAb148), and the corresponding isotype controls (IgG1: anti-HBV core [NBe]; IgG2a: anti-small hydrophobic protein of HRSV [SHe]).

A. Elution of mAbs from Protein G Chromatography



B. Analysis of purified recombinant OKT8 mAbs (P3X) by Coomassie gel and Western Blot



C. Comparison of purified recombinant OKT8 mAbs by Coomassie gel

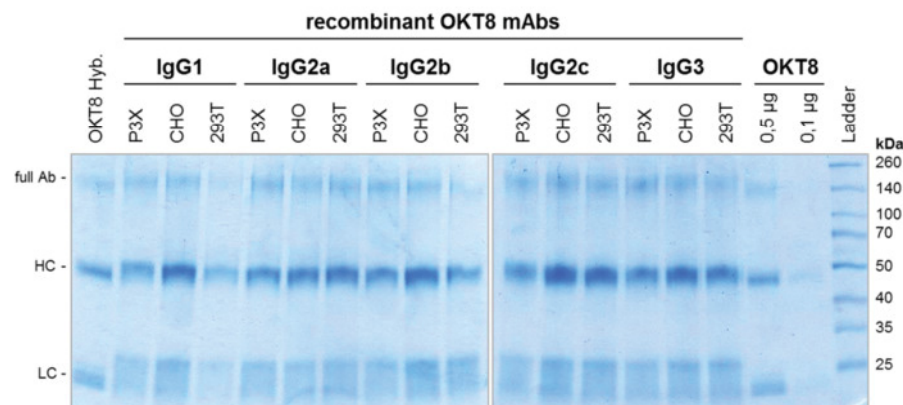


FIGURE 4.12. Purification of the recombinant OKT8 mAbs by Protein G affinity chromatography. A(i). Model of IgG elution from a Protein G affinity column. After equilibration of the column with PBS and application of the tissue culture supernatant, the unbound material is washed off with PBS, and the IgGs are eluted with 0,1 M Glycine (pH 2,7). The eluate is collected in fractions and neutralized with 1 M Tris-HCl (pH 9.0). A(ii) 4 µl of the supernatant (SN) or fraction of recombinant OKT8 (P3X) IgG2b were separated by 10% SDS PAGE and stained with colloidal Coomassie. 1,2 µg of purified OKT8 hybridoma supernatant serves as control. A(iii) Dot Blot of IgG2b P3X fractions, 1 µl per dot, 1/10 dilution series, detection with anti-mouse Fab-POD. B/C. Fractions were pooled and dialyzed against PBS (P3X: fractions 3 and 4; HEK293T, CHO: fractions 4 and 5) B. 4 µl or respectively 1 µl of purified recombinant OKT8 (P3X) were separated by 10% SDS PAGE and stained with colloidal coomassie or detected with goat anti mouse POD in Western Blot. As control 1,2 µg of purified OKT8 hybridoma supernatant or the indicated amount of commercially available OKT8 (eBioscience) were utilized. C. 3 µl of purified recombinant OKT8 (P3X) were separated by 10% SDS PAGE and stained with colloidal coomassie. As control 1,8 µg of purified OKT8 hybridoma supernatant or the indicated amount commercially available OKT8 (eBioscience) were used. HC: heavy chain; LC: light chain.

5. Material

5.1. Devices

Agarose Gel electrophoresis chambers	Agagel mini and maxi, Biometra Vari-gel System SVG-SYS MINI and TVG-SYS MIDI, Scie-Plas
Blot-Shaker	Type 3011, Type 3013, Type 3017, GFL Polymax 2040, Heidolph WS42, Hartenstein
Blotting-Equipment	Fastblot B64, B33/B34, B44, Biometra
Centrifuges	5810R, 5415D, 5417R, 5424, Eppendorf Sigma 3K30, Sartorius Avanti J-E, Beckman Coulter Sorvall RC28S, Du Pont Heraeus Fresco 21, Thermo Scientific Megafuge 1.0R, Heraeus Optima L-70K Ultracentrifuge, Beckman Coulter
Chromatography System	ÄKTA basic with UNICORN Control Software, GE Healthcare ÄKTA basic/purifier with UV-900, pH/C-900, Frac-920, P-960, UNICORN Control Software, GE Healthcare
µCuvette G10	Eppendorf
Douncer	Wheaton, VWR
Electroporator	Genepulser II, Biorad
ELISA Reader	Rainbow ELISA Reader, Tecan
Film developer machine	Curix 60, Agfa Cawo Cawomat 2000 IR, Hohmann Röntgentechnik
Flow cytometer	FACSCanto II with FACSDiva software, BD Pharming
Freezing container	Qualifreeze, Qualilab Nalgene Cryo 1°C Freezing Container, Thermo Scientific
Fluorescence Microscope	TE2000-S, Nikon
Gel Dryer	Model 583, Biorad
Gel Imager	Gel-Doc EZ Imager, Bio-Rad
Hybridization oven and bottles	OV5, Biometra
Incubator (Cell Culture)	BBD 6220 and BBD 6620 CU, Heraeus Instruments HeraCell 240i, Thermo Scientific
Incubator (Bacteria)	New Brunswick Scientific B 6200, Heraeus Instruments
Incubator Shaker	G25 Incubator Shaker, New Brunswick Scientific Innova 40, New Brunswick Scientific
Luminometer	Mithras LB 940, Berthold
Magnetic mixer (heatable)	RSM-10HS, Phoenix Instruments RCT standard, IKA Labortechnik
Microscope	Axiovert 25 and 40 CFL, Zeiss TS100, Nikon Leitz Labovert FS, Typ 090-127.017, Leica Microsystems
Multimode microplate reader	Infinite M200 with Tecan i-control 1.10.4.0 software, Tecan
Nitrogen Dewar Flask	Nalgene 4150-4000, Thermo Scientific
Nitrogen Tank	Biosafe MD and ApolloLIN, Cryotherm Chronos, Messer Griesheim
Rotors	JLA 16.250, JA-10, SW32 Ti, Beckman Coulter Sorvall GS-3, Sorvall GSA, Du Pont

Pipettes	Pipetman, Gilson Research Plus, Eppendorf Multichannel Research Plus, Eppendorf Multichannel Pipet-Lite XLS, Mettler Toledo Multipette M4, Eppendorf Pipetboy, Integra Bioscience
Power-Supplies	Power Pac 300, Biorad EPS 301, Amersham / GE Healthcare EV245 and EV261, Consort
Scales	PC200, AJ50, and AB54, Mettler Toledo CPA3202S-OCE, Sartorius Pro, Ohaus Scout
SDS Electrophoresis chambers	Minigel-Twin, Biometra Standard Twin Plate Gel Unit, Mini or Wide Format, SCIE-PLAS
Spectrophotometer	UV-VIS Spectrophotometer UVmini 1240, Shimadzu Nanodrop 1000, Thermo Scientific BioPhotometer D30, Eppendorf
Sonicator	Branson Sonifier II 450
SEC Columns	Superdex 200 10/300 GL, GE Healthcare Superdex 200 HiLoad 16/600 Prep Grade, GE Healthcare
Thermocycler	T1 and T3000, Biometra FlexCycler ² , Analytik Jena
Thermoblock	ThermoStat plus, Eppendorf Thermomixer Comfort, Eppendorf
Turbo Blotter (Southern Blot)	Schleicher und Schuell
UV crosslinker	CL-1000, UVP
UV transilluminator	Gel iX Imager, Intrax
Vacuum pump	AP86, Hartenstein
Vortexer	L46, Labinco VV3, VWR Vortex 4 basic, IKA
Water bath	Type 1002, Type 1083, Type 1092 GFL
Working sterile banks	Hera Safe, Heraeus BIO-CL190, Ehret

5.2. Consumables

Bottle Top Filters	Disposable Nalgene Rapid-Flow Sterile PES 0,45 µm, Thermo Scientific
Cell culture dishes	10 cm (60 cm ²), TPP
Cell culture flasks	25 cm ² / 75 cm ² / 175 cm ² , TPP or Nunc
Cell culture plates	48 well, Nunc or Greiner 96 flat well / 24 well / 12 well / 6 well, TPP
Cell strainer	Falcon Cell strainer 70 µm Nylon, Corning Incorporated
Centrifugal filters	Amicon Ultra-4 Ultracel 50 K, Merck Millipore
Cryo tubes	Nunc 1,5 ml, Thermo Scientific
Cuvettes	Disposable 2,5 ml semi-micro PS, Brand
Dialyse tubing	Spectra/Por MWCO 20k CE sterile 16 mm, Roth
Dialysis membrane	Drop Dialysis V-series membrane, Millipore
DNA marker	Hyperladder I, Bioline Generuler 1 kb or 100 kb, Thermo Scientific
Electroporation cuvettes	0,2 cm Bio-Rad
ELISA plates	Nunc Maxi Sorp F, Thermo Fisher

Micro-Hematocrit Capillaries	non-heparinisiert, B. Braun
Hemocytometer	Kova
Film	Biomax MR, Kodak
	Amersham Hyperfilm ECL, GE Healthcare
Filter for flow cytometry	Cell Tris 50 µm, REF 04-004-2327, Sysmex Partec
Flow cytometry tubes	BD Falcon
Protein G Column	HiTrap Protein G HP 1 ml, GE Healthcare
Nitrocellulose membrane	Protran Nitrocellulose Transfer Membrane 0,45 µm, Schleicher & Schuell
	Amersham Protran 0,45 µm NC, Amersham/GE Healthcare
Nylon membrane	Nylon membrane positively charged, Roche
PCR tubes	0,2 ml/ 0,5 ml, Starlab, Biozym Scientific, or Eppendorf
Pipet tips	with and without filter, TipOne, Starlab
Polyallome tubes	Beckman Coulter
Protein marker	Kaleidoscope prestained standards, Bio-Rad
	Spectra Multicolor Broad Range Protein Ladder, Thermo Scientific
	Color Prestained Protein Standard Broad Range, New England Biolabs
Reaction tubes	1,5 ml/ 2ml/ 5 ml, Eppendorf
	15 ml/ 50 ml, TPP, Greiner, or Falcon
Reagent Reservoirs	60 ml, Thermo Scientific
Reblot Plus Stripping Solution	Millipore
Scalpel	Disposable, No.21, Feather
Sterile pipettes	5 ml / 10 ml / 25 ml, Costar
	Combitips advanced 25 ml Biopure, Eppendorf
Whatman-Paper	3 mm Cellulose Filter Paper, Whatman / GE Healthcare
Needles	20G x 1 ½"; 24G x 1", Sterican, B. Braun
Syringe filters	0,45 µm sterile Acrodisc Supor membrane, PALL Life Science
Syringes	BD Micro Fine U100 Insulin 0,5 ml 30G 8 mm, BD Pharming
	1 ml / 5 ml / 10 ml Omnitix, B. Braun
White 96 well F Plates	Lumitrac 200, Greiner
	Nunc 96F non-treated white microwell SH, Thermo Fischer Scientific

5.3. Cell culture media and supplements

All media and supplement were from the provider Gibco by Life Technology / Thermo Scientific if not stated otherwise.

Beta-Mercaptoethanol (50 mM)	
Dulbecco's Modified Eagle Medium (DMEM)	
Dulbecco's Modified Eagle Medium (DMEM) without Met and Cys (starvation medium)	
Fetal calf serum (FCS)	Gibco Lot. 41G1780K; Biochrome Lot. 0907B
Geneticin G-418 Sulfate	Gibco, Sigma
L-Glutamine (200 mM)	
10x MEM	
Penicillin-Streptomycin (10000 U/ml)	
Dubecco's Phosphate buffered saline (PBS)	Gibco, Cell Concepts
Puromycin	Sigma-Aldrich
RPMI 1640 Medium GlutaMAX	
Trypsin 2,5%	
Sodium pyruvate (100x, 100 mM)	
Zeocin	

5.4. Chemicals and Biochemicals

1-Step Ultra TMB ELISA	Thermo Scientific	Isoflurane	Forne, Baxter
30 % Acrylamid-/Bisacrylamid	Rothphorese 30, Roth	Isopropanol	Merck
Accutase Solution	Sigma-Adlrch	Kanamycin	Sigma
Acetic acid (C ₂ H ₄ O ₂)	Roth	LB medium	Roth
Agarose	Biozym, Lonza	Lymphoprep	Axis-Shield
Aluminium sulphate Al ₂ (SO ₄) ₃	Fluka	Magnesium chloride	Sigma, Merck
Ammonium Persulfate (APS)	Merck, Roth	Maleic acid	Merck
Ampicillin	Roth	Methanol	Merck
Bacto-Agar	Oxoid /Thermo Scient.	Methyl cellulose	Methocel MC or 4AM, Sigma
Bacto-Trypton	Oxoid /Thermo Scient.	Dublecco's PBS (tablets, powder)	Oxoid/Thermo Scient., Biochrome
Bacto-Yeast-Extract	Oxoid /Thermo Scient.	Phenol/Chloroform	Roth
Beta-Mercaptoethanol	Roth, Merck	Phosphoric acid	Sigma
Boric acid (H ₃ BO ₃)	J.T. Baker	Polybrene	Roth
Bovine Serum albumin (BSA)	PAA Laborator., Sigma	Polyethylenimine (PEI, CAS Nr 9002-98-6)	Millipore
Bromophenol blue	Merck	Potassium chloride (KCl)	Merck
Calcium Chloride (CaCl ₂)	Roth	Proteinase K	Roche
Chemiluminescent Substrate	CDP-Star, Roche	Protein G Sepharose 4 fast flow	GE Healthcare
Cell Dissociation Solution	Sigma	Re-Blot Plus Strong Solution 10x	Millipore
chloramphenicol	Sigma-Aldrich	Saccharose	Roth
Ciprofloxacin Hydrochloride	ICN Biochemicals	Saponin	Roth
Complete Protease Inhibitor	Roche	Skim milk powder	Sucofin, Frema
Coomassie Brilliant Blue G250	Serva	Sodium bicarbonate (NaHCO ₃)	Roth
Deoxycholic acid sodium salt	Roth	Sodium chloride (NaCl)	Roth
Deoxyribonucleotide tri- phosphat mix (dNTPs)	Qiagen, Invitrogen/ Thermo Sient.	Sodium citrate	Roth
4',6-Diamidino-2-phenylindo- ledihydrochloride (DAPI)	BioLegend	Sodium dodecyl sulfate (SDS)	Roth
DIG Easy Hyb Granules	Roche	sodium hydrogen phosphate (Na ₂ HPO ₄)	Merck
Dimethyl sulfoxide (DMSO, >99,5%)	Roth	Sodium hydroxide (NaOH)	Merck
Digitonin, high purity	Calbiochem	Sulfuric acid (H ₂ SO ₄)	Roth
Dithiothreitol (DTT)	Merck, Serva	N, N, N', N'- Tetramethyl- ethylenediamine(TEMED)	Roth
Erythrocyte Lysis Buffer	BD Pharm Lyse Buffer, BD Pharming	Tris ultrapure	Applichem
Ethanol	Merck	Tris-Base	Roth, AppliChem
Ethidiumbromid	Roth	Tween-20	ApplChem, Sigma
Ethidiumbromid 0,07%	AppliChem		
Ethylenedinitrilo tetraacetic acid (EDTA)	Serva, Merck		
Glycerol	Roth		
Glycin	Neolab Roth		
Hydrochloric acid (HCl)	Sigma-Adlrch		

5.5. Buffers and Solutions

Laird's Tail Buffer

10 mM Tris-HCl (pH 8,5)
5 mM EDTA
0,2% (w/v)SDS
200 mM Natrim chlorid

LB Agar

1,5% (w/v) Agar in LB medium

LB Medium (Luria Bertani)

1% (w/v) Bacto-Trypton
5% (w/v) Bacto-Yeast-Extract
1% (w/v) NaCl

FC buffer

1x PBS
3% FCS
Optional 2 mM EDTA

PEI transfection reagent

Stock 10 mg/ml in H₂O, steril filtrated,
storage at -80°C

Buffers and solution for agarose gels

6x DNA sample buffer

10% (v/v) Glycerol

6x TBE

Bromophenol blue

50x Tris-Acetate-EDTA buffer (TAE)

200mM Tris-HCl (pH 8,0)

50mM EDTA

5,71% (v/v) acetic acid

10x Tris-Borat-EDTA-Buffer (TBE)

900 mM Tris

900 mM Boric acid

20 mM EDTA (pH8)

Buffers and solution for ELISA

ELISA coating buffer

0,1 M Na₂HPO₄ (pH 9)

ELISA Wash buffer

1x PBS

0,1% Tween-20

ELISA blocking buffer

1x PBS

0,1% Tween-20

10% FCS or 5% BSA

Buffers and solution for MCMV

MCMV saccharose buffer

50 mM Tris/HCl (pH 7,8)

10 mM KCl

5 mM EDTA

15% Saccharose

autoclaved

Methyl cellulose

7-9 g Methyl cellulose in 360 ml ddH₂O

autoclaved and stirred oN at 4°C

45 ml 10x MEM

20 ml FCS

20 ml NaHCO₃ (55 g/l, autoclaved)

5 ml Penicillin / Streptavidin (10000 U/ml)

5 ml L-Glutamine (200 mM)

Stirred oN at 4°C and

centrifuged at 4000 rpm, 1 h

Buffers and solution for and Western Blots

Anode buffer (native PAGE)

25 mM Tris/HCl (pH 8,4)

192 mM Glycin

Bradford Solution

8,5% (v/v) phosphoric acid

4,75% (v/v) ethanol

100 mg/l Coomassie Blue G250

Filtrated 0,45 µm

10x Blot Buffer (semi dry)

480 mM Tris

280 mM Glycin

20% (v/v) ml MeOH

Cathode buffer (native PAGE)

25 mM Tris/HCl (pH 8,4)

192 mM Glycin

0,2% Deoxycholic acid

Colloidal Coomassie staining
0,02% (w/v) Coomassie G250
% (v/v) phosphoric acid
10% (v/v) ethanol
5% (w/v) aluminium sulphate

2x native sample buffer
125 mM Tris/HCl (pH 6,8)
3% (v/v) Glycerol
14% Saccharose
Bromophenol blue

resolving gel with 10% acrylamide-bisacrylamide (SDS-PAGE)
33% (v/v) 30% acrylamide-bisacrylamide mix
417 mM Tris (pH 8,8)
0,1% (w/v) SDS
0,12% (w/v) APS
0,2% (v/v) TEMED

stacking gel (SDS-PAGE)
16% (v/v) 30% acrylamide-bisacrylamide mix
138 mM Tris (pH 6,8)
0,1% (w/v) SDS
0,13% (w/v) APS
0,13% (v/v) TEMED

Solutions for Protein G affinity chromatography

Elute neutralization buffer
1 M Tris-HCl (pH 9.0)

10x Laemmli Electrophoresis Buffer
252 mM Tris
1,92 mM Glycin
1% (w/v) SDS

10x TBST
0,1 M Tris/HCl (pH 8,0)
1,5 M NaCl
5% (v/v) Tween-20

5x SDS sample buffer
0,25 M Tris/HCl (pH 6,8)
25% (v/v) Glycerol
20% (w/v) SDS
0,5% (v/v) beta-Mercaptoethanol
Bromophenol blue

Solutions for Southern Blot

Maleic acid buffer
0,1 M maleic acid (pH 7,5)
0,15 M Sodium chloride

20x sodium citrate standard buffer (SSC)
3 M Sodium chloride
0,3 M Sodium citrate

Stringency wash buffer I
2x SSC buffer
0,1% (w/v) SDS

Stringency wash buffer II
0,5x SSC buffer
0,1% (w/v) SDS

Stripping Solution
0, 1% SDS
8% (w/v) Sodium hydroxide

Buffers and solution for IP (added shortly before usage)*

IP lysis puffer
140 mM NaCl
5 mM MgCl₂
20 mM Tris, pH 7,6
1% (w/v) Digitonin*
Complete Protease Inhibitor (Roche)*

IP-B wash buffer
150 mM NaCl
10 mM Tris, pH7,6
2 mM EDTA
0,2% (w/v) Digitonin*

IP-C wash buffer

500 mM NaCl
 10 mM Tris, pH 7,6
 2 mM EDTA
 0,2% (w/v) Digitonin*

5x PNG puffer

250 mM Sodiumphosphat (pH 6,5)
 50 mM EDTA
 1 % (w/v) SDS
 1 % (v/v) Nonidet P-40
 1 % (v/v) 1 M beta-Mercaptoethanol

IP-D was h buffer

10 mM Tris, pH8

5x IP running buffer

250 mM Tris base
 2 M glycin
 0,1% SDS (to 1x buffer)

4x IP sample buffer

250 mM Tris/HCl, pH 6,8
 20 mM EDTA
 8% (w/v) SDS
 60% (w/v) sucrose
 Bromophenol blue
 11,% SDS*
 80 mM DTT*

5.6. Antibodies**5.6.1. Antibodies**

Antigen	Clone	Label	Host	Sub-class	Provider	Catalogue Nr.	Appli-cation
Primary antibodies							
Beta-Actin	AC-74	-	mouse	IgG2a	Sigma-Aldrich	A2228	WB
Human Erp57 (ascites)		-	mouse	IgG	Merck Millipore	05-728	NP
Human CD3	OKT3	FITC	mouse	IgG2a	Affymetrix / eBios.	11-0037-41	FC
Human CD4	OKT4	-	mouse	IgG2b	Affymetrix / eBios.	14-0048	FC, C, NP
		FITC				11-0048	
		APC				17-0048	
Human CD8	OKT8	-	mouse	IgG2a	Affymetrix / eBios.	14-0086	FC, NP
		FITC				11-0086	
		APC				17-0086	
	RTA-T8	FITC	mouse	IgG1	Affymetrix / eBios.	11-0088	FC
Human pan MHC-I (ascites)	W6/32	-	mouse	IgG2a	ATCC	HB95	FC, ivFcA, NP
Human tapasin	N-17	-	mouse	IgG1	Santa Cruz Biotech.	sc-14373	NP
Human tapasin	(PaSta1, STC2)	-	mouse	IgG1	Dick et al., 2002	-	NP
Mouse CD3	145-2C11	PerCP	hamster	IgG1	BD Pharming	553067	FC
		PE				553063	FC
Mouse CD4	RM4-5	PerCP	rat	IgG2a	BD Pharming	553052	FC
Mouse CD8	KT15	FITC	rat	IgG2a	Prolimmune	A502-3B-E	FC
	53-6.7	APC	rat	IgG2a	Affymetrix / eBios.	17-0081	FC
Mouse CD11b	M1/70	APC-Cy7	rat	IgG2b	BD Pharming	561039	FC
Mouse CD11c	HL3	APC	hamster	IgG1	BD Pharming	561119	FC
Mouse CD19	1D3	APC	rat	IgG2a	BD Pharming	550992	FC
		PerCP-Cy5.5				561113	FC
Mouse CD49b	DX5	APC	rat	IgM	Mitleny Biotec	130-102-803	FC
		PE-Cy7	rat	IgM	Affymetrix / eBios.	25-5971	FC
Mouse CD86	GL-1	PE-Cy7	rat	IgG2a	BioLegend	105013	FC

Mouse Ly-6C	HK1.4	AlexaFluor 488	rat	IgG2c	BioLegend	128021	FC
Mouse F4/80	BM8	FITC	rat	IgG2a	Affymetrix / eBios.	53-4801	FC
	BM9	PE			BioLegend	123109	FC
Mouse FcγRI	290322	-	rat	IgG2a	R and D systems	MAB20741	FC
Mouse FcγRII/III	2.4G2	-	rat	IgG2b	ATCC	HB-197	FC
Mouse FcγRIII	275003	-	rat	IgG2a	R and D systems	MAB19601	FC, ivFcA
		PE				FAB19601P	FC
Mouse FcγRIV	E9E	Alexa Flour 647	hamster		Prof. Dr. Nimmerjahn, University of Erlangen-Nuremberg		FC
Anti-viral antibodies							
MCMV gB	97.3	-	mouse	IgG2c	Prof. Dr. M. Mach, University of Erlangen-Nuremberg		FC, NP
	MCMV 1.01	-	mouse	IgG2b	Prof. Dr. Jonjic, University of Rijeka		FC, WB, NP
MCMV pM45	4D4-A3	-	mouse	IgG2a	Prof. Dr. Jonjic, University of Rijeka; Dr. G. Androsiac, Heinrich Heine University Düsseldorf		NP
MCMV pp89 (IE1)	2C10-C2	-	mouse	IgG1			FC, NP
	CHROMA 101	-	mouse		Prof. Dr. Jonjic, University of Rijeka		WB
Influenza A M2 ectopic domain	mA65	-	mouse	IgG2a	Silvie van den Hoecke , Prof. Dr. Xavier Saelens, VIB Medical Biotechnology Center UGent		ivFcA
	mAb37	-	mouse	IgG1			ivFcA
	mAb148	-	mouse	IgG1			ivFcA
Capture antibodies							
Mouse IL-2	JES6-1A12	-	rat	IgG2a	BD Pharmingen	554424	E
Rat IgG	polyclonal, F(ab) ₂	-	rabbit		AbD Serotech	STAR16B	ivFcA
Isotype controls							
Mouse Immunoglobulin Panel gG1, IgG2a, IgG2b; IgG3, IgA, IgM		-	mouse		Southern Biotech	5300-01	NP
T-2 mycotoxin	15H6	biotin	mouse	IgG1	Genetex	GTX35016	FC
unknown	HOPC-1	biotin	mouse	IgG2a	Genetex	GTX35021	FC
Chicken IgA	A-1	biotin	mouse	IgG2b	Genetex	GTX35025	FC
unknown	6.3	biotin	mouse	IgG2c	Genetex	GTX35013	FC
unknown	B10	biotin	mouse	IgG3	Genetex	GTX35029	FC
unknown	eBMG2b	FITC	mouse	IgG2b	Affymetrix / eBios.	11-4732	FC
unknown	eBMG2b	APC	mouse	IgG2a	Affymetrix / eBios.	17-4724	FC
Ectodomain of the small hydrophobic protein of HRSV		-	mouse	IgG2a	Silvie van den Hoecke , Prof. Dr. Xavier Saelens, VIB Medical Biotechnology Center UGent		ivFcA
Ectodomain of the HBV core		-	mouse	IgG1			ivFcA
Detection antibodies							
Mouse IgG	polyclonal	APC	goat		DB Pharming	550826	FC
Mouse IgG	polyclonal	Cy5	goat		Dianova	115-175-146	FC
Mouse IgG	polyclonal	FITC	goat		Sigma-Aldrich	F2012	FC
Mouse IgG	polyclonal	POD	goat		J. ImmunoResearch	115-035-003	WB, E
Rat IgG	polyclonal	FITC	goat		Sigma	F2012	FC
DIG-AP	Polyclonal, Fab	alkaline phosphatase	sheep	-	Roche	11093274910	SB
Mouse IL-2	JES6-5H4	Biotin	rat	IgG2b	BD Pharmingen	554426	E
Fc Block							
Mouse FcγRII/III	2.4G2	-	rat	IgG2b	BP Pharming	553141	FC
Human FcγR		-			Miltenyi Biotech	130-059-901	FC
other detection reagents							
Streptavidin		POD			J. ImmunoResearch	016-030-084	E, WB
Streptavidin		APC			BD Pharming	554067	FC

C: Coomassie stained SDS-PAGE, E: ELISA, FC: Flow Cytometry, ivFcA: *in vitro* FcγR activation assay; NP: Native PAGE, SB: Southern Blot, WB: Western Blot, POD: Horseradish Peroxidase

5.6.2. Sera and IgG from sera

Name	Mouse strain	Infection	Provider
Purified IgG from naive mouse serum	Non swiss albino	-	Chrompure Lot. 99042, Jackson ImmunoResearch
Naive mouse serum (pool)	BALB/c	-	In house
MCMV immune serum (pool)	BALB/c	28 dpi MCMV	
H1N1 immune serum	C57BL/6	H1N1 (RP8) 16 dpi	Prof. Dr. P. Stähli, Albert Ludwigs University, Freiburg

5.7. Kits

DIG High Prime	Roche
DNeasy Blood and Tissue Kit	Qiagen
Film developer and fixer	Adeco UV, Adeco Chemie
Gel and PCR Extraction Kit	QIAquick, Qiagen
	NucleoSpin Gel and PCR Clean-up, Macherey-Nagel
Luciferase Reporter Gene Assay, high sensitivity	Roche
NucloBond AX100 (BACmid DNA Isolation)	Macherey-Nagel
OneStep RT-PCR Kit	Qiagen
PCR Master Mix with Taq (for mouse screening)	Promega
Plasmid Mini and Midi Kit	Qiagen
	NucleoSpin Plasmid, Macherey-Nagel
QIAshredder	Qiagen, Hilden, Deutschland
QuickChange II XL Site-Directed Mutagenesis Kit	Stratagene
RNeasy Mini Kit	Qiagen
Superfect Transfection Reagent	Qiagen
TOPO TA Cloning® Kit	Life Technology / Thermo Scientific
TA Cloning Kit Dual Promoter, pCRII vector	Life Technology / Thermo Scientific
Western Blotting Detection System	ECL/ ECL Plus, GE Healthcare
	Clarity Western ECL Substrate, Bio-Rad

5.8. Enzymes

AmpliTaq DNA Polymerase	Applied Biosystems
Alkaline Phosphatase (Calf Intestinal Phosphatase, CIP)	New England Biolabs
Antarctic Phosphatase	New England Biolabs
Collagenase D	Roche
DNase I	Roche
DNA restriction endonucleases (<i>EcoRI</i> , <i>BamHI</i> , <i>HindIII</i> ,...)	New England Biolabs
DNA restriction endonuclease Eco47III	Promega
Expand High Fidelity PCR System	Roche
Peptide-N-Glycosidase F (PNGase F)	Roche
Phusion High-Fidelity DNA Polymerase	Finnzymes / Thermo Scientific
Proteinase K	Roche
RNase A	Fermentas
RNase H	Fermentas
SuperScript II Reverse Transcriptase	Invitrogen / Thermo Scientific
T4 DNA Ligase	New England Biolabs
OneTaq DNA Polymerase	New England Biolabs
Terminal Deoxynucleotidyl Transferase (TdT)	Invitrogen / Thermo Scientific

5.9. Primer

All primers (oligonucleotides) were order at Erofins MWG-Biotech or Integrated DNA Technologies (IDT). The lyophilised DNA was solved in DNase-free water with a final concentration of 100 mM and stored at -20°C. For PCR, the stock solution was diluted with ddH2O to the working concentration of 10 mM.

Primer name	sequence	Restriction sites
Oligo-dT	T(20)	-
Expression cassette for insertion into the MCMV genome		
5-MscI-Luc	AATATGGCCACAACCATGGAAGACGCCAAAAACATAAA	MscI
3-Luc-NotI	AGTCGCGGCCGCTCACGGCGATCTTTCCGC	NotI
5-EcoRI-hCD8	AAGAATTCATGGCCTTACCAGTGACCGC	EcoRI
5-EcoRI-hCD4	AAGAATTCATGAACCGGGGAGTCCCTTT	
3-hCD8-BglII	TCTCAGATCTTTAGACGTATCTCGCCGAAAGGC	BglII
3-hCD4-BglII	TCTCAGATCTTCAAATGGGGCTACATGTCTTCTG	
5-Spe-m157	GAGACTAGTCGTCCCGGGTGTGCGCT	SpeI
5'RACE		
5-AnhcorP	CTACTAGAATTCACTAGTACGGGZZGGGZZGGGZZG Z: deoxyinosine	EcoRI, SpeI
3-GSP1-HC	CCAGTTGTATCTCCACAC	
3-GSP1-LC	TGCTCACTGGATGGTG	
Insertion of OKT8 V _H and V _L into pFUSE vectors		
5-8HC-EcoRI	AGAATTCGCCACCATGAAATGCAGCTGGGTTATC	EcoRI
3-8HC-BstUI	TTCGCGAGGAGACTGTGAGAGTGGTG	BstUI
5-8LC-AgeI	AACCGGTGCCACCATGAGGTTCCAGGTTCCAGG	AgeI
3-8LC-BstAPI	GCTGCAGCATCTGCCCGTCTCAGCTCC	BstAPI
Insertion of OKT8 kappa LC into puc vectors		
5-XhoI-8LC	CTCGAGACCGGTGCCACCATGAGG	XhoI
3- 8LC-BglII	AGATCTTGCCAGCTAGCTCTC	BglII
Cloning of the IgG2c heavy chain		
5-IgG2c-HC	TGCTAGCAGCGCCAAAACAACAGCCCCATCGG	NheI
3-IgG2c-HC	GTCTGGCCAGCTAGGGCTGAGCTCATTTACCCAGA GACCGGGAGATGGTCTTAGTCG	MscI
5-IgG2c-HC-Eco	TGCTAGCAGCGCTAAAACAACAGCCCCATCGG	Eco47III
3-IgG2c-HC-Eco	CCGATGGGGCTGTTGTTTTCAGCGCTGCTAGCA	
FcγR-CD3z chimeras		
5-FcγRI-SpeI	CCCACTAGTGGGGCCGCATCCATGATTCTTACCAGC	SpeI
3-FcγRI-Zeta	GTAGCAGAGAAACCAGACAGGAGCTGATGACTGGG	-
5-Zeta-FcγRI	CTCCTGTCTGTTTCTCTGCTACTTGCTAGATGGA	-
5-FcγRII-SpeI	CCCACTAGTGGGGCCGCATCCATGGGAATCCTGCCGTTT	SpeI
3-FcγRII-Zeta	GTAGCAGAGTGTCAATACTGGTAAAGACCT	-
5-Zeta-FcγRII	GTATTGACACTCTGCTACTTGCTAGATGGA	-
5-FcγRIII-SpeI	CCCACTAGTGGGGCCGCATCCATGTTTCAGAATGCACAC	SpeI
3-FcγRIII-Zeta	GTAGCAGAGCCAGACTAGAGAGATGGAGGA	-
5-Zeta-FcγRIII	CTAGTCTGGCTCTGCTACTTGCTAGATGGA	-
5-FcγRIV-SpeI	CCCACTAGTGGGGCCGCATCCATGTGGCAGCTACTACTA	SpeI
3-FcγRIV-Zeta	GTAGCAGAGCGGTGGAAACATGGATGGAGA	-
5-Zeta-FcγRIV	TTCCACCGCTCTGCTACTTGCTAGATGGA	-
3-Zeta-SpeI	AAGACTAGTCTTAGCGAGGGGCCAGGGTCTG	SpeI
5-SpeI-Balb-FIII	TTGACTAGTGGGGCCGCATCCATGTTT	SpeI
3-OverI-FIII	GACCTGGCTCCGGATGGACCTCCCGTTGTGG	-

5-Overl-FIII	CATCCGGAGCCAGGTCCAAGCCAGC	-
3-SpeI-FIII	ATACTAGTCTTAGCGAGGGGCCAGGG	<i>SpeI</i>
Mouse strain genotyping		JAX name
y-KO-For	CTCGTGCTTTACGGTATCGCC	IMR0618
y-WT-For	CTCACGGCTGGCTATAGCTGCCTT	IMR0622
y-COM-Rev	ACCCTACTCTACTGTCGACTCAAG	IMR0621
RI-KO-For	GATTCGCAGCGCATCGCCTTCTATCG	-
RI-WT-For	ACCATCCGTTCTGCTGCTGCTTGA	-
RI-COM-Rev	TTGCCGAAAATCCACTCTAAATACAG	-
RIII-KO-For	GCACGAGACTAGTGAGACGTG	IMR7696
RIII-WT-For	CTACATCCTCCATCTCTCTAG	IMR0848
RIII-COM-Rev	GTGGCTGAAAAGTTGCTGCTG	IMR0847
RIV-KO-For	GAGCCGAGTGA	-
RIV-WT-For	CCAAACAGCGGTCTCCT	-
RIV-COM-Rev	CCTTATCACCTTGCTCCTTAG	-
RAG1-KO-For	TGGATGTGGAATGTGTGCGAG	IMR8162
RAG1-WT-For	TCTGGACTTGCTCCTCTGT	IMR23267
RAG1-COM-Rev	CATTCCATCGCAAGACTCCT	IMR23268
Sequencing		Vector / gene
5-Seq-pFUSE	TTACAGATCCAAGCTGTGACCG	HTLV promotor
5-Seq-puc-for	GCTCACAACCCCTCACTCGGCGC	Puc vector
3-Seq-puc-rev	TAACATATAGACAAACGCACACCG	Puc vector
M13 (life technology)	GTAAAACGACGGCCAG	TOPO vectors
5-Seq-IRES-for	GGTAGGCGTGACGGTGG	pIRES vector
3-Seq-IRES-rev	CACCGGCTTATTCC	IRES
5-Seq-LucM	CCTGCGTGAGATTCTCGCATGC	Luciferase
5-Seq-IRES	CGAACCACGGGGACGTGGTTT	pIRES-Luc
3-Seq-Luc	AGCAAGTAAACCTCTACAAATCTGGT	pIRES-Luc

5.10. Plasmids and BACmids

5.10.1. Plasmids

pC20	Cherepanov and Wackernagel, 1995
pTA-Luc-m157FLK	PD Dr. Albert Zimmermann (Heinrich Heine University, Düsseldorf)
pFRTZ-MIEP-IRES-eGFP	Dr. Vu Thy Khanh Le Trilling (University Duisburg-Essen)
pcDNA3.1-hFcyRIII-CD3zeta	Dr. E. Corrales-Aguilar
pCMV6-XL5-hCD8	Origene, SC111602
pIRES-eGFP	Clontech
pCRII-TOPO, pCR2.1-TOPO	Life Technology / Thermo Scientific
pFUSE-CHlg-m1	InVivogen
pFUSE-CHlg-m2a	InVivogen
pFUSE-CHlg-m2b	InVivogen
pFUSE-CHlg-m3	InVivogen
pFUSE-CLlg-mk	InVivogen
puc2CL6IPwo	Prof. Dr. Hanenberg (Heinrich Heine University, Düsseldorf)
puc2CL6INwo	Prof. Dr. Hanenberg (Heinrich Heine University, Düsseldorf)
puc2CL6IGwo	Prof. Dr. Hanenberg (Heinrich Heine University, Düsseldorf)
Pseudotyping vector "VSV-G"	Prof. Dr. Hanenberg (Heinrich Heine University, Düsseldorf)
Packing vector "Gagpol"	Prof. Dr. Hanenberg (Heinrich Heine University, Düsseldorf)

5.10.2. BACmids

MCMV C3X	PD Dr. Barbara Adler (Ludwig Maximilians University, Munich; Jordan et al., 2011)
MCMV C3X Δ m157 FRT	PD Dr. Albert Zimmermann (HHU Düsseldorf, Germany)

5.11. Viruses

MCMV C3X	Recombinant MCMV virus basing on the pSM3fr BACmid (Messerle et al., 1997) with repaired frameshift mutation in the MCK-2 ORF (<i>m129</i>)(kindly provided by B. Adler, Ludwig-Maximilians University, Jordan et al., 2011)
MCMV Δ m157-Luc	MCMV Δ m157-luc was constructed by Dr. Albert Zimmermann (Heinrich Heine University, Düsseldorf) based on the MCMV C3X BACmid. Deletion of the m157 ORF and insertion of the luciferase sequence into the m157 locus was performed exactly as described in Trilling et al. 2011.
MCMV hCD8	Insertion of the expression cassette of MIEP-hCD8-IRES-Luc-Zeocin via FRT/FLP recombination into MCMV Δ m157 FRT
MCMV hCD4	Insertion of the expression cassette of MIEP-hCD4-IRES-Luc-Zeocin via FRT/FLP recombination into MCMV Δ m157 FRT
MCMV C3X _{MCK2} -	Recombinant MCMV virus basing on the pSM3fr BACmid (Messerle et al., 1997; Jordan et al, 2011)
MCMV C3X _{MCK2} - Δ m138	Recombinant MCMV virus based on the pSM3fr BACmid (Messerle et al., 1997; Jordan et al, 2011) with deletion of <i>m138</i> by introduction of a premature stop codon by a frame shift mutation (Crnkovic-Mertens et al., 1998)

Infectious MCMV was reconstituted by the Superfect transfection (Qiagen, Germany) procedure. BAC sequences were removed by serial passage in MEF before use of the recombinant virus.

Influenza A virus	A/RP/8/34, abbreviation H1N1 RP8 (Prof. Dr. P. Stähli, Albert Ludwigs University, Freiburg)
-------------------	---

5.12. Bacteria

<i>E.coli</i> , strain XLI-Blue	F':Tn10 pro A B lacI Δ (lacZ)M15/recA1 end A1 gyrA96 (Na1) thi hsdR17 (rkMk) glnV44 relA1 lac
<i>E.coli</i> , strain DH10B	F ⁻ mcrA Δ (mrr-hsdRMS-mcrBC) Φ 80lacZ Δ M15 Δ lacX74 deoR recA1 endA1 araD139 Δ (ara, leu) 7697 galU galK rpsL nupG λ -

5.13 Cells

5.13.1. Cell Lines

Name	Host species	origin	cell type	property	ATCC Nr./Provider
HeLa	human	cervix adenocarcinoma	epithelial	adherent	CCL-2
BIM	mouse	BALB/c embryo tissue	fibroblast	adherent	Prof. Dr. M. Trilling, University Duisburg-Essen
BW:5147	mouse	AKR/J thymoma	T lymphocyte	suspension	TIB-47
CHO	Chinese hamster	ovary	epithelial-like	adherent	Tjio et al., 1958
CIM	mouse	C57BL/6 embryo tissue	fibroblast	adherent	Prof. Dr. Mirko Trilling, University Duisburg-Essen
HEK293T	human	fetal kidney	epithelial	adherent	CRL-11268
MDCK	dog	kidney	epithelial	adherent	Prof. Dr. P. Stähli, Albert-Ludwigs University Freiburg

NIH3T3	mouse	Swiss albino embryo tissue	fibroblast	adherent	CRL-1658
OKT8	mouse	hybridoma	B lymphocyte	suspension	CRL-8014; Christiane Steeg, BNITM, Hamburg
OKT4	mouse	hybridoma	B lymphocyte	suspension	CRL-8002; Christiane Steeg, BNITM, Hamburg
P3X63Ag 8.6533	mouse	BALB/c myeloma	B lymphocyte	suspension	CRL-1580; Brigitte Dorner, RKI, Berlin

5.13.2. Primary cells

Primary MEF were generated from BALB/c mice as described in 4.3.3. and cultured in complete DMEM medium.

5.14. Mouse strains

Name	Abbreviation	Provider	Reference
B6;129P2-Fcγ1 ^{tm1Rav}	Fcγ-KO	Prof. Dr. F. Nimmerjahn, University of Erlangen-Nuremberg	Takai et al., 1994
B6;129-Fcγ1 ^{tm1Rav} Rag1 ^{tm1Mom} /J (B6;129P2 x B6.129S7)	Fcγ x RAG-KO	Prof. Dr. M. Mach, University of Erlangen-Nuremberg	Bootz, 2014
C57BL/6J;B6(B6(Cg)-Tyr ^{C-2J})-FcγRIV tm	FcγRIV-KO	Prof. Dr. F. Nimmerjahn, University of Erlangen-Nuremberg	Nimmerjahn et al., 2005
C57BL/6.129S1/Sv(129SvJ)-FcγR1 ^{tm1Sjv}	FcγRI-KO	Prof. Dr. F. Nimmerjahn, University of Erlangen-Nuremberg	Barnes et al., 2002; Ioan-Facsinay et al., 2002
B6.129P2-FcγR3 ^{tm1Sjv} /SjvJ	FcγRIII-KO	JAX Stock 009637, Jackson Laboratories	Hazenbos et al., 1996
C57BL/6J	C57BL/6J	Heinrich Heine University, Düsseldorf	

Mice were bred in the animal facility of the Heinrich Heine University, Düsseldorf, or in the animal facilities at the Albert Ludwigs University, Freiburg (ZBMZ or Institute for Virology). The experiments were performed in IV cages.

5.15. Software

5.15.1. Software

Name	Manufacture	Function
Microsoft Office 7 (Word, Excel, PowerPoint)	Microsoft	Storage, organization, analysis, and presentation of data
Prism 6	Graphpad Software	Data graphing and statistical analysis
FACSDiva	BD Bioscience	Flow cytometer setup, data acquisition, and data analysis
FlowJo V10	Tree Star, Inc.	Analysis of flow cytometry data
Vector NTI	Invitrogen / Thermo Scientific	sequence analysis application and management
Geneious R7, R8	Biomatters Limited	
MicroWin 2000	Berthold Technologies	Operation and definition of instrument settings for the Mithras plate reader
ND-1000	Thermo Scientific	Operation and definition of instrument settings of the Nanodrop 1000
i-control 1.10.4.0	Tecan	Operation and definition of instrument settings for the multimode microplate reader

5.15.2. Online Software

Function	Abbreviation	Full name	Link
3D structures of proteins, nucleic acids, and complex assemblies	PDB	RCSB Protein Data Base	http://www.rcsb.org/pdb/home/home.do

Multiple sequence alignment	Clustal W2; Clustal Omega		http://www.ebi.ac.uk/Tools/msa/clustalw2/ http://www.ebi.ac.uk/Tools/msa/clustalo/
Protein domain predication	SMART	Simple Modular Architecture Research Tool	http://smart.embl-heidelberg.de/
Reverse-complement DNA sequence			http://www.bioinformatics.org/sms/rev_comp.html
Translation of nucleotide sequences	ExPASy Translate	Expert Protein Analysis System	http://web.expasy.org/translate/
NetNGlyc 1.0 Server			http://www.cbs.dtu.dk/services/NetNGlyc/
NetOGlyc 4.0 Server			http://www.cbs.dtu.dk/services/NetOGlyc/

5.15.3. Online Databases

Abbreviation	Full name	Link
IMGT/Gene-DB	The International Immunogenetics Information System®	http://www.imgt.org/genedb/
MGI	Mouse Genome Informatics	http://www.informatics.jax.org/
NCBI Protein	National Center for Biotechnology Information (Protein / Gene/ Nucleotide/ Genbank/ Reference Sequence) Database	http://www.ncbi.nlm.nih.gov/protein/
NCBI Gene		http://www.ncbi.nlm.nih.gov/gene/
NCBI Nucleotide		http://www.ncbi.nlm.nih.gov/nucleotide/
NCBI Genbank		http://www.ncbi.nlm.nih.gov/genbank/
NCBI RefSeq		http://www.ncbi.nlm.nih.gov/refseq/
NCBI Blast	Basic Local Alignment Search Tool	http://blast.ncbi.nlm.nih.gov/Blast.cgi
UniProt	Universal Protein Resource	http://www.uniprot.org/

6. SUPPLEMENT

6.1. Characterisation of the immune cell populations in the SG

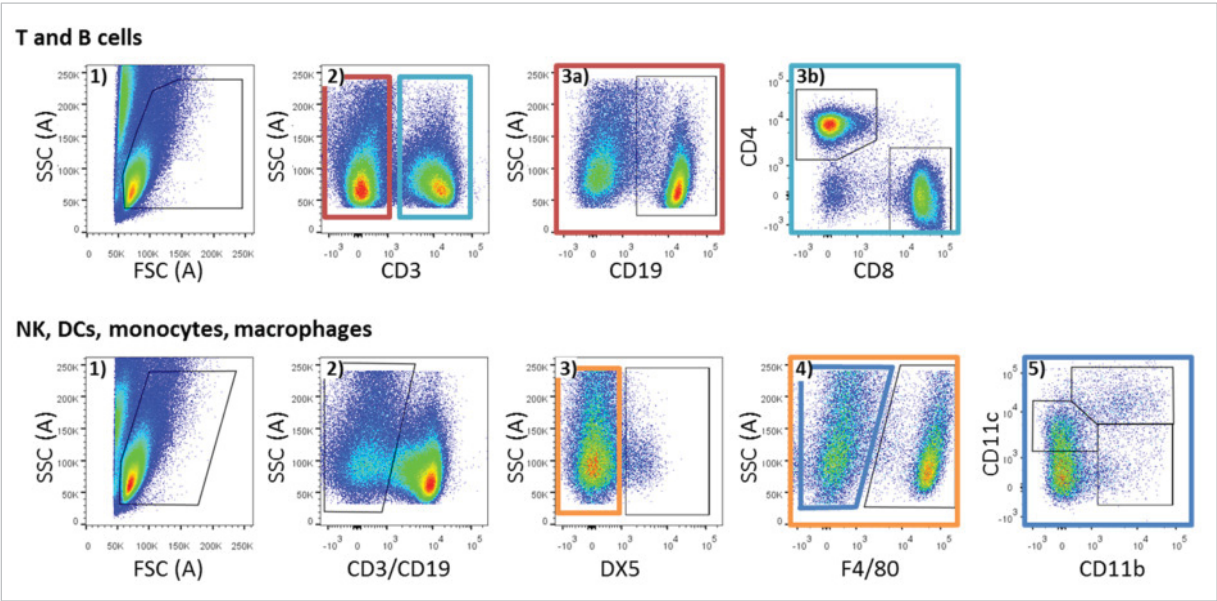


FIGURE S1. Flow cytometry gating strategies to characterize the immune cell population in the SG in MCMV infected FcR γ -KO vs. FcR γ -HET mice. 8 - 12 wks old FcR γ -KO and FcR γ -HET control mice were infected i.p. with 2×10^5 PFU MCMV Δ m157 Luc for 14 or 28 (10 - 12 mice/group). The SG were harvested, the tissue was mechanically and enzymatically dissolved, the immune cells were separated by density gradient centrifugation, and stained. First, living and single cells were gated (data not shown). The surface molecules stained and the gating strategy are indicated. Cells were measured by flow cytometry (BD FACS Canto II, FACS Diva software) and analysed with FlowJo (Tree Star Inc). As example, one FcR γ -HET mouse at 28 dpi is shown.

6.2. Structure of the human CD8 $\alpha\alpha$ homodimer

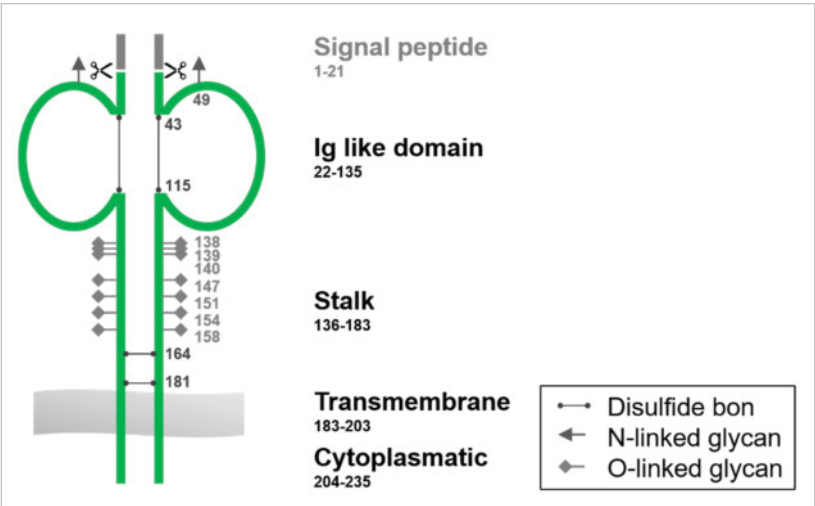


FIGURE S2. Schematic representation of the structure of the human CD8 $\alpha\alpha$ homodimer. Annotations are according to P01732. N- and O-glycosylation sites were predicted with the NetNGlyc1.0 and NetOGlyc4.0 Server.

6.3. Polymorphisms of mouse IgG subclasses

The analysis was performed as described in 2.4.1.

IgG1	$\Sigma 53$ sequence identity: 99-100%
Domain	Sequence
N	- AKT ^S TP

C_{H1}	-	PSVYPLAPGSA ^S AQTNSMVTLGCLVKGYFPEPVTVTWNSGSLSSGVHTFPAVL ^Q L ^E (5)
		SDLYTLSSSVTVPSSTW ^{PR} (9)PS ^Q (10)TVTCNVAHPASSTKVDDKIV
Hinge	-	PRDCG ^{CG} (1)CKPCICTVPEV
C_{H2}	-	SSVFIFPPKPKDVLITITLTPKVTCVVVDISKDDPEVQFSWFVDDVEVHTAQTL ^K (10)PR
		EEQ ^F (5)NSTFRSVSELPIMHQDWL ^F NGKEFKCRVNSAAFPAPIEKTIS
-	-	KTKGRPKA
C_{H3}	-	P ^S (2)QVYTIPPPKEQMAKDKVSLTCMIT ^D N(5)FFPEDITVEWQWNGQPAENYKNTQPI
		MD ^{NTN} (11)SYFV ^I YSKLVNQKSNWEAGNT ^X FTCSVLHEGLHNHHTEKS ^N LS
C	-	HSPGK

IgG2a	$\Sigma 26$ sequence identity: 98-100%
Domain	Sequence
N	- AKTTA
C_{H1}	- PSVYPLAPVCGDITGSSVTLGCLVKGYFPEPVTLTWNSG ^S PLSSGVHTFPA ^V VLQSDLY
	TLSSSVTVTSSTWPSQITCNVAHPASSTKVDDKIE
Hinge	- PRGPTIKPCPPCKCPAPNLLGG
C_{H2}	- PSVFIFPPKIKDVLMLISL ^P M(14)VTCVVVDVSEDDPDVQISWFVNNVEV ^H L(12)TAQ
	TQTHREDY ^N STLRVVSALPIQH ^Q QDWMSGKEFKCKVNNK ^A (10)LPAPIERTIS
-	- KPKGSVRA
C_{H3}	- PQVYVLPPEEEMTKQVTLTCMVTDFMPEDIYVEWTNNGKTELNYKNTPEVLDSDG
	SYFMYSKLRVEKKNWVERNSYSCSVVHEGLHNHHTTKS ^F LS
C	- RTPGK

IgG2b	$\Sigma 17$ sequence identity: (96) 98-100%
Domain	Sequence
N	- AKTTP
C_{H1}	- PSVYPLAPGCG ^D GTTGSSVT ^I S(2)GCLVKGYFPE ^S P(2)VTVTWNSGSLSSSVHT ^F FL ^{LSQ}
	ALLQSGLYTMSSSVTVPSSTWPSQTVTCVAHPASSTTVDDKLE
Hinge	- PSGP ^I TSTINPCPPCKECKCPAPNLEGG
C_{H2}	- PSVFIFPPNIKDVLMLISLTPKVTCVVVDVSEDDPDV ^R Q(14)ISWFVNNVEV ^H LTAQTQ
	THREDY ^N STIRVVS ^A H(1)T(8)LP ^I QH ^Q QDWMSGKEFKCKVNNKDLP ^S APIERTIS
-	- K ^T P ^K GL ^I VRA
C_{H3}	- PQVY ^T (2)LP ^S PPA ^P EQLSRK ^E EDVSLTCLV ^V AVGF ^N SP ^E DISVEWTSNGHTEENYKDTAP
	VLDSDGSYFIYSKL ^D TM(10)KTSKWEKTD ^S FCNVRHEGLKNYYLKKTIS
C	- RSPGK

IgG2c	$\Sigma 8$ sequence identity: 98-100%
Domain	Sequence
N	- AKTTA
C_{H1}	- PSVYPLA ^V PVCGGTGSSVTLGCLVKGYFPEPVTLTWNSGSLSSGVHTFPALLQSG
	YTLSSSVTVTSNTWPSQTITCNVAHPASSTKVDDKIE
Hinge	- PRVPITQNPCPP ^L KEC ^{HQRV} PPCAAPDLLGG
C_{H2}	- PSVFIFPPKIKDVLMLISLSPMVTVCVVVDVSEDDPDVQISWFVNNVEVHTAQQTTHRE
	DY ^N STLRVVSALPIQH ^Q QDWMSGKEFKCKVNNRALPSPIEKTIS
-	- KPRGPVRA
C_{H3}	- PQVYVLPPEAEEMTKKEFSLTCMITGFLPAEIAVDWTSNGRTEQNYKNTATVLDSDG
	SYFMYSKLRVQKSTWERGSLFACSVVHE ^V (3)LHNHLTTKTIS
C	- RSLGK

IgG3	$\Sigma 7$ sequence identity: 99-100%
Domain	Sequence
N	- ATTTA
C_{H1}	- PSVYPLVPGC ^S G(2)DTSGSSVTLGCLVKGYFPEPVTVKWNYGALSSGVRTVSSVLQSG
	FYSLSSLVTVPSSTWPSQTVICNVAHPASKTELKIE
Hinge	- PRIPKPSTPPGSSCPPGNILGG
C_{H2}	- PSVFIFPPKPKDALMISLTPKVTCVVVDVSEDDPDVHVSWFVDNKEVHTAWTQPREAQ
	Y ^N STFRVVSALPIQH ^Q QDWMRGKEFKCKVNNKALPAPIERTIS
-	- KPKGRAQTPQV
C_{H3}	- YTIPPPREQMSKKKVSITCLVTNFFSEAISVEWERNGELEQDYKNTPPILSDSGTYFL
	YSKLTVDTDSWLQGEIFTCSVVHEALHNHHTQKNLS
C	- RSPGK

FIGURE S3. Amino acid polymorphism within IgG subclasses. The sequences were identified by *NCBI protein blast* in the database of non-redundant protein sequences for *mus musculus* (taxid 10090). The query sequences were the heavy chain sequences present in the pFUSE vectors of InVivogen and the newly cloned IgG2c heavy chain (2.4.3.) and are shown. Sequences with a cover of $\geq 98\%$ (IgG1 $\geq 99\%$) and a sequence identity of $> 86\%$ were compared. Amino acid substitutions are colored in green and the superscript specifies the alternative amino acids with the number of affected sequences in brackets. The light green colour indicates that the amino acid substitution was only present in one sequence. Grey color marks one IgG2b HC sequence with a sequence identity of only 96%; – deletion, + insertion, Σ number of compared sequences. Missing of one or two AA at the N- and C-terminus was not included. C_H1 - C_H3 annotation from P0186, bold N: N-glycosylation side at Asn297. NCBI sequence identification numbers (gi) are listed in the appendix.

NCBI sequence identification numbers (gi), * membrane bound form.

IgG1: 557129232*, 597955649, 28624968, 121040, 21304450*, 21304449, 194434, 300244464, 1617396, 74190484, 758371624, 754501555, 121038*, 194435*, 26334307*, 148589114, 194362, 23958196, 34785917, 14198347, 12805309, 19353759, 145203137*, 195162, 997831417, 18568340, 374672075, 32309129, 21071089, 45789811, 5114265, 13097381, 14091947*, 148540420, 7439167, 89477416, 89477420, 26665404, 1513182, 99783142, 89477424, 440121, 289666439, 340941670, 89477408, 261343156, 927228224, 549515808, 29786361, 50346336, 89477412, 14091948, 148686600; IgG2a: 34784630, 407280298, 13278043, 63100280, 82568938, 13278069, 17390662, 51593434, 481974, 17391266, 62204132, 21594583, 17644233, 462078938, 614497827, 282721924, 480895, 290877931, 734459144, 27127160, 26665400, 121048, 194438, 148686604, 148686605*, 62901522*; IgG2b: 90677 (96% sequence identity), 62201498, 19343851, 16307557, 62024579, 815099083, 816196921, 223428, 54827, 1333985, 387221, 62901523*, 148540416, 997831425, 148540424, 261343152, 223194; IgG2c: 121049, 12841781, 802199554, 62028521, 1806128, 194445, 553939; IgG3: 121044, 1304160, 50346340, 821369807, 179955, 226374242, 558122

6.4. Characterization of the parental mAb used for grafting of the variable domains: OKT8 mouse-anti-human CD8 IgG2a_K

An OKT8 mAb containing supernatant (OKT8 SN) was produced as described in (4.2.7.1.), whereby 1×10^6 cells were cultivated for 15 days in 8 ml.

6.4.1. Secretion of mAb by the OKT8 hybridoma

A sufficient mAb gene expression by the hybridoma cells is necessary to allow the cloning of the variable regions of the mAb. Therefore, the OKT8 supernatant was analysed by Western Blot detecting the heavy (HC) and the light chain (LC). A high amount of secreted IgG was detectable and (Figure S4). The purified anti MCMV-gB mAb MCMV1.01 served as control.

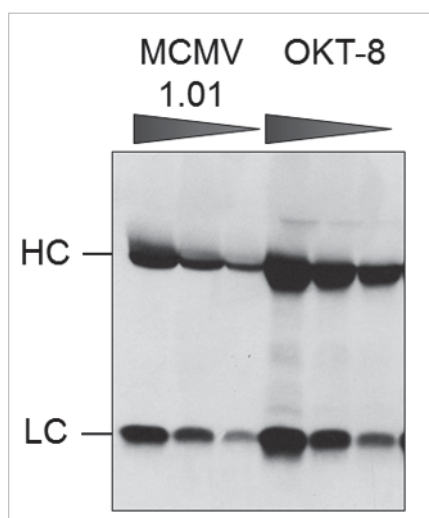


FIGURE S4. Secretion of OKT8 mAbs into the cell culture supernatant. OKT8 hybridoma supernatant (50 μ l, 20 μ l, and 10 μ l) and MCMV1.01 (1 μ g, 0.5 μ g, and 0.025 μ g; purified) were separated in a 10% SDS PAGE at 12 mA/170 V for 17 h. IgG was detected with goat anti mouse-POD by Western Blot.

6.4.2. Antigen binding specificity of OKT8

To verify the binding to its antigen, the human CD8, and to exclude a cross reactivity to the murine CD8, human PBMCs and murine splenocytes were first stained with the directly labelled OKT8-APC mAb, which is commercial available (Figure S5). To identify T cells, CD3 was stained as well. As expected, the OKT8-APC labelled the subset of the CD3 positive cells of the human PBMCs, which are human CD8 T cells. In contrast, it did not bind to murine cells. As a side note, the CD3 positive and CD8 negative population consisted mainly of CD4 T cells.

In addition, the human PBMCs and murine splenocytes were stained with different dilutions of the OKT8 SN (Figure S6). Predictably, the OKT8 SN stained the CD8 T cells whereby the signal magnitude decreased with the increasing dilution of the OKT8 SN. Furthermore, no binding of OKT8 mAb either derived from the hybridoma supernatant or of directly labelled purchased mAb to mouse T cells was detectable. These results confirm the antigen specificity of the OKT8 mAb.

SUMMARY

- *The OKT8 hybridoma secretes high amounts of monoclonal antibodies, which bind to human CD8 T cells but not to mouse CD8 T cells.*

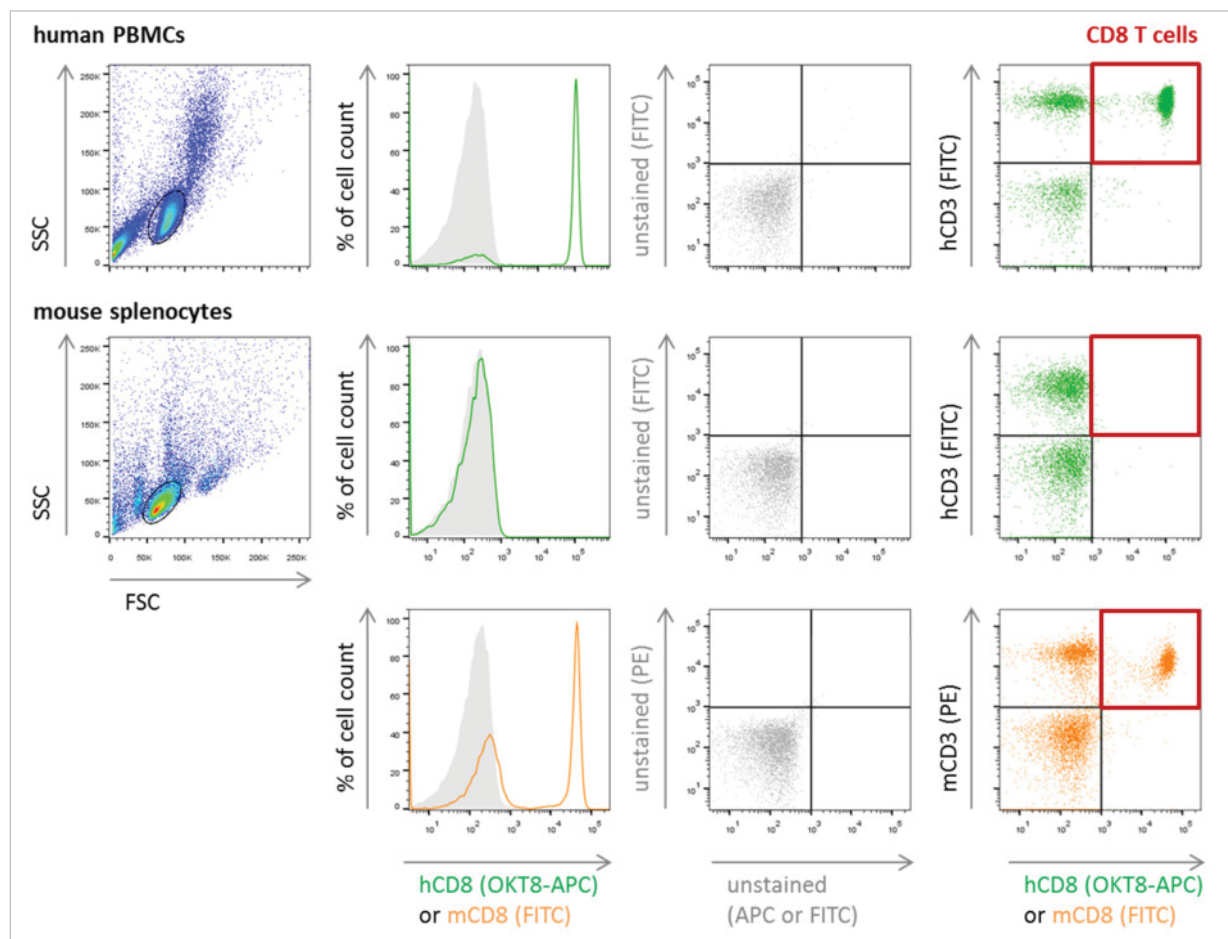


FIGURE S5. OKT8-APC binds to human but not to mouse T cells. Human PBMCs and murine splenocytes were preincubated with Fc block and stained with the anti-CD8 (anti-hCD8-APC clone OKT8; anti-mCD8-FITC) and anti-CD3 (anti-hCD3-FITC; anti-mCD3-PE). Unstained cells are shown in grey. At least 3×10^4 cells were measured by flow cytometry (BD FACS Canto II, FACS Diva software) and analysed with FlowJo (Tree Star Inc). It was gated on the lymphocyte population in the FSC/SSC gate. Histograms show the CD3 positive cell population.

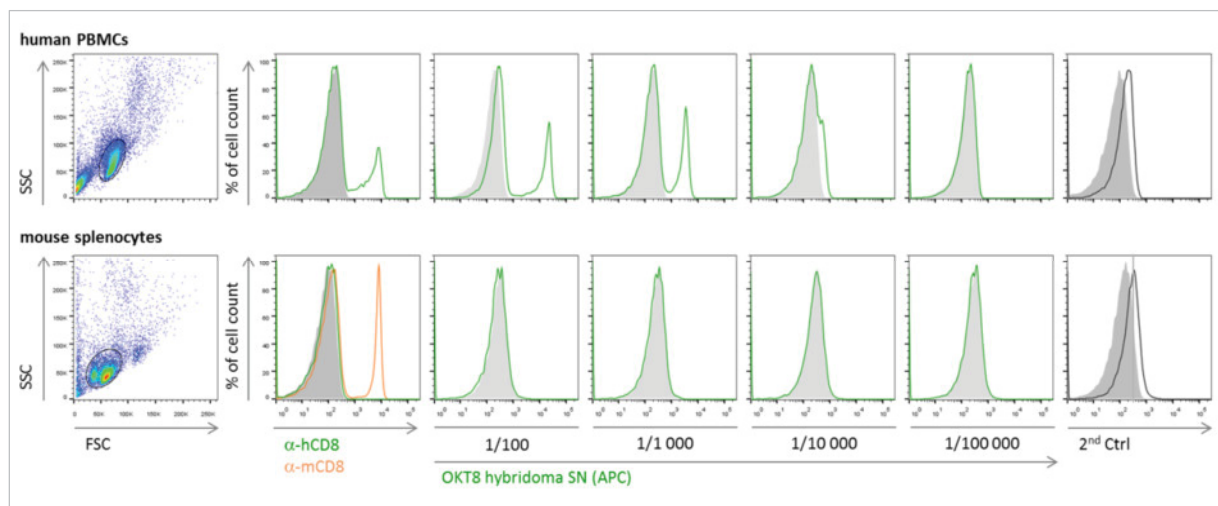


FIGURE S6. The OKT8 mAb binds to human but not to mouse T cells. Human PBMCs and murine splenocytes were stained with a 10-fold dilution series of the OKT8 SN starting at 1/100. For detection a goat anti-mouse Cy5 labeled antibody was used (2nd Ab). Furthermore the cells were preincubated with Fc block and stained with anti-CD3 (anti-hCD3-FITC; anti-mCD3-PerCP) allowing to gate on T cells. As controls, direct labelled anti-hCD8 and anti-mCD8 were utilized. Unstained cells are shown in solid dark grey and control stained cells (2nd Ab and anti-CD3) in solid light grey. At least 3×10^4 cells were measured by flow cytometry (BD FACS Canto II, FACS Diva software) and analysed with FlowJo (Tree Star Inc). It was gated on living cells (DAPI negative) and on the lymphocyte population in the FSC/SSC gate. Histograms show the CD3 positive cell population, excepted for the direct label controls.

6.5. Reproducibility of the *in vitro* FcγR activation assay

The results obtained by BW:FcγR-ζ activation assay were independent of the following parameters: (1) cultivation duration of BW:FcγR-ζ reporter cells (Figure S8), (2) batch of produced mAbs (Figure S9), type of cell line for (3) stable hCD8 expression (Figure 2.36A and data not shown) or (4) MCMV hCD8 infection (MEF, CIM, BIM, data not shown).

6.5.1. Cultivation duration of BW:FcγR-ζ reporter cells

To demonstrate the reproducibility of the *in vitro* FcγR activation assay, the responsiveness of two different passages of the BW:FcγRIII-ζ cell aliquots to HeLa hCD8 target cells opsonized with the recombinant OKT8 mAbs were compared (Figure S8). The general activation level was tested by coating anti-FcγRIII mAbs to activate the reporter cells by FcγRIII cross-linking. The crosslinking demonstrated a similar level of activation (aka amount IL-2 secretion) dependent on the amount of coated anti-FcγRIII mAb. The hierarchy of the IgG subclasses leading to different levels of FcγRIII-ζ activation was indistinguishable between both aliquots.

SUMMARY

- The BW:FcγR-ζ reporter cells showed an unchanged hierarchy of IgG subclass dependent activation independent of the number of reporter cell passages.

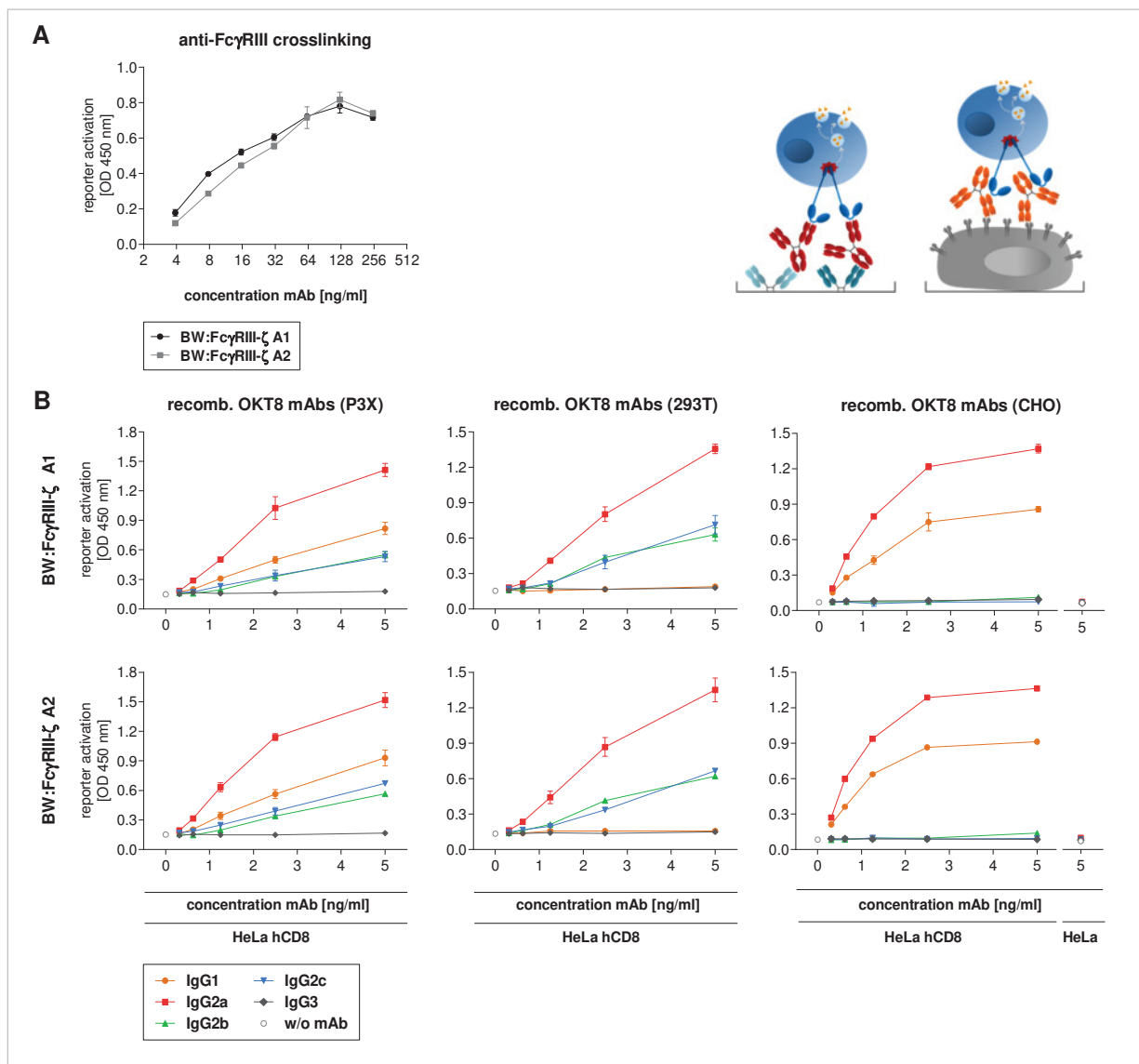


FIGURE S7. Reproducibility of the *in vitro* FcγRIII activation assay. (A) Crosslinking of FcγRIII on the reporter cells. BW:FcγRIII-ζ reporter cells were co-cultivated overnight on a plate exhibiting graded concentrations of rat anti-mouse FcγRIII bound to coated anti-rat F(ab)2 fragment (4 μg/ml). (B) The hierarchy of the IgG subclasses leading to different levels of FcγRIII activation is indistinguishable among two aliquots of BW:FcγRIII-ζ. HeLa hCD8 cells were opsonized with graded concentrations of recombinant OKT8 mAbs and co-cultivated with 2×10^5 BW:FcγRIII-ζ cells overnight. (A+B) The secreted amount of IL-2, which is the surrogate marker for FcγR activation, was quantified by sandwich ELISA. Co-cultures were performed in triplicates and the mean with SD is shown (GraphPad Prism).

6.5.2. Batch of produced mAbs

The culturing conditions can influence the glycan composition of mAbs. Several studies analysed the glycan profile dependent on culturing duration, culturing conditions, and batches of collected mAb. Mostly, no significant alteration in the glycoforms dependent on transfection and transduction methods, culturing duration, batch-to-batch or up scaling were found (Nallet et al., 2012; Corset et al., 2012; Muller et al., 2007). Comparing different culturing conditions or methods, e.g. bioreactors, oxygen supply, nutrition, pH, might lead to differences in the proportion of the glycoforms, but in general, differences in the glycoforms are more determined by cell line than by the culturing conditions (Kumpel et al., 1994; Patel et al., 1994; van Berkel et al., 2009).

Here, all recombinant OKT8 mAb preparations were produced under the same conditions and thus no significant batch-to-batch variation was expected. To exclude an influence of the production process on the mAbs, two batches, which were produced successively, were compared for BW:Fc γ R- ζ activation on recombinant OKT8 mAb opsonized HeLa hCD8 target cells (Figure S9). No difference in the hierarchy of the IgG subclasses for BW:Fc γ R- ζ activation was observed. However, the magnitude of the signal was a little less with P3X batch I. To note, the initial batch I was produced in a very small scale whereas batch II was used for all *in vitro* BW:Fc γ R- ζ activation analysis. The upscaling of the mAb production had only minor effects on their performance in the *in vitro* Fc γ R activation assay. Nevertheless, to ensure comparability between mAb batches, standardized conditions and protocols for the mAb production are of importance.

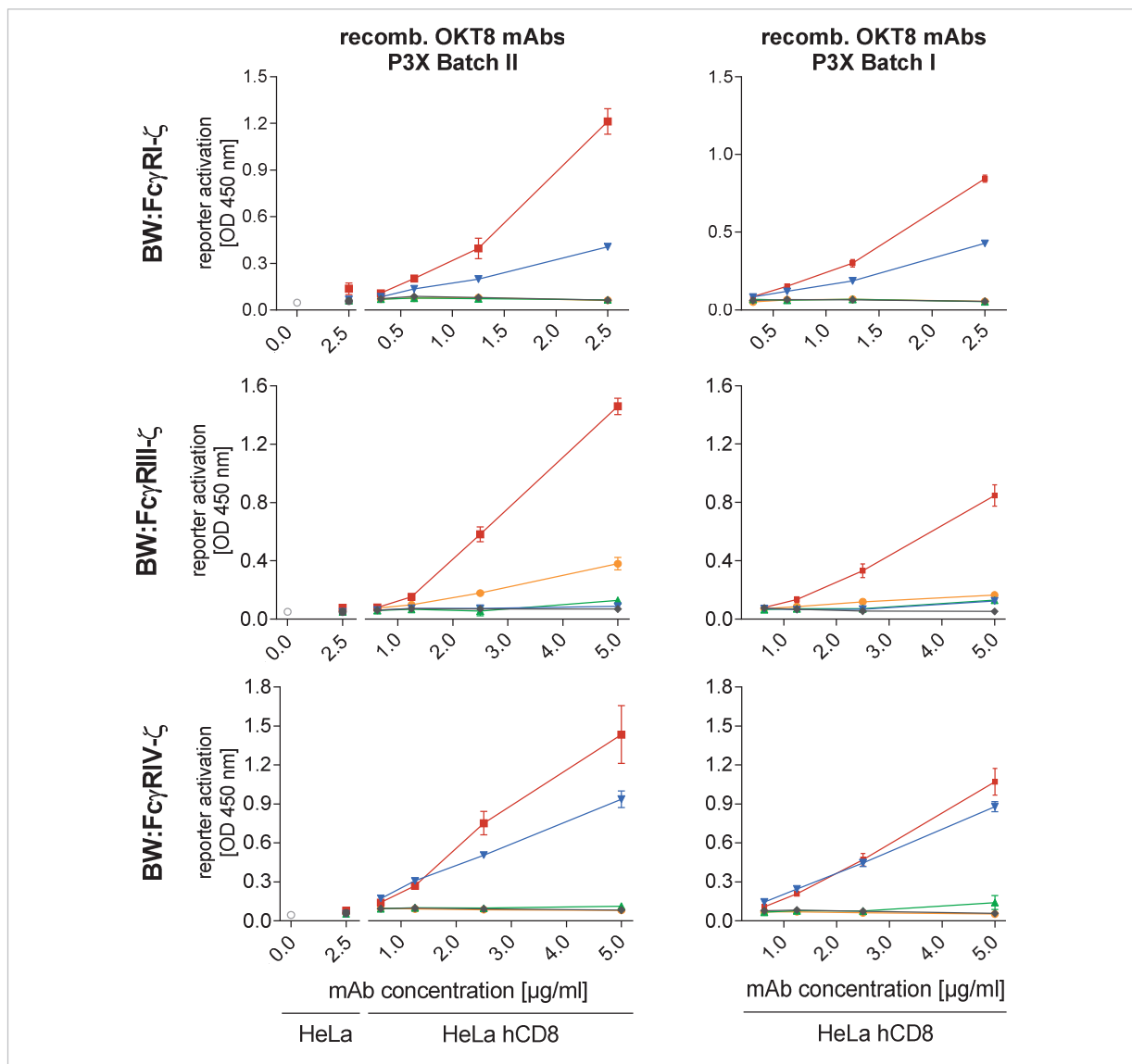


FIGURE S8. Hierarchy of distinct Fc γ R activation by individual IgG subclasses is independent on the IgG batch. HeLa hCD8 were opsonized with grades concentrations of recombinant OKT8 mAbs (P3X) from two different batches and co-cultivated with 2×10^5 reporter cells overnight. IL-2, the surrogate marker for Fc γ R activation, was quantified by sandwich ELISA. Triplicates were measured. The data were analysed with GraphPad Prism and means with SD are shown. One representative out of 2 - 3 experiments is shown.

SUMMARY

- No significant differences for the IgG subclass dependent activation of the BW:Fc γ R- ζ s was observed for two different batches of the recombinant OKT8 mAbs produced in P3X myeloma cells.

6.6. Hierarchy of FcγR activation by distinct subclasses is independent of the duration of infection

Since vFcγRs are expressed during the early and late phase of the CMV replication cycle, the time of infection might influence the amount of vFcγR and therefore the magnitude of their inhibitory effect. The hCD8 antigen is expressed under the HCMV major IE promoter (MIEP) leading to a high and mostly early expression of this ectopic antigen as seen on the surface staining of infected fibroblasts (Figure 2.13.). Figure S10 shows the BW:FcγRII–ζ activation by OKT8 mAbs (HEK293T) opsonized HeLa hCD8 and MCMV hCD8 infected MEF at 1, 2, or 3 dpi. The BW:FcγRII–ζ was chosen as example because it is efficiently activated by most IgG subclasses so that an alteration of the IgG subclass hierarchy for the activation would be easily detectable. The hierarchy of the IgG subclasses for the FcγRII–ζ activation was not changed dependent on the duration of infection. At 1 dpi, the activation was very low presumably caused by insufficient amounts of hCD8 expressed on the cell surface. The magnitude of BW:FcγRII–ζ activation on MCMV infected cells in comparison to HeLa hCD8 cells varied between experiments. For example, the BW:FcγR–ζ activation was reduced at 3 dpi in comparison to 2 dpi for two out of three experiments (data not shown). Even if the amount of hCD8 antigen and vFcγR expression varies during infection, the duration of MCMV infection did not influence the hierarchy of the IgG subclass dependent BW:FcγR–ζ activation for an ectopically expressed antigen by MCMV.

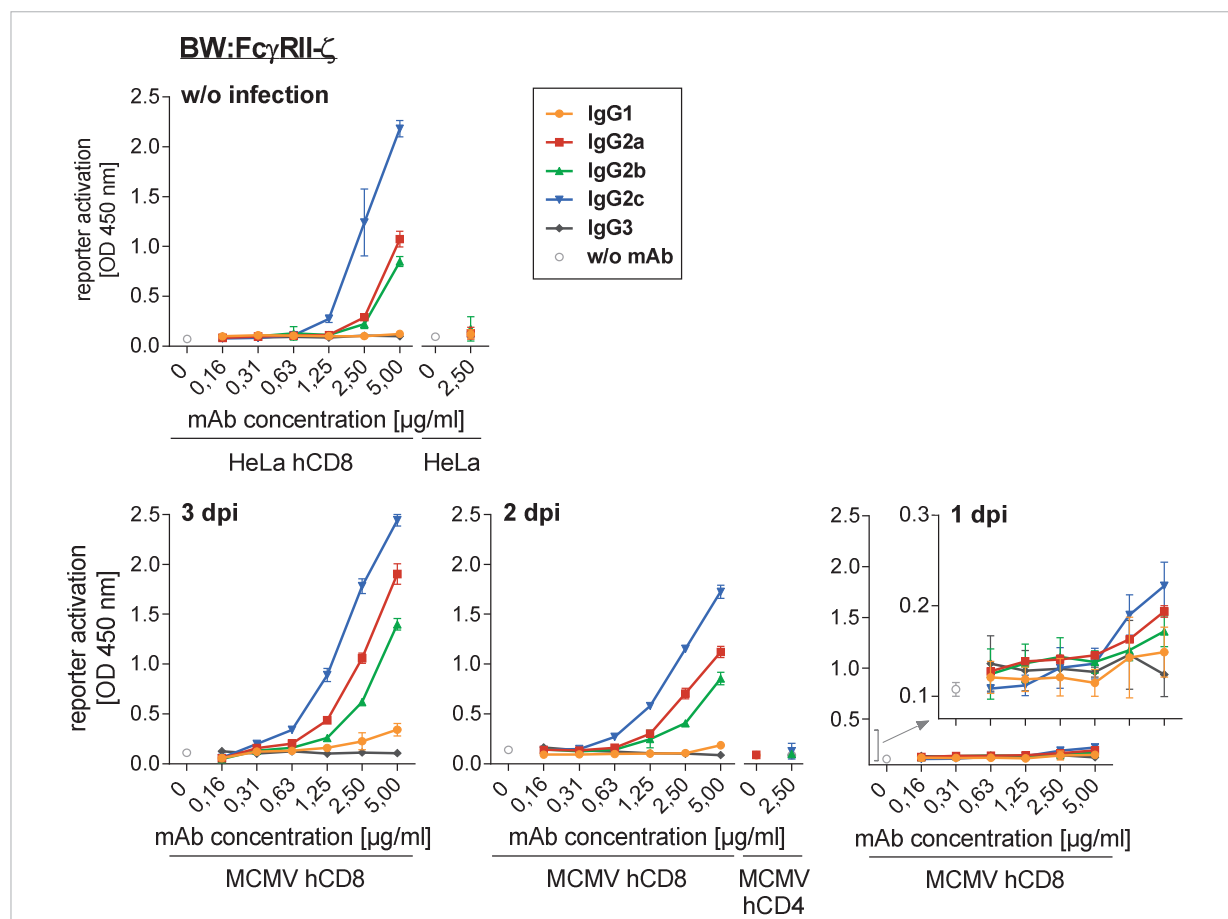
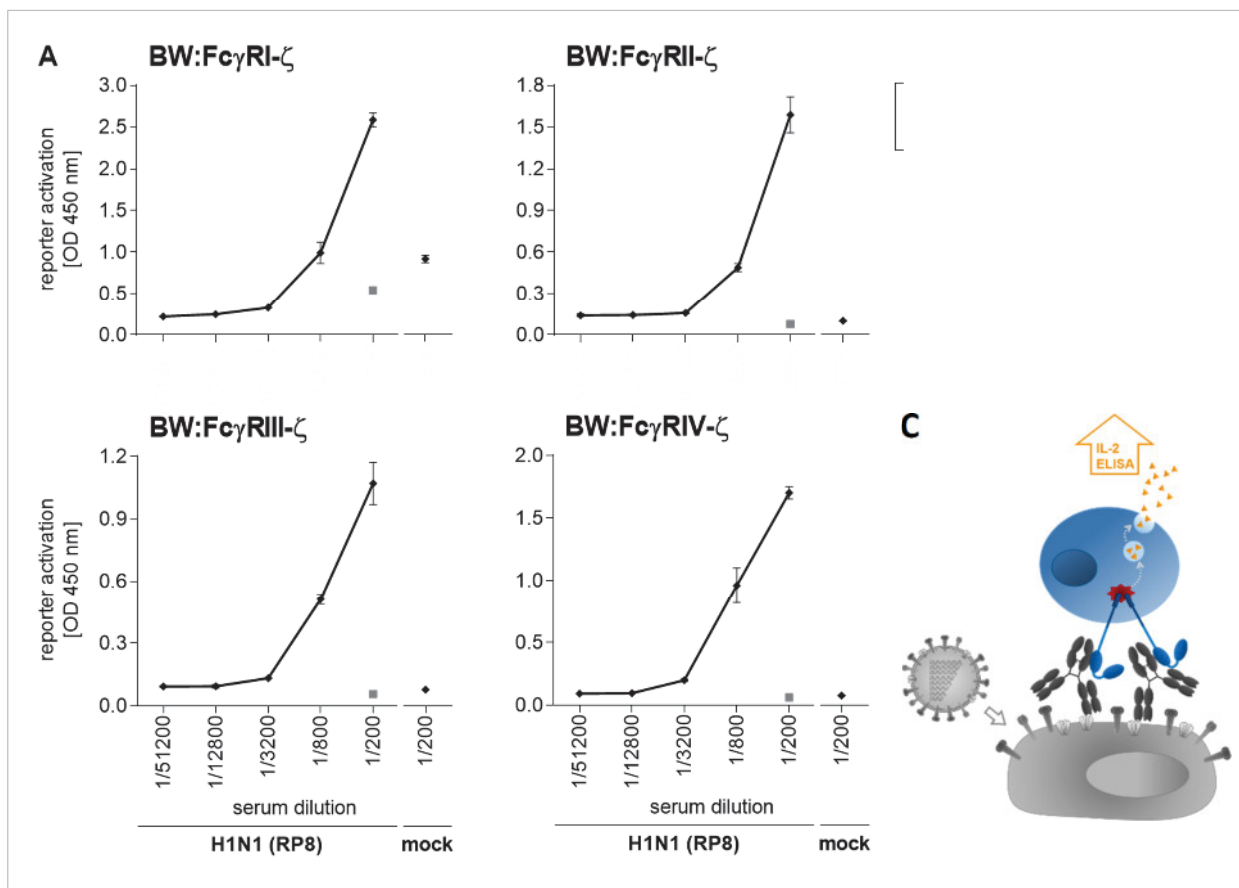


FIGURE S9. Influence of time of MCMV infection for selective IgG subclass dependent FcγRII activation pattern *in vitro*. Target cells were opsonized with grades concentrations of recombinant OKT8 mAbs produced in HEK293T cells (human) and co-cultivated 2×10^5 reporter cells overnight. Target cells were HeLa hCD8 or MCMV hCD8 infected MEF (MOI 1,5; 1, 2 or 3 dpi) and HeLa or MCMV hCD4 infected MEF served as controls. IL-2, the surrogate marker for FcγR activation, was quantified by sandwich ELISA. Colorimetric reaction was stopped after 70s for HeLa hCD8 and 90s for MCMV hCD8 infected target cells. Triplicates were measured for samples and duplicates for controls. The data were analysed with GraphPad Prism and means with SD are shown. One representative out of three experiments is shown.

6.7. Differential *in vitro* FcγR activation by mAbs targeting the ectodomain of M2 of Influenza A viruses

The M2 ion channel of influenza A viruses is very conserved between subtypes and therefore it is a promising candidate for a universal influenza vaccine (Gerhard et al., 2006). M2 is a small protein of 97 AA and its homotrimer is forming a proton-selective ion channel, which is present on the surface of infected cells and on the virion. The two most prominent functions are on the one hand its ion channel activity which causes the acidification and consequently the uncoating of the endocytosed virions and on the other hand the involvement of its cytoplasmic tail in virion assembly and budding. Antibodies targeting the N-terminal ectodomain of M2 (M2e), which only consists of 24 amino acids, are *in vitro* non-neutralizing but protective against lethal infection in the mouse model (Bakkouri et al., 2011). Their protection relies on the engagement of FcγRs. To define the contribution of distinct FcγRs for the protection of M2 antibodies dependent on their IgG subclass, Silvie van den Hoecke and Xavier Saelens (Medical Biotechnology Center (VIB) and Department of Biomedical Molecular Biology, Ghent University, Ghent, Belgium) generated mAbs against the tetrameric form of M2e. BALB/c mice were immunized and the isolated splenocytes were fused with SP2/0-Ag14 myeloma cells to generate hybridoma cell lines. The resulting mAb37 (IgG1) and mAb65 (IgG2a) bind in all likelihood the same epitope with comparable affinities (K_D) as shown by binding to M2e alanine scan mutants and SPR measurements. These preconditions allowed assessing and comparing the *in vitro* FcγR activation capacity of these non-neutralizing anti-M2e mAbs (4.7.5.) with their protectively *in vivo*. All FcγR-ζs were activated by influenza infected target cells opsonized with H1N1 immune serum in a dose-dependent manner (Figure S10A).



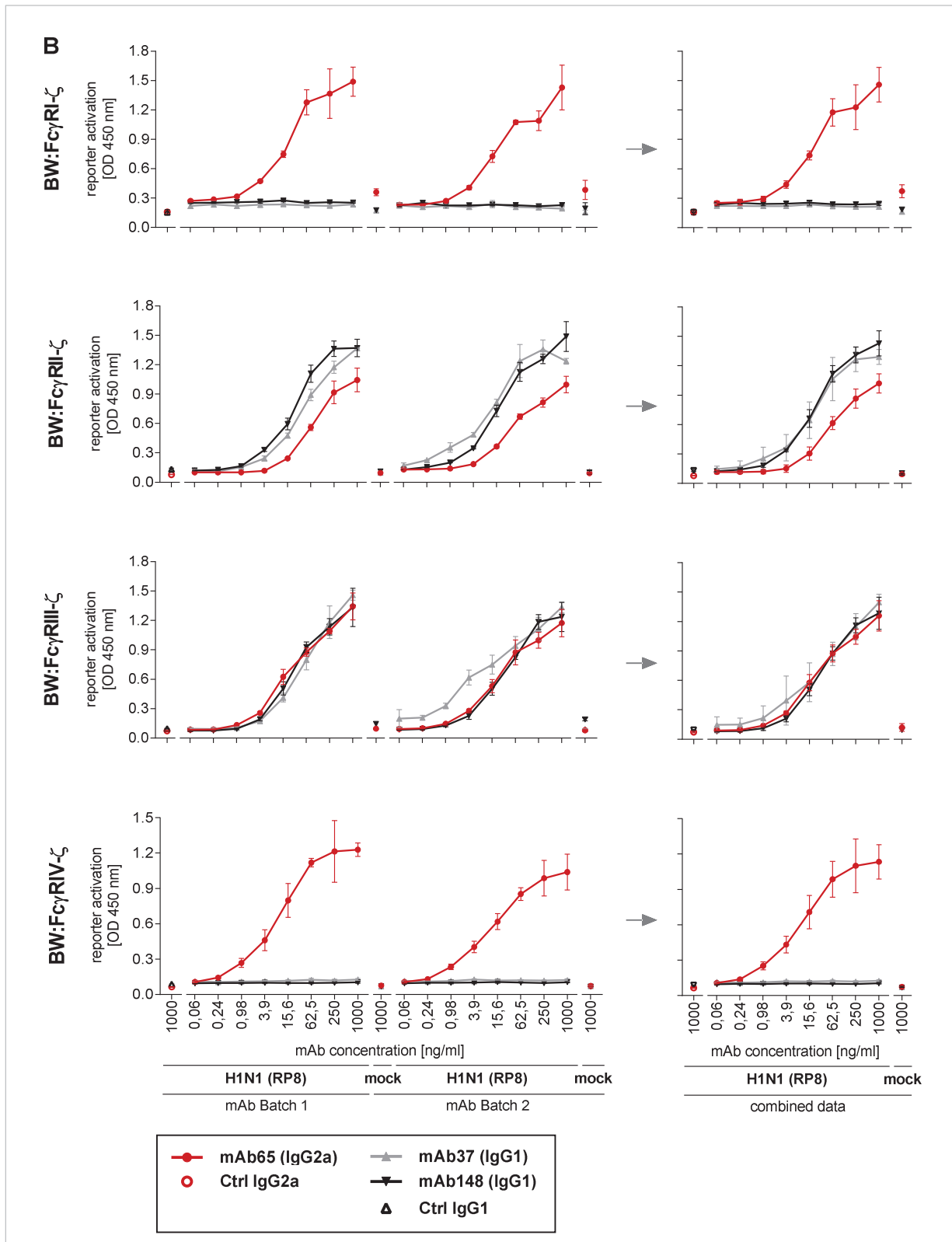


FIGURE S10. *In vitro* Fc γ R activation by polyclonal immune serum and anti-M2 mAbs. MDCK cells were infected with MOI 5 of H1N1 (PR8) for one hour, unbound virus was removed by washing, and cells were co-cultured over night with the BW:Fc γ R- ζ reporter cells and graded concentrations of immune serum derived from C57BL/6 16 dpi post infection with PR8 (A) or anti-M2 mAbs (B). As controls, mock infected cells, naïve serum, and the corresponding isotype controls (IgG2a anti-NBe; IgG2 anti-SHe) were included. Produced IL-2, a surrogate marker for Fc γ R activation, was quantified by sandwich ELISA. Data points were determined in triplicates. A representative result out of three experiments and mean values with standard deviation are shown (GraphPad Prism). C. Model of the *in vitro* Fc γ R activation assay on Influenza infected cells.

BW:FcγR-ζ	comparison			mAb concentration [ng/ml]							
	subclasses	name of mAbs		0,06	0,24	0,98	3,9	15,6	62,5	250	1000
FcγRI-ζ	IgG2a vs. IgG1	mAb65	mAb148	ns	ns	ns	***	***	***	***	***
	IgG2a vs. IgG1	mAb65	mAb37	ns	ns	ns	***	***	***	***	***
	IgG1 vs. IgG1	mAb148	mAb37	ns	ns	ns	ns	ns	ns	ns	ns
FcγRII-ζ	IgG2a vs. IgG1	mAb65	mAb148	ns	ns	ns	**	***	***	***	***
	IgG2a vs. IgG1	mAb65	mAb37	ns	ns	*	***	***	***	***	***
	IgG1 vs. IgG1	mAb148	mAb37	ns	ns	ns	ns	ns	ns	ns	*
FcγRIII-ζ	IgG2a vs. IgG1	mAb65	mAb148	ns	ns	ns	ns	ns	ns	ns	ns
	IgG2a vs. IgG1	mAb65	mAb37	ns	ns	ns	ns	ns	ns	ns	ns
	IgG1 vs. IgG1	mAb148	mAb37	ns	ns	ns	**	ns	ns	ns	ns
FcγRIV-ζ	IgG2a vs. IgG1	mAb65	mAb148	ns	ns	***	***	***	***	***	***
	IgG2a vs. IgG1	mAb65	mAb37	ns	ns	**	***	***	***	***	***
	IgG1 vs. IgG1	mAb148	mAb37	ns	ns	ns	ns	ns	ns	ns	ns

TABLE S1. *In vitro* FcγR activation by polyclonal immune serum and anti-M2 mAbs – statistical analysis. Two-way ANOVA with Tukey's multiple comparisons test was applied for the statistical analysis of the combined data of mAb batch 1 and 2 (Prism 6, GraphPad).

Next, the engagement of individual FcγRs by graded dilutions of the anti-M2e mAbs was analysed (Figure S10B). As expected, mAb65 (IgG2a) was able to activate all FcγR-ζs. In contrast, both IgG1 mAbs, mAb37 and mAb148, only triggered FcγRIII and FcγRII but failed to activate FcγRI and FcγRIV at any tested concentration (0,06 - 1 ng/ml). Moreover, both IgG1 mAbs exhibit similar activation capacities, which are comparable with mAb65 for FcγRIII and higher for the inhibitory FcγRII. The corresponding isotype controls failed to trigger the FcγR-ζ reporter cells as well as the anti-M2e mAbs in absence of the antigen, e.g. on mock infected cells. Furthermore, two independently produced batches of the anti-M2e mAbs were compared revealing equivalent *in vitro* FcγR activation capacities. The absence of IgG aggregates was confirmed by analytic size exclusion chromatography for selected mAbs preparations (Superdex 200 10/300 GL; data not shown). Taken together, mAb65 and mAb37 exhibited similar F(ab)₂-mediated but clearly different and distinct Fc-mediated functions *in vitro*.

Comparing these results with the ones obtained with the recombinant OKT8 mAbs, the type of FcγR which can be triggered by IgG2a (all FcγRs) or IgG1 (only FcγRII and FcγRIII) is in accordance. The subclass dependent pattern of FcγR activation (IgG1 in relation to IgG2a) differs strongly from the P3X derived recombinant OKT8 mAbs but is similar to the OKT8 mAbs produced CHO cells. There are two possible explanations: the Asn297 mediated Fc glycosylation pattern of the antibodies and / or an influence of the epitope of the antibodies (affinity, accessibility / avidity). The hybridoma of the M2 specific mAbs were generated with the murine myeloma cell line Sp2/0 and it was observed that the FcγR activation capabilities of recombinant OKT8 IgG1 was dependent on the cell line by which the isotype was produced (see 2.7. and 3.2.5.).

The *in vivo* protection of the passively transferred anti-M2e mAbs (mAb37 and mAb65) was determined by weight loss and survival after a potentially lethal influenza virus challenge in different FcγR deficient mouse strains (BALB/c background; data not shown; Silvie van den Hoecke and Xavier Saelens, manuscript submitted). Remarkably, the differential protective efficacies of anti-M2e mAbs *in vivo* are reflecting their *in vitro* FcγR activation capacities and are briefly summarized: The non-neutralizing M2e mAbs depend on FcγRs since both mAbs fail to protect mice lacking all activating FcγRs (FcRγ-KO). mAb37 (IgG1) protected wild type and FcγRIV-KO similarly showing that IgG1 does not engage FcγRIV. However, it is unable to protect FcγRIII-KO, confirming its sole dependency on FcγRIII for its mode of action. Protection by mAb65 (IgG2a) is superior to mAb37 (IgG1) in wild type mice probably due to its broader FcγR activation capacities. The protection of mAb65 is comparable

for wild type and FcγRIII-KO mice, whereas it is compromised in FcγRI x FcγRIII double KO. FcγRIV-KO mice are less protected by mAb65 than wild type mice, verifying the contribution of FcγRIV. Consequently, FcγRIII and therefore ADCC mediated by NK cells seem to be dispensable, while FcγRI and FcγRIV are contributing to the mode of action of the IgG2a mAb.

SUMMARY

- All BW:FcγR-ζ cell lines were activated by influenzainfected targets opsonized with immune serum.
- As expected, M2e specific mAb65 (IgG2a) was able to activate all FcγR-ζs.
- Both M2e specific IgG1 mAbs, mAb37 and mAb148, triggered only FcγRIII and FcγRII.
- Protection from lethal influenza challenge by non-neutralizing anti-M2e antibodies mAb65 (IgG2a) depends on activating FcγRs.
- Protection of the IgG2a subclass was superior to IgG1 probably because IgG2a can trigger all FcγRs in contrast to IgG1 relying solely on FcγRIII.
- FcγRI and FcγRIV contribute to the protection by mAb65 (IgG2a).

6.8. Overview of generated plasmid, BACmids, and cell lines

6.8.1. Generated plasmids and BACmids

plasmid	parental plasmid	insert	cloning method
pCRII-mk-OKT8VL	pCRII	OKT8 LC (kappa)	PCR: pFUSE-CLIg-OKT8-mk with 5-XhoI-8VL / 3-BglII-8VL
pCRII-TOPO-hCD8	pCRII-TOPO	human CD8	PCR: pCMV6-XL5-hCD8 with 5-EcoRI-hCD8, 3-BglII-hCD8
pCRII-TOPO-IgG2c-HC		IgG2c HC	PCR: cDNA of C57BL/6 splenocytes 14 dpi with MCMV Δm157-Luc with 5-IgG2c / 3-IgG2c
pCRII-TOPO-OKT8VH		OKT8 V _H	5' RACE with cDNA from the OKT8 hybridoma cell line
pCRII-TOPO-OKT8VL		OKT8 V _L	
pIRES-Luc	pIRES-eGFP	Luciferase gene from pTA-Luc-m157FLK	PCR: pTA-Luc-m157FLK with 5-MscI-Luc / 3-Luc-Not; DNA digestion with <i>MscI</i> , <i>NotI</i> and vector with <i>NotI</i> , <i>MscI</i> (partial)
phCD4-IRES-Luc	pIRES-Luc	human CD4	PCR: cDNA from Jurkat cells with 5-EcoRI-hCD4 / 3-BglII-hCD4; DNA digestion: <i>EcoRI</i> , <i>BamHI</i> ;
phCD8-IRES-Luc		human CD8	PCR: pCMV6-XL5-hCD8 with 5-EcoRI-hCD8 / 3-BglII-hCD8; DNA digestion: <i>EcoRI</i> , <i>BamHI</i> ;
pFRTZ-MIEP-hCD4-IRES-Luc-Zeocin	pFRTZ-MIEP-IRES-eGFP	"MIEP-hCD4-IRES-Luc" from phCD4-IRES-Luc	DNA digestion: <i>NotI</i> , <i>SnaBI</i>
pFRTZ-MIEP-hCD8-IRES-Luc-Zeocin		"MIEP-hCD8-IRES-Luc" from phCD4-IRES-Luc	
pFUSE-CHlg-m2c	pFUSE-CHlg-m2a	IgG2c-HC from pCRII-TOPO-IgG2c-HC	DNA digestion: plasmid with <i>NheI</i> , <i>MscI</i> (partial), insert with <i>NheI</i> , <i>MscI</i>
pFUSE-CHlg-m2c-Eco47III	pFUSE-CHlg-m2c	Generation of an Eco47III restriction recognition site at the 5' IgG2c HC	QuickChange with 5-IgG2cEco / 3-IgG2cEco; Reinsertion of the 5' IgG2c HC gene into the original vector with <i>NheI</i> , <i>NcoI</i>
pFUSE-CHlg-m1-OKT8HC	pFUSE-CHlg-m1	OKT8 V _H from pCRII-TOPO-OKT8VH	PCR: pCRII-TOPO-OKT8VH with 5-OKT8-HC / 3-OKT8-HC; DNA digestion plasmid with <i>EcoRI</i> , <i>Eco47III</i> , insert with <i>EcoRI</i> , <i>BstUI</i>
pFUSE-CHlg-m2a-OKT8HC	pFUSE-CHlg-m2a		
pFUSE-CHlg-m2b-OKT8HC	pFUSE-CHlg-m2b		
pFUSE-CHlg-m2c-OKT8HC	pFUSE-CHlg-m2c-Eco47III		
pFUSE-CHlg-m3-OKT8HC	pFUSE-CHlg-m3		

pFUSE-CLlg-mk-OKT8VL	pFUSE-CLlg-mk	OKT8 V _L	PCR: cDNA from OKT8 hybridoma with 5-OKT8-LC /3-OKT8-LC; DNA digestion with <i>AgeI</i> , <i>BstAPI</i>
puc2CL6PI-m1-OKT8	puc2CL6IPwo	OKT8 V _H +HC from pFUSE-CHlg-m1-OKT8VH	DNA digestion: vector with <i>BamHI</i> , blunt end generation with Phusion polymerase, <i>EcoRI</i> , insert with <i>EcoRI</i> , <i>MscI</i> (IgG1: <i>MscI</i> partial)
puc2CL6PI-m2a-OKT8		OKT8 V _H +HC from pFUSE-CHlg-m2a-OKT8VH	
puc2CL6PI-m2b-OKT8		OKT8 V _H +HC from pFUSE-CHlg-m2b-OKT8VH	
puc2CL6PI-m2c-OKT8		OKT8 V _H +HC from pFUSE-CHlg-m2c-OKT8VH	
puc2CL6PI-m3-OKT8		OKT8 V _H +HC from pFUSE-CHlg-m3-OKT8VH	
puc2CL6NI-mk-OKT8		OKT8 V _L +LC from pCRII-mk-OKT8VL	DNA digestion: vector with <i>BamHI</i> , <i>XhoI</i> , insert with <i>XhoI</i> , <i>BglII</i>
puc2CL6IP-hCD8	puc2CL6IP-mFcγRIII-ζ (C57BL/6)	pCRII-TOPO-hCD8	DNA digestion: <i>EcoRI</i>
puc2CL6IP-FcγRI-ζ		chimera of FcγR and CD3zeta	overlap extension PCR: 1. cDNA from murine splenocytes with 5-FcγR-SpeI, 3-FcγR-Zeta 2. pcDNA3.1-hFcγRIII-CD3zeta with 5-Zeta-FcγR, 3-Zeta-SpeI 3. 5-FcγR-Spe, 3-Zeta-SpeI; DNA digestion: vector with <i>NheI</i> , insert with <i>SpeI</i>
puc2CL6IP-FcγRII-ζ			
puc2CL6IP-FcγRIII-ζ (B6)			
puc2CL6IP-FcγRIV-ζ			
puc2CL6IP-FcγRIII-ζ (BALB)			overlap extension PCR: 1. 5-SpeI-BALB-FIII, 3-OverI-FIII 2. 5-OverI-FIII, 3-SpeI-FIII, 3. 5-SpeI-Balb-FIII, 3-Spe-FIII, <i>SpeI</i> , DNA digest: vector with <i>NheI</i> , insert with <i>SpeI</i>
BACmid	parental BACmid	insert	recombination method
MCMV C3X Δm157 MIEP hCD4 IRES Luc Zeo	MCMV C3X Δm157 FRT	pFRTZ-MIEP-hCD8-IRES-Luc-Zeocin	FRT/FLP recombination
MCMV C3X Δm157 MIEP hCD8 IRES Luc Zeo		pFRTZ-MIEP-hCD4-IRES-Luc-Zeocin	FRT/FLP recombination

HC : heavy chain, LC : light chain, V_H : variable region of the HC, V_L : variable region of the LC

6.8.1. Generated cell lines

generated cell line	parental cell line	transgene(s)	selection marker	method
P3X OKT8 IgG1	P3X63Ag 8.6533	OKT8 V _H IgG HC with the respective subclass, OKT8 V _L kappa light chain	Puromycin / Geneticin	Td
P3X OKT8 IgG2a				
P3X OKT8 IgG2b				
P3X OKT8 IgG2c				
P3X OKT8 IgG3				
HEK293T OKT8 IgG1	HEK293T	OKT8 V _H IgG HC with the respective subclass, OKT8 V _L kappa light chain	Zeocin / Blasticidin	Tf
HEK293T OKT8 IgG2a				
HEK293T OKT8 IgG2b				
HEK293T OKT8 IgG2c				
HEK293T OKT8 IgG3				
CHO OKT8 IgG1	CHO	OKT8 V _H IgG HC with the respective subclass, OKT8 V _L kappa light chain	Puromycin	Td
CHO OKT8 IgG2a				
CHO OKT8 IgG2b				
CHO OKT8 IgG2c				
CHO OKT8 IgG3				
HeLa hCD8	HeLa	hCD8	Puromycin	Td
BIM hCD8	BIM	hCD8	Puromycin	Td
CIM hCD8	CIM	hCD8	Puromycin	Td
NIH 3T3 hCD8	NIH 3T3	hCD8	Puromycin	Td
BW:FcγRI-ζ	BW:5147	chimera of the extracellular domain of respective mouse FcγR and the transmembrane and cytosolic domain of CD3-zeta	Puromycin	Td
BW:FcγRII-ζ	BW:5147			
BW:FcγRIII-ζ B6	BW:5147			
BW:FcγRIII-ζ BALB	BW:5147			
BW:FcγRIV-ζ	BW:5147			

REFERENCE LIST

- Abboud N, Chow SK, Saylor C, Janda A, Ravetch JV, Scharff MD, Casadevall A. A requirement for FcγR in antibody-mediated bacterial toxin neutralization. *J Exp Med*. 2010 Oct 25;207(11):2395-405.
- Ackerman ME, Crispin M, Yu X, Baruah K, Boesch AW, Harvey DJ, Dugast AS, Heizen EL, Ercan A, Choi I, Streeck H, Nigrovic PA, Bailey-Kellogg C, Scanlan C, Alter G. Natural variation in Fc glycosylation of HIV-specific antibodies impacts antiviral activity. *J Clin Invest*. 2013 May;123(5):2183-92.
- Aderem A, Underhill DM. Mechanisms of phagocytosis in macrophages. *Annu Rev Immunol*. 1999;17:593-623.
- Adler SP, Nigro G. Findings and conclusions from CMV hyperimmune globulin treatment trials. *J Clin Virol*. 2009 Dec;46 Suppl 4:S54-7.
- Adler SP. Molecular epidemiology of cytomegalovirus: a study of factors affecting transmission among children at three day-care centers. *Pediatr Infect Dis J*. 1991 Aug;10(8):584-90
- Albanesi M, Mancardi DA, Macdonald LE, Iannascoli B, Zitvogel L, Murphy AJ, Daëron M, Leusen JH, Bruhns P. Cutting edge: FcγRIII (CD16) and FcγRI (CD64) are responsible for anti-glycoprotein 75 monoclonal antibody TA99 therapy for experimental metastatic B16 melanoma. *J Immunol*. 2012 Dec 15;189(12):5513-7.
- Albert H, Collin M, Dudziak D, Ravetch JV, Nimmerjahn F. In vivo enzymatic modulation of IgG glycosylation inhibits autoimmune disease in an IgG subclass-dependent manner. *Proc Natl Acad Sci U S A*. 2008 Sep 30;105(39):15005-9.
- Alexandre YO, Cocita CD, Ghilas S, Dalod M. Deciphering the role of DC subsets in MCMV infection to better understand immune protection against viral infections. *Front Microbiol*. 2014 Jul 29;5:378
- Amigorena S, Bonnerot C. Role of B-cell and Fc receptors in the selection of T-cell epitopes. *Curr Opin Immunol*. 1998 Feb;10(1):88-92.
- Anderson CL, Ganesan LP, Robinson JM. The biology of the classical Fcγ receptors in non-hematopoietic cells. *Immunol Rev*. 2015 Nov;268(1):236-40.
- Andrén M, Johanneson B, Alarcón-Riquelme ME, Kleinau S. IgG Fc receptor polymorphisms and association with autoimmune disease. *Eur J Immunol*. 2005 Oct;35(10):3020-9.
- Androsiac GA. Characterization of IgG Effector Responses to Mouse Cytomegalovirus in Susceptible and Resistant Mouse Strains. Dissertation HHU Düsseldorf, Germany 2012.
- Arapović J, Lenac Rovis T, Reddy AB, Krmpotić A, Jonjić S. Promiscuity of MCMV immunoevasin of NKG2D: m138/fcr-1 down-modulates RAE-1ε in addition to MULT-1 and H60. *Mol Immunol*. 2009 Nov;47(1):114-22.
- Arase H, Mocarski ES, Campbell AE, Hill AB, Lanier LL. Direct recognition of cytomegalovirus by activating and inhibitory NK cell receptors. *Science*. 2002 May 17;296(5571):1323-6.
- Araullo-Cruz TP, Ho M, Armstrong JA. Protective effect of early serum from mice after cytomegalovirus infection. *Infect Immun*. 1978 Sep;21(3):840-2.
- Arduin E, Arora S, Bamert PR, Kuiper T, Popp S, Geisse S, Grau R, Calzascia T, Zenke G, Kovarik J. Highly reduced binding to high and low affinity mouse Fc gamma receptors by L234A/L235A and N297A Fc mutations engineered into mouse IgG2a. *Mol Immunol*. 2015 Feb;63(2):456-63.
- Arens R, Wang P, Sidney J, Loewendorf A, Sette A, Schoenberger SP, Peters B, Benedict CA. Cutting edge: murine cytomegalovirus induces a polyfunctional CD4 T cell response. *J Immunol*. 2008 May 15;180(10):6472-6.
- Armour KL, Atherton A, Williamson LM, Clark MR. The contrasting IgG-binding interactions of human and herpes simplex virus Fc receptors. *Biochem Soc Trans*. 2002 Aug;30(4):495-500.
- Arnold JN, Wormald MR, Sim RB, Rudd PM, Dwek RA. The impact of glycosylation on the biological function and structure of human immunoglobulins. *Annu Rev Immunol*. 2007;25:21-50.
- Arnold JN, Wormald MR, Sim RB, Rudd PM, and Raymond A. Dwek RA. The Impact of Glycosylation on the Biological Function and Structure of Human Immunoglobulins. *Annu. Rev. Immunol*. 2007.25:21-50
- Atalay R, Zimmermann A, Wagner M, Borst E, Benz C, Messerle M, Hengel H. Identification and expression of human cytomegalovirus transcription units coding for two distinct Fc gamma receptor homologs. *J Virol*. 2002 Sep;76(17):8596-608.
- Avery RK. Special considerations regarding CMV in lung transplantation. *Transpl Infect Dis*. 1999;1 Suppl 1:13-8.
- Axford JS. Glycosylation and rheumatic disease. *Biochim Biophys Acta*. 1999 Oct 8;1455(2-3):219-29.
- Baker K, Qiao SW, Kuo TT, Aveson VG, Platzer B, Andersen JT, Sandlie I, Chen Z, de Haar C, Lencer WI, Fiebiger E, Blumberg RS. Neonatal Fc receptor for IgG (FcRn) regulates cross-presentation of IgG immune complexes by CD8-CD11b+ dendritic cells. *Proc Natl Acad Sci U S A*. 2011 Jun 14;108(24):9927-32

- Baker K, Rath T, Pyzik M, Blumberg RS. The Role of FcRn in Antigen Presentation. *Front Immunol*. 2014; 5: 408.
- Barahona Afonso AF, João CM. The Production Processes and Biological Effects of Intravenous Immunoglobulin. *Biomolecules*. 2016 Mar 9;6(1). pii:
- Barnes N, Gavin AL, Tan PS, Mottram P, Koentgen F, Hogarth PM. Fc gamma RI-deficient mice show multiple alterations to inflammatory and immune responses. *Immunity*. 2002 Mar;16(3):379-89.
- Bartholomaeus WN, O'Donoghue H, Foti D, Lawson CM, Shellam GR, Reed WD. Multiple autoantibodies following cytomegalovirus infection: virus distribution and specificity of autoantibodies. *Immunology*. 1988 Jul;64(3):397-405.
- Baudino L, Nimmerjahn F, Azeredo da Silveira S, Martinez-Soria E, Saito T, Carroll M, Ravetch JV, Verbeek JS, Izui S. Differential contribution of three activating IgG Fc receptors (Fc gamma RI, Fc gamma RIII, and Fc gamma RIV) to IgG2a- and IgG2b-induced autoimmune hemolytic anemia in mice. *J Immunol*. 2008 Feb 1;180(3):1948-53.
- Baudino L, Nimmerjahn F, Shinohara Y, Furukawa J, Petry F, Verbeek JS, Nishimura S, Ravetch JV, Izui S. Impact of a three amino acid deletion in the CH2 domain of murine IgG1 on Fc-associated effector functions. *J Immunol*. 2008 Sep 15;181(6):4107-12.
- Baudino L, Shinohara Y, Nimmerjahn F, Furukawa J, Nakata M, Martínez-Soria E, Petry F, Ravetch JV, Nishimura S, Izui S. Crucial role of aspartic acid at position 265 in the CH2 domain for murine IgG2a and IgG2b Fc-associated effector functions. *J Immunol*. 2008 Nov 1;181(9):6664-9.
- Becker M, Lemmermann NA, Ebert S, Baars P, Renzaho A, Podlech J, Stassen M, Reddehase MJ. Mast cells as rapid innate sensors of cytomegalovirus by TLR3/TRIF signaling-dependent and -independent mechanisms. *Cell Mol Immunol*. 2015 Mar;12(2):192-201.
- Becker S, Frankel MB, Schneewind O, Missiakas D. Release of protein A from the cell wall of *Staphylococcus aureus*. *Proc Natl Acad Sci U S A*. 2014 Jan 28;111(4):1574-9.
- Benedict CA, De Trez C, Schneider K, Ha S, Patterson G, Ware CF. Specific remodeling of splenic architecture by cytomegalovirus. *PLoS Pathog*. 2006 Mar;2(3):e16.
- Bernstein DI. Vaccines for cytomegalovirus. *Infect Disord Drug Targets*. 2011 Oct;11(5):514-25
- Biburger M, Aschermann S, Schwab I, Lux A, Albert H, Danzer H, Woigk M, Dudziak D, Nimmerjahn F. Monocyte subsets responsible for immunoglobulin G-dependent effector functions in vivo. *Immunity*. 2011 Dec 23;35(6):932-44.
- Bigl A. Untersuchungen zur Struktur und Funktion von Cytomegalovirus - kodierten Fcγ-Rezeptoren. Dissertation, Robert Koch-Institut, 2010
- Bloom JW, Madana MS, Marriott D, Wong T, Chan SY. Intrachain disulfide bond in the core hinge region of human IgG4. *Protein Sci*. 1997 Feb; 6(2): 407–415.
- Boeckh M, Bowden RA, Storer B, Chao NJ, Spielberger R, Tierney DK, Gallez-Hawkins G, Cunningham T, Blume KG, Levitt D, Zaia JA. Randomized, placebo-controlled, double-blind study of a cytomegalovirus-specific monoclonal antibody (MSL-109) for prevention of cytomegalovirus infection after allogeneic hematopoietic stem cell transplantation. *Biol Blood Marrow Transplant*. 2001;7(6):343-51.
- Boesch AW, Brown EP, Ackerman ME. The role of Fc receptors in HIV prevention and therapy. *Immunol Rev*. 2015 Nov;268(1):296-310.
- Böhm S, Kao D, Nimmerjahn F. Sweet and sour: the role of glycosylation for the anti-inflammatory activity of immunoglobulin G. *Curr Top Microbiol Immunol*. 2014;382:393-417.
- Bootz A. Die Rolle von Fcγ-Rezeptoren bei der humoralen Immunantwort gegen das Cytomegalovirus. Dissertation Friedrich-Alexander-University, Erlangen-Nuremberg, Germany 2014
- Boppana SB, Britt WJ. Antiviral antibody responses and intrauterine transmission after primary maternal cytomegalovirus infection. *J. Infect. Dis*. 1995. 171:1115-1121.
- Boppana SB, Fowler Kb in *Human Herpesviruses: Biology, Therapy, and Immunoprophylaxis*. Cambridge University Press; 2007.
- Boross P, Verbeek JS. The complex role of Fc gamma receptors in the pathology of arthritis. *Springer Semin Immunopathol*. 2006 Dec;28(4):339-50.
- Boshart M, Weber F, Jahn G, Dorsch-Häsler K, Fleckenstein B, Schaffner W. A very strong enhancer is located upstream of an immediate early gene of human cytomegalovirus. *Cell*. 1985 Jun;41(2):521-30
- Bournazos S, DiLillo DJ, Ravetch JV. The role of Fc-FcγR interactions in IgG-mediated microbial neutralization. *J Exp Med*. 2015 Aug 24;212(9):1361-9.
- Bournazos S, Klein F, Pietzsch J, Seaman MS, Nussenzweig MC, Ravetch JV. Broadly neutralizing anti-HIV-1 antibodies require Fc effector functions for in vivo activity. *Cell*. 2014 Sep 11;158(6):1243-53.

Brinkmann MM, Dağ F, Hengel H, Messerle M, Kalinke U, Čičin-Šain L. Cytomegalovirus immune evasion of myeloid lineage cells. *Med Microbiol Immunol*. 2015 Jun;204(3):367-82.

Bruhns P, Iannascoli B, England P, Mancardi DA, Fernandez N, Jorieux S, Daëron M. Specificity and affinity of human Fc gamma receptors and their polymorphic variants for human IgG subclasses. *Blood*. 2009 Apr 16;113(16):3716-25

Bruhns P, Jönsson F. Mouse and human FcR effector functions. *Immunol Rev*. 2015 Nov;268(1):25-51.

Bruhns P. Properties of mouse and human IgG receptors and their contribution to disease models. *Blood*. 2012 Jun 14;119(24): 5640-9.

Brune W, Ménard C, Heesemann J, Koszinowski UH. A ribonucleotide reductase homolog of cytomegalovirus and endothelial cell tropism. *Science*. 2001 Jan 12;291(5502):303-5.

Brune W, Messerle M, Koszinowski UH. Forward with BACs: new tools for herpesvirus genomics. *Trends Genet*. 2000 Jun;16(6):254-9.

Bubić I, Wagner M, Krmpotić A, Saulig T, Kim S, Yokoyama WM, Jonjić S, Koszinowski UH. Gain of virulence caused by loss of a gene in murine cytomegalovirus. *J Virol*. 2004 Jul;78(14):7536-44.

Budt M, Reinhard H, Bigl A, Hengel H. Herpesviral Fc gamma receptors: culprits attenuating antiviral IgG? *Int Immunopharmacol*. 2004 Sep;4(9):1135-48.

Burioni R, Williamson RA, Sanna PP, Bloom FE, Burton DR. Recombinant human Fab to glycoprotein D neutralizes infectivity and prevents cell-to-cell transmission of herpes simplex viruses 1 and 2 in vitro. *Proc Natl Acad Sci U S A*. 1994 Jan 4;91(1):355-9.

Burnet FM. A modification of Jerne's theory of antibody production using the concept of clonal selection. *CA Cancer J Clin*. 1976 Mar-Apr;26(2):119-21.

Burton DR, Saphire EO, Parren PW. A model for neutralization of viruses based on antibody coating of the virion surface. *Curr Top Microbiol Immunol*. 2001;260:109-43.

Caaveiro JM, Kiyoshi M, Tsumoto K. Structural analysis of Fc/FcγR complexes: a blueprint for antibody design. *Immunol Rev*. 2015 Nov;268(1):201-21.

Campbell AE, Cavanaugh VJ, Slater JS. The salivary glands as a privileged site of cytomegalovirus immune evasion and persistence. *Med Microbiol Immunol*. 2008 Jun;197(2):205-13.

Caron E, Hall A. Identification of two distinct mechanisms of phagocytosis controlled by different Rho GTPases. *Science*. 1998 Nov 27;282(5394):1717-21.

Carroll VA, Lundgren A, Wei H, Sainz S, Tung KS, Brown MG. Natural killer cells regulate murine cytomegalovirus-induced sialadenitis and salivary gland disease. *J Virol*. 2012 Feb;86(4):2132-42.

Cavanaugh VJ, Deng Y, Birkenbach MP, Slater JS, Campbell AE. Vigorous innate and virus-specific cytotoxic T-lymphocyte responses to murine cytomegalovirus in the submaxillary salivary gland. *J Virol*. 2003 Feb;77(3):1703-17.

Cekinović D, Golemac M, Pugel EP, Tomac J, Cicin-Sain L, Slavuljica I, Bradford R, Misch S, Winkler TH, Mach M, Britt WJ, Jonjić S. Passive immunization reduces murine cytomegalovirus-induced brain pathology in newborn mice. *J Virol*. 2008 Dec;82(24):12172-80.

Cheeran MC, Lokensgard JR, Schleiss MR. Neuropathogenesis of congenital cytomegalovirus infection: disease mechanisms and prospects for intervention. *Clin Microbiol Rev*. 2009 Jan;22(1):99-126

Cherepanov PP, Wackernagel W. Gene disruption in *Escherichia coli*: TcR and KmR cassettes with the option of Flp-catalyzed excision of the antibiotic-resistance determinant. *Gene*. 1995 May 26;158(1):9-14.

Chung S, Quarmby V, Gao X, Ying Y, Lin L, Reed C, Fong C, Lau W, Qiu ZJ, Shen A, Vanderlaan M, Song A. Quantitative evaluation of fucose reducing effects in a humanized antibody on Fcγ receptor binding and antibody-dependent cell-mediated cytotoxicity activities. *MAbs*. 2012 May-Jun;4(3):326-40.

Clémenceau B, Congy-Jolivet N, Gallot G, Vivien R, Gaschet J, Thibault G, Vié H. Antibody-dependent cellular cytotoxicity (ADCC) is mediated by genetically modified antigen-specific human T lymphocytes. *Blood*, 107 (2006), p. 4669

Clynes R, Ravetch JV. Cytotoxic antibodies trigger inflammation through Fc receptors. *Immunity*. 1995 Jul;3(1):21-6

Coffman RL, Savelkoul HF, Lebman DA. Cytokine regulation of immunoglobulin isotype switching and expression. *Semin Immunol*. 1989 Sep;1(1):55-63.

Collin M, Ehlers M. The carbohydrate switch between pathogenic and immunosuppressive antigen-specific antibodies. *Exp Dermatol*. 2013 Aug;22(8):511-4.

Collins TM, Quirk MR, Jordan MC. Biphasic viremia and viral gene expression in leukocytes during acute cytomegalovirus infection of mice. *J Virol*. 1994 Oct;68(10):6305-11.

Corbett AJ, Coudert JD, Forbes CA, Scalzo AA. Functional consequences of natural sequence variation of murine cytomegalovirus m157 for Ly49 receptor specificity and NK cell activation. *J Immunol*. 2011 Feb 1;186(3):1713-22.

Corrales-Aguilar E, Hoffmann K, Hengel H. CMV-encoded Fcγ receptors: modulators at the interface of innate and adaptive immunity. *Semin Immunopathol*. 2014 Nov;36(6):627-40.

Corrales-Aguilar E, Trilling M, Hunold K, Fiedler M, Le VT, Reinhard H, Ehrhardt K, Mercé-Maldonado E, Aliyev E, Zimmermann A, Johnson DC, Hengel H. Human cytomegalovirus Fcγ binding proteins gp34 and gp68 antagonize Fcγ receptors I, II and III. *PLoS Pathog*. 2014 May 15;10(5):e1004131.

Corrales-Aguilar E, Trilling M, Reinhard H, Mercé-Maldonado E, Widera M, Schaal H, Zimmermann A, Mandelboim O, Hengel H. A novel assay for detecting virus-specific antibodies triggering activation of Fcγ receptors. *J Immunol Methods*. 2013 Jan 31;387(1-2):21-35.

Corrales-Aguilar E. A Novel Method for Measuring IgG-Dependent Triggering of Host FcγRs CD16, CD32 and CD64 Reveals a Selective Inhibition through Herpesviral FcγRs. Dissertation, Humboldt-Universität zu Berlin, 2008.

Cortese M, Calò S, D'Aurizio R, Lilja A, Pacchiani N, Merola M. Recombinant human cytomegalovirus (HCMV) RL13 binds human immunoglobulin G Fc. *PLoS One*. 2012;7(11):e50166.

Cortez VS, Fuchs A, Cella M, Gilfillan S, Colonna M. Cutting edge: Salivary gland NK cells develop independently of Nfil3 in steady-state. *J Immunol*. 2014 May 15;192(10):4487-91.

Coutelier JP, van der Logt JT, Heessen FW, Vink A, van Snick J. Virally induced modulation of murine IgG antibody subclasses. *J Exp Med*. 1988 Dec 1;168(6):2373-8.

Coutelier JP, van der Logt JT, Heessen FW, Warnier G, Van Snick J. IgG2a restriction of murine antibodies elicited by viral infections. *J Exp Med*. 1987 Jan 1;165(1):64-9.

Couzi L, Pitard V, Sicard X, Garrigue I, Hawchar O, Merville P, Moreau JF, Déchanet-Merville J. Antibody-dependent anti-cytomegalovirus activity of human γδ T cells expressing CD16 (FcγRIIIa). *Blood*. 2012 Feb 9;119(6):1418-27.

Crnković-Mertens I, Messerle M, Milotić I, Szepan U, Kucić N, Krmpotić A, Jonjić S, Koszinowski UH. Virus attenuation after deletion of the cytomegalovirus Fc receptor gene is not due to antibody control. *J Virol*. 1998 Feb;72(2):1377-82.

Daëron M, Yodoi J, Néauport-Sautès C, Moncuit J, Fridman WH. Receptors for immunoglobulin isotypes (FcR) on murine T cells. I. Multiple FcR expression on T lymphocytes and hybridoma T cell clones. *Eur. J. Immunol.*, 15 (1985), p. 662

Daley-Bauer LP, Roback LJ, Wynn GM, Mocarski ES. Cytomegalovirus hijacks CX3CR1(hi) patrolling monocytes as immune-privileged vehicles for dissemination in mice. *Cell Host Microbe*. 2014 Mar 12;15(3):351-62.

Dalziel M, Crispin M, Scanlan CN, Zitzmann N, Dwek RA. Emerging principles for the therapeutic exploitation of glycosylation. *Science*. 2014 Jan 3;343(6166):1235681.

Dangl JF, Wensel TG, Morrison SL, Stryer L, Herzenberg LA, Oi VT. Segmental flexibility and complement fixation of genetically engineered chimeric human, rabbit and mouse antibodies. *Emboj* 1988; 7(7):1989-1994

Davis HE, Rosinski M, Morgan JR, Yarmush ML. Charged polymers modulate retrovirus transduction via membrane charge neutralization and virus aggregation. *Biophys J*. 2004 Feb;86(2):1234-42.

de Parseval A, Lerner DL, Borrow P, Willett BJ, Elder JH, Shariff DM, et al. Blocking of feline immunodeficiency virus infection by a monoclonal antibody to CD9 is via inhibition of virus release rather than interference with receptor binding. *J Virol* 1997;71:5742–9.

Dick TP, Bangia N, Peaper DR, Cresswell P. Disulfide bond isomerization and the assembly of MHC class I-peptide complexes. *Immunity*. 2002 Jan;16(1):87-98.

DiLillo DJ, Palese P, Wilson PC, Ravetch JV. Broadly neutralizing anti-influenza antibodies require Fc receptor engagement for in vivo protection. *J Clin Invest*. 2016 Feb 1;126(2):605-10.

DiLillo DJ, Ravetch JV. Differential Fc-Receptor Engagement Drives an Anti-tumor Vaccinal Effect. *Cell*. 2015 May 21;161(5):1035-45.

DiLillo DJ, Tan GS, Palese P, Ravetch JV. Broadly neutralizing hemagglutinin stalk-specific antibodies require FcγR interactions for protection against influenza virus in vivo. *Nat Med*. 2014 Feb;20(2):143-51.

Dimmock NJ. Neutralization of animal viruses. *Curr Top Microbiol Immunol*. 1993;183:1-149.

Dognin MJ, Lauwereys M, Strosberg AD. Multiple amino acid substitutions between murine gamma 2a heavy chain Fc regions of Ig1a and Ig1b allotypic forms. *Proc Natl Acad Sci U S A*. 1981 Jul;78(7):4031-5.

Dubin G, Socolof E, Frank I, Friedman HM. Herpes simplex virus type 1 Fc receptor protects infected cells from antibody-dependent cellular cytotoxicity. *J Virol*. 1991 Dec;65(12):7046-50.

Ebert S, Becker M, Lemmermann NA, Büttner JK, Michel A, Taube C, Podlech J, Böhm V, Freitag K, Thomas D, Holtappels R, Reddehase MJ, Stassen M. Mast cells expedite control of pulmonary murine cytomegalovirus infection by enhancing the recruitment of protective CD8 T cells to the lungs. *PLoS Pathog*. 2014 Apr 24;10(4):e1004100.

Ecker DM, Jones SD, Levine HL. The therapeutic monoclonal antibody market. *MAbs*. 2015 Jan-Feb; 7(1): 9–14. Chan CE, Lim El Bakkouri K, Descamps F, De Filette M, Smet A, Festjens E, Birkett A, Van Rooijen N, Verbeek S, Fiers W, Saelens X. Universal vaccine based on ectodomain of matrix protein 2 of influenza A: Fc receptors and alveolar macrophages mediate protection. *J Immunol*. 2011 Jan 15;186(2):1022-31.

Elgert KD. *Immunology: Understanding the Immune System*. John Wiley & Sons, Inc. 1998

Eryilmaz E, Janda A, Kim J, Cordero RJ, Cowburn D, Casadevall A. Global structures of IgG isotypes expressing identical variable regions. *Mol Immunol*. 2013 Dec;56(4):588-98.

Ey PL, Prowse SJ, Jenkin CR. Complement-fixing IgG1 constitutes a new subclass of mouse IgG. *Nature*. 1979 Oct 11;281(5731):492-3.

Farrell HE, Shellam GR. Protection against murine cytomegalovirus infection by passive transfer of neutralizing and non-neutralizing monoclonal antibodies. *J Gen Virol*. 1991 Jan;72 (Pt 1):149-56.

Ferrara C, Grau S, Jäger C, Sondermann P, Brünker P, Waldhauer I, Hennig M, Ruf A, Rufer AC, Stihle M, Umaña P, Benz J. Unique carbohydrate-carbohydrate interactions are required for high affinity binding between Fc gamma RIII and antibodies lacking core fucose. *Proc Natl Acad Sci U S A*. 2011 Aug 2;108(31):12669-74.

Finkelman FD, Holmes J, Katona IM, Urban JF Jr, Beckmann MP, Park LS, Schooley KA, Coffman RL, Mosmann TR, Paul WE. Lymphokine control of in vivo immunoglobulin isotype selection. *Annu Rev Immunol*. 1990;8:303-33.

Forthal D, Hope TJ, Alter G. New paradigms for functional HIV-specific nonneutralizing antibodies. *Curr Opin HIV AIDS*. 2013 Sep;8(5):393-401.

Forthal DN. Functions of Antibodies. *Microbiol Spectr*. 2014 Aug;2(4):AID-0019-2014.

Foss S, Watkinson R, Sandlie I, James LC, Andersen JT. TRIM21: a cytosolic Fc receptor with broad antibody isotype specificity. *Immunol Rev*. 2015 Nov;268(1):328-39.

Fossati-Jimack L, Ioan-Facsinay A, Reininger L, Chicheportiche Y, Watanabe N, Saito T, Hofhuis FM, Gessner JE, Schiller C, Schmidt RE, Honjo T, Verbeek JS, Izui S. Markedly different pathogenicity of four immunoglobulin G isotype-switch variants of an antierythrocyte autoantibody is based on their capacity to interact in vivo with the low-affinity Fc gamma receptor III. *J Exp Med*. 2000 Apr 17;191(8):1293-302.

Fowler KB, Stagno S, Pass RF, Britt WJ, Boll TJ, Alford CA. The outcome of congenital cytomegalovirus infection in relation to maternal antibody status. *N Engl J Med*. 1992 Mar 5;326(10):663-7.

Fowler KB, Stagno S, Pass RF. Maternal immunity and prevention of congenital cytomegalovirus infection. *JAMA*. 2003 Feb 26;289(8):1008-11.

Frank I, Friedman HM. A novel function of the herpes simplex virus type 1 Fc receptor: participation in bipolar bridging of antiviral immunoglobulin G. *J Virol*. 1989 Nov;63(11):4479-88.

Frenzel A, Hust M, Schirrmann T. Expression of recombinant antibodies. *Front Immunol*. 2013 Jul 29;4:217.

Gao GF, Jakobsen BK. Molecular interactions of coreceptor CD8 and MHC class I: the molecular basis for functional coordination with the T-cell receptor. *Immunol Today*. 2000 Dec;21(12):630-6.

Garred P, Michaelsen TE, Aase A. The IgG subclass pattern of complement activation depends on epitope density and antibody and complement concentration. *Scand J Immunol*. 1989 Sep;30(3):379-82.

Gavin AL, Barnes N, Dijstelbloem HM, Hogarth PM. Identification of the mouse IgG3 receptor: implications for antibody effector function at the interface between innate and adaptive immunity. *J Immunol*. 1998 Jan 1;160(1):20-3.

Gavin AL, Hamilton JA, Hogarth PM. Extracellular mutations of non-obese diabetic mouse Fc gamma RI modify surface expression and ligand binding. *J Biol Chem*. 1996 Jul 19;271(29):17091-9.

Gavin AL, Leiter EH, Hogarth PM. Mouse Fc gamma RI: identification and functional characterization of five new alleles. *Immunogenetics*. 2000 Mar;51(3):206-11.

Gavin AL, Tan PS, Hogarth PM. Gain-of-function mutations in Fc gamma RI of NOD mice: implications for the evolution of the Ig superfamily. *EMBO J*. 1998 Jul 15;17(14):3850-7.

Gerhard W, Mozdzanowska K, Zharikova D. Prospects for universal influenza virus vaccine. *Emerg Infect Dis*. 2006 Apr;12(4):569-74.

Gerna G, Baldanti F, Revello MG. Pathogenesis of human cytomegalovirus infection and cellular targets. *Hum Immunol*. 2004 May;65(5):381-6.

Gershoni JM, Palade GE. Protein blotting: principles and applications. *Anal Biochem*. 1983 May;131(1):1-15.

Getahun A, Cambier JC. Of ITIMs, ITAMs, and ITAMis: revisiting immunoglobulin Fc receptor signaling. *Immunol Rev.* 2015 Nov;268(1):66-73.

Goding JW. *Monoclonal Antibodies: principles and practice.* Academic Press; 3rd edition, 1996

Gómez-Román VR, Florese RH, Patterson LJ, Peng B, Venzon D, Aldrich K, Robert-Guroff M. A simplified method for the rapid fluorometric assessment of antibody-dependent cell-mediated cytotoxicity. *J. Immunol. Methods*, 308 (2006), p. 53

Gordan S, Biburger M, Nimmerjahn F. bIgG time for large eaters: monocytes and macrophages as effector and target cells of antibody-mediated immune activation and repression. *Immunol Rev.* 2015 Nov;268(1):52-65.

Gorman S, Harvey NL, Moro D, Lloyd ML, Voigt V, Smith LM, Lawson MA, Shellam GR. Mixed infection with multiple strains of murine cytomegalovirus occurs following simultaneous or sequential infection of immunocompetent mice. *J Gen Virol.* 2006 May;87(Pt 5):1123-32.

Gray CA, Lawrence RA. A role for antibody and Fc receptor in the clearance of *Brugia malayi* microfilariae. *Eur J Immunol.* 2002 Apr;32(4):1114-20.

Grundy JE, Lawson KM, MacCormac LP, Fletcher JM, Yong KL. Cytomegalovirus-infected endothelial cells recruit neutrophils by the secretion of C-X-C chemokines and transmit virus by direct neutrophil-endothelial cell contact and during neutrophil transendothelial migration. *J Infect Dis.* 1998 Jun;177(6):1465-74.

Guilliams M, Bruhns P, Saeys Y, Hammad H, Lambrecht BN. The function of Fcγ receptors in dendritic cells and macrophages. *Nat Rev Immunol.* 2014 Feb;14(2):94-108.

Hahn G, Jores R, Mocarski ES. Cytomegalovirus remains latent in a common precursor of dendritic and myeloid cells. *Proc Natl Acad Sci U S A.* 1998 Mar 31;95(7):3937-42.

Hamaguchi Y, Xiu Y, Komura K, Nimmerjahn F, Tedder TF. Antibody isotype-specific engagement of Fc gamma receptors regulates B lymphocyte depletion during CD20 immunotherapy. *J Exp Med.* 2006 Mar 20;203(3):743-53.

Hamano S, Yoshida H, Takimoto H, Sonoda K, Osada K, He X, Minamishima Y, Kimura G, Nomoto K. Role of macrophages in acute murine cytomegalovirus infection. *Microbiol Immunol.* 1998;42(9):607-16.

Hamilton RG. The human IgG subclasses. 2001 *Calbiochem, Novabiochem*

Hamprecht K, Vochem M, Baumeister A, Boniek M, Speer CP, Jahn G. Detection of cytomegaloviral DNA in human milk cells and cell free milk whey by nested PCR. *Virol Methods.* 1998 Feb;70(2):167-76.

Hangartner L, Zinkernagel RM, Hengartner H. Antiviral antibody responses: the two extremes of a wide spectrum. *Nat Rev Immunol.* 2006 Mar;6(3):231-43.

Hanson LK, Slater JS, Karabekian Z, Virgin HW 4th, Biron CA, Ruzek MC, van Rooijen N, Ciavarra RP, Stenberg RM, Campbell AE. Replication of murine cytomegalovirus in differentiated macrophages as a determinant of viral pathogenesis. *J Virol.* 1999 Jul;73(7):5970-80.

Hanson QM, Barb AW. A perspective on the structure and receptor binding properties of immunoglobulin G Fc. *Biochemistry.* 2015 May 19;54(19):2931-42.

Hazenbos W.L.W., Heijnen I.A.F.M., Meyer D., Hofhuis F.M.A., de Lavalette C.R., Schmidt R.E., Capel P.J.A., Van de Winkel J.G.J., Gessner J.E., van den Berg T.K. Murine IgG1 complexes trigger immune effector functions predominantly via FcγRIII (CD16) *J. Immunol.* 1998;161:3026–3032.

Hengel H, Brune W, Koszinowski UH. Immune evasion by cytomegalovirus-survival strategies of a highly adapted opportunist. *Trends Microbiol.* 1998 May;6(5):190-7.

Hengel H, Reusch U, Geginat G, Holtappels R, Ruppert T, Hellebrand E, Koszinowski UH. Macrophages escape inhibition of major histocompatibility complex class I-dependent antigen presentation by cytomegalovirus. *J Virol.* 2000 Sep;74(17):7861-8.

Henson D, Strano AJ. Mouse cytomegalovirus. Necrosis of infected and morphologically normal submaxillary gland acinar cells during termination of chronic infection. *Am J Pathol.* 1972 Jul;68(1):183-202.

Hessell AJ, Hangartner L, Hunter M, Havenith CE, Beurskens FJ, Bakker JM, Lanigan CM, Landucci G, Forthal DN, Parren PW, Marx PA, Burton DR. Fc receptor but not complement binding is important in antibody protection against HIV. *Nature.* 2007 Sep 6;449(7158):101-4.

Hirayama N, Hirano T, Köhler G, Kurata A, Okumura K, Ovary Z. Biological activities of antitrinitrophenyl and antidinitrophenyl mouse monoclonal antibodies. *Proc Natl Acad Sci U S A.* 1982 Jan;79(2):613-5.

Hodson EM, Jones CA, Strippoli GF, Webster AC, Craig JC. Immunoglobulins, vaccines or interferon for preventing cytomegalovirus disease in solid organ transplant recipients. *Cochrane Database Syst Rev.* 2007 Apr 18;(2):CD005129.

Hogarth PM, Pietersz GA. Fc receptor-targeted therapies for the treatment of inflammation, cancer and beyond. *Nat Rev Drug Discov.* 2012 Mar 30;11(4):311-31.

Honjo K, Kubagawa Y, Jones DM, Dizon B, Zhu Z, Ohno H, Izui S, Kearney JF, Kubagawa H. Altered Ig levels and antibody responses in mice deficient for the Fc receptor for IgM (FcμR). *Proc Natl Acad Sci U S A*. 2012 Sep 25;109(39):15882-7.

Hsu KM, Pratt JR, Akers WJ, Achilefu SI, Yokoyama WM. Murine cytomegalovirus displays selective infection of cells within hours after systemic administration. *J Gen Virol*. 2009 Jan;90(Pt 1):33-43.

Huber VC, Lynch JM, Bucher DJ, Le J, Metzger DW. Fc receptor-mediated phagocytosis makes a significant contribution to clearance of influenza virus infections. *J Immunol*. 2001 Jun 15;166(12):7381-8.

Hudson, J. B. 1979. The murine cytomegalovirus as a model for the study of viral pathogenesis and persistent infections. *Arch. Virol*. 62:1-29.

Hutt-Fletcher LM, Balachandran N, Elkins MH. B cell activation by cytomegalovirus. *J Exp Med*. 1983 Dec 1;158(6):2171-6.

Igietseme JU, Eko FO, He Q, Black CM. Antibody regulation of T cell immunity: implications for vaccine strategies against intracellular pathogens. *Expert Rev Vaccines*. 2004 Feb;3(1):23-34.

Ioan-Facsinay A, de Kimpe SJ, Hellwig SM, van Lent PL, Hofhuis FM, van Ojik HH, Sedlik C, da Silveira SA, Gerber J, de Jong YF, Roozendaal R, Aarden LA, van den Berg WB, Saito T, Mosser D, Amigorena S, Izui S, van Ommen GJ, van Vugt M, van de Winkel JG, Verbeek JS. Fc gamma RI (CD64) contributes substantially to severity of arthritis, hypersensitivity responses, and protection from bacterial infection. *Immunity*. 2002 Mar;16(3):391-402.

Irani V, Guy AJ, Andrew D, Beeson JG, Ramsland PA, Richards JS. Molecular properties of human IgG subclasses and their implications for designing therapeutic monoclonal antibodies against infectious diseases. *Mol Immunol*. 2015 Oct;67(2 Pt A):171-82.

Ito K, Furukawa J, Yamada K, Tran NL, Shinohara Y, Izui S. Lack of galactosylation enhances the pathogenic activity of IgG1 but Not IgG2a anti-erythrocyte autoantibodies. *J Immunol*. 2014 Jan 15;192(2):581-8.

Jackson SE, Mason GM, Wills MR. Human cytomegalovirus immunity and immune evasion. *Virus Res*. 2011 May;157(2):151-60.

Jakus Z, Németh T, Verbeek JS, Mócsai A. Critical but overlapping role of Fc gamma RIII and Fc gamma RIV in activation of murine neutrophils by immobilized immune complexes. *J Immunol*. 2008 Jan 1;180(1):618-29.

Janda A, Bowen A, Greenspan NS, Casadevall A. Ig Constant Region Effects on Variable Region Structure and Function. *Front Microbiol*. 2016 Feb 4;7:22.

Janda A, Casadevall A. Circular Dichroism reveals evidence of coupling between immunoglobulin constant and variable region secondary structure. *Mol Immunol*. 2010 Apr;47(7-8):1421-5.

Janda A, Eryilmaz E, Nakouzi A, Cowburn D, Casadevall A. Variable region identical immunoglobulins differing in isotype express different paratopes. *J Biol Chem*. 2012 Oct 12;287(42):35409-17.

Jassal R, Jenkins N, Charlwood J, Camilleri P, Jefferis R, Lund J. Sialylation of human IgG-Fc carbohydrate by transfected rat alpha2,6-sialyltransferase. *Biochem Biophys Res Commun*. 2001 Aug 17;286(2):243-9.

Jean Beltran PM, Cristea IM. The life cycle and pathogenesis of human cytomegalovirus infection: lessons from proteomics. *Expert Rev Proteomics*. 2014 Dec;11(6):697-711

Jefferis R. Antibody therapeutics: isotype and glycoform selection. *Expert Opin Biol Ther*. 2007 Sep;7(9):1401-13.

Jeitziner SM, Walton SM, Torti N, Oxenius A. Adoptive transfer of cytomegalovirus-specific effector CD4+ T cells provides antiviral protection from murine CMV infection. *Eur J Immunol*. 2013 Nov;43(11):2886-95.

Ji H, Ohmura K, Mahmood U, Lee DM, Hofhuis FM, Boackle SA, Takahashi K, Holers VM, Walport M, Gerard C, Ezekowitz A, Carroll MC, Brenner M, Weissleder R, Verbeek JS, Duchatelle V, Degott C, Benoist C, Mathis D. Arthritis critically dependent on innate immune system players. *Immunity*. 2002 Feb;16(2):157-68.

Jonjić S, Mutter W, Weiland F, Reddehase MJ, Koszinowski UH. Site-restricted persistent cytomegalovirus infection after selective long-term depletion of CD4+ T lymphocytes. *J Exp Med*. 1989 Apr 1;169(4):1199-212.

Jonjić S, Pavić I, Lucin P, Rukavina D, Koszinowski UH. Efficacious control of cytomegalovirus infection after long-term depletion of CD8+ T lymphocytes. *J Virol*. 1990 Nov;64(11):5457-64.

Jonjić, S., I. Pavić, B. Polić, I. Crnković, P. Lucin, U. H. Koszinowski. 1994. Antibodies are not essential for the resolution of primary cytomegalovirus infection but limit dissemination of recurrent virus. *J. Exp. Med*. 179: 1713-1717.

Jönsson F, Mancardi DA, Kita Y, Karasuyama H, Iannascoli B, Van Rooijen N, Shimizu T, Daëron M, Bruhns P. Mouse and human neutrophils induce anaphylaxis. *J Clin Invest*. 2011 Apr;121(4):1484-96.

Jordan S, Krause J, Prager A, Mitrovic M, Jonjić S, Koszinowski UH, Adler B. Virus progeny of murine cytomegalovirus bacterial artificial chromosome pSM3fr show reduced growth in salivary Glands due to a fixed mutation of MCK-2. *J Virol*. 2011 Oct;85(19):10346-53.

Jouvin-Marche E, Morgado MG, Leguern C, Voegtli D, Bonhomme F, Cazenave PA. The mouse Igh-1a and Igh-1b H chain constant regions are derived from two distinct isotypic genes. *Immunogenetics*. 1989;29(2):92-7.

Kalland KH, Ke XS, Øyan AM. Tumour virology-history, status and future challenges. *APMIS*. 2009 May;117(5-6):382-99.

Kaneko Y, Nimmerjahn F, Ravetch JV. Anti-inflammatory activity of immunoglobulin G resulting from Fc sialylation. *Science*. 2006 Aug 4;313(5787):670-3.

Kantakamalakul W, Pattanapanyasat K, Jongrakthaitae S, Assawadarachai V, Ampol S, Sutthent R. A novel EGFP-CEM-NK flow cytometric method for measuring antibody dependent cell mediated-cytotoxicity (ADCC) activity in HIV-1 infected individuals. *J Immunol Methods*. 2006 Aug 31;315(1-2):1-10.

Kao D, Danzer H, Collin M, Groß A, Eichler J, Stambuk J, Lauc G, Lux A, Nimmerjahn F. A Monosaccharide Residue Is Sufficient to Maintain Mouse and Human IgG Subclass Activity and Directs IgG Effector Functions to Cellular Fc Receptors. *Cell Rep*. 2015 Dec 22;13(11):2376-85.

Karbach A. Protection from Cytomegalovirus Infection by Glycoprotein-specific Monoclonal Antibodies. Dissertation 2012, Friedrich-Alexander-University Erlangen-Nürnberg, Germany

Karrer U, Sierro S, Wagner M, Oxenius A, Hengel H, Koszinowski UH, Phillips RE, Klennerman P. Memory inflation: continuous accumulation of antiviral CD8+ T cells over time. *J Immunol*. 2003 Feb 15;170(4):2022-9.

Karupiah G, Sacks TE, Klinman DM, Fredrickson TN, Hartley JW, Chen JH, Morse HC 3rd. Murine cytomegalovirus infection-induced polyclonal B cell activation is independent of CD4+ T cells and CD40. *Virology*. 1998 Jan 5;240(1):12-26.

Kenneson A, Cannon MJ. Review and meta-analysis of the epidemiology of congenital cytomegalovirus (CMV) infection. *Rev Med Virol* 2007;17(4):253–276.

Kenneth MP. Janeway's immunobiology. 2012 by Garland Science, Taylor & Francis Group, LLC

Keusch J, Levy Y, Shoenfeld Y, Youinou P. Analysis of different glycosylation states in IgG subclasses. *Clin Chim Acta*. 1996 Aug 30;252(2):147-58.

Khairallah C, Netzer S, Villacreces A, Juzan M, Rousseau B, Dulanto S, Giese A, Costet P, Praloran V, Moreau JF, Dubus P, Vermijlen D, Déchanet-Merville J, Capone M. $\gamma\delta$ T cells confer protection against murine cytomegalovirus (MCMV). *PLoS Pathog*. 2015 Mar 6;11(3):e1004702.

Kim HY, Kim S, Chung DH. Fc gamma RIII engagement provides activating signals to NKT cells in antibody-induced joint inflammation. *J Clin Invest*. 2006 Sep;116(9):2484-92.

Kindt TJ, Osborne BA. Kuby Immunology, Sixth Edition, Aug 15, 2006

Kitamura K, et al. Critical role of the Fc receptor gamma-chain on APCs in the development of allergen-induced airway hyperresponsiveness and inflammation. *J Immunol* 2007;178:480–488.

Kiyoshi M, Caaveiro JM, Kawai T, Tashiro S, Ide T, Asaoka Y, Hatayama K, Tsumoto K. Structural basis for binding of human IgG1 to its high-affinity human receptor Fc γ RI. *Nat Commun*. 2015 Apr 30;6:6866.

Klasse PJ, Sattentau QJ. Occupancy and mechanism in antibody-mediated neutralization of animal viruses. *J Gen Virol*. 2002 Sep;83(Pt 9):2091-108.

Klenovsek K, Weisel F, Schneider A, Appelt U, Jonjić S, Messerle M, Bradel-Tretheway B, Winkler TH, Mach M. Protection from CMV infection in immunodeficient hosts by adoptive transfer of memory B cells. *Blood*. 2007 Nov 1;110(9):3472-9.

Koffron AJ, Hummel M, Patterson BK, Yan S, Kaufman DB, Fryer JP, Stuart FP, Abecassis MI. Cellular localization of latent murine cytomegalovirus. *J Virol*. 1998 Jan;72(1):95-103.

Köhler G, Milstein C. Continuous cultures of fused cells secreting antibody of predefined specificity. *Nature*. 1975 Aug 7;256(5517):495-7.

Köhler G, Milstein C. Derivation of specific antibody-producing tissue culture and tumor lines by cell fusion. *Eur J Immunol*. 1976 Jul;6(7):511-9.

Kumpel BM, Rademacher TW, Rook GA, Williams PJ, Wilson IB. Galactosylation of human IgG monoclonal anti-D produced by EBV-transformed B-lymphoblastoid cell lines is dependent on culture method and affects Fc receptor-mediated functional activity. *Hum Antibodies Hybridomas*. 1994;5(3-4):143-51.

Kurath S, Halwachs-Baumann G, Müller W, Resch B. Transmission of cytomegalovirus via breast milk to the prematurely born infant: a systematic review. *Clin Microbiol Infect*. 2010 Aug;16(8):1172-8.

Kurosaki T, Gander I, Ravetch JV. A subunit common to an IgG Fc receptor and the T-cell receptor mediates assembly through different interactions. *Proc Natl Acad Sci U S A*. 1991 May 1;88(9):3837-41.

Laemmli UK. Cleavage of structural proteins during the assembly of the head of bacteriophage T4. *Nature*. 1970 Aug 15;227(5259):680-5.

- Lambert SL, Okada CY, Levy R. TCR vaccines against a murine T cell lymphoma: a primary role for antibodies of the IgG2c class in tumor protection. *J Immunol.* 2004 Jan 15;172(2):929-36.
- Lanier LL, Le AM, Phillips JH, Warner NL, Babcock GF. Subpopulations of human natural killer cells defined by expression of the Leu-7 (HNK-1) and Leu-11 (NK-15) antigens. *J Immunol.* 1983 Oct;131(4):1789-96.
- Lanier LL, Yu G, Phillips JH. Co-association of CD3 zeta with a receptor (CD16) for IgG Fc on human natural killer cells. *Nature.* 1989 Dec 14;342(6251):803-5.
- László G, Rajnavölgyi E, Andó I, Gergely J. The influence of Igh-1 genes on the class and subclass distribution of oxazolone-specific antibodies. *Immunogenetics.* 1985;21(5):429-43.
- Lawson CM, Grundy JE, Shellam GR. Antibody responses to murine cytomegalovirus in genetically resistant and susceptible strains of mice. *J Gen Virol.* 1988 Aug;69 (Pt 8):1987-98.
- Lee J, Zhang T, Hwang I, Kim A, Nitschke L, Kim M, Scott JM, Kamimura Y, Lanier LL, Kim S. Epigenetic modification and antibody-dependent expansion of memory-like NK cells in human cytomegalovirus-infected individuals. *Immunity.* 2015 Mar 17;42(3):431-42.
- Lee YN, Lee YT, Kim MC, Hwang HS, Lee JS, Kim KH, Kang SM. Fc receptor is not required for inducing antibodies but plays a critical role in conferring protection after influenza M2 vaccination. *Immunology.* 2014 Oct;143(2):300-9.
- Lefranc MP, Pommié C, Kaas Q, Duprat E, Bosc N, Guiraudou D, Jean C, Ruiz M, Da Piédade I, Rouard M, Foulquier E, Thouvenin V, Lefranc G. IMGT unique numbering for immunoglobulin and T cell receptor constant domains and Ig superfamily C-like domains. *Dev Comp Immunol.* 2005;29(3):185-203.
- Lenac T, Budt M, Arapovic J, Hasan M, Zimmermann A, Simic H, Krmpotic A, Messerle M, Ruzsics Z, Koszinowski UH, Hengel H, Jonjić S. The herpesviral Fc receptor fcr-1 down-regulates the NKG2D ligands MULT-1 and H60. *J Exp Med.* 2006 Aug 7;203(8):1843-50.
- Léonetti M, Galon J, Thai T, Sautès-Fridman C, Moine G, Ménez A. Presentation of Antigen in Immune Complexes Is Boosted by Soluble Bacterial Immunoglobulin Binding Proteins. *J Exp Med.* 1999 Apr 19; 189(8): 1217–1228.
- Letourneur O, Kennedy IC, Brini AT, Ortaldo JR, O'Shea JJ, Kinet JP. Characterization of the family of dimers associated with Fc receptors (Fc epsilon RI and Fc gamma RIII). *J Immunol.* 1991 Oct 15;147(8):2652-6.
- Li X, Gibson AW, Kimberly RP. Human FcR polymorphism and disease. *Curr Top Microbiol Immunol.* 2014;382:275-302
- Lichtenfels R, Biddison WE, Schulz H, Vogt AB, Martin R. CARE-LASS (calcein-release-assay), an improved fluorescence-based test system to measure cytotoxic T lymphocyte activity. *J. Immunol. Methods*, 172 (1994), p. 227
- Lifely MR, Hale C, Boyce S, Keen MJ, Phillips J. Glycosylation and biological activity of CAMPATH-1H expressed in different cell lines and grown under different culture conditions. *Glycobiology.* 1995 Dec;5(8):813-22.
- Liu W, Won Sohn H, Tolar P, Meckel T, Pierce SK. Antigen-induced oligomerization of the B cell receptor is an early target of Fc gamma RIIb inhibition. *J Immunol.* 2010 Feb 15;184(4):1977-89.
- Loukas A, Jones MK, King LT, Brindley PJ, McManus DP. Receptor for Fc on the surfaces of schistosomes. *Infect Immun.* 2001 Jun;69(6):3646-51.
- Lu J, Chu J, Zou Z, Hamacher NB, Rixon MW, Sun PD. Structure of FcγRI in complex with Fc reveals the importance of glycan recognition for high-affinity IgG binding. *Proc Natl Acad Sci U S A.* 2015 Jan 20;112(3):833-8.
- Lu J, Sun PD. Structural mechanism of high affinity FcγRI recognition of immunoglobulin G. *Immunol Rev.* 2015 Nov;268(1):192-200.
- Lu X, Pinto AK, Kelly AM, Cho KS, Hill AB. Murine cytomegalovirus interference with antigen presentation contributes to the inability of CD8 T cells to control virus in the salivary gland. *J Virol.* 2006 Apr;80(8):4200-2.
- Lucin P, Pavić I, Polić B, Jonjić S, Koszinowski UH. Gamma interferon-dependent clearance of cytomegalovirus infection in salivary glands. *J Virol.* 1992 Apr;66(4):1977-84.
- Lund J, Pound JD, Jones PT, Duncan AR, Bentley T, Goodall M, Levine BA, Jefferis R, Winter G. Multiple binding sites on the CH2 domain of IgG for mouse Fc gamma RII. *Mol Immunol.* 1992 Jan;29(1):53-9.
- Lux A, Aschermann S, Biburger M, Nimmerjahn F. The pro and anti-inflammatory activities of immunoglobulin. *Ann Rheum Dis* 2010;69:i92-i96.
- Lux A, Yu X, Scanlan CN, Nimmerjahn F. Impact of immune complex size and glycosylation on IgG binding to human FcγRs. *J Immunol.* 2013 Apr 15;190(8):4315-23.
- Maeda S, Irie Y, Ichii S, Yasuraoka K. The killing effect of subclasses of mouse IgG antibodies on schistosomula of *Schistosoma japonicum*. *Jpn J Exp Med.* 1986 Feb;56(1):27-33.

Maidji E, Nigro G, Tabata T, McDonagh S, Nozawa N, Shiboski S, Muci S, Anceschi MM, Aziz N, Adler SP, Pereira L. Antibody treatment promotes compensation for human cytomegalovirus-induced pathogenesis and a hypoxia-like condition in placentas with congenital infection. *Am J Pathol*. 2010 Sep;177(3):1298-310.

Maillard P, Lavergne JP, Sib  ril S, Faure G, Roohvand F, Petres S, Teillaud JL, Budkowska A. Fc gamma receptor-like activity of hepatitis C virus core protein. *J Biol Chem*. 2004 Jan 23;279(4):2430-7.

Maloney DG, Smith B, Rose A. Rituximab: mechanism of action and resistance. *Semin Oncol*. 2002 Feb;29(1 Suppl 2):2-9.

Mancardi DA, Albanesi M, J  nsson F, Iannascoli B, Van Rooijen N, Kang X, England P, Da  ron M, Bruhns P. The high-affinity human IgG receptor Fc  RI (CD64) promotes IgG-mediated inflammation, anaphylaxis, and antitumor immunotherapy. *Blood*. 2013 Feb 28;121(9):1563-73.

Manicklal S, Emery VC, Lazzarotto T, Boppana SB, Gupta RK. The "silent" global burden of congenital cytomegalovirus. *Clin Microbiol Rev*. 2013 Jan;26(1):86-102. doi: 10.1128/CMR.00062-12.

Manischewitz JE, Quinnan GV Jr. Antivirus antibody-dependent cell-mediated cytotoxicity during murine cytomegalovirus infection. *Infect Immun*. 1980 Sep;29(3):1050-4.

Manning WC, Stoddart CA, Lagenaur LA, Abenes GB, Mocarski ES. Cytomegalovirus determinant of replication in salivary glands. *J Virol*. 1992 Jun;66(6):3794-802.

Mannini-Palenzona A, Costanzo F, Fiorilli MP, Derenzini M. Growth, spread, and extracellular localization of herpes simplex virus 1 in Vero cells in the presence of an anti-gD plaque inhibiting monoclonal antibody. *New Microbiol* 1998;21:65–76

Marasco WA, Sui J. The growth and potential of human antiviral monoclonal antibody therapeutics. *Nat Biotechnol*. 2007 Dec;25(12):1421-34.

Martin RM, Silva A, Lew AM. The Igh-1 sequence of the non-obese diabetic (NOD) mouse assigns it to the IgG2c isotype. *Immunogenetics*. 1997;46(2):167-8.

Maschke M, Kastrup O, Diener HC. CNS manifestations of cytomegalovirus infections: diagnosis and treatment. *CNS Drugs*. 2002;16(5):303-15.

Masuda K, Kubota T, Kaneko E, Iida S, Wakitani M, Kobayashi-Natsume Y, Kubota A, Shitara K, Nakamura K. Enhanced binding affinity for Fc gamma RIIIa of fucose-negative antibody is sufficient to induce maximal antibody-dependent cellular cytotoxicity. *Mol Immunol*. 2007 May;44(12):3122-31.

Merc   Maldonado E. Identification and functional characterization of a novel HCMV-encoded Fc   receptor blocking CD16-mediated activation of human natural killer cells. Dissertation, HHU D  sseldorf, 2011.

Messerle M, Crnkovic I, Hammerschmidt W, Ziegler H, Koszinowski UH. Cloning and mutagenesis of a herpesvirus genome as an infectious bacterial artificial chromosome. *Proc Natl Acad Sci U S A*. 1997 Dec 23;94(26):14759-63.

Mettenleiter TC. Herpesvirus assembly and egress. *J Virol*. 2002 Feb;76(4):1537-47.

Michaelsen TE, Kolberg J, Aase A, Herstad TK, H  iby EA. The four mouse IgG isotypes differ extensively in bactericidal and opsonophagocytic activity when reacting with the P1.16 epitope on the outer membrane PorA protein of *Neisseria meningitidis*. *Scand J Immunol*. 2004 Jan;59(1):34-9.

Mimura Y, Kelly RM2, Unwin L, Albrecht S, Jefferis R, Goodall M, Mizukami Y, Mimura-Kimura Y, Matsumoto T, Ueoka H, Rudd PM. Enhanced sialylation of a human chimeric IgG1 variant produced in human and rodent cell lines. *J Immunol Methods*. 2016 Jan;428:30-6.

Mintern JD, Klemm EJ, Wagner M, Paquet ME, Napier MD, Kim YM, Koszinowski UH, Ploegh HL. Viral interference with B7-1 costimulation: a new role for murine cytomegalovirus fc receptor-1. *J Immunol*. 2006 Dec 15;177(12):8422-31.

Mitrovi   M, Arapovi   J, Jordan S, Fodil-Cornu N, Ebert S, Vidal SM, Krmpot  i   A, Reddehase MJ, Jonji   S. The NK cell response to mouse cytomegalovirus infection affects the level and kinetics of the early CD8(+) T-cell response. *J Virol*. 2012 Feb;86(4):2165-75.

Mocarski Jr ES, Thomas Shenk T, Griffiths PD, Pass RF. In: Fields Virology. Lippincott Williams & Wilki, 6th revised edition 2013.

Morel PA, Ernst LK, Metes D. Functional CD32 molecules on human NK cells. *Leuk Lymphoma*. 1999 Sep;35(1-2):47-56

Moretta A, Bottino C, Vitale M, Pende D, Cantoni C, Mingari MC, Biassoni R, Moretta L. Activating receptors and coreceptors involved in human natural killer cell-mediated cytotoxicity. *Annu Rev Immunol*. 2001;19:197-223.

Morgado MG, Cam P, Gris-Liebe C, Cazenave PA, Jouvin-Marche E. Further evidence that BALB/c and C57BL/6 gamma 2a genes originate from two distinct isotypes. *EMBO J*. 1989 Nov;8(11):3245-51.

Morgado MG, Jouvin-Marche E, Gris-Liebe C, Bonhomme F, Anand R, Talwar GP, Cazenave PA. Restriction fragment length polymorphism and evolution of the mouse immunoglobulin constant region gamma loci. *Immunogenetics*. 1993;38(3):184-92.

Mosmann TR, Coffman RL. TH1 and TH2 cells: different patterns of lymphokine secretion lead to different functional properties. *Annu Rev Immunol.* 1989;7:145-73.

Muller N, Derouazi M, Van Tilborgh F, Wulhfard S, Hacker DL, Jordan M, Wurm FM. Scalable transient gene expression in Chinese hamster ovary cells in instrumented and non-instrumented cultivation systems. *Biotechnol Lett.* 2007 May;29(5):703-11

Mutnal MB, Hu S, Lokensgard JR. Persistent humoral immune responses in the CNS limit recovery of reactivated murine cytomegalovirus. *PLoS One.* 2012;7(3):e33143.

Naing ZW, Scott GM, Shand A, Hamilton ST, van Zuylen WJ, Basha J, Hall B, Craig ME, Rawlinson WD. Congenital cytomegalovirus infection in pregnancy: a review of prevalence, clinical features, diagnosis and prevention. *Aust N Z J Obstet Gynaecol.* 2016 Feb;56(1):9-18.

Nallet S, Fornelli L, Schmitt S, Parra J, Baldi L, Tsybin YO, Wurm FM. Glycan variability on a recombinant IgG antibody transiently produced in HEK-293E cells. *N Biotechnol.* 2012 May 15;29(4):471-6.

Nathanson N, Moss WJ. In: *Fields Virology*. Lippincott Williams & Wilki, 6th revised edition 2013.

Ndjamen B, Farley AH, Lee T, Fraser SE, Bjorkman PJ. The herpes virus Fc receptor gE-gI mediates antibody bipolar bridging to clear viral antigens from the cell surface. *PLoS Pathog.* 2014 Mar 6;10(3):e1003961.

Ndjamen B, Joshi DS, Fraser SE, Bjorkman PJ. Characterization of Antibody Bipolar Bridging Mediated by the Human Cytomegalovirus Fc Receptor gp68. *J Virol.* 2016 Jan 6;90(6):3262-7.

Neuberger MS, Rajewsky K. Activation of mouse complement by monoclonal mouse antibodies. *Eur J Immunol.* 1981 Dec;11(12):1012-6.

Nichols WG, Boeckh M. Recent advances in the therapy and prevention of CMV infections. *J Clin Virol.* 2000 Feb;16(1):25-40.

Nigro G, Adler SP, La Torre R, Best AM; Congenital Cytomegalovirus Collaborating Group. Passive immunization during pregnancy for congenital cytomegalovirus infection. *N Engl J Med.* 2005 Sep 29;353(13):1350-62.

Nigro G, Adler SP, Parruti G, Anceschi MM, Coclite E, Pezone I, Di Renzo GC. Immunoglobulin therapy of fetal cytomegalovirus infection occurring in the first half of pregnancy--a case-control study of the outcome in children. *J Infect Dis.* 2012 Jan 15;205(2):215-27.

Nigro G, La Torre R, Pentimalli H, Taverna P, Lituania M, de Tejada BM, Adler SP. Regression of fetal cerebral abnormalities by primary cytomegalovirus infection following hyperimmunoglobulin therapy. *Prenat Diagn.* 2008 Jun;28(6):512-7.

Nimmerjahn F, Anthony RM, Ravetch JV. Agalactosylated IgG antibodies depend on cellular Fc receptors for in vivo activity. *Proc Natl Acad Sci U S A.* 2007 May 15; 104(20): 8433-8437.

Nimmerjahn F, Bruhns P, Horiuchi K, Ravetch JV. Fc gamma RIV: a novel FcR with distinct IgG subclass specificity. *Immunity* 2005;23:41-51.

Nimmerjahn F, Gordan S, Lux A. FcγR dependent mechanisms of cytotoxic, agonistic, and neutralizing antibody activities. *Trends Immunol.* 2015 Jun;36(6):325-36

Nimmerjahn F, Lux A, Albert H, Woigk M, Lehmann C, Dudziak D, Smith P, Ravetch JV. FcγRIV deletion reveals its central role for IgG2a and IgG2b activity in vivo. *Proc Natl Acad Sci U S A.* 2010 Nov 9;107(45):19396-401.

Nimmerjahn F, Ravetch JV. Divergent immunoglobulin G subclass activity through selective Fc receptor binding. *Science.* 2005 Dec 2;310(5753):1510-2.

Nimmerjahn F, Ravetch JV. Fc gamma receptors as regulators of immune responses. *Nat Rev Immunol.* 2008 Jan;8(1):34-47.

Nimmerjahn F, Ravetch JV. Fc gamma receptors: old friends and new family members. *Immunity.* 2006 Jan;24(1):19-28.

Nimmerjahn F, Ravetch JV. FcγRs in health and disease. *Curr Top Microbiol Immunol.* 2011;350:105-25.

Nomura M, Kurita-Taniguchi M, Kondo K, Inoue N, Matsumoto M, Yamanishi K, Okabe M, Seya T. Mechanism of host cell protection from complement in murine cytomegalovirus (CMV) infection: identification of a CMV-responsive element in the CD46 promoter region. *Eur J Immunol.* 2002 Oct;32(10):2954-64

Oefner CM, Winkler A, Hess C, Lorenz AK, Holecska V, Huxdorf M, Schommartz T, Petzold D, Bitterling J, Schoen AL, Stoeck AD, Vu Van D, Darcan-Nikolaisen Y, Blanchard V, Schmutte I, Laumonier Y, Ströver HA, Hegazy AN, Eiglmeier S, Schoen CT, Mertes MM, Loddenkemper C, Löhning M, König P, Petersen A, Luger EO, Collin M, Köhl J, Hutloff A, Hamelmann E, Berger M, Wardemann H, Ehlers M. Tolerance induction with T cell-dependent protein antigens induces regulatory sialylated IgGs. *J Allergy Clin Immunol.* 2012 Jun;129(6):1647-55.e13.

Ohlin M, Söderberg-Nauclér C. Human antibody technology and the development of antibodies against cytomegalovirus. *Mol Immunol.* 2015 Oct;67(2 Pt A):153-70. doi: 10.1016/j.molimm.2015.02.026. Epub 2015 Mar 20.

Oleszak EL, Leibowitz JL. Immunoglobulin Fc binding activity is associated with the mouse hepatitis virus E2 peplomer protein. *Virology.* 1990 May;176(1):70-80.

Ollo R, Rougeon F. Gene conversion and polymorphism: generation of mouse immunoglobulin gamma 2a chain alleles by differential gene conversion by gamma 2b chain gene. *Cell*. 1983 Feb;32(2):515-23.

Ono M, Okada H, Bolland S, Yanagi S, Kurosaki T, Ravetch JV. Deletion of SHIP or SHP-1 reveals two distinct pathways for inhibitory signaling. *Cell*. 1997 Jul 25;90(2):293-301.

Otten MA, van der Bij GJ, Verbeek SJ, Nimmerjahn F, Ravetch JV, Beelen RH, van de Winkel JG, van Egmond M. Experimental antibody therapy of liver metastases reveals functional redundancy between Fc gammaRI and Fc gammaRIV. *Immunol Lett*. 2012 Mar 30;143(1):44-52.

Pantaleo G, Demarest JF, Vaccarezza M, Graziosi C, Bansal GP, Koenig S, Fauci AS. Effect of anti-V3 antibodies on cell-free and cell-to-cell human immunodeficiency virus transmission. *Eur J Immunol*. 1995 Jan;25(1):226-31.

Parekh BS, Berger E, Sibley S, Cahya S, Xiao L, Lacerte MA, Vaillancourt P, Wooden S, Gately D. Development and validation of an antibody-dependent cell-mediated cytotoxicity-reporter gene assay. *MAbs*, 4 (2012)

Parren PW, Burton DR. The antiviral activity of antibodies in vitro and in vivo. *Adv Immunol*. 2001;77:195–262.

Patel TP, Parekh RB, Moellering BJ, Prior CP. Different culture methods lead to differences in glycosylation of a murine IgG monoclonal antibody. *Biochem J*. 1992 Aug 1;285 (Pt 3):839-45.

Pati SK, Novak Z, Purser M, Arora N, Mach M, Britt WJ, Boppana SB. Strain-specific neutralizing antibody responses against human cytomegalovirus envelope glycoprotein N. *Clin Vaccine Immunol*. 2012 Jun;19(6):909-13.

Pavić I, Polić B, Crnković I, Lucin P, Jonjić S, Koszinowski UH. Participation of endogenous tumour necrosis factor alpha in host resistance to cytomegalovirus infection. *J Gen Virol*. 1993 Oct;74 (Pt 10):2215-23

Pellett PE, Roizman B. In: *Fields Virology*. Lippincott Williams & Wilki, 6th revised edition 2013.

Petrushina I, Tran M, Sadzikava N, Ghochikyan A, Vasilevko V, Agadjanyan MG, Cribbs DH. Importance of IgG2c isotype in the immune response to in amyloid precursor protein/transgenic mice. *Neurosci Lett*. 2003 Feb 20;338(1):5-8.

Plotkin S. The history of vaccination against cytomegalovirus. *Med Microbiol Immunol*. 2015 Jun;204(3):247-54.

Plotkin SA, Gilbert PB. Nomenclature for immune correlates of protection after vaccination. *Clin Infect Dis*. 2012 Jun;54(11):1615-7.

Plotkin SA. Complex correlates of protection after vaccination. *Clin Infect Dis*. 2013 May;56(10):1458-65.

Podlech J, Ebert S, Becker M, Reddehase MJ, Stassen M, Lemmermann NA. Mast cells: innate attractors recruiting protective CD8 T cells to sites of cytomegalovirus infection. *Med Microbiol Immunol*. 2015 Jun;204(3):327-34.

Polić B, Hengel H, Krmpotić A, Trgovcich J, Pavić I, Luccaroni P, Jonjić S, Koszinowski UH. Hierarchical and redundant lymphocyte subset control precludes cytomegalovirus replication during latent infection. *J Exp Med*. 1998 Sep 21;188(6):1047-54

Pötzsch S, Spindler N, Wiegers AK, Fisch T, Rücker P, Sticht H, Grieb N, Baroti T, Weisel F, Stamminger T, Martin-Parras L, Mach M, Winkler TH. B cell repertoire analysis identifies new antigenic domains on glycoprotein B of human cytomegalovirus which are target of neutralizing antibodies. *PLoS Pathog*. 2011 Aug;7(8):e1002172.

Price P, Olver SD, Gibbons AE, Shellam GR. B-cell activation following murine cytomegalovirus infection: implications for autoimmunity. *Immunology*. 1993 Jan;78(1):14-21.

Pucić M, Knezević A, Vidic J, Adamczyk B, Novokmet M, Polasek O, Gornik O, Supraha-Goreta S, Wormald MR, Redzić I, Campbell H, Wright A, Hastie ND, Wilson JF, Rudan I, Wuhler M, Rudd PM, Josić D, Lauc G. High throughput isolation and glycosylation analysis of IgG-variability and heritability of the IgG glycome in three isolated human populations. *Mol Cell Proteomics*. 2011 Oct;10(10): M111.010090.

Raanani P, Gafter-Gvili A, Paul M, Ben-Bassat I, Leibovici L, Shpilberg O. Immunoglobulin prophylaxis in hematopoietic stem cell transplantation: systematic review and meta-analysis. *J Clin Oncol*. 2009 Feb 10;27(5):770-81.

Raju TS, Briggs JB, Borge SM, Jones AJ. Species-specific variation in glycosylation of IgG: evidence for the species-specific sialylation and branch-specific galactosylation and importance for engineering recombinant glycoprotein therapeutics. *Glycobiology*. 2000 May;10(5):477-86.

Raju TS, Jordan RE. Galactosylation variations in marketed therapeutic antibodies. *MAbs*. 2012 May-Jun;4(3):385-91.

Ramezani A, Hawley RG. Overview of the HIV-1 Lentiviral Vector System. *Curr Protoc Mol Biol*. 2002 Nov;Chapter 16:Unit 16.21.

Rawlinson WD, Farrell HE, Barrell BG. Analysis of the complete DNA sequence of murine cytomegalovirus. *J Virol*. 1996 Dec;70(12):8833-49.

Raymond C, Robotham A, Kelly J, Lattová E, Perreault H, Durocher Y(2012). Production of Highly Sialylated Monoclonal Antibodies, Glycosylation, Dr. Stefana Petrescu (Ed.), InTech, DOI: 10.5772/51301.

Reddehase MJ, Balthesen M, Rapp M, Jonjić S, Pavić I, Koszinowski UH. The conditions of primary infection define the load of latent viral genome in organs and the risk of recurrent cytomegalovirus disease. *J Exp Med*. 1994 Jan 1;179(1):185-93.

Reddehase MJ, Mutter W, Münch K, Bühring HJ, Koszinowski UH. CD8-positive T lymphocytes specific for murine cytomegalovirus immediate-early antigens mediate protective immunity. *J Virol*. 1987 Oct;61(10):3102-8.

Regnault A, Lankar D, Lacabanne V, Rodriguez A, Théry C, Rescigno M, Saito T, Verbeek S, Bonnerot C, Ricciardi-Castagnoli P, Amigorena S. Fc gamma receptor-mediated induction of dendritic cell maturation and major histocompatibility complex class I-restricted antigen presentation after immune complex internalization. *J Exp Med*. 1999 Jan 18;189(2):371-80.

Reinhard HC. Struktur-Funktions-Beziehung der HCMV-kodierten Fcγ-Rezeptoren gp34 und gp68. Dissertation, Humboldt-Universität zu Berlin, 2009

Reinherz EL, Kung PC, Goldstein G, Levey RH, Schlossman SF. Discrete stages of human intrathymic differentiation: analysis of normal thymocytes and leukemic lymphoblasts of T-cell lineage. *Proc Natl Acad Sci U S A*. 1980 Mar;77(3):1588-92.

Revello MG, Lazzarotto T, Guerra B, Spinillo A, Ferrazzi E, Kustermann A, Guaschino S, Vergani P, Todros T, Frusca T, Arossa A, Furione M, Rognoni V, Rizzo N, Gabrielli L, Klersy C, Gerna G; CHIP Study Group. A randomized trial of hyperimmune globulin to prevent congenital cytomegalovirus. *N Engl J Med*. 2014 Apr 3;370(14):1316-26.

Riedel S. Edward Jenner and the history of smallpox and vaccination. *Proc (Bayl Univ Med Cent)*. 2005 Jan;18(1):21-5.

Robbins SH, Bessou G, Cornillon A, Zucchini N, Rupp B, Ruzsics Z, Sacher T, Tomasello E, Vivier E, Koszinowski UH, Dalod M. Natural killer cells promote early CD8 T cell responses against cytomegalovirus. *PLoS Pathog*. 2007 Aug 24;3(8):e123

Sacher T, Mohr CA, Weyn A, Schlichting C, Koszinowski UH, Ruzsics Z. The role of cell types in cytomegalovirus infection in vivo. *Eur J Cell Biol*. 2012 Jan;91(1):70-7.

Sacher T, Podlech J, Mohr CA, Jordan S, Ruzsics Z, Reddehase MJ, Koszinowski UH. The major virus-producing cell type during murine cytomegalovirus infection, the hepatocyte, is not the source of virus dissemination in the host. *Cell Host Microbe*. 2008 Apr 17;3(4):263-72.

Saederup N, Lin YC, Dairaghi DJ, Schall TJ, Mocarski ES. Cytomegalovirus-encoded beta chemokine promotes monocyte-associated viremia in the host. *Proc Natl Acad Sci U S A*. 1999 Sep 14;96(19):10881-6.

Sakamoto N, Shibuya K, Shimizu Y, Yotsumoto K, Miyabayashi T, Sakano S, Tsuji T, Nakayama E, Nakauchi H, Shibuya A. A novel Fc receptor for IgA and IgM is expressed on both hematopoietic and non-hematopoietic tissues. *Eur J Immunol*. 2001 May;31(5):1310-6.

Sawyer LA. Antibodies for the prevention and treatment of viral diseases. *Antiviral Res*. 2000 Aug;47(2):57-77.

Scallan BJ, Tam SH, McCarthy SG, Cai AN, Raju TS. Higher levels of sialylated Fc glycans in immunoglobulin G molecules can adversely impact functionality. *Mol Immunol*. 2007 Mar;44(7):1524-34.

Schleiss MR. Cytomegalovirus in the neonate: immune correlates of infection and protection. *Clin Dev Immunol*. 2013;2013:501801

Schoppel K, Schmidt C, Einsele H, Hebart H, Mach M. Kinetics of the antibody response against human cytomegalovirus-specific proteins in allogeneic bone marrow transplant recipients. *J Infect Dis*. 1998 Nov;178(5):1233-43.

Schreier PH, Bothwell AL, Mueller-Hill B, Baltimore D. Multiple differences between the nucleic acid sequences of the IgG2aa and IgG2ab alleles of the mouse. *Proc Natl Acad Sci U S A*. 1981 Jul;78(7):4495-9.

Schroeder HW Jr, Cavacini L. Structure and function of immunoglobulins. *J Allergy Clin Immunol*. 2010 Feb;125(2 Suppl 2):S41-52.

Seckert CK, Griebel M, Büttner JK, Freitag K, Lemmermann NAW, Hummel MA, Liu XF, Abecassis MI, Angulo A, Messerle M, Cook CH, Reddehase MJ. In: *Cytomegaloviruses: From Molecular Pathogenesis to Intervention*. Caister Academic Press 2013

Seino J, Eveleigh P, Warnaar S, van Haarlem LJ, van Es LA, Daha MR. Activation of human complement by mouse and mouse/human chimeric monoclonal antibodies. *Clin Exp Immunol*. 1993 Nov;94(2):291-6.

Sell S, Dietz M, Schneider A, Holtappels R, Mach M, Winkler TH. Control of murine cytomegalovirus infection by γδ T cells. *PLoS Pathog*. 2015 Feb 6;11(2):e1004481.

Seppälä I, Sarvas H, Péterfy F, Mäkelä O. The four subclasses of IgG can be isolated from mouse serum by using Protein A-Sepharose. *Scand J Immunol*. 1981 Oct;14(4):335-42.

Shanley JD, Jordan MC, Stevens JG. Modification by adoptive humoral immunity of murine cytomegalovirus infection. *J Infect Dis* 1981;143:231-237.

Shields RL, Lai J, Keck R, O'Connell LY, Hong K, Meng YG, Weikert SH, Presta LG. Lack of fucose on human IgG1 N-linked oligosaccharide improves binding to human Fc gamma RIII and antibody-dependent cellular toxicity. *J Biol Chem*. 2002 Jul 26;277(30):26733-40.

Shields RL, Namenuk AK, Hong K, Meng YG, Rae J, Briggs J, Xie D, Lai J, Stadlen A, Li B, Fox JA, Presta LG. High resolution mapping of the binding site on human IgG1 for Fc gamma RI, Fc gamma RII, Fc gamma RIII, and FcRn and design of IgG1 variants with improved binding to the Fc gamma R. *J Biol Chem*. 2001 Mar 2;276(9):6591-604.

Shinkawa T, Nakamura K, Yamane N, Shoji-Hosaka E, Kanda Y, Sakurada M, Uchida K, Anazawa H, Satoh M, Yamasaki M, Hanai N, Shitara K. The absence of fucose but not the presence of galactose or bisecting N-acetylglucosamine of human IgG1 complex-type oligosaccharides shows the critical role of enhancing antibody-dependent cellular cytotoxicity. *J Biol Chem*. 2003 Jan 31;278(5):3466-73.

Sidorin EV, Solov'eva TF. IgG-binding proteins of bacteria. *Biochemistry (Mosc)*. 2011 Mar;76(3):295-308

Slavuljica I, Busche A, Babić M, Mitrović M, Gašparović I, Cekinović D, Markova Car E, Pernjak Pugel E, Ciković A, Lisnić VJ, Britt WJ, Koszinowski U, Messerle M, Krmpotić A, Jonjić S. Recombinant mouse cytomegalovirus expressing a ligand for the NKG2D receptor is attenuated and has improved vaccine properties. *J Clin Invest*. 2010 Dec;120(12):4532-45.

Slingsby JH, Hogarth MB, Walport MJ, Morley BJ. Polymorphism in the Ly-17 alloantigenic system of the mouse FcγRII gene. *Immunogenetics*. 1997;46(4):361-2.

Sondermann P, Huber R, Oosthuizen V, Jacob U. The 3.2-Å crystal structure of the human IgG1 Fc fragment-Fc gammaRIII complex. *Nature*. 2000 Jul 20;406(6793):267-73.

Spiller OB, Morgan BP, Tufaro F, Devine DV. Altered expression of host-encoded complement regulators on human cytomegalovirus-infected cells. *Eur J Immunol*. 1996 Jul;26(7):1532-8.

Sprague ER, Reinhard H, Cheung EJ, Farley AH, Trujillo RD, Hengel H, Bjorkman PJ. The human cytomegalovirus Fc receptor gp68 binds the Fc CH2-CH3 interface of immunoglobulin G. *J Virol*. 2008 Apr;82(7):3490-9.

Sprague ER, Wang C, Baker D, Bjorkman PJ. Crystal structure of the HSV-1 Fc receptor bound to Fc reveals a mechanism for antibody bipolar bridging. *PLoS Biol*. 2006 Jun;4(6):e148.

Stadlmann J, Pabst M, Kolarich D, Kunert R, Altmann F. Analysis of immunoglobulin glycosylation by LC-ESI-MS of glycopeptides and oligosaccharides. *Proteomics*. 2008 Jul;8(14):2858-71.

Starr SE, Allison AC. Role of T lymphocytes in recovery from murine cytomegalovirus infection. *Infect Immun*. 1977 Aug;17(2):458-62.

Steenfot C, Vakhrushev SY, Joshi HJ, Kong Y, Vester-Christensen MB, Schjoldager KT, Lavrsen K, Dabelsteen S, Pedersen NB, Marcos-Silva L, Gupta R, Bennett EP, Mandel U, Brunak S, Wandall HH, Lavery SB, Clausen H. Precision mapping of the human O-GalNAc glycoproteome through SimpleCell technology. *EMBO J*, 32(10):1478-88, May 15, 2013.

Stern-Ginossar N, Weisburd B, Michalski A, Le VT, Hein MY, Huang SX, Ma M, Shen B, Qian SB, Hengel H, Mann M, Ingolia NT, Weissman JS. Decoding human cytomegalovirus. *Science*. 2012 Nov 23;338(6110):1088-93.

Stoddart CA, Cardin RD, Boname JM, Manning WC, Abenes GB, Mocarski ES. Peripheral blood mononuclear phagocytes mediate dissemination of murine cytomegalovirus. *J Virol*. 1994 Oct;68(10):6243-53.

Storcksdieck genannt Bonsmann M, Niezold T, Temchura V, Pissani F, Ehrhardt K, Brown EP, Osei-Owusu NY, Hannaman D, Hengel H, Ackerman ME, Streeck H, Nabi G, Tenbusch M, Überla K. Enhancing the Quality of Antibodies to HIV-1 Envelope by GagPol-Specific Th Cells. *J Immunol*. 2015 Nov 15;195(10):4861-72.

Straub T, Schweier O, Bruns M, Nimmerjahn F, Waisman A, Pircher H. Nucleoprotein-specific nonneutralizing antibodies speed up LCMV elimination independently of complement and FcγR. *Eur J Immunol*. 2013 Sep;43(9):2338-48.

Subedi GP, Barb AW. The Structural Role of Antibody N-Glycosylation in Receptor Interactions. *Structure*. 2015 Sep 1;23(9):1573-83.

Subedi GP, Hanson QM, Barb AW. Restricted motion of the conserved immunoglobulin G1 N-glycan is essential for efficient FcγRIIIa binding. *Structure*. 2014 Oct 7;22(10):1478-88.

Sung H, Schleiss MR. Update on the current status of cytomegalovirus vaccines. *Expert Rev Vaccines*. 2010 Nov;9(11):1303-14.

Suvas S, Singh V, Sahdev S, Vohra H, Agrewala JN. Distinct role of CD80 and CD86 in the regulation of the activation of B cell and B cell lymphoma. *J Biol Chem*. 2002 Mar 8;277(10):7766-75.

Syed SN, Konrad S, Wiege K, Nieswandt B, Nimmerjahn F, Schmidt RE, Gessner JE. Both Fc gamma RIV and Fc gamma RIII are essential receptors mediating type II and type III autoimmune responses via FcRgamma-LAT-dependent generation of C5a. *Eur J Immunol*. 2009 Dec;39(12):3343-56.

Sylvestre DL, Ravetch JV. Fc receptors initiate the Arthus reaction: redefining the inflammatory cascade. *Science*. 1994 Aug 19;265(5175):1095-8.

Takai T, Li M, Sylvestre D, Clynes R, Ravetch JV. FcR gamma chain deletion results in pleiotropic effector cell defects. *Cell*. 1994 Feb 11;76(3):519-29

Takai T, Ono M, Hikida M, Ohmori H, Ravetch JV. Augmented humoral and anaphylactic responses in Fc gamma RII-deficient mice. *Nature*. 1996 Jan 25;379(6563):346-9.

Takai T. A novel recognition system for MHC class I molecules constituted by PIR. *Adv Immunol*. 2005;88:161-92.

Takai T. Multiple loss of effector cell functions in FcR gamma-deficient mice. *Int Rev Immunol*. 1996;13(4):369-81.

Takai T. Roles of Fc receptors in autoimmunity. *Nat Rev Immunol*. 2002 Aug;2(8):580-92.

Tessmer MS, Reilly EC, Brossay L. Salivary gland NK cells are phenotypically and functionally unique. *PLoS Pathog*. 2011 Jan 13;7(1):e1001254.

Thäle R, Lucin P, Schneider K, Eggers M, Koszinowski UH. Identification and expression of a murine cytomegalovirus early gene coding for an Fc receptor. *J Virol*. 1994 Dec;68(12):7757-65.

Thom JT, Walton SM, Torti N, Oxenius A. Salivary gland resident APCs are Flt3L- and CCR2-independent macrophage-like cells incapable of cross-presentation. *Eur J Immunol*. 2014 Mar;44(3):706-14.

Thomann M, Reckermann K, Reusch D, Prasser J, Tejada ML. Fc-galactosylation modulates antibody-dependent cellular cytotoxicity of therapeutic antibodies. *Mol Immunol*. 2016 May;73:69-75.

Thomann M, Schlothauer T, Dashivets T, Malik S, Avenal C, Bulau P, Rüger P, Reusch D. In vitro glycoengineering of IgG1 and its effect on Fc receptor binding and ADCC activity. *PLoS One*. 2015 Aug 12;10(8):e0134949

Tian X, Vestergaard B, Thorolfsson M, Yang Z, Rasmussen HB, Langkilde AE. In-depth analysis of subclass-specific conformational preferences of IgG antibodies. *IUCr*. 2015 Jan 1;2(Pt 1):9-18.

Tiller T, Kofer J, Kreschel C, Busse CE, Riebel S, Wickert S, Oden F, Mertes MM, Ehlers M, Wardemann H. Development of self-reactive germinal center B cells and plasma cells in autoimmune Fc gammaRIIB-deficient mice. *J Exp Med*. 2010 Nov 22;207(12):2767-78.

Tjio JH, Puck TT. Genetics of somatic mammalian cells. II. Chromosomal constitution of cells in tissue culture. *J Exp Med*. 1958 Aug 1;108(2):259-68

Tonegawa S. Somatic generation of antibody diversity. *Nature*. 1983 Apr 14;302(5909):575-81.

Uchida J, Hamaguchi Y, Oliver JA, Ravetch JV, Poe JC, Haas KM, Tedder TF. The innate mononuclear phagocyte network depletes B lymphocytes through Fc receptor-dependent mechanisms during anti-CD20 antibody immunotherapy. *J Exp Med*. 2004 Jun 21;199(12):1659-69.

van Berkel PH, Gerritsen J, Perdok G, Valbjørn J, Vink T, van de Winkel JG, Parren PW. N-linked glycosylation is an important parameter for optimal selection of cell lines producing biopharmaceutical human IgG. *Biotechnol Prog*. 2009 Jan-Feb;25(1):244-51.

Veomett N, Dao T, Liu H, Xiang J, Pankov D, Dubrovsky L, Whitten JA, Park SM, Korontsvit T, Zakhaleva V, Casey E, Curcio M, Kharas MG, O'Reilly RJ, Liu C, Scheinberg DA. Therapeutic efficacy of an Fc-enhanced TCR-like antibody to the intracellular WT1 oncoprotein. *Clin Cancer Res*. 2014 Aug 1;20(15):4036-46.

Verma S, Weiskopf D, Gupta A, McDonald B, Peters B, Sette A, Benedict CA. Cytomegalovirus-Specific CD4 T Cells Are Cytolytic and Mediate Vaccine Protection. *J Virol*. 2015 Oct 21;90(2):650-8.

Vidarsson G, Dekkers G, Rispens T. IgG subclasses and allotypes: from structure to effector functions. *Front Immunol*. 2014 Oct 20;5:520

Vidarsson G, Stermerding AM, Stapleton NM, Spliethoff SE, Janssen H, Rebers FE, de Haas M, van de Winkel JG. FcRn: an IgG receptor on phagocytes with a novel role in phagocytosis. *Blood*. 2006 Nov 15;108(10):3573-9.

Vogt MR, Dowd KA, Engle M, Tesh RB, Johnson S, Pierson TC, Diamond MS. Poorly neutralizing cross-reactive antibodies against the fusion loop of West Nile virus envelope protein protect in vivo via Fc gamma receptor and complement-dependent effector mechanisms. *J Virol*. 2011 Nov;85(22):11567-80.

Voigt V, Forbes CA, Tonkin JN, Degli-Esposti MA, Smith HR, Yokoyama WM, Scalzo AA. Murine cytomegalovirus m157 mutation and variation leads to immune evasion of natural killer cells. *Proc Natl Acad Sci U S A*. 2003 Nov 11;100(23):13483-8.

Vora KA, Ravetch JV, Manser T. Amplified follicular immune complex deposition in mice lacking the Fc receptor gamma-chain does not alter maturation of the B cell response. *J Immunol*. 1997 Sep 1;159(5):2116-24.

Wagner M, Jonjić S, Koszinowski UH, Messerle M. Systematic excision of vector sequences from the BAC-cloned herpesvirus genome during virus reconstitution. *J Virol*. 1999 Aug;73(8):7056-60.

Wallace RB, Shaffer J, Murphy RF, Bonner J, Hirose T, Itakura K. Hybridization of synthetic oligodeoxyribonucleotides to phi chi 174 DNA: the effect of single base pair mismatch. *Nucleic Acids Res*. 1979 Aug 10;6(11):3543-57.

- Walton SM, Mandaric S, Torti N, Zimmermann A, Hengel H, Oxenius A. Absence of cross-presenting cells in the salivary gland and viral immune evasion confine cytomegalovirus immune control to effector CD4 T cells. *PLoS Pathog.* 2011 Aug;7(8):e1002214.
- Walton SM, Wyrsh P, Munks MW, Zimmermann A, Hengel H, Hill AB, Oxenius A. The dynamics of mouse cytomegalovirus-specific CD4 T cell responses during acute and latent infection. *J Immunol.* 2008 Jul 15;181(2):1128-34.
- Wang C, Zhang X, Bialek S, Cannon MJ. Attribution of congenital cytomegalovirus infection to primary versus non-primary maternal infection. *Clin Infect Dis.* 2011 Jan 15;52(2):e11-3.
- Wegener AM, Letourneur F, Hoeveler A, Brocker T, Luton F, Malissen B. The T cell receptor/CD3 complex is composed of at least two autonomous transduction modules. *Cell* 1992, 68, p. 83
- Welten SP, Redeker A1, Toes RE2, Arens R. Viral Persistence Induces Antibody Inflation without Altering Antibody Avidity. *J Virol.* 2016 Apr 14;90(9):4402-11
- Wenig K, Chatwell L, von Pawel-Rammingen U, Björck L, Huber R, Sonderrmann P. Structure of the streptococcal endopeptidase IdeS, a cysteine proteinase with strict specificity for IgG. *Proc Natl Acad Sci U S A.* 2004 Dec 14;101(50):17371-6.
- Wipke BT, Wang Z, Nagengast W, Reichert DE, Allen PM. Staging the initiation of autoantibody-induced arthritis: a critical role for immune complexes. *J Immunol.* 2004 Jun 15;172(12):7694-702.
- Wirtz N, Schader SI, Holtappels R, Simon CO, Lemmermann NA, Reddehase MJ, Podlech J. Polyclonal cytomegalovirus-specific antibodies not only prevent virus dissemination from the portal of entry but also inhibit focal virus spread within target tissues. *Med Microbiol Immunol.* 2008 Jun;197(2):151-8.
- Wormald MR, Rudd PM, Harvey DJ, Chang SC, Scragg IG, Dwek RA. Variations in oligosaccharide-protein interactions in immunoglobulin G determine the site-specific glycosylation profiles and modulate the dynamic motion of the Fc oligosaccharides. *Biochemistry.* 1997 Feb 11;36(6):1370-80.
- Wuhrer M, Stam JC, van de Geijn FE, Koeleman CA, Verrips CT, Dolhain RJ, Hokke CH, Deelder AM. Glycosylation profiling of immunoglobulin G (IgG) subclasses from human serum. *Proteomics.* 2007 Nov;7(22):4070-81.
- Xiang Z, Cutler AJ, Brownlie RJ, Fairfax K, Lawlor KE, Severinson E, Walker EU, Manz RA, Tarlinton DM, Smith KG. Fc gamma RIIB controls bone marrow plasma cell persistence and apoptosis. *Nat Immunol.* 2007 Apr;8(4):419-29.
- Yamamoto AY, Mussi-Pinhata MM, Boppana SB, Novak Z, Wagatsuma VM, Oliveira Pde F, Duarte G, Britt WJ. Human cytomegalovirus reinfection is associated with intrauterine transmission in a highly cytomegalovirus-immune maternal population. *Am J Obstet Gynecol.* 2010 Mar;202(3):297.e1-8.
- Yamasaki S, Ishikawa E, Sakuma M, Hara H, Ogata K, Saito T. Mincle is an ITAM-coupled activating receptor that senses damaged cells. *Nat Immunol.* 2008 Oct;9(10):1179-88. doi: 10.1038/ni.1651.
- Ye J, Kober V, Tellers M, Naji Z, Salmon P, Markusen JF. High-level protein expression in scalable CHO transient transfection. *Biotechnol Bioeng.* 2009 Jun 15;103(3):542-51.
- Zhang T, Scott JM, Hwang I, Kim S. Cutting edge: antibody-dependent memory-like NK cells distinguished by FcRγ deficiency. *J Immunol.* 2013 Feb 15;190(4):1402-6
- Zhang Z, Goldschmidt T, Salter H. Possible allelic structure of IgG2a and IgG2c in mice. *Mol Immunol.* 2012 Mar;50(3):169-71.

ACKNOWLEDGEMENTS

I would like to thank all the people who supported and accompanied me. It is not easy to find the right words to express the appreciation everybody had and still has for my scientific and personal life.

Firstly, I would like to express my gratitude to Prof. Hartmut Hengel for the opportunity to perform my PhD thesis in his lab and for the scientific discussions, motivation, and his knowledge, which guided me in my development as a scientist.

I want to thank Prof. Johannes Hegemann for the co-supervision of my PhD. Furthermore, I want to thank the MOI graduate school at the Heinrich Heine University Düsseldorf, which is funded by the Jürgen Manchot Stiftung, and the VISTRIE research consortium for financial support and for creating a great environment for scientific exchange and the building of networks.

Thanks to Albert and Zsolt for their guidance in molecular cloning and science in general, to Anne, Khanh, and Mirko for many great suggestions to improve my experiments, to Eugi for the “BW assay”, to Stef and Domi for the “technical” support with the mouse experiments, and thank you to Kerstin for her support with the ÄKTA. Thank you to all technicians in general. I would like to thank all members of the Institute of Virology in Düsseldorf and Freiburg. I enjoyed the great and supportive atmosphere in the labs, which always was a motivation during hard times. Thank you for sharing expertise, great science-related and non-science-related discussions inside and outside of the lab. I feel blessed that I had the chance to get to know so many great people.

Thank you to our collaboration partners for sharing expertise, methods, and materials.

Thank you to all the people in Bochum and San Diego for my scientific education prior to my PhD thesis.

Und natürlich möchte ich mich herzlich bei meiner Familie und Hendrik bedanken, die mir Wurzeln und Flügel gegeben haben, so dass dies alles mir möglich war.

CURRICULUM VITAE

PERSONAL DETAILS

Name Katrin Ehrhardt
Date of Birth 26.10.1983
Place of Birth Celle, Germany
E-mail katrin-ehrhardt@web.de

RESEARCH EXPERIENCE

02/2010 – 11/2016 **Ph.D. Thesis**
Institute for Virology (Prof. Dr. Hartmut Hengel)
• Ph.D. thesis “Analysis of activating Fc gamma receptors and IgG subclasses in the mouse model of cytomegalovirus infection”
02/2010 – 07/2013 Heinrich Heine University Düsseldorf, Germany
08/2013 – 03/2016 Albert Ludwigs University Freiburg, Germany

01/2009 – 12/2009 **La Jolla Institute for Allergy and Immunology (LIAI), La Jolla, USA**
Department of Autoimmune Research (Prof. Dr. Matthias von Herrath)
• Position as graduate student
• Experimental studies with Dr. Christophe Filippi and Dr. Tobias Boettler (see publications)

EDUCATION

10/2006 – 12/2008 **Master of Science in Biochemistry**
Ruhr-University Bochum, Germany
• Master thesis: “Influence of Rev-protein and splicing on encapsidation of different HIV-1 RNA classes in vector particles”
• Department of Medical and Molecular Virology (Prof. Dr. Klaus Überla)

10/2003 – 10/2006 **Bachelor of Science in Biochemistry**
Ruhr-University Bochum, Germany
• Bachelor thesis: “Production and characterization of adenoviral vectors for targeted vaccination via bicistronic expression of α -Dec205-single chain-antibody and cytokines”
• Department of Medical and Molecular Virology (Prof. Dr. Klaus Überla)

08/1996 – 06/2003 **General Qualification for University Entrance (*Abitur*)**
Kaiserin-Auguste-Viktoria-Gymnasium (high school), Celle, Germany

SCHOLARSHIPS

08/2013 – 03/2016 **VISTRIE (Viral Strategies of Immune Evasion)**
Helmholtz Centre for Infection Research, Braunschweig, Germany

02/2010 – 07/2013 **Manchot Graduate School „Molecules of Infection“ (MOI)**
Heinrich Heine University Düsseldorf, Germany

12/2005 – 12/2006 **e-fellows.net**
Career Network and Online Scholarship Programme

ADDITIONAL SCIENTIFIC QUALIFICATIONS

01/2015 – 03/2016 **Deputy Animal Project Leader**
Institute for Virology, Albert Ludwigs University Freiburg, Germany

03/2008 **Laboratory Animal Science**
Department of Biochemistry, Ruhr-University Bochum and Bayer HealthCare, Wuppertal, Germany

- Certificate according to the recommendations of FELASA (category B) and GV-SOLAS

LANGUAGES

German (native), English (fluent), French (basic)

MENTORING EXPERIENCE

10/2005 – 3/2006 **Tutor of 1st Semester Students (Bachelor's Degree Programme in Biochemistry)**
Ruhr-University Bochum, Germany

10/2007 – 3/2008 **Thekla Mentoring Programme: Vocational Orientation for Science and Economy**
Ruhr-University Bochum, Germany

PUBLICATIONS

Anti-apoptotic Bcl-XL but not Mcl-1 contributes to protection against virus-induced apoptosis. Ohmer M, Weber A, Sutter G, Ehrhardt K, Zimmermann A, Häcker G. Cell Death Dis. 2016 Aug 18;7(8):e2340.

Immunoactivation induced by chronic viral infection inhibits viral replication and drives immunosuppression through sustained IFN-I responses. Honke N, Shaabani N, Merches K, Gassa A, Kraft A, Ehrhardt K, Häussinger D, Löhning M, Dittmer U, Hengel H, Recher M, Lang PA, Lang KS. Eur J Immunol. 2015 Oct 28.

Enhancing the Quality of Antibodies to HIV-1 Envelope by GagPol-Specific Th Cells. Storcksdieck genannt Bonsmann M, Niezold T, Temchura V, Pissani F, Ehrhardt K, Brown EP, Osei-Owusu NY, Hannaman D, Hengel H, Ackerman ME, Streeck H, Nabi G, Tenbusch M, Überla K. J Immunol. 2015 Oct 14. pii: 1501377.

Human cytomegalovirus Fcγ binding proteins gp34 and gp68 antagonize Fcγ receptors I, II and III. Corrales-Aguilar E, Trilling M, Hunold K, Fiedler M, Le VT, Reinhard H, Ehrhardt K, Mercé-Maldonado E, Aliyev E, Zimmermann A, Johnson DC, Hengel H. PLoS Pathog. 2014 May 15;10(5):e1004131.

Direct infection of dendritic cells during chronic viral infection suppresses antiviral T cell proliferation and induces IL-10 expression in CD4 T cells. Baca Jones C, Filippi C, Sachithanatham S, Rodriguez-Calvo T, Ehrhardt K, von Herrath M. PLoS One. 2014 Mar 10;9(3):e90855.

The HIV-1 Rev protein enhances encapsidation of unspliced and spliced, RRE-containing lentiviral vector RNA. Grewe B, Ehrhardt K, Hoffmann B, Blissenbach M, Brandt S, Uberla K. PLoS One. 2012; 7(11):e48688.

TGF- β blockade does not improve control of an established persistent viral infection. Boettler T, Cheng Y, Ehrhardt K, von Herrath M. Viral Immunol. 2012 Jun;25(3):232-8.

TLR2 signaling improves immunoregulation to prevent type 1 diabetes. Filippi CM, Ehrhardt K, Estes EA, Larsson P, Oldham JE, von Herrath MG. Eur J Immunol. 2011 May;41(5):1399-409.

Essential role for TLR9 in prime but not prime-boost plasmid DNA vaccination to activate dendritic cells and protect from lethal viral infection. Rottembourg D, Filippi CM, Bresson D, Ehrhardt K, Estes EA, Oldham JE, von Herrath MG. J Immunol. 2010 Jun 15;184(12):7100-7.

MANUSCRIPTS IN PREPARATION

Different serum abundance and disparate Fc gamma receptor activation capacity of mouse antiviral IgG2a versus IgG2c. Ehrhardt K*, Androsiac GA*, Corrales-Aguilar E, Zimmermann A, Hengel H. (* shared first authorship)

Specificity of Fc γ R-mediated protection against influenza disease by M2e-specific IgG1 and IgG2a antibodies. Van den Hoecke S, Katrin Ehrhardt K, Annasaheb Kolpe A, Karim El Bakkouri B, Deng L, Schoonooghe S, Anouk Smet A, Bentahir M, Roose K, Schotsaert M, Bert Schepens B, Fiers W, Nimmerjahn F, Staeheli T, Hengel H, Saelens X.

ORAL PRESENTATIONS

Impact of IgG subclasses on antiviral antibody effector function *in vitro* and *in vivo*: towards optimized antiviral IgG-based therapies for CMV disease. Ehrhardt K, Androsiac GE, Corrales-Aguila E, Zimmermann A, Hengel H. 2015. VISTRIE PhD & Postdoc Retreat, Punat, Croatia

IgG2a and IgG2c are unequal: distinct alleles, different serum abundance, disparate Fc-gamma receptor (Fc γ R) activation capacities. Ehrhardt K, Androsiac G, Corrales-Aguilar E, Zimmermann A, Hengel H. 2013. 43rd Annual Meeting German Society for Immunology, Mainz, Germany

POSTER PRESENTATIONS

Mouse cytomegalovirus induced IgG subclass selective hypergammaglobulinemia and emergence of Fc gamma receptor mediated antiviral IgG effector functions. Ehrhardt K, Androsiac A, Corrales-Aguilar E, Zimmermann Z, Hengel H. 2016. 41st Annual International Herpesvirus Workshop in Madison, Wisconsin, USA

Impact of IgG subclasses on antiviral antibody effector function *in vivo*: towards optimized antiviral IgG-based therapies for CMV disease. Ehrhardt K, Androsiac GE, Corrales-Aguila E, Zimmermann A, Hengel H. 2015. 3rd International Symposium of the Virtual Institute "Viral Strategies of Immune Evasion" VISTRIE. Braunschweig, Germany

IgG2a and IgG2c are unequal: distinct alleles, different serum abundance, disparate Fc-gamma-receptor (Fc γ R) activation. 2014. Ehrhardt K, Androsiac GE, Corrales-Aguilar E, Zimmermann A, Hengel

H. 2nd Waldthausen Castle Symposium "Margaret Gladys Smith 60th Anniversary of Cytomegalovirus Isolation" in Waldthausen, Germany

IgG2a and IgG2c are unequal: distinct alleles, different serum abundance, disparate Fc-gamma receptor (FcγR) activation capacities. Ehrhardt K, Androsiac G, Corrales-Aguilar E, Zimmermann A, Hengel H. 2014. 2nd International Symposium of the Virtual Institute "Viral Strategies of Immune Evasion" VISTRIE. Braunschweig, Germany

The HIV-1 Rev Protein Enhances Encapsidation of Unspliced and Spliced, RRE-Containing Lentiviral Vector RNA. 2013. Grewe B, Ehrhardt K, Hoffmann B, Blissenbach M, Brandt S, Ueberla K; 23rd Annual Meeting of the Society for Virology in Kiel, Germany

Fcγ-Receptor Mediated IgG Effector Functions Govern Cytomegalovirus Replication *In Vivo*. 2012. Ehrhardt K, Androsiac G, Corrales-Aguilar E, Nimmerjahn F, Zimmermann A, Hengel H; 14th international CMV/beta-Herpervirus Workshop, 4th Congenital Cytomegalovirus Conference in San Francisco, USA

Analysis of the protective capabilities of virus-specific IgG antibodies mediated by Fcγ-Receptors in the MCMV-Infection. 2012. Ehrhardt K, Androsiac G, Zimmermann A, Hengel H. 22rd Annual Meeting of the Society for Virology in Essen, Germany

Fcγ-Receptor mediated immune control of cytomegalovirus infection *in vivo*. 2011. Ehrhardt K, Nimmerjahn F, Hengel H; 16th FEBS International Summer School on Immunology in Hvar, Croatia

Splicing does not inhibit encapsidation of HIV-1-derived lentiviral vector. 2009. Brandt S, Ehrhardt K, Grewe B, Blißenbach M, Stang A, Überla K. 19th Annual Meeting of the Society for Virology in Leipzig, Germany